Agonists, Antagonists, and Constitutive Activation of the Melanocortin-1 Receptor (MC1-R)

by

Dongsi Lu

A DISSERTATION

Presented to the Department of Cell and Developmental Biology
and the Oregon Health Sciences University
School of Medicine
in partial fulfillment of
the requirements for the degree of
Doctor of Philosophy
May 1997

School of Medicine
Oregon Health Sciences University

CERTIFICATE OF APPROVAL

This is certify that the Ph.D. thesis of
Dongsi Lu
has been approved

[redacted]
Professor in charge of thesis

[redacted]
Member

[redacted]
Member

[redacted]
Member

[redacted]
Member

Associate Dean for Graduate Studies

To My Parents, Mr. Fengming Lu and Mrs. YuLan Ji,

and Grandmother, Mrs. Shenzhen Xu

To My in-Laws, Mr. Yan Xia and Mrs. Xiulan Pang

To My Loving Husband, Xiaoming

ACKNOWLEDGMENT

Many people deserve my thanks for their support and help during past several years. While it would be impossible to acknowledge all of them here, certain people have made an important impact both on the works comprising this dissertation and on my life.

I am especially grateful to my mentor, Dr. Roger D. Cone, who has been an outstanding advisor, from whom I have learned a tremendous number of valuable lessons that will be with me through my professional life. I thank him for his critical advice, support, encouragement, stimulating ideas, and for his efforts to ensure that I received the highest level of training possible.

I would like to express my appreciation to all those individuals in the Cone Lab, Wenbiao Chen, Bob Kesterson, Carrie Haskell-Leuvano, Linda Robbins, Kathy Kong, Wei Fan, Ximena Opitz-Araya, Daniela Dinulescu, and former members of the Cone Lab, Sandhya Koppula , Bruce Boston, Katie Blaydon and Maya Hunter, who have contributed much to this project through their friendship, suggestions and support.

I would like to thank the faculty, staff, and my fellow students in the Vollum Institute and in the department of cell and developmental biology. I would also like to thank the dissertation committee consisting of Dr. John Adelman, Dr. Roger Cone, Dr. David Farrens, Dr. Richard Goodman, and Dr. David Grandy.

I wish to thank following family members for their encouragement, support, and enthusiasm: Fengming Lu, Yulan Ji, Shenzhen Xu, Yan Xia, Xiulan Pang, Ensi Lu, Ningsi Lu, Xiaoguang Xia, Xuefeng Xia, Xueqin Xia, Jijin Li, and Jing Shen. Of special recognition is my husband, Xiaoming, his love, humour, advice and understanding have always being with me and giving me the strength to fulfill this study.

During the preparation of this dissertation, my father in-law, Yan Xia and my good friend, Linda Robbins passed away, they will be remembered always in my heart.

TABLE OF CONTENTS

TABLE OF CONTENTS-continued

LIST OF ILLUSTRATIONS

LIST OF ILLUSTRATIONS-continued

LIST OF ILLUSTRATIONS-continued

LIST OF ILLUSTRATIONS-continued

LIST OF TABLES

LIST OF TABLES-continued

LIST OF TABLES-continued

ABSTRACT

Pigmentation in mice is determined by over 60 genetic loci. *Agouti* and *extension* are two loci involved in the regulation of pigmentation. These two loci have opposite effects on coat color pigmentation. The molecular mechanism of the interaction between gene products of *agouti* and *extension*, the agouti peptide and the melanocortin-1 receptor (MC1-R, or melanocyte-stimulating-hormone receptor, MSH-R), was examined in this study. Mouse agouti peptide functions as a highly potent competitive antagonist of the MC1-R, resulting in the yellow pigmentation in mice expressing agouti in the hair follicle. In addition, the agouti peptide is also a highly potent antagonist of the melanocortin-4 receptor (MC4-R). Based on this finding, a hypothesis that antagonism of the MC4-R by ectopically expressed agouti causes the agouti obesity syndrome found in the lethal yellow mouse (A^y) was proposed.

Although dominant *extension* alleles are epistatic to dominant *agouti* alleles in the mouse, the significantly different distribution of black and red pigments in fox *Vulpes vulpes* indicated a non-epistatic interaction of these two loci. This study demonstrated the proposed dominant *extension* allele (E^A) encodes a constitutively active MC1-R with a C125R mutation in the middle of the presumed third transmembrane domain, while the proposed recessive *agouti* allele (a) results from a 166 nt deletion in its second exon. Demonstration that the proposed *agouti* and *extension* loci encoded agouti peptide and the MC1-R convincingly argued for a novel non-epistatic relationship between these alleles in the fox.

To test the hypothesis that antagonism of the MC4-R was responsible for the agouti obesity syndrome, we sought to identify the first peptide antagonists of the central MC3-R and MC4-R. Cyclic lactam α-melanotropic analogues of Ac-Nle^4-cyclo[Asp^5,D-Phe^7,Lys^{10}] α-Melanocyte-Stimulating Hormone-(4-10)-NH_2 were tested for both agonist and antagonist activities on MC1-R, MC3-R, MC4-R and MC5-R. Analysis of a series of analogues demonstrated that the size of the amino acid substitutions at position 7 determined the antagonist function of Ac-Nle^4-c[Asp^5,D-Phe^7,Lys^{10}] α-MSH-(4-10)-NH_2 analogues on the MC3 and MC4 melanocortin receptors. Two analogues, SHU8914 [Ac-Nle^4-c[Asp^5,D-Phe(pI)^7,Lys^{10}] α-MSH-(4-10)-NH_2] and SHU9119 [Ac-Nle^4-c[Asp^5,D-Nal(2)^7,Lys^{10}] α-MSH-(4-10)-NH_2], with bulky aromatic amino acids at position 7, showed high antagonist activities of only the MC3-R and the MC4-R, and full agonist activities of the MC1-R and the MC5-R. The other two analogues, SHU9128 [Ac-Nle^4-c[Asp^5,D-Phe(pF)^7,Lys^{10}] α-MSH-(4-10)-NH_2] and SHU9203 [Ac-Nle^4-c[Asp^5,D-Phe(pCl)^7,Lys^{10}] α-MSH-(4-10)-NH_2], with smaller aromatic amino acids at position 7, showed full agonist activities for all melanocortin receptors tested.

Mutations that constitutively activate the MC1-R are found in a variety of mammals with dark coat color pigmentation. These mutations include a glu92lys in the sombre-3J mouse, leu98pro in the sombre mouse, cys125arg in the Alaska Silver fox, leu99pro in black Norwegian cattle, and met71lys plus asp119asn in black Norwegian Dala sheep. Extensive *in vitro* mutagenesis studies were performed at each of these amino acid residues in the mouse MC1-R to determine

the requirement at each of these positions for constitutive activation of the receptor. The results showed that a basic residue in each of the glu-92, asp-119, and cys-123 positions is required for constitutive activation. In addition, three different amino acid substitutions at asp-115 position can also constitutively activate the receptor, as well as the leu98pro and the met71lys mutations. Binding studies demonstrated that none of the residues implicated in constitutive activation are required for high affinity ligand binding except asp-119. Replacement of this acidic residue decreased affinity for ligand 10-100 fold irrespective of the changes made at that position. Computer modeling suggests that the three acidic residues, glu-92, asp-115 and asp-119 are located at the site of the receptor-ligand interaction, and the basic arg-8 residue in the His-Phe-Arg-Trp pharmacophore of the ligand contacts this site when the ligand is docked to the receptor. Based on mutagenesis studies and computer modeling, a "ligand-mimetic" model is proposed for the mechanism of constitutive activation of the melanocortin-1 receptor. When ligand binds to the wild type receptor, arg-8 in the pharmacophore of the ligand interacts with the negative charged acidic residue(s), glu-92, asp-115, and glu-119, to activate the receptor. Insertion of a basic residue at either of the glu-92, asp-119, and cys-123 positions is mimicking the ligand-receptor interaction to constitutively activate the receptor. Since constitutive activation mimics events proximal to ligand binding, agonist affinity and efficacy are dramatically reduced. This finding requires a modification of the current allosteric ternary complex model of G protein-coupled receptor (GPCR) activation, which states that constitutively active GPCR mutants should have higher affinity for ligand since they shift the equilibrium between R and R* towards the high affinity active receptor conformation, R*.

Chapter 1

Introduction

Pigmentation

Pigmentation is a fascinating mammalian phenotype, and is mainly determined by the density and distribution of melanin pigments (Szabo et al., 1972). Melanin is synthesized in specialized cytoplasmic organelles, known as melanosomes, within the melanocytes. Melanocytes are specialized dendritic cells derived from the neural crest, and actively migrate to the peripheral sites, including hair bulbs, dermis, and the dermoepidermal junction of the skin. One epidermal melanin unit consists one mature melanocyte and many surrounding keratinocytes (Lynch, 1994). The absorption of melanin by keratinocytes or by the growing hair shaft is responsible for the pigmentation of skin and hair, respectively.

Phaeomelanin and eumelanin are the two types of melanin pigments produced in melanocytes. The distribution of red-yellow phaeomelanin, and brown-black eumelanin, is an important determinant of the pigmentation pattern in mammals. Tyrosinase is the rate-limiting enzyme in formation of both types of melanin, and it catalyzes three different reactions: 1) the hydroxylation of tyrosine to 3,4-dihydroxyphenylalanine (DOPA); 2) the oxidation of DOPA to DOPAquinone; and 3) the oxidation of 5,6-dihydroxyindole (DHI) to indole-quinone (Korner and Pawelek, 1982; Hearing, 1987; Hearing and Jimenez, 1987; Hearing and Tsukamoto, 1991). When low levels of tyrosinase are present in the melanocyte, phaeomelanins are synthesized exclusively (Burchill et al., 1986; Burchill et al., 1989); when high levels of tyrosinase are present in the melanocyte, eumelanins are synthesized (Tamate and Takeuchi, 1984; Takeuchi et

al., 1989). It appears, therefore, that the phaeomelanin biosynthetic pathway is a default pathway. The summary of the melanin synthetic pathway in mammals is shown in **Figure 1.1**. Tyrosinase activity in melanocytes is regulated by cAMP levels , and elevated cAMP causes the activation of tyrosinase both transcriptionally (Kwon et al., 1988; Hoganson et al., 1989) and posttranslationally (Wong and Pawelek, 1975; Halaban et al., 1984). α-MSH is the primary melanocortin peptide that regulates the eumelanin/phaeomelanin switch by increasing the intracellular cAMP level in melanocytes via binding to the MC1 receptor and activating Gs and adenylyl cyclase (Pawelek, 1976).

In addition to tyrosinase, DHICA oxidase (tyrosinase related protein 1, TRP1) (del Marmol et al., 1993; del Marmol and Beermann, 1996; Zhao et al., 1996) and DOPAchrome tautomerase (TRP2) (Jackson et al., 1992; Tsukamoto et al., 1992), which share 35%-45% amino acid identity with tyrosinase, and DHICA polymerase (pmel 17) (Kwon, 1993; Kobayashi et al., 1994; Chakraborty et al., 1996; Lee et al., 1996) are also involved in the regulation of the eumelanin synthesis pathway. It appears that tyrosinase and tyrosinase related proteins are important in the proximal steps of this pathway, and the pmel 17 gene family might be important in distal steps of this pathway. These four proteins, tyrosinase, TRP-1, TRP-2, and pmel 17, involved in the eumelanin biosynthetic pathway, are encoded by four pigmentation loci: *albino* (Beermann et al., 1990), *brown* (Jackson, 1988), *slaty* (Jackson et al., 1992), and *silver* (Kwon et al., 1991), respectively. Enzymes specific to the phaeomelanin biosynthetic pathway have not yet been identified.

In the mouse, over 60 loci affecting pigmentation have been identified (Silvers, 1979; Jackson, 1994; Barsh, 1996). These loci are divided into 6 different categories according to their sites of action in the regulation of pigmentation: 1) melanocyte development and migration (*steel, piebald*), 2) melanocyte gene expression (*microphthalmia*), 3) melanocyte morphology (*dilute, leaden*), 4) melanosome structure and function (*silver, pink-eyed dilution*), 5) melanogenic enzymes (*albino, brown, slaty*), and 6) regulators of melanogenesis (*extension, agouti, mahogany, mahoganoid, umbrous*) (Jackson, 1994).

Recently, several studies have focused on two of the pigmentation loci that regulate melanogenesis, *extension* and *agouti*. These two loci regulate melanogenesis by controlling the relative amounts of eumelanin and phaeomelanin in the melanocyte, and have opposite effects. The *extension* locus increases brown/black pigment when dominant or extends red/yellow pigment when recessive, while the *agouti* locus increases red/yellow pigment when dominant and extends brown/black pigment when recessive. Previous experiments have shown that the *extension* gene product acts continuously within the hair follicle melanocyte (Geschwind, 1966; Geschwind et al., 1972; Lamoreux and Mayer, 1975), whereas the *agouti* gene product acts within the surrounding hair follicle cells only at certain times during development (Silvers and Russel, 1955; Silvers, 1958). Examples of mammalian *extension* alleles are shown in **Table 1.1**.

The phenotype of mice with the genotype A^{vy}/A E^{so}/E is black with maturity-onset obesity (Wolff et al., 1978), which demonstrated that dominant *extension* alleles are epistatic to dominant *agouti* alleles in mouse (Bateman, 1961; Wolff et al., 1978). In addition, the fact that dominant *extension* alleles had no

ability to abrogate the obesity syndrome caused by dominant *agouti* alleles indicated that there are probably separate pathways for the agouti-induced pigmentation and obesity phenotypes (Wolff et al., 1978).

Table 1.1 Examples of Mammalian *Extension* Alleles.

Mouse	Fox	Cattle
E^{so} ($E^{so\text{-}3J}$).....dominant black	E^{A}.....dominant black	E^{d}.....dominant black
E^{tob}.....dominant black		*E*...normal extension of black
E .....normal extension of black	*E*.....normal extension of black	e^{br}.....brindled
e .....non-extension of black		*e*...non-extension of black

Melanocortin peptides

The α-melanocyte stimulating hormone (α-MSH) and adrenocorticotropic hormone (ACTH) are representatives of the melanocortin peptide family with either melanotropic or adrenocorticotropic activity, respectively. These two peptides, along with the other members of the melanocortin peptide family, β-MSH, γ-MSH, and β-lipotropic hormone (β-LPH), are processed from the same polypeptide precursor, POMC (proopiomelanocortin), which is expressed primarily in the pituitary, the arcuate nucleus of the hypothalamus, and the nucleus of solitary tract in the brain stem. As shown in **Figure 1.2A**, POMC contains three fragments, the N-terminal fragment, ACTH, and β-LPH. α-MSH, β-MSH and γ-MSH are cleaved from the 39 amino acid ACTH precursor, the

carboxyl-terminal 91 amino acid peptide β-LPH and the N-terminal fragment, respectively. α-MSH contains the first 13 amino acids of ACTH, β-MSH contains 18 amino acids from the middle of β-LPH, and γ-MSH contains 12 amino acids from the middle of the N-terminal fragment. The major melanocortin peptides, such as α-MSH, ACTH, β-MSH, and γ-MSH, all have the same core sequence of -His-Phe-Arg-Trp-, which acts as the pharmacophore for the ligand-receptor interaction (Eberle et al., 1984; Eberle, 1988). The primary sequences of the major melanocortin peptide are shown in **Figure 1.2B**.

α-MSH is one of the best characterized melanocortin peptides, and several biological activities have been attributed to this peptide. The most well-known function of this peptide is the regulation of pigmentation (Geschwind, 1966; Geschwind et al., 1972; Eberle, 1988). Other biological activities, related to both the central and peripheral nervous systems, endocrine system, and other systems in mammals, are attributed to α-MSH as well. These proposed biological activities include: the potential role in learning and memory processes including motivation, attention, and concentration (de Wied, 1977; Donovan, 1978; Sandman et al., 1980; van Wimersma Greidanus et al., 1981; Beckwith and Sandman, 1982; Nyakas et al., 1985; de Wied, 1990), the neurotrophic influence in accelerated recovery of sensorimotor function (Bijlsma et al., 1983; Edwards et al., 1984; Nyakas et al., 1985; Strand et al., 1993) acquisition and maintenance of conditioned behavior (de Wied, 1977), modification of acute and chronic effects of opioids (Swaab and Martin, 1981; Jhamandas, 1984; de Wied, 1990), anti-inflammatory, antipyretic, and anti-cytokine effects (Hiltz et al., 1992; Catania and Lipton, 1994; Ceriani et al., 1994; Lyson et al., 1994; Star et al., 1995; Chiao et al., 1996), stimulation of sebaceous gland function (Thody and Shuster, 1975; Thody

et al., 1976), regulation of intrauterine growth, labor and brain development (Swaab et al., 1976; Swaab and Visser, 1977; Swaab et al., 1978; Swaab and Martin, 1981; Strand et al., 1993), and antidiuretic activity (Wesley and Gilmore, 1985). Decades later, five members of the melanocortin receptor family have been cloned, and demonstrated to bind both α-MSH and ACTH peptides.

Before the cloning of the MC1-R, studies to further understand the structure-function relationships of α-MSH were performed using several pigmentation test systems in which α-MSH increases dark color pigmentation. Different MSH analogues, as well as MSH fragments, were synthesized and tested. Some important features of these peptides were revealed by melanophore stimulation of the lizard *Anolis carolinensis* and the frog *Rana pipiens* (Shizume et al., 1954; Huntington and Hadley, 1974; Castrucci et al., 1984). As mentioned above, the core sequence His-Phe-Arg-Trp of α-MSH, conserved in other melanocortins, is the smallest fragment required for pigmentation in those assays (Hruby et al., 1987; Eberle, 1988). Some modifications in this core sequence of α-MSH produced both unique α-MSH agonists and antagonists (Sawyer et al., 1988; al-Obeidi et al., 1990; Sawyer et al., 1990; Hruby and Sharma, 1991). NDP-α-MSH ([4-norleucine, 7-D-phenylalanine]-α-MSH) is one of these compounds, which has prolonged melanosome-dispersing effect on frog (*Rana pipiens*) melanophores in vitro, and has a longer half-life in the serum. Since the initial cleavage site of enzyme degradation for α-MSH is probably located between the phenylalanine-7 and arginine-8 residues of this peptide, the change of L-Phe^7 to D-Phe^7 in NDP-α-MSH possibly hides the cleavage site of α-MSH stereostructurally (Sawyer et al., 1980). Thus, the longer half life of NDP-α-MSH in the serum is most likely due to resistance to serum enzymes that inactivate α-

MSH. NDP-α-MSH also has greater biological potency than α-MSH in stimulating adenylyl cyclase and tyrosinase (Sawyer et al., 1980). After the cloning of the melanocortin 1 receptor, the effect of the NDP-α-MSH at the MC1-R was tested and demonstrated to have a two log greater efficacy for activation of the MC1-R than α-MSH (Mountjoy et al., 1992; Cone et al., 1993).

Melanocortin peptide receptors

At the present, five genes encoding receptors for melanocortin peptides have been identified, and all belong to the superfamily of G protein-coupled receptors. According to the order in which they were cloned, the five receptors are named melanocortin 1 receptor (MC1-R), melanocortin 2 receptor (MC2-R), melanocortin 3 receptor (MC3-R), melanocortin 4 receptor (MC4-R), and melanocortin 5 receptor (MC5-R). The MC1-R and MC2-R were known from classical physiological and pharmacological studies prior to their cloning, and were previously called melanocyte-stimulating-hormone receptor (MSH- R), and adrenocorticotropin receptor (ACTH-R), respectively.

The human MC1-R was the first melanocortin receptor to be cloned by PCR methods using degenerate oligonucleotides, using cDNA from a human melanoma with a high number of α-MSH binding sites as the starting material. This receptor has 317 amino acids (315 amino acids in mouse), and its messenger RNA is expressed exclusively in melanocytes (Mountjoy et al., 1992). A second group also cloned the human MC1-R from a human melanoma sample using similar method (Chhajlani and Wikberg, 1992). From the same human melanoma tissue, another fragment closely related to the human MSH receptor was also isolated by PCR (Mountjoy et al., 1992). This fragment had a unique sequence,

hybridized specifically to an adrenal mRNA, and was considered a candidate for the human MC2-R. Subsequently, the human MC1-R was used as a probe to clone the genomic human MC1-R sequence as well as the mouse MC1-R cDNA (Mountjoy et al., 1992), and the putative MC2-R was used to clone the genomic human MC2-R sequence (Mountjoy et al., 1992) as well as the bovine MC2-R cDNA (Cone and Mountjoy, 1993). Both human and bovine MC2-Rs have 298 amino acids, and the human MC2-R mRNA is expressed almost exclusively in adrenocortical cells.

The cloning of MC1-R and MC2-R quickly led to the discovery of the latter three members of the melanocortin receptor family, the MC3-R, MC4-R, and MC5-R (Chhajlani et al., 1993; Roselli-Rehfuss et al., 1993; Gantz et al., 1993b; Barret et al., 1994; Desarnaud et al., 1994; Griffon et al., 1994; Labbe et al., 1994; Mountjoy et al., 1994; Gantz et al., 1994a; Fathi et al., 1995). Some of the expression sites of these three melanocortin receptors were determined by northern hybridization, RT-PCR, and *in situ* hybridization methods. Although the expression of MC3-R mRNA has been detected in stomach, duodenum, and pancreas by RT-PCR (Gantz et al., 1993a), the expression of MC3-R mRNA has been found mainly in the brain (Roselli-Rehfuss et al., 1993) and placenta (Gantz et al., 1993a). Besides the MC3-R, the MC4-R mRNA is also expressed in the brain (Gantz et al., 1993b; Mountjoy et al., 1994). The difference is that the MC4-R mRNA has been found only in the brain, and is expressed much more widely in the rat brain than the MC3-R. The MC4-R mRNA has been found by in situ hybridization to be expressed in 148 different rat brain nuclei (Mountjoy et al., 1994), whereas the MC3-R mRNA has only been found in 30 different rat brain nuclei (Roselli-Rehfuss et al., 1993). In addition, the MC4-R mRNA is

expressed in almost every brain region including: cortex, thalamus, hypothalamus and limbic system, brain stem, and spinal cord (Mountjoy et al., 1994), whereas the MC3-R mRNA is expressed primarily in hypothalamus and other limbic system structures (Roselli-Rehfuss et al., 1993).

Unlike the other four members of the melanocortin receptor family, whose expression is relatively restricted to either the melanocyte, the adrenocortical cells, or the brain area, the MC5-R mRNA has been found expressed at low levels in almost every organ, including the skin, muscle, thymus, spleen, ovary, testis, adrenal cortex, lung, brain, and pars tuberalis (Barret et al., 1994; Griffon et al., 1994; Labbe et al., 1994; Gantz et al., 1994a; Fathi et al., 1995). The summary of the distribution of melanocortin peptide receptors is shown in **Table 1.2**. There is 39-61% identity among these five melanocortin receptors on the amino acid level, which is summarized in **Table 1.3**.

Table 1.2 Distribution and functions of melanocortin peptide receptors

Receptor	Sites of expression	Functions
MC1-R	Melanocytes	Pigmentation
MC2-R	Adrenal cortex, adipocytes	Steroidogenesis
MC3-R	Hypothalamus, limbic system, placenta, gut	Unknown
MC4-R	Hypothalamus, limbic system, cortex, brain stem	Energy balance regulation , cardiovascular function regulation, thermoregulation
MC5-R	Muscle, liver, spleen, lung, brain, adipocytes...	Regulation of exocrine gland function

Table 1.3 The primary amino acid sequence identity among the five melanocortin receptors.

	MC1-R	MC2-R	MC3-R	MC4-R	MC5-R
MC1-R	___	39%	46%	47%	44%
MC2-R	___	___	46%	46%	43%
MC3-R	___	___	___	55%	59%
MC4-R	___	___	___	___	61%

Compared to other members of the G protein-coupled receptor superfamily, the melanocortin receptors are smaller (298-372 amino acids), resulting from a short amino terminal extracellular domain, a short carboxyl-terminal intracellular domain, and a small second extracellular domain (Cone et al., 1993). Also, some residues conserved amongst most G protein-coupled receptors are absent in the melanocortin receptors. For example, one or both of two cysteine residues, thought to form a disulfide bond (Dixon et al., 1987; Karnik et al., 1988) between the first and second extracellular loops (Probst et al., 1992), are missing in the melanocortin receptors.

Several conserved residues among the five melanocortin receptors are located close to the extracelluar face of the plasma membrane. Some of them are negative charged residues, such as glu-92 near the presumed extracellular margin of the second transmembrane domain, and two aspartic acid residues, asp-115 and asp-119 in the border of the presumed third transmembrane domain and the extracelluar environment; some of them are neutral amino acids with aromatic rings, such as two phenylalanine residues, phe-43 and phe-278 in the presumed

exterior portion of the first and the seventh transmembrane domains, respectively; and some of them are positive charged residues, such as his-258 in the presumed exterior portion of the sixth transmembrane domain (Cone et al., 1996). Since the ligand α-MSH has a positive charged residue (Arg-8), as well as neutral amino acids with aromatic rings (Phe-7 and Trp-9) in its pharmacophore, the conserved residues in the melanocortin receptors might play a role in ligand binding to the receptor. However, each of the melanocortin receptors has its unique sequence. As in the MC1-R, about 20% of its sequence is unique. These unique amino acids probably define the specific interactions among different residues of a receptor and give the receptor its unique pharmacological properties.

The chromosomal location of all five melanocortin receptors is determined in human (Vamvakopoulos et al., 1993; Gantz et al., 1993b; Magenis et al., 1994; Malas et al., 1994; Gantz et al., 1994b; Chowdhary et al., 1995), and four of the five have been determined in the mouse (Magenis et al., 1994), as shown in **Table 1.4**. Except for the MC1-R, which mapped to the distal end of chromosome 8 in the

Table 1.4 Human and mouse chromosomal location of melanocortin receptors.

Receptor	Mouse Chromosome	Human Chromosome
MC1-R	Distal end of Chr 8 identical with the *extension* locus	16q2
MC2-R	Distal end of Chr 18 near *Pdea*	18p11.2
MC3-R	Distal half of Chr 2 near *El-2*	20q13.2
MC4-R	RFLP not yet found	18q22
MC5-R	Distal end of Chr 18, near D18Mit9 and *sy*	18p11

mouse near the pigmentation locus mentioned above as *extension*, none of the other receptors mapped to known gene loci either in man or in the mouse.

As mentioned above, all five melanocortin receptors belong to the superfamily of G protein-coupled receptors. All five receptors have been shown to couple to Gs, activate adenylyl cyclase, and raise the cytoplasmic cAMP level upon activation. However, one report suggests MC3-R may also couple to a Gq-activated pathway (Konda et al., 1994). Although the downstream pathway is common, each of these five receptors has unique pharmacological profile for activation by different melanocortin peptides (**Figure 1.3**). Both the MC1-R and the MC4-R have the highest affinity for NDP-α-MSH (Mountjoy et al., 1992; Mountjoy et al., 1994), the MC2-R can only be activated by ACTH (Buckley and Ramachandran, 1981), and only MC3-R has high affinity for γ-MSH (Roselli-Rehfuss et al., 1993; Gantz et al., 1993a). MC1-R has a unique pharmacological profile, showing a similar EC_{50} for NDP-α-MSH as the MC4-R around 10^{-11} M, a similar EC_{50} for ACTH as the MC5-R around 10^{-8} M, and an EC_{50} for α-MSH around 10^{-9} M. Most mammalian MC1-Rs have lower EC_{50} values for stimulation by α-MSH than for ACTH, except for the human MC1-R which has a similar or even lower EC_{50} value for ACTH (Hunt et al., 1994; Mountjoy, 1994; Abdel-Malek et al., 1995). The lack of a distinct pars intermediate of the pituitary gland in adult human results in low levels of serum α-MSH (Eberle, 1988), thus ACTH may be the major hormone related to pigmentation in humans. This might explain why ACTH activates the human MC1-R more efficiently than α-MSH does.

The functions of the MC1-R and the MC2-R, regulation of pigmentation and adrenocortical steroidogenesis, respectively , were known long before the

cloning of these two receptors. Most recently, pharmacological experiments (Fan et al., 1997) and gene knockout experiments (Huszar et al., 1997) demonstrated the involvement of the MC4-R in the regulation of mouse body weight. Gene knockout has also been used to identify a role for the MC5-R in the regulation of exocrine gland function (Chen, W. and Cone, R.D., unpublished data). The known functions of melanocortin receptors are summarized in **Table 1.2**.

Genetics and biology of Agouti

The *Agouti* locus, named after the South American rodent *Dasyprocta agouti*, is one important pigmentation locus. Along with *extension*, it functions as a switch of pigment synthesis between the black-brown pigment eumelanin and the red-yellow pigment phaeomelanin, which are produce by the hair-bulb melanocytes (Silvers, 1979).

Around 20 different alleles of the *agouti* locus have been identified by genetic studies in the mouse. The phenotype of wild type *agouti* alleles (A^w, A) is a sub-apical yellow band along the shaft of a black hair (Silvers, 1979). From the dominant *agouti* alleles, such as the *lethal yellow* (A^y), to recessive *agouti* alleles, such as the *extreme nonagouti* (a), the mouse shows gradual color change from pure yellow to pure black (Siracusa, 1994). Besides the effects on coat color, four dominant *agouti* alleles (A^y, A^{vy}, A^{iy}, A^{sy}) are associated with pleiotropic effects, including adult-onset obesity, hyperinsulinemia and hyperglycemia (Siracusa, 1994; Yen et al., 1994). In addition, A^y and A^{vy} are associated with tumor susceptibility, and A^y, along with *lethal light-bellied nonagouti* (a^x), is associated with embryonic lethality (Siracusa, 1994).

The mouse *agouti* gene was cloned in 1992, and has four exons, the latter three containing the coding region (Bultman et al., 1992; Miller et al., 1993). The gene is normally expressed in the skin from postnatal day 3 to day 7 (Bultman et al., 1992; Miller et al., 1993). However, in heterozygous lethal yellow mice (A^y/a), the agouti gene is continuously expressed in every tissue examined (Bultman et al., 1992; Miller et al., 1993). The mouse agouti protein is a 131-amino acid polypeptide. It is composed of a signal peptide of 22 amino acids (Met-1 to Ser-22), a lysine-rich basic domain (His-23 to Lys-82) with an N-linked glycosylation site at Asn-39, and a cysteine-rich domain containing ten cysteine residues (Val-83-Cys-131) (Bultman et al., 1992; Miller et al., 1993; Willard et al., 1995), as shown in **Figure 1.4**. Sequence comparisons showed remarkable similarities between the agouti protein and some short peptide toxins isolated from the venom of predatory cone snails and spiders, such as ω-conotoxins and ω-agatoxins, which consist of a signal peptide, a middle portion with unknown function, and a cysteine rich domain (Olivera et al., 1994). The cysteine rich domain has been shown to be critical for toxin activity (Olivera et al., 1994).

When different *agouti* alleles were analyzed, the results showed large insertions or deletions of agouti's neighboring gene, which are responsible for some effects of *agouti* alleles other than the hair color pigmentation. For example, the embryonic lethality of A^y mice resulted from the deletion of all coding and 3' sequence of a ubiquitously expressed gene (*Raly*) sitting upstream of the *agouti* gene (Michaud et al., 1993; Duhl et al., 1994; Michaud et al., 1994), and the *Raly* promoter-driven agouti was ubiquitously expressed to cause the pleiotropic effects of agouti, since the *agouti* promoter was also deleted along with other regions of *Raly*. Few mutations in the agouti coding sequence were

found. In order to find why the ventral skin showed more agouti expression than the dorsal skin (Bultman et al., 1992), gene expression in different body regions was further analyzed. Four different wild-type A^w transcripts were revealed by this study (Vrieling et al., 1994). As shown in **Figure 1.5**, all of them have the same coding region, but different 5' untranslated regions, which result in two hair-cycle specific forms and two ventrum-specific forms (Siracusa, 1994; Vrieling et al., 1994). Different regional expression of the mouse agouti gene is responsible for differences in dorsal and ventral pigmentation (Vrieling et al., 1994).

Naturally occurring mutations in MC1-R

In 1993, Robbins et al. demonstrated that the *extension* locus encodes the mouse MC1-R, and variant *extension* locus alleles result from point mutations of the MC1-R that alter the function of the receptor (Robbins et al., 1993). This was one of the first reports of functional variants of the G protein-coupled receptors. There are four alleles of the *extension* locus in the mouse, which are wild type (E^+), sombre (including two independent sombre alleles, E^{so} and $E^{so\text{-}3J}$), tobacco (E^{tob}), and recessive yellow (e). In the *recessive yellow* mouse, a frameshift mutation at position 183 between the fourth and the fifth transmembrane domains results in a prematurely terminated nonfunctional MC1-R. In the *sombre* mice, there is a glu-to-lys change at position 92 in the $E^{so\text{-}3J}$ allele, a leu-to-pro change at position 98 in the E^{so} allele, with both of these mutations located in the putative exterior margin of the second transmembrane domain of the receptor. When expressed in the heterologous 293 cell line, both *sombre-3J* and *sombre* receptors are constitutively activated to 30 to 50% of the maximal stimulation levels of the wild type receptor, which refers to the activation level of the MC1-R stimulated by 10^{-6} M α-MSH.

The *sombre-3J* receptor is not further stimulated by higher concentration of α-MSH, however, the super-potent melanocortin analogue Nle^4-D-Phe^7-α-MSH (NDP-α-MSH) is capable of further activating the sombre receptor (Cone et al., 1996). The MC1-R of another kind of black mouse, the *tobacco* mouse, which has a ser-to-leu change at position 69, has different pharmacological features from the *sombre* receptor. The *tobacco* receptor only has a slightly elevated basal activity but can be further stimulated by α-MSH and stimulates a much higher maximal adenylyl cyclase level than the wild type receptor (Robbins et al., 1993).

After the discovery of the naturally occurring mutations in the mouse MC1-R, naturally occurring mutations have also been reported in humans (Valverde et al., 1995; Koppula et al., 1997), cattle (Klungland et al., 1995), fox (Vage et al., 1997), chicken (Takeuchi et al., 1996), and horse (Marklund et al., 1996). Naturally occurring mutations from different species are shown in **Figure 1.6** except the human mutations, which are shown in **Figure 1.7**.

Three *extension* alleles were postulated in cattle based on genetic studies, E^D for dominate black, *e* for recessive red, and E^+, the only allele in cattle and mice that allows phenotypic expression of *agouti* (Vanetti et al., 1994). A leu-to-pro change at position 99, homologous to position 97 of the mouse, has been found in the E^D allele, and a frameshift mutation resulting from a single base deletion at position 104 has been found in the *e* allele of the cattle (Adalsteinsson et al., 1995). The E^D allele has not been characterized pharmacologically, but is likely to have a functional similarity to the *sombre* receptor with a leu-to-pro change at position 98 in the mouse. Since all three mutations, glu92lys, leu98pro, and leu97pro (homologous to leu99pro in cattle), are clustered in the same portion of

the MC1-R, they are predicted to constitutively activate the receptor via the same mechanism.

There are three reports focusing on the studies of the naturally occurring mutations in the hMC1-R (Valverde et al., 1995; Xu et al., 1996; Koppula et al., 1997). In the first report, the human MC1-R coding sequence was examined from 30 unrelated British or Irish individuals with different shades of red hair and a poor tanning response, and from another 30 unrelated British or Irish control individuals with brown or black hair with a good tanning response (Valverde et al., 1995). Several amino acid changes have been found, with most clustered around the second transmembrane domain, except for the most commonly observed variant, asp294his. The other variants are all conservative changes, as shown in **Figure 1.7**. Two of the mutations, val92met and asp84glu, were also discovered independently by Sandhya Koppula in our laboratory using patient skin samples from the OHSU dermatology clinic (Koppula et al., 1997).

There is a much higher percentage of MC1-R variant alleles in people with fair skin and/or red hair than the control group in both studies. Valverde's study showed that 80% of red-haired fair skinned individuals had one or more MC1-R variants, while only 20% of the control group had the similar MC1-R changes (Valverde et al., 1995). Koppula's study showed that the val92met allele was found at a frequency of 0.11 in individuals with skin type I, which was more than five times higher than that in the individuals with skin type II. Although the association between the phenotype and MC1-R variants are striking, whether the MC1-R allele variants are causative factors of the phenotype is still an open question at this time. Based on MC1-R mutations found in other mammals, red hair often results from of loss-of-function mutations of the MC1-R gene, and the

loss-of-function mutations should be recessive. However, most individuals in both studies were not homozygous or even compound heterozygous for variant MC1-Rs, and all variants are conservative changes except asp294his (Valverde et al., 1995; Koppula et al., 1997). It is possible that an unidentified mutation of another locus is associated with the heterozygous individual. The cluster of mutations around the second transmembrane domain, along with mutations found in other species, suggested that this region might be important in MC1-R function and also a hot spot for mutation.

One of the human MC1-R variants, the val92met mutant, has been pharmacologically characterized, and there is no difference between the wild type receptor and the mutant receptor for α-MSH, $ACTH_{1-39}$, and β-MSH stimulations (Koppula et al., 1997). However, the val92met mutant receptor has about 5 times lower affinity for the ligand α-MSH than the wild type receptor according to one report (Xu et al., 1996). The reduced affinity of the val92met mutant for the ligand might explain the reduced eumelanin and enhanced phaeomelanin synthesis, resulting in the phenotype of red hair and easy burning of type I and type II skin (Xu et al., 1996).

Two proposed *extension* alleles were identified in the fox, *Vulpes vulpes*, the Alaska Silver allele E^A from Alaska Silver fox with dark pigmentation and the normal *extension* allele *E* from the red fox with red pigmentation, respectively (Ashbrook, 1937; Adalsteinsson et al., 1987).

As mentioned above, dominant *extension* alleles are epistatic to dominant *agouti* alleles in the mouse (Wolff et al., 1978), and dominant *extension* alleles result in the constitutive activation of the mouse MC1-R (Robbins et al., 1993). In chapter 2, we demonstrated that the murine agouti peptide is a highly potent

competitive antagonist of the mouse MC1-R. Based on the genetic observations and the pharmacological properties of both the constitutively active MC1-R and the murine agouti, the reason for the epistasis seen in the mouse is probably due to the inability of murine agouti peptide to antagonize the constitutively active MC1-R. However, the proposed *extension* locus is not epistatic to the *agouti* locus in the fox, *Vulpes vulpes* (Ashbrook, 1937; Adalsteinsson et al., 1987). In chapter 4, we show that both the MC1-R and *agouti* genes have been cloned from fox, *Vulpes vulpes* with different genotypes to attempt to understand this novel relationship between the receptor and its antagonist.

Although the pigmentation phenotypes of large felines are fascinating, it is difficult to study them due to the shortage of experimental materials. Also, undefined *extension* locus in domestic felines further complicated the study of the role of the MC1-R in feline pigmentation. However, several large cats with dark black pigmentation are reported to result from a dominant gene (Searle, 1968). Fortunately, our laboratory obtained blood samples from Boltar and Chewy, black and tan *Panthera pardus*, respectively, living at the Octagon Wildlife Sanctuary in Florida. They have been bred twice and gave birth to both black and tan offspring. Cloning and sequence analysis of the MC1-R from Boltar and Chewy demonstrated that Boltar was heterozygous for an arg106leu change while Chewy was homozygous with arg-106 in both alleles (Cone, R.D., unpublished data). Since Boltar, with an arg106leu change, transmits dominant black gene, and this change abolished a basic charge residue, in comparison to the constitutive activating mutations in MC1-Rs of the mouse, cattle and fox, it is reasonable to hypothesize that this change may constitutively activate the

panther MC1-R, and represents a dominant allele of the MC1-R in *Panthera pardus*.

In a recent study, presented in chapter 5, the arg106leu change, along with the arg106asp change, were introduced into the mouse MC1-R to test whether this arginine (homologous to arg-107 in the mouse MC1-R) plays an important role in constitutively activating the mouse MC1-R.

The high percentage of amino acid identity among MC1-Rs from different species (**Table 1.5**) provides us the basis for introducing naturally occurring mutations of MC1-Rs from different species into the mouse MC1-R to further understand the function of these spontaneous mutations and the mechanism of the activation of the MC1-R.

Table 1.5 The primary amino acid sequence identity of MC1-Rs cloned to date from different species .

	HMC1-R[b]	BMC1-R[c]	FMC1-R[d]	CMC1-R[e]
MMC1-R[a]	76%	75%	74%	59%
HMC1-R	___	80%	80%	62%
BMC1-R	___	___	82%	65%
FMC1-R	___	___	___	63%

a, MMC1-R, Mouse MC1-R; b, HMC1-R, Human MC1-R; c, BMC1-R, Bovine MC1-R; d, FMC1-R, Fox MC1-R; e, CMC1-R, Chicken MC1-R.

Constitutively active G protein-coupled receptors

The term "constitutive activation" has been used to refer to those G protein - coupled receptors which are active even in the absence of agonist. Mutations of residues in the third intracellular loop of the α_1-adrenergic receptor, made by *in vitro* mutagenesis, were first identified to yield constitutively active G protein-coupled receptors in 1990 (Cotecchia et al., 1990). Later, mutations of nearby residues of α_1-, α_2-, and β_2-adrenergic receptors were found to cause constitutive activation of these receptors as well (Kjelsberg et al., 1992; Lefkowitz et al., 1993; Ren et al., 1993; Samama et al., 1993). Studies of the constitutively active mutations of these receptors suggested a modification of the classical ternary complex model for G protein-coupled receptor activation (DeLean et al., 1980), and the new model is called the allosteric ternary complex model (Lefkowitz et al., 1993). The allosteric ternary complex model emphasizes two new concepts of receptor activation based on the pharmacological properties of the constitutively active mutations of the adrenergic receptor.
1), Receptors exist in equilibrium between two states: R and R*, and only R* can effectively interact with the G protein. Thus, the process of receptor activation comprises at least two distinguishable steps, conversion from R to R*, and binding of R* to G protein. 2), Ligand binding facilitates the conversion from R to R*, and stabilizes the ternary complex consisting of agonist-bound R* and G protein. In the absence of ligand, receptor mutation can shift the equilibrium towards the active state, R*, and results in a constitutively active receptor (Lefkowitz et al., 1993).

Meanwhile, studies on the G protein-coupled receptor rhodopsin have been carried out. Oprian's group identified mutations at two residues, glu-113 and lys-296, in the rhodopsin molecule that result in constitutive activation of opsin, and causes

the activation of G protein transducin in the absence of added chromophore or light (Robinson et al., 1992).

Lys-296 is the site of attachment of 11-cis-retinal chromophore to opsin through a protonated Schiff base linkage (Dratz and Hargrave, 1083; Bownds, 1967; Ovchinnikov et al., 1982; Findlay and Pappin, 1986), and glu-113 is the Schiff base counterion (Sakmar et al., 1989; Zhukovsky and Oprian, 1989; Nathans, 1990). It has been known that these two residues interact electrostatically when the chromophore is bound to the protein (Sakmar et al., 1989; Zhukovsky and Oprian, 1989; Nathans, 1990). Based on the results that mutations at either lys-296 or glu-113 can constitutively activate opsin, a salt bridge model was proposed to explain functions of these two residues in constraining the receptor in the inactive state, R. This model suggested that a salt bridge between lys-296 and glu-113 is a dominant feature of the inactive state of opsin. This electrostatic interaction constrains opsin in an inactive state, and absorption of light or mutations at either residue can break the salt bridge and activate opsin (Robinson et al., 1992).

Unlike the wild type opsin, the lys296gly and lys296ala mutants do not form a complex with 11-cis-retinal because of the loss of the covalent linkage to the chromophore as well as the long side chain of lys-296. However, the activation of the lys296gly and lys296ala mutants can be suppressed by the addition of an n-propylamine and ethylamine, respectively. The addition of n-alkylamine, such as n-propylamine and ethylamine, can rebuild Schiff bases for lys296gly and lys296ala to form complexes with 11-cis-retinal, called nPrSB chromophore and EtSB chromophore, respectively. Although the new Schiff base chromophore is not covalently bound to lys296gly or lys296ala, the new complexes, including the mutant opsin, and the nPrSB chromophore or the EtSB chromophore, have similar spectral

properties as the wild type opsin (Zhukovsky et al., 1991; Robinson et al., 1992). Also, the size of the n-alkylamine, as well as the residue size at position 296, are critical for the complex forming between the mutant and the n-alkylamineSB chromophore, which indicated that building a salt bridge requires both the right charge and the right distance. For example, the wild type opsin has a lysine at position 296 with a four carbon side chain, the mutant lys296gly has a glycine with one hydrogen side chain and the mutant lys296ala has an alanine with one carbon side chain. The mutant lys296gly with a smaller glycine substitution can bind either nPrSB chromophore or the EtSB chromophore, which has three and two carbons, respectively in the part of n-alkylamine, but can not bind nBuSB, which has four carbons in the part of n-alkylamine (Zhukovsky et al., 1991). Also, the mutant lys296ala with alanine substitution, one carbon bigger than the glycine substitution, only binds the smaller EtSB chromophore with two carbons in the part of n-alkylamine, but not the one carbon bigger nPrSB chromophore (Zhukovsky et al., 1991). Thus, reconstitution of a salt bridge in the mutants suppresses the constitutive activation of the opsin, further supporting the salt bridge model.

Since constitutively active mutations of the α_{1B}-adrenergic receptor enhance mitogenesis and tumorigenicity (Allen et al., 1991), and mutants of opsin, lys296glu and lys296met, which also result in the constitutively activation of opsin (Robinson et al., 1992; Rim and Oprian, 1995), were found in families with autosomal dominate retinitis pigmentosa (Keen et al., 1991; Sullivan et al., 1993), more studies started to focus on the identification of mutations in diverse G-protein coupled receptors in hyperfunctional tumors or genetic diseases. The mutations of rhodopsin found in congenital stationary night blindness (Dryja et al., 1993; Rao et al., 1994), the mutations of the thyrotropin receptor found in

hyperfunctioning thyroid adenoma (Russo et al., 1991; Parma et al., 1993; Paschke et al., 1994; Parma et al., 1995; Porcellini et al., 1995; Van Sande et al., 1995) and autosomal dominant toxic thyroid hyperplasia (Tonacchera et al., 1996; Tonacchera et al., 1996; Vassart et al., 1996), the mutations of the luteinizing hormone receptor found in familial male precocious puberty (Shenker et al., 1993; Kawate et al., 1995; Kosugi et al., 1995; Kraaij et al., 1995; Latronico et al., 1995; Laue et al., 1995; Yano et al., 1995), the mutation of the parathyroid hormone-parathyroid hormone-related peptide receptor found in Jansen-type metaphyseal chondrodysplasia (Schipani et al., 1995), mutations of a calcium-sensing receptor found in familial hypocalciuric hypercalcaemia and neonatal severe hyperparathyroidism (Pollak et al., 1994; Tominaga and Takagi, 1996), and a constitutively active putative G-protein coupled receptor encoded by human herpesvirus Kaposi's sarcoma-associated herpesvirus (KSHV) in Kaposi's sarcoma (Arvanitakis et al., 1997), are known examples of these studies as of this writing.

Naturally occurring mutations in the MC1-Rs of mice (Robbins et al., 1993) and other species (Klungland et al., 1995; Valverde et al., 1995; Koppula et al., 1997; Vage et al., 1997) represent millions of years of nature's efforts at informative mutagenesis of the MC1-R. Likewise, the study of agouti, and other antagonists of the melanocortin receptors may provide information regarding structure and function of the MC1-R, and thus these two areas of study have provided the basis for my thesis research entitled, "Agonists, Antagonists and Constitutive Activation of the Melanocortin-1 Receptor (MC1-R)".

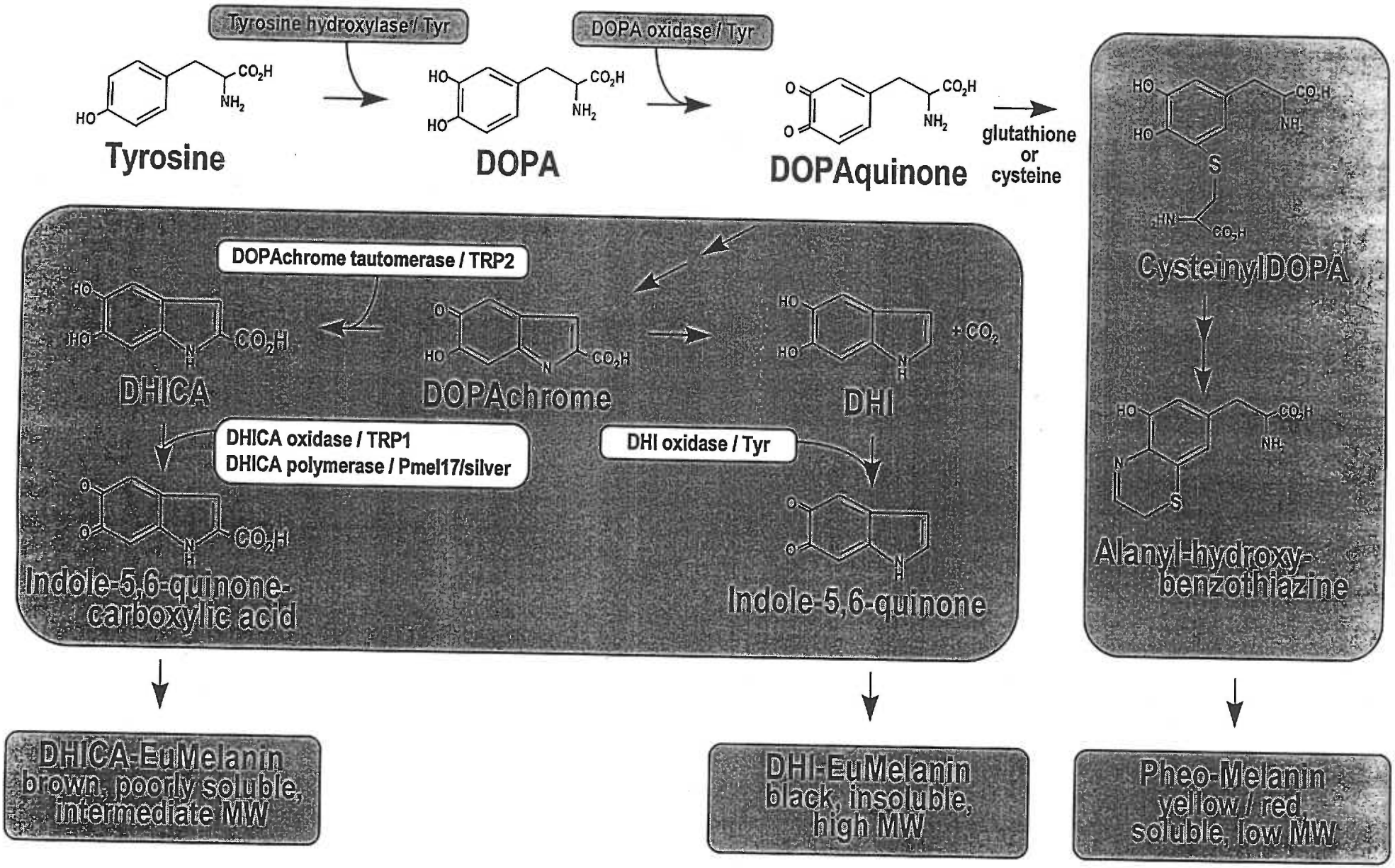

Figure 1.1 Melanin Synthetic Pathways in Mammals. Characterized enzymes are indicated, followed by the genetic locus encoding the enzyme.

A

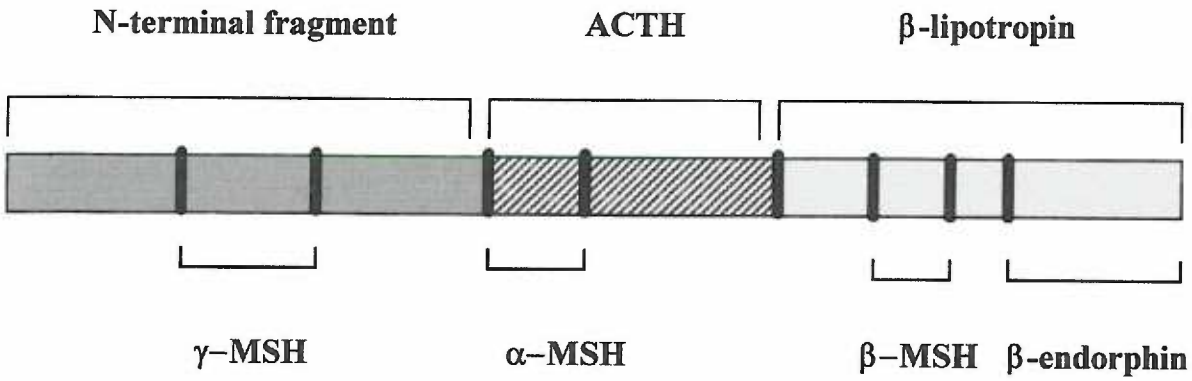

B

ACTH	H_2N-SYSMEHFRWGKPVGKKRRPVKVYPNGAEDESAEAFPLEF-OH
α-MSH	Ac-SYSMEHFRWGKPV-NH_2
β-MSH	H_2N-AEKKDEGPYRMEHFRWGSPPKD-OH
γ-MSH	H_2N-YVMGHFRWDRFG-OH
NDP-α-MSH	Ac-SYSXEHZRWGKPV-NH_2

Figure 1.2 The melanocortin peptides. (A) Structure of the proopiomelanocortin (POMC) precursor. Major melanocortin peptides are indicated by brackets and basic dipeptide proteolytic cleavage sites are indicated by the heavy bars. (B) Amino acid sequence of the major melanocortin peptides. All peptides are derived from human POMC except the potent synthetic analogue [Nle^4, D-Phe^7]-α-MSH (NDP-α-MSH). The conserved H-F-R-W pharmacophore is underlined. In the sequence of NDP-α-MSH, X represents norleucine and Z represents D-phenylalanine (Cone et al., 1996).

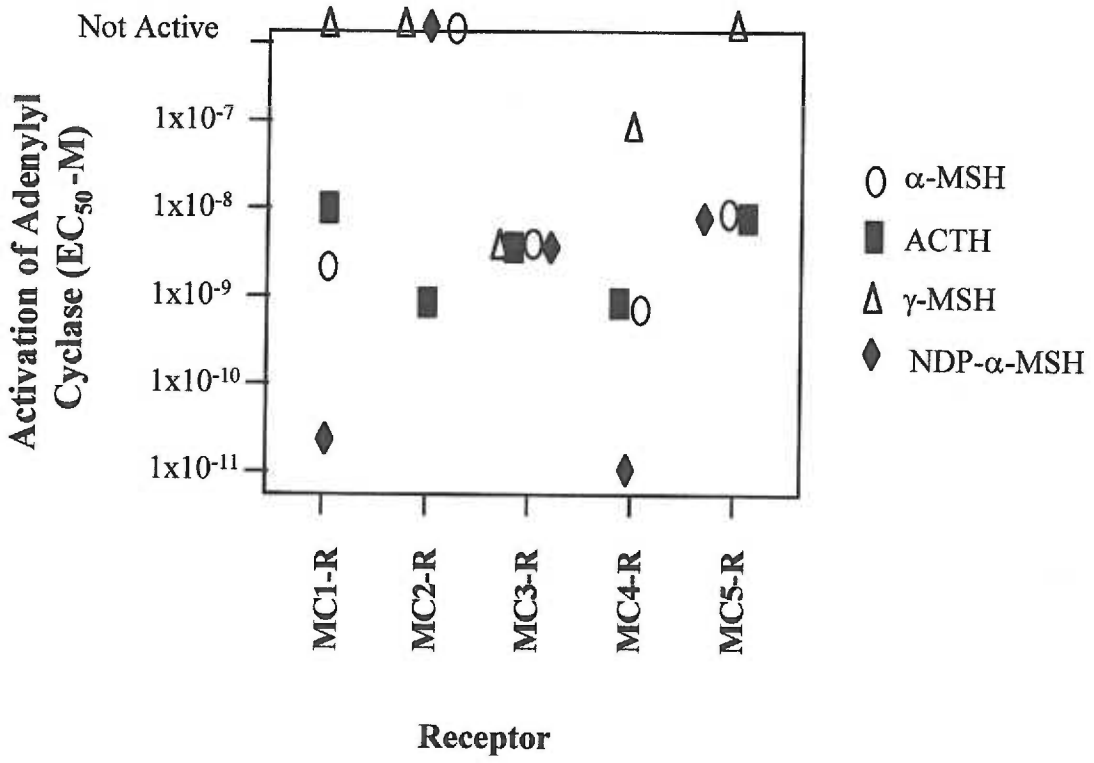

Figure 1.3 Pharmacology of the melanocortin receptors. Data represent published EC_{50} values for activation of adenylyl cyclase for each receptor by the peptide indicated. Not active means an $EC_{50} >> 10^{-7}$ M. In the case of the MC2-R, except for ACTH, no activity at all is seen at peptide concentration up to 10^{-6} M. Data from Mountjoy et al., 1992 (MC1-R), Buckley et al., 1981 (MC2-R), Roselli-Rehfuss et al., 1993(MC3-R), Mountjoy et al., 1994 (MC4-R), and Chen, unpublished data (MC5-R).

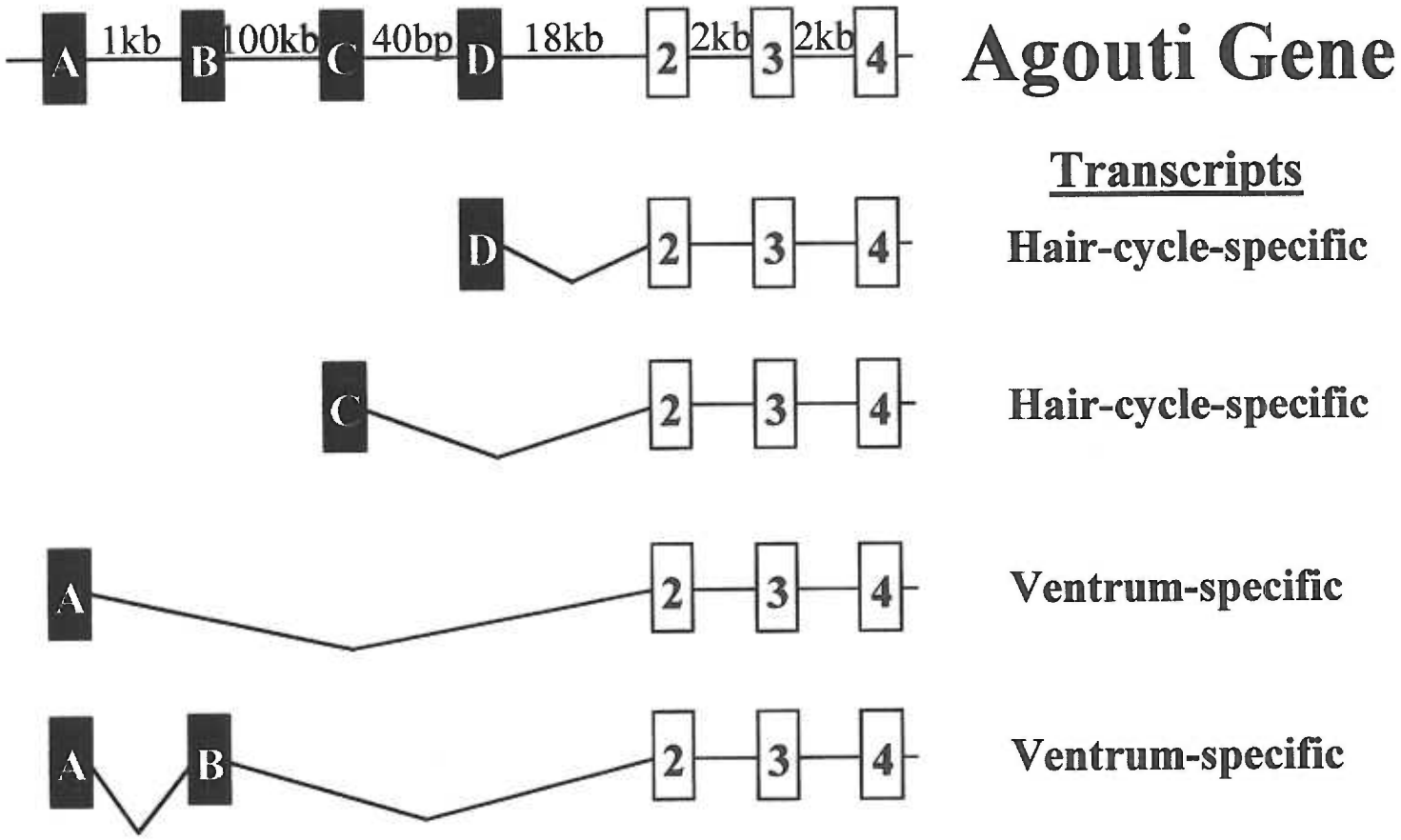

Figure 1.5. Genetic organization and multiple forms of wild type A^W transcripts (Siracusa, 1994).

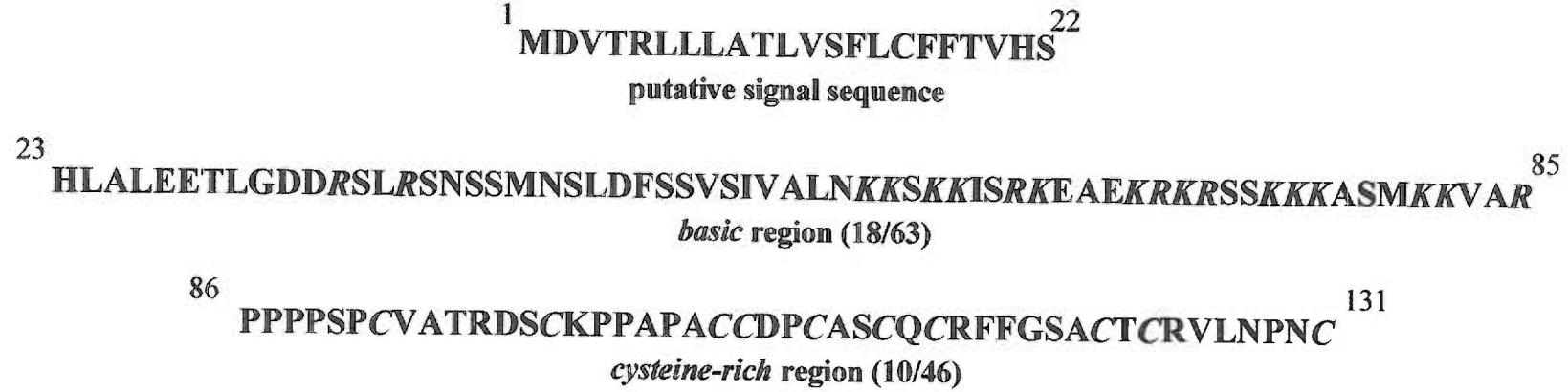

Figure 1.4 Sequence of Murine Agouti Signaling Peptides.

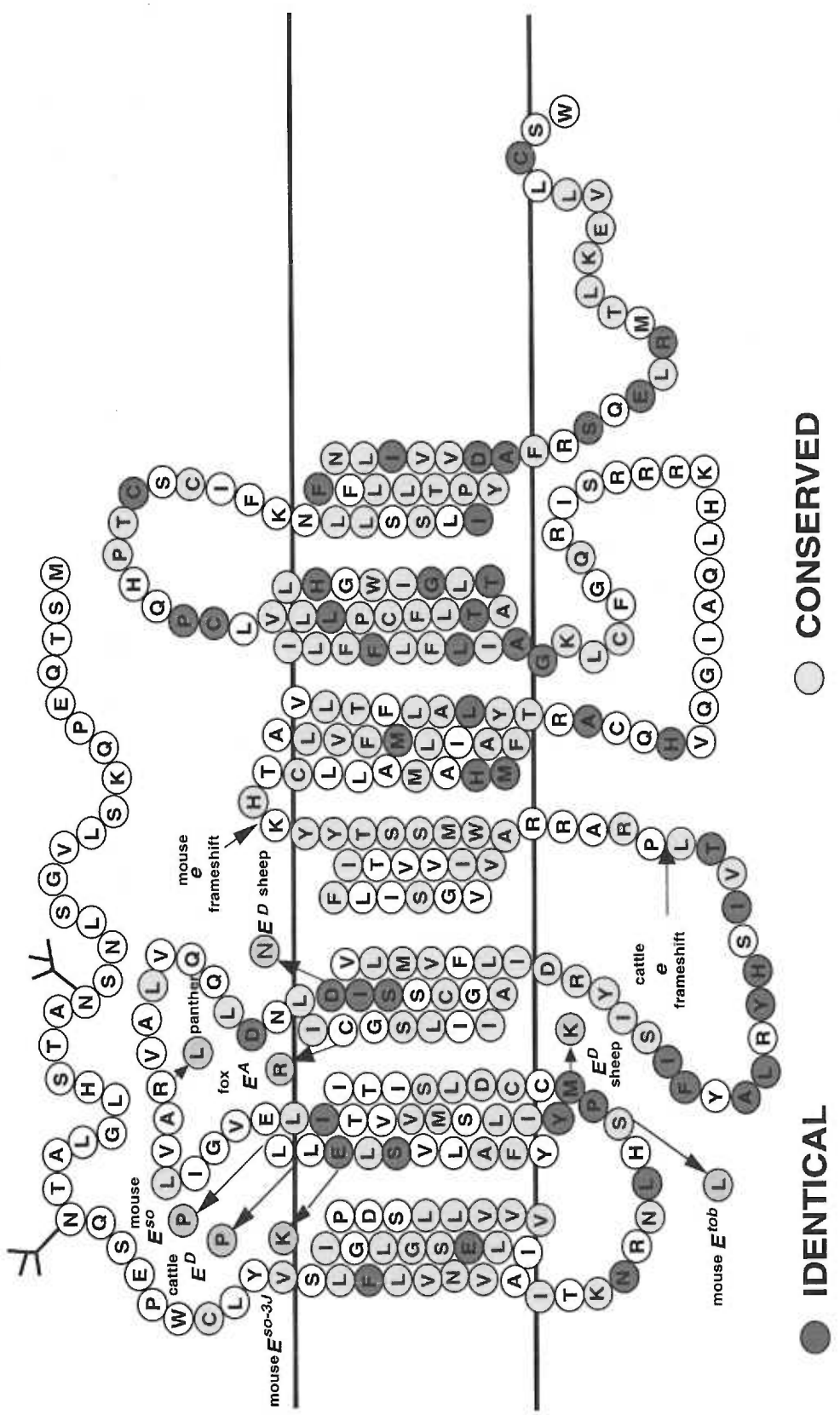

Figure 1.6 Naturally Occuring Variants of the MC1-R

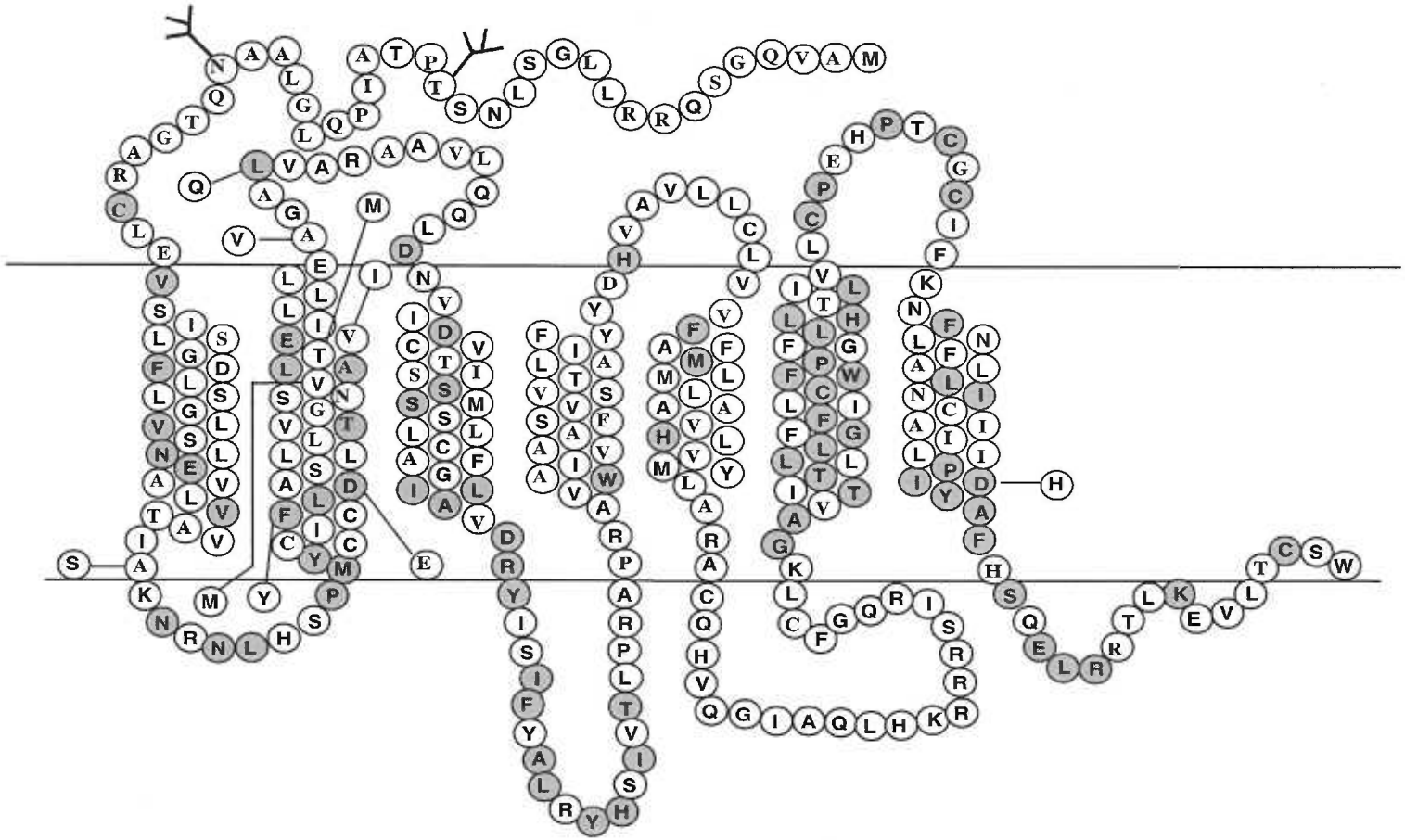

Figure 1.7 Allelic Variants of the human MC1-R

Chapter 2

Agouti Protein is an Antagonist of the Melanocyte Stimulating Hormone Receptor

Dongsi Lu*,&, Derril Willard@, Indravadan R. Patel@, Sue Kadwell@, Laurie Overton@, Tom Kost@, Michael Luther@, Wenbiao Chen*, Richard P. Woychik#, William O. Wilkison@!, and Roger D. Cone*

**Vollum Institute for Advanced Biomedical Research,*

& Department of Cell and Developmental Biology,

Oregon Health Sciences University, Portland, Oregon 97201, USA

@Division of Molecular Sciences, Glaxo Research Institute, Research Triangle Park, North Carolina 27709, USA

#Biology Division, Oak Ridge National Laboratory, Oak Ridge, Tennessee 37831-8077, USA

! To whom correspondence should be addressed.

Published in Nature, Vol. 371, 799-802 (1994)

ABSTRACT

The genetic loci *agouti* and *extension* control the relative amounts of eumelanin (brown-black) and phaeomelanin (yellow-red) pigments in mammals (Silvers, 1979): *extension* encodes the receptor for melanocyte-stimulating hormone (MSH) (Robbins et al., 1993) and *agouti* encodes a novel 131-amino-acid protein containing a signal sequence (Bultman et al., 1992; Miller et al., 1993). Agouti, which is produced in the hair follicle (Silvers and Russel, 1955), acts on follicular melanocytes (Lamoreux and Mayer, 1975) to inhibit α-MSH induced eumelanin production, resulting in the subterminal band of phaeomelanin often visible in mammalian fur. Here we used partially purified agouti protein to demonstrate that agouti is a high-affinity antagonist of the MSH receptor and blocks α-MSH stimulation of adenylyl cyclase, the effector through which α-MSH induces eumelanin synthesis. Agouti was also found to be an antagonist of the melanocortin-4 receptor (Gantz et al., 1993b; Mountjoy et al., 1994), a related MSH-binding receptor. Consequently, the obesity caused by ectopic expression of agouti in the lethal yellow (A^y) mouse (Dickerson and Gowen, 1947) may be due to the inhibition of melanocortin receptor(s) outside the hair follicle.

INTRODUCTION, RESULTS, AND DISCUSSION

Two models have been proposed for the mechanism by which agouti protein inhibits stimulation of melanogenesis by α-MSH: 1) agouti is a negative regulator of the cAMP signalling pathway acting through a unique agouti receptor (Conklin and Bourne, 1993), or 2) agouti is a competitive antagonist of α-MSH (Jackson, 1993). We produced recombinant agouti protein using the baculovirus expression system in order to test these hypotheses. The band indicated by the arrow in **Fig 2.1** was absent from *Trichiplusia* cells not infected with the agouti/baculovirus vector, and its identity as the *agouti* gene product was verified by N-terminal sequencing (data not shown). Agouti pooled from the 0.8M NaCl elution shown in this preparation was estimated to be 75% pure, resulting in an effective agouti concentration of ~ 0.14 mg ml^{-1}.

Agouti action was examined initially on the B16F10 murine melanoma cell line (Siegrist et al., 1988). Agouti (0.7 nM) shifted the half-maximal effective concentration (EC_{50}) for stimulation of adenylyl cyclase by α-MSH in these cells from 1.7 $\pm$ 0.24 nM to 13.4 $\pm$ 3.3 nM (data not shown). To characterize agouti action further, we examined the effects of agouti on the MSH receptor (MSH-R) and other G-protein-coupled receptors stably transfected into the human embryonic kidney 293 cell (Frazier et al., 1990; Mountjoy et al., 1992; Roselli-Rehfuss et al., 1993; Mountjoy et al., 1994). α-MSH had no effect on the cAMP pathway in untransfected 293 cells, demonstrating the absence of endogenous melanocortin receptors in this cell line (**Fig 2.2a**). Furthermore, addition of agouti (0.7 nM) had no effect on the basal adenylyl cyclase levels. Agouti also had no

effect on the ability of thyroid-stimulating hormone (TSH) to bind to its receptor and stimulate adenylyl cyclase in TSH-R-transfected 293 cells (**Fig 2.2b**). As the TSH-R couples to the same G protein as do the melanocortin receptors, G_S, this experiment shows that agouti acts upstream of G_S in the cAMP signalling pathway.

In contrast, the same concentration of agouti protein produced a significant shift in the adenylyl cyclase/functional coupling curve of the murine MSH-R expressed in 293 cells (**Fig 2.3a**). Control supernatants from baculovirus-infected cells at the same total protein concentration had no effect. Agouti protein (0.7 nM) increased the EC_{50} for activation of adenylyl cyclase from $1.5 \pm 1.1 \times 10^{-9}$ M to $2.2 \pm 1.2 \times 10^{-8}$ M, but did not alter the maximally induced activity of the receptor. The apparent *K*i value calculated from four independent experiments was $3.2 \pm 2.6 \times 10^{-10}$ M. A dose-response curve demonstrated increasing inhibition of the murine MSH-R by agouti at concentrations from below 10^{-9} M up to 10^{-6} M(**Fig 2.3b**). The human MSH receptor was also inhibited by agouti but only at much higher protein concentrations (**Fig 2.3c**). It is conceivable that, unlike its murine counterpart, human agouti is a high-affinity antagonist of the human MSH-R. But as the wild-type agouti pigmentation phenotype is not commonly observed in man, it is possible that agouti no longer antagonizes MSH-R function in the human hair follicle.

The ability of agouti to shift the MSH-R functional coupling curve without affecting maximal receptor activation suggested that agouti was acting as a

competitive antagonist. To investigate this further, the ability of the protein to compete with another melanocortin peptide for binding to the mMSH-R was examined. Adrenocorticotropic hormone (ACTH), which contains the α-MSH peptide in its first 13 amino acids, can be radiolabelled at Tyr23 without loss of potency and binds to the same site on the melanocortin receptors as does α-MSH (Gantz et al., 1993a; Gantz et al., 1993b; Roselli-Rehfuss et al., 1993). Competition binding experiments were performed with ^{125}I-labeled $ACTH_{1-39}$ and the M-3 subclone of the Cloudman murine melanoma cell line. This cell line was used because of the high density of MSH receptors expressed on the plasma membrane (10,000-50,000), in contrast to the MSH-R-transfected 293 cells, which were estimated to express under 1000 MSH receptors per cell (data not shown). ACTH bound the MSH-R with a *K*d of 6.3 $\pm$ 13.3 x 10^{-8} M, within the range of previously reported values (Siegrist et al., 1988) (**Fig 2.3d**). Using a single site model, agouti protein blocked 50% of specific ACTH binding to the MSH receptor at a concentration of 1.2 $\pm$ 0.7 ng/ml (*K*i=IC_{50} (half-maximal inhibitory concentration) = 6.6 $\pm$ 3.8 x 10^{-10} M) (**Fig 2.3e**). Similar results were obtained when a synthetic radiolabelled α-MSH analogue (Nle^4,D-Phe^7-α-MSH) was used as the radiolabelled ligand (data not shown). As a control, baculovirus supernatant from *T. ni* cells infected with a baculovirus construct containing an unrelated gene insert was purified as described for agouti. The protein had no activity in this assay (**Fig 2.3e**), or on α-MSH stimulation of adenylyl cyclase in MSH-R-transfected 293 cells (data not shown).

So far there are five members of the melanocortin receptor family, MC1-R (MSH-R) (Chhajlani and Wikberg, 1992; Mountjoy et al., 1992) , MC2-R (ACTH-

R) (Mountjoy et al., 1992), MC3-R (Gantz et al., 1993a; Roselli-Rehfuss et al., 1993) , MC4-R (Gantz et al., 1993b; Mountjoy et al., 1994), and MC5-R (Chhajlani et al., 1993; Desarnaud et al., 1994). No functions have yet been described for the latter three members of the family, but the MC3-R and MC4-R are expressed primarily in the central nervous system in brain nuclei involved in neuroendocrine and autonomic control. Surprisingly, agouti was also found to be a potent antagonist of α-MSH activation of the MC4-R (**Fig 2.4a**). Once again, the protein appeared to act like a competitive antagonist, not significantly interfering with maximal activation of the receptor. The same concentration of agouti (0.7 nM) did not antagonize activation of the MC3 or MC5 receptors, and the MC5-R was unaffected even at 100 nM agouti concentrations (**Fig 2.4b,c**).

Our results show that agouti is a high-affinity antagonist of the MSH-R, and of at least one of the other melanocortin receptors. Agouti appears to function as a competitive antagonist, inhibiting agonist binding to the MSH-R. This unique bifunctional regulation of the MSH-R by α-MSH and agouti allows for fine spatial and temporal regulation of eumelanin and phaeomelanin synthesis. These findings also provide a context for understanding the complex interactions of agouti and extension (MSH-R) responsible for many mammalian coat color variants, such as the variable black and tan markings in the German Shepherd, resulting from combinations of two extension (E^m, E) and three agouti (A^s, a^y,a^t) alleles (Little, 1957).

Because agouti also antagonizes MC4-R function, ectopic overexpression of agouti may lead to obesity in the lethal yellow mouse (A^y) through

pathological antagonism of melanocortin receptor(s) expressed outside the hair follicle. Although no agouti pigmentation phenotype has ever been reported in humans, a gene encoding a conserved human agouti protein has been found (Kwon et al., 1994) and so may a physiological role.

Acknowledgments

This work was supported in part by NIH grants (RDC), and by the office of Health and Environmental Research, US Department of Energy, under contract with Martin Marietta Energy Systems, Inc. (R.P.W.). We gratefully acknowledge the help of James Weiel, Pam DeLacey, and Kelly Lewis. We also thank Mark Furth and Terry Kenakin for helpful discussions.

METHODS

Production and Purification of recombinant agouti polypeptide.

Trichiplusia ni cells were infected at an MOI of 2 with pAcMP3-M.agouti virus or control virus and media were collected 48 h post-infection. This media was directly loaded onto a Poros-20 HS cation exchange column (PerSeptive Biosystems, MA) and bound protein eluted with NaCl concentrations from 0.2-1.0M. The 0.8M fraction was dialyzed into 50 mM NaCl, 20 mM PIPES, pH 6.5 and then diluted for assay. Agouti concentrations were estimated from gel electrophoresis and amino-acid analysis of purified protein. Media controls consisted of unrelated baculovirus supernatants collected 48 h post-infection and purified by NaCl elution of a Poros-20 HS column as for agouti.

Adenylyl cyclase assay.

Agouti protein was prepared as described above. Two independent preparations of agouti yielded similar results. 293 cells ($5x10^5$) and 293 cells expressing human TSH-R were preloaded with 5 μCi [^{3}H]-adenine for 1.5 hours at 37^{o}C, in a 5% CO_2 incubator. Cells were stimulated with varying concentrations of α-MSH (a) or bovine TSH (b) in the presence or absence of 0.7 nM agouti for 40 min. in cyclase assay incubation media (Dulbecco's modified Eagle's medium containing 0.1 mg ml $^{-1}$ bovine serum albumin and 0.1 mM isobutylmethylxanthine). Medium was aspirated and 2.5% perchloric acid containing 0.1 mM cAMP was used to stop the incubation. Adenylyl cyclase activity was calculated by determining the percent conversion of [^{3}H]-adenine to [^{3}H]-cAMP as described (Johnson and Salomon, 1991; Salomon, 1991). Correlation of cAMP accumulation measured in

this assay with actual adenylyl cyclase activity is made under the assumption that isobutymethylxanthine effectively blocks cAMP degradation. Data represent means and standard deviations from triplicate data points. EC_{50} values were calculated using GraphPad InPlot version 4.0.

Competition binding experiment.

Competition binding with radiolabelled ACTH has been described (Rainey et al., 1989). $1x10^6$ cells were washed twice with binding medium (F-10 medium containing 0.5% bovine serum albumin, 0.1% bacitracin, prewarmed to room temperature) and incubated in binding medium containing 9×10^{-11} M ^{125}I-labeled $ACTH_{1-39}$ (200,000 c.p.m.; Amersham) and different concentrations of agouti, control protein or cold ACTH for 2 h at 22 °C. Cells were then washed 3 times with ice cold binding medium, lysed with 1 ml of lysis buffer (0.5M NaOH, 0.4% deoxycholate) and counted as before (Rainey et al., 1989). Data were analyzed using the Kaleidagraph software package. Non-specific binding, determined as the amount of radioactivity bound at 10^{-5} M cold ACTH, was 10% of the total counts bound.

Figure Legends

Figure 2.1 Production and purification of recombinant agouti polypeptide. A 614 bp XbaI/PstI fragment of the full-length mouse agouti cDNA was subcloned into a XbaI/PstI digested baculovirus expression vector pAcMP3 (PharMingen, San Diego). Virus was produced using standard methods (Summers and Smith, 1987). 1 μg of each sample was electrophoresed on a 4-20% Tris-glycine gel (Novex, San Diego) and was visualized by ProBlue (Integrated Separation Systems, MA) staining. The agouti protein eluted with the 0.8M-NaCl wash. The 18.5K agouti species (arrow) was not observed in media infected with wild-type virus, and was demonstrated, after elution from the gel, to contain agouti by N-terminal sequencing. Lanes: 1, 48 h post-infection media from pAcMP3-M.agouti-infected cells; 2, follow-through from Poros-20 HS column; 3-7, NaCl elutions from Poros-20 HS column. Arrow indicates authentic agouti protein.

Figure 2.2 Agouti does not affect basal or TSH-R stimulated adenylyl cyclase activity. **a**, Adenylyl cyclase assay showing no effect of agouti on basal levels of this enzyme in untransfected 293 cells. α-MSH treatment also elicits no response, demonstrating the absence of endogenous melanocortin receptors in this cell line. **b**, Adenylyl cyclase assay showing no effect of agouti protein on the cAMP signalling pathway following activation by bovine thyroid-stimulating hormone (TSH) of adenylyl cyclase in 293 cells transfected with human TSH-receptor.

Fig. 2.3 Agouti is an antagonist of α-MSH at the murine MSH receptor. **a**, Agouti inhibits activation of the mMSH-R by α-MSH in stably transfected 293 cells, as monitored by stimulation of adenylyl cyclase. **b**, Agouti inhibition of murine MSH-R activation is dose-responsive. mMSH-R expressing 293 cells were stimulated with 10 nM α-MSH in the presence of agouti (10^{-12} - 7 x 10^{-7} M). **c**, Agouti inhibits activation of human MSH-R at high protein concentrations. No inhibition of human MSH-R activation by 0.7 nM agouti was observed. EC_{50} values were 2.3 $\pm$ 0.8 x 10^{-10} M (no agouti), 8.8 $\pm$ 2.1 x 10^{-10} M (154 nM agouti), and 1.1 $\pm$ 1.5 x 10^{-9} M (770 nM agouti). **d**, Competition binding demonstrates murine MSH-R expression in the Cloudman M-3 melanoma cell line. **e**, Competition binding demonstrates agouti protein blocks ^{125}I-labeled $ACTH_{1-39}$ binding to murine MSH-R. Baculovirus supernatants from SF9 cells infected with a virus containing an unrelated gene insert were purified in parallel with agouti protein and did not block ^{125}I-labeled $ACTH_{1-39}$ binding to murine MSH-R at concentrations up to 0.01 mg ml^{-1}. Values are shown as protein concentrations to compare agouti with control protein.

Figure 2.4 Agouti is an antagonist of the human MC4-R. **a**, Agouti antagonizes α-MSH activation of human MC4-R. **b**, Agouti protein does not effect α-MSH activation of rat MC3-R. **c**, Agouti protein does not effect α-MSH activation of mouse MC5-R. EC_{50} values for adenylyl cyclase activation by rat MC3-R or human MC4-R stimulated with α-MSH, or α-MSH plus 0.7 nM agouti,

respectively, were: rMC3-R, 4.2 $\pm$ 0.8 x10^{-9} M; 4.1 $\pm$ 0.9 x10^{-9} M; hMC4-R, 4.9 $\pm$ 2.4 x10^{-9} M; 3.3 $\pm$ 0.5 x10^{-8} M.

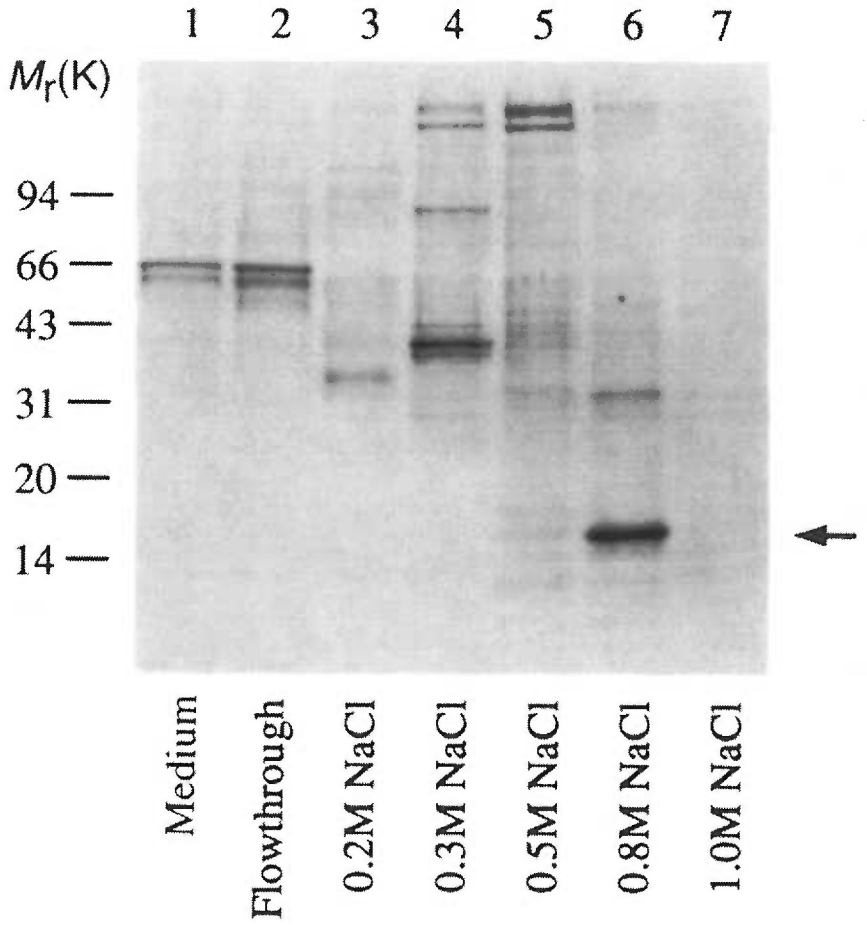

Figure 2.1 Production and Purification of Recombinant Agouti Polypeptide.

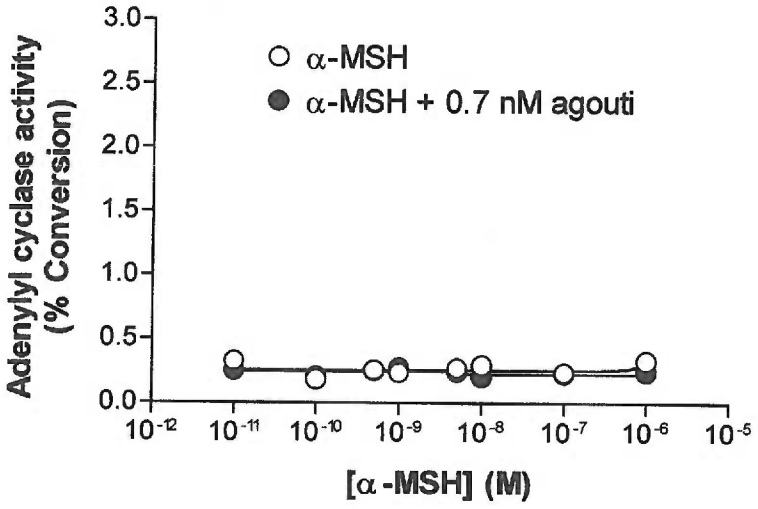

Figure 2.2a

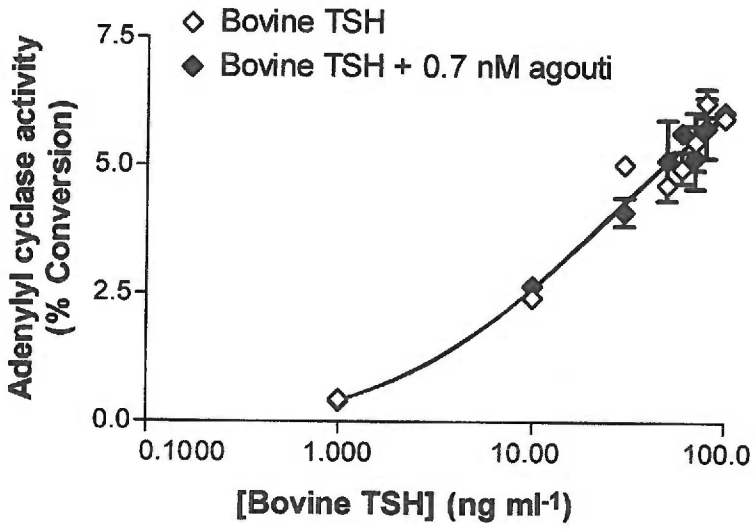

Figure 2.2b

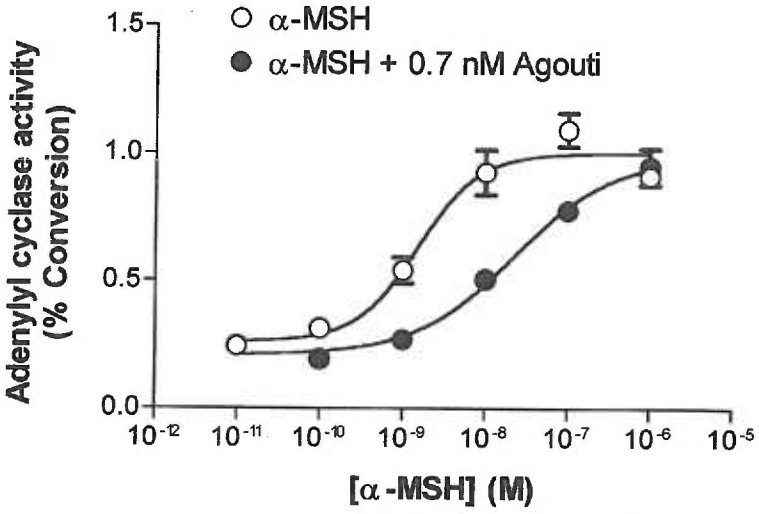

Figure 2.3a

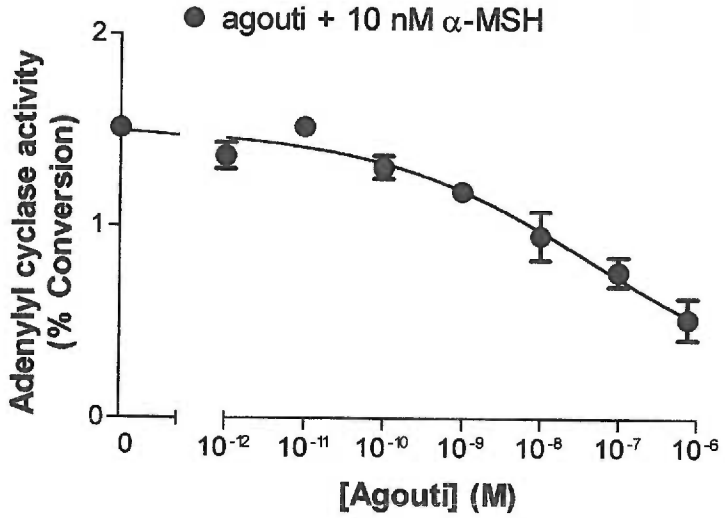

Figure 2.3b

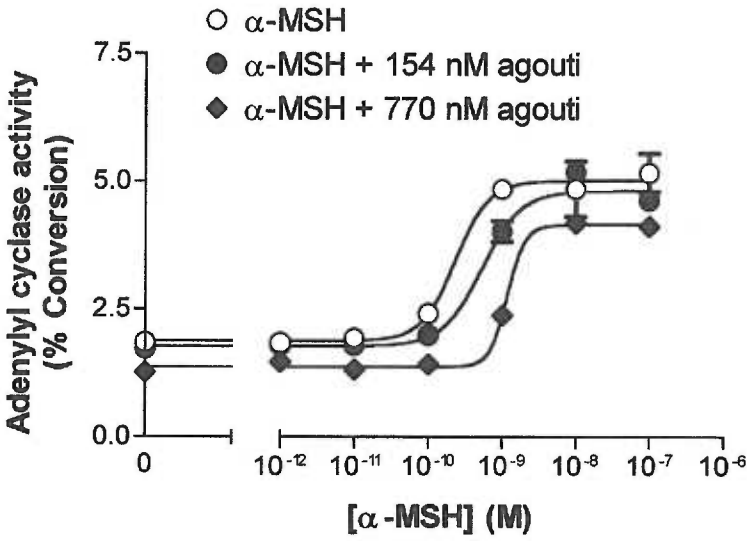
α-MSH
α-MSH + 154 nM agouti
α-MSH + 770 nM agouti
Adenylyl cyclase activity (% Conversion)
7.5
5.0
2.5
0.0
0
10-12
10-11
10-10
10-9
10-8
10-7
10-6
[α-MSH] (M)

Figure 2.3c

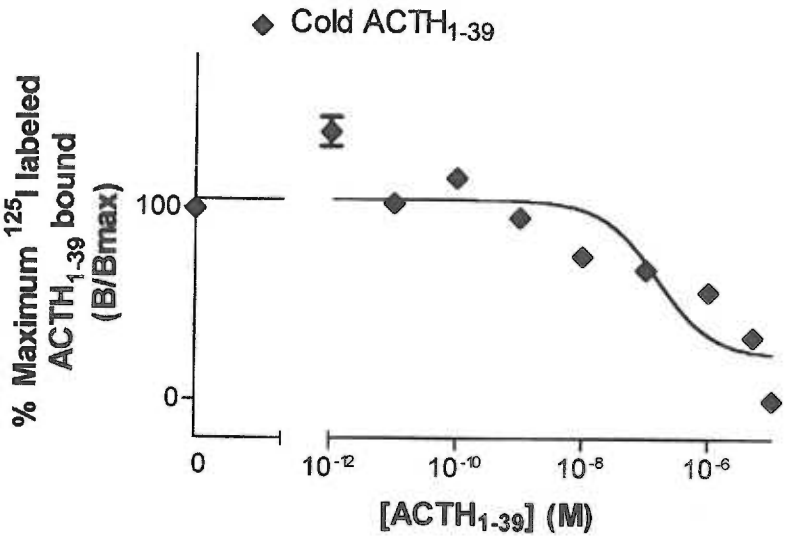

Figure 2.3d

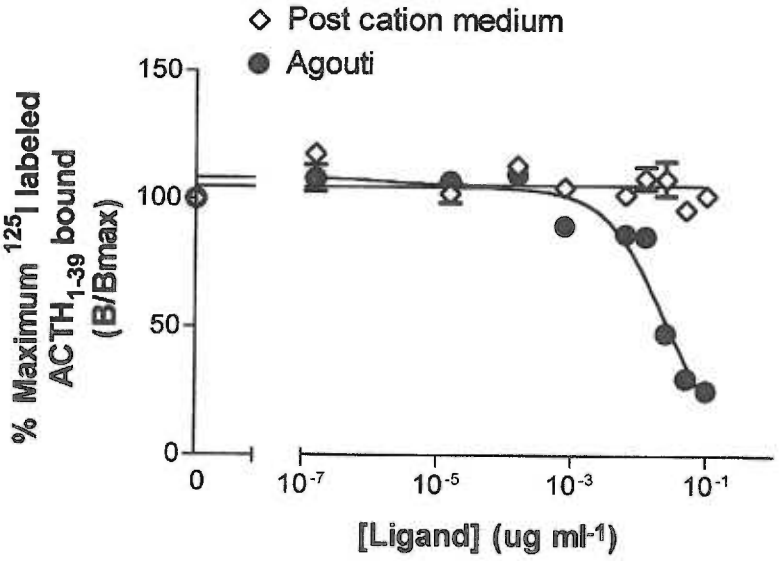

Figure 2.3e

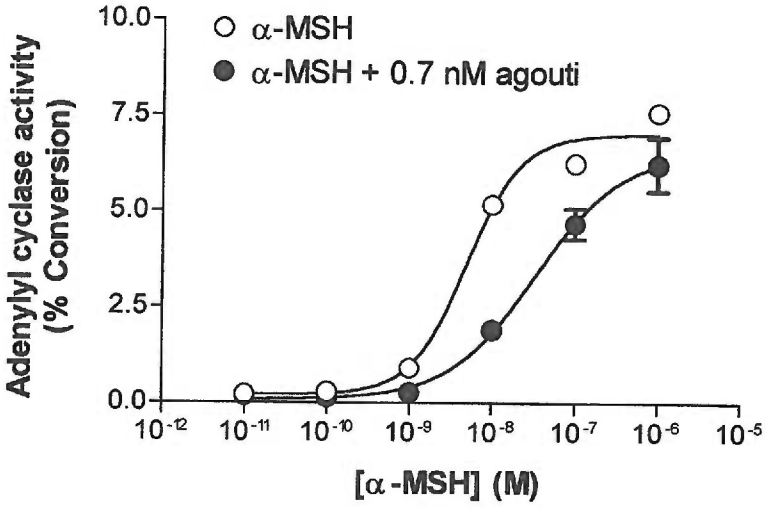
10.0
7.5
5.0
2.5
0.0
α-MSH
α-MSH + 0.7 nM agouti
Adenylyl cyclase activity
(% Conversion)
10-12
10-11
10-10
10-9
10-8
10-7
10-6
10-5
[α-MSH] (M)

Figure 2.4a

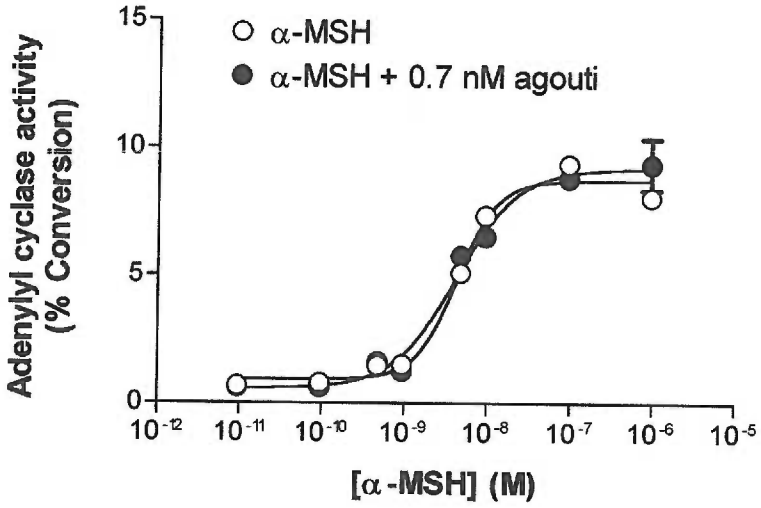

Figure 2.4b

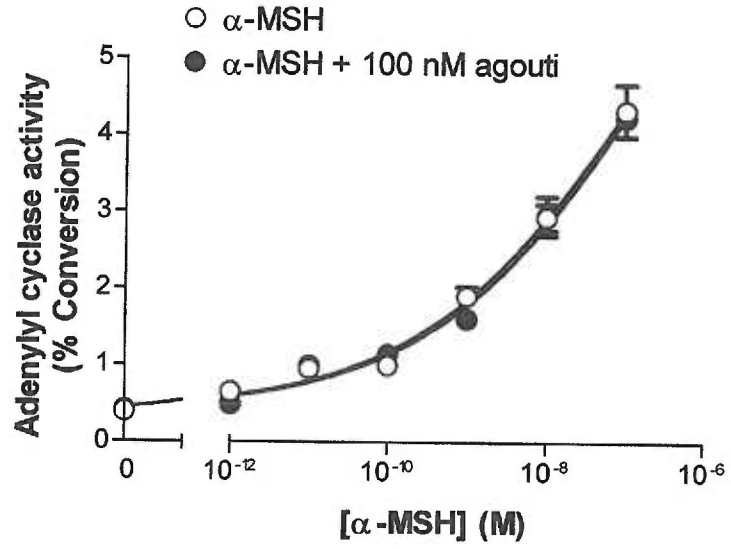

Figure 2.4c

Chapter 2 Appendix

As shown in chapter 2, the competition binding experiment with agouti peptide and the MC1-R was done using Cloudman M-3 cell lines and ^{125}I-ACTH$_{1-39}$, due to the availability of materials at that time. Later, the experiment was repeated using the heterogeneous 293 cell line stably transfected with the mMC1-R and ^{125}I-NDP-α-MSH, a superpotent analogue of α-MSH. The agouti peptide inhibited the binding of ^{125}I-NDP-α-MSH to the MC1-R with an IC_{50} of 0.8 x 10^{-10} M, while the control medium had no effect in inhibiting the ^{125}I-NDP-α-MSH binding (**Figure 2A .1**).

Since the agouti peptide used in chapter 2 was only 75% pure, the antagonist action of agouti on MC1 and MC4 receptors was questioned. One of the cysteine residues in agouti, cys107 was shown to be critical for agouti function (Perry et al., 1996). A transgenic mouse was made with a cys107ser mutation of the *agouti* cDNA expressed behind the β-actin promoter, and it showed no pigmentation or obesity phenotype compared to the control, which indicated that the cys107ser mutation impairs the function of normal agouti. Cys107 is one of the 10 conserved cysteines in agouti, and, by comparison with the ω-conotoxins and ω-agatoxins, is likely to play a critical role in stabilizing the tertiary structure of the protein through the formation of disulfide bonds (Olivera et al., 1994). Therefore, cys107 is likely to have the same effect in agouti peptide as those in ω-conotoxins and ω-agatoxins. This mutant served as a useful control for agouti peptide function. Both wild type and cys107ser agouti polypeptide were made by the baculovirus expression system and purified as described (Lu et al., 1994). In contrast to the wild type agouti peptide, the cys107ser agouti polypeptide showed no ability to compete with and ^{125}I–NDP-α-MSH for binding

melanocortin-1 receptor, probably due to the partially unfolded structure of the mutant polypeptide (Kesterson, R.A., and Cone, R.D., unpublished data). The data is shown in **Figure 2A.2**. This result further supported the argument that antagonism of MC1 and MC4 receptors was due to the specific action of agouti on each receptor.

Figure Legends

Figure 2A.1. Competition binding on MC1-R stably transfected 293 cells. a. Competition binding by cold NDP-α-MSH. B. Competition binding demonstrates that agouti peptide block the binding of ^{125}I-NDP-α-MSH to the MC1-R. The agouti peptide and the control medium are at the same protein concentration.

Figure 2A.2. Competition binding of the hMC1-R with wild type agouti peptide and cys107ser mutant. In contrast to the wild type agouti peptide, the cys107ser mutant of agouti can not block the binding of ^{125}I-NDP-α-MSH to the MC1-R.

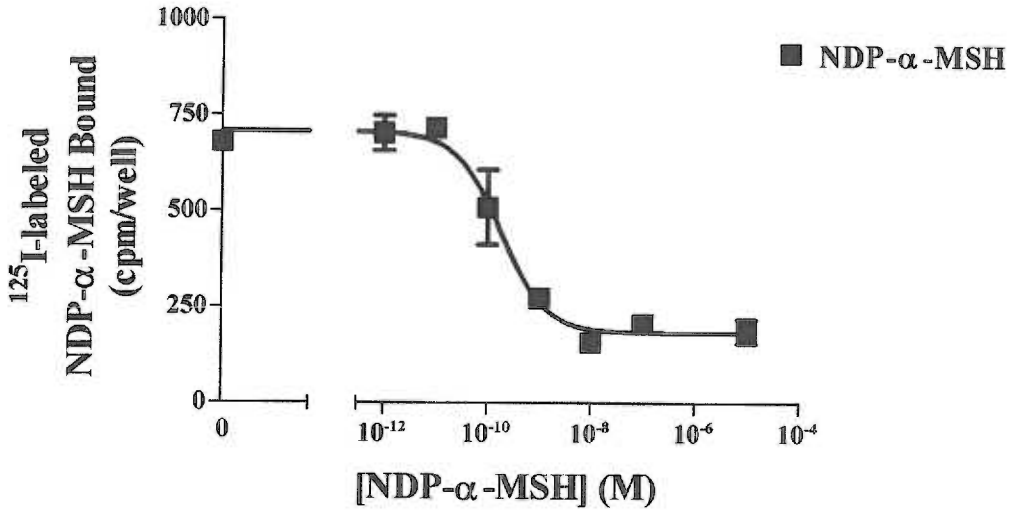

Figure 2A .1a

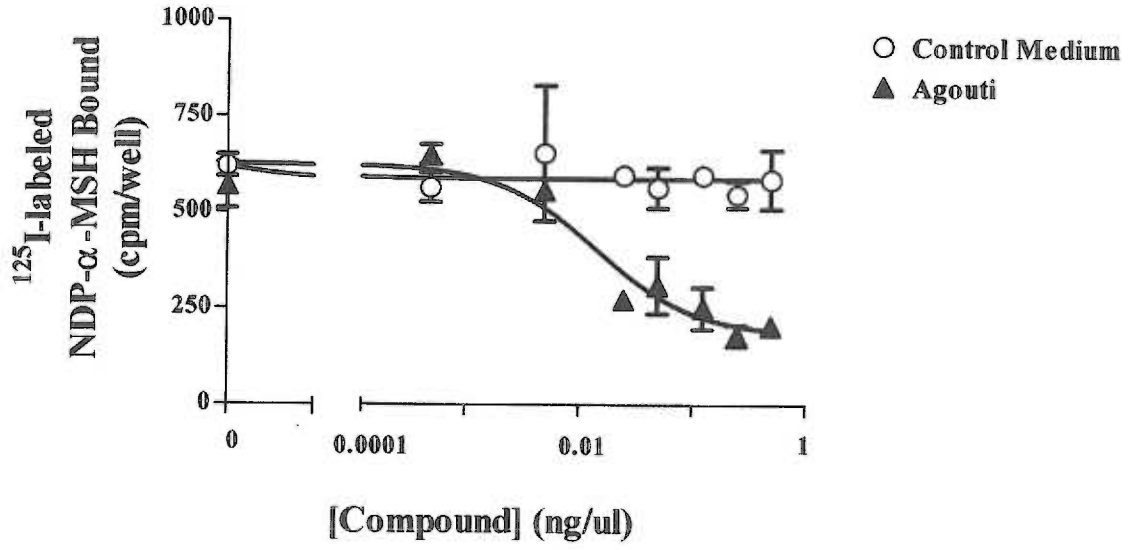

Figure 2A . 1b

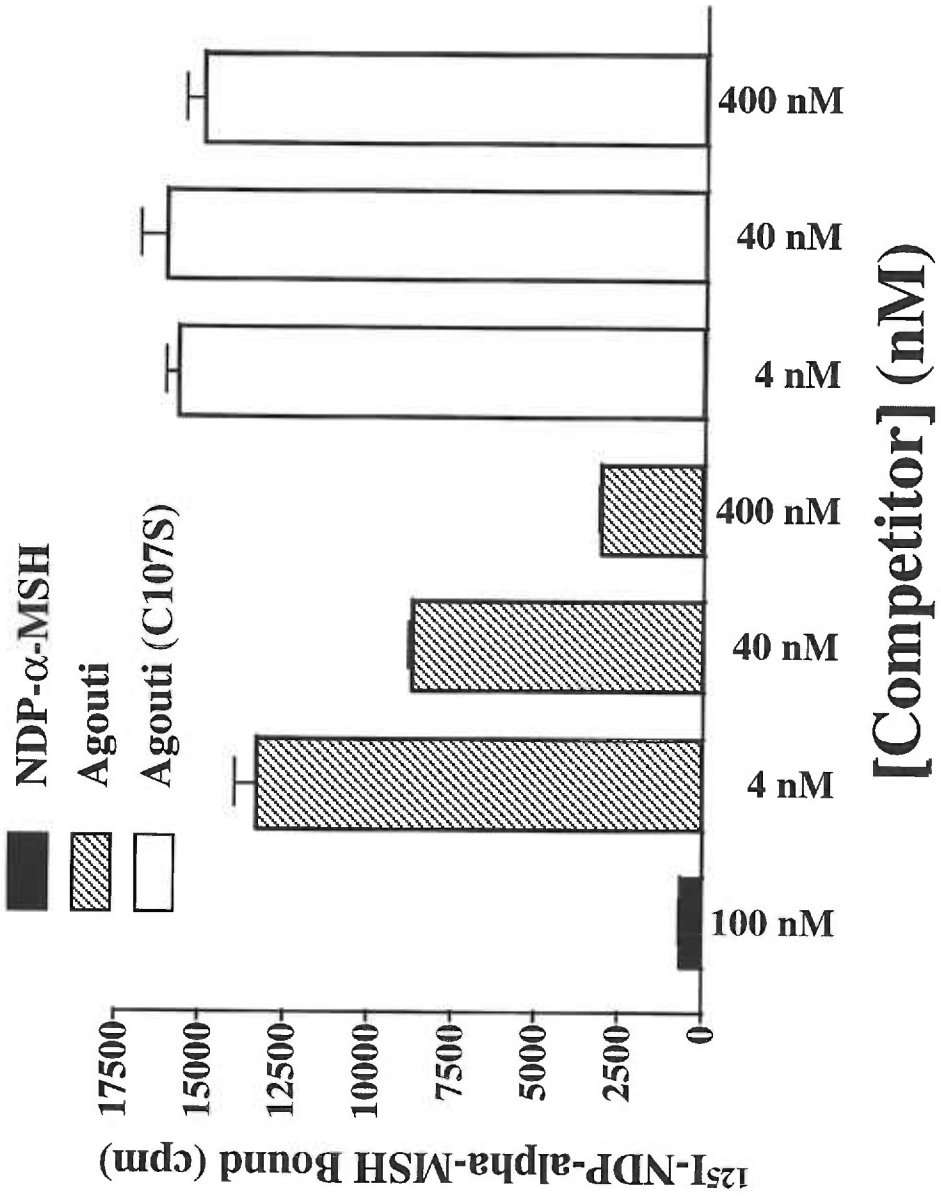
NDP-α-MSH
Agouti
Agouti (C107S)
125I-NDP-alpha-MSH Bound (cpm)
17500
15000
12500
10000
7500
5000
2500
0
100 nM
4 nM
40 nM
400 nM
4 nM
40 nM
400 nM
[Competitor] (nM)

Figure 2A.2

Chapter 3

Cyclic Lactam α-Melanotropin Analogues of Ac-Nle^4-cyclo[Asp^5,D-Phe^7,Lys^{10}] α-Melanocyte-Stimulating Hormone-(4-10)-NH_2 with Bulky Aromatic Amino Acids at Position 7 Show High Antagonist Potency and Selectivity at Specific Melanocortin Receptors

Victor J. Hruby,[*,!] Dongsi Lu,[@,&] Shubh D. Sharma,[!] Ana de L. Castrucci,[#] Robert A. Kesterson,[@] Fahad A. Al-Obeidi,[!] Mac E. Hadley,[#] and Roger D. Cone[*,@]

@ Vollum Institute for Advanced Biomedical Research, Oregon Health Sciences University L-474, Portland, Oregon 97201

& Department of Cell and Developmental Biology, Oregon Health Sciences University, L-474, Portland, Oregon 97201

! Department of Chemistry, University of Arizona, Tucson, Arizona 85721

 # Department of Cell Biology and Anatomy, University of Arizona, Tucson, Arizona 85721

* Authors to whom reprints should be addressed

Published in Journal of Medicinal Chemistry, 38, 3454-3461, 1995

Abstract

The cloning of the melanocyte-stimulating hormone (MSH) and adrenocorticotropic hormone (ACTH) receptors (MC1-R and MC2-R, respectively) recently has led to the identification of three additional melanocortin receptors, MC3-R, MC4-R, and MC5-R. The MC2 receptor primarily recognizes only ACTH peptides, but the other four receptors all recognize a-melanocyte-stimulating hormone (α-MSH) and potent α-MSH agonists such as [Nle^4,D-Phe^7]α-MSH-NH_2 and Ac-Nle^4-c[Asp^5,D-Phe^7,Lys^{10}]α-MSH-(4-10)-NH_2 as well as ACTH. The absence of any known physiological role for these new receptors, expressed both in the brain (MC3-R and MC4-R) and throughout a number of peripheral tissues (MC5-R), has necessitated a search for potent and receptor selective agonists and antagonists. We report here that analogues of the superpotent cyclic agonist analogue Ac-Nle^4-c[Asp^5,D-Phe^7,Lys^{10}]α-MSH-(4-10)-NH_2, in which a bulky aromatic amino acid is substituted in the 7-position, can produce potent and selective antagonists for melanocortin receptors. Thus, the D-*p*-iodophenylalanine 7-containing analogue Ac-Nle^4-c[Asp^5,D-Phe(pI)^7,Lys^{10}]α-MSH-(4-10)-NH_2 is a potent antagonist (pA_2 = 10.3) in the classical frog skin (*Rana pipiens*) assay (MC1-R), as is the D-2'-naphthylalanine^7 (D-Nal(2)^7)-containing analogue Ac-Nle^4-c[Asp^5,D-Phe^7,Lys^{10}]α-MSH-(4-10)-NH_2 ($pA_2 > 10.3$). Interestingly, the D-*p*-chloro- and D-*p*-fluorophenylalanine^7-containing analogues lacked antagonist activities at all melanotropin receptors, and both exhibited full agonist potency in the frog skin assay. The activity of these analogues also was examined at four mammalian melanocortin receptors. Interestingly, analogue Ac-Nle^4-c[Asp^5,(D-Nal(2)^7),Lys^{10}]

α-MSH-(4-10)-NH_2 was found to be a potent antagonist of the MC4-R (pA_2 = 9.3) with minimal agonist activity, a less potent antagonist of the MC3-R (pA_2 = 8.3) with minimal agonist activity, and a full agonist of the MC1 and MC5 receptors. Surprisingly, Nle^4-c[Asp^5,D-Phe(pI)^7,Lys^{10}]α-MSH-(4-10)-NH_2 was found to be a potent agonist at the cloned human MC1-R (EC_{50} = 0.055 nM) and mouse MC1-R (EC_{50} = 0.19 nM) but had potent antagonist activities at the human MC4-R (pA_2 = 9.7) and human MC3-R (pA_2 = 8.3) with significant partial agonist activities (EC_{50} = 0.57 and 0.68 nM, respectively) as well. Thus, highly potent and receptor selective antagonist analogues can arise from substitution of the D-Phe^7 residue with a bulky aromatic amino acid. These analogues can be used to help determine the functional roles of these receptors.

Introduction

While pharmacological methods have been traditionally used to define receptor subtypes, receptor-cloning experiments have often led to the discovery of novel receptor subtypes within many receptor families. Following the cloning of the melanocyte-stimulating hormone (MSH) and adrenocorticotropic hormone (ACTH) receptor genes (Chhajlani and Wikberg, 1992; Mountjoy et al., 1992), for example, three unique yet related genes were identified that also encoded functional, high-affinity receptors for the melanocortin (MSH/ACTH) peptides (Chhajlani et al., 1993; Gantz et al., 1993a; Gantz et al., 1993b; Roselli-Rehfuss et al., 1993; Barrett et al., 1994; Desarnaud et al., 1994; Gantz et al., 1994a; Griffon et al., 1994; Labbe et al., 1994; Mountjoy et al., 1994) . Labeled numerically in the order of their discovery, the melanocortin-3, melanocortin-4, and melanocortin-5 receptor genes have been demonstrated to be expressed primarily in the hypothalamus, midbrain, and brain stem (MC3-R and MC4-R) or in a wild distribution of peripheral tissues (MC5-R).

α-melanotropin (α-MSH, Ac-Ser-Tyr-Ser-Met-Glu-His-Phe-Arg-Trp-Gly-Lys-Pro-Val-NH_2) was among the first peptide hormone to be isolated and to have its structure determined. This hormone plays an important biological role in pigmentation (Hadley, 1988; Vaudry and Eberle, 1993)and numerous central nervous system (CNS)-related activities also have been proposed for this hormone (O. Donohue and Dorsa, 1982; Eberle, 1988; Hadley, 1988; Vaudry and Eberle, 1993). Extensive structure-activity relationships have established the central role of α-melanotropin in pigmentation in vertebrates, and super potent, enzymatically stable, super prolonged acting agonist analogues such as [Nle^4,D-

Phe^7,]α-MSH (Sawyer et al., 1980) and the cyclic lactam analogue Ac-Nle^4-c[Asp^5,(D-Nal(2)^7),Lys^{10}]α-MSH-(4-10)-NH_2 (Al-Obeidi et al., 1989; Al-Obeidi et al., 1989) have been developed and widely used in biological studies related to the role of α-melanotropin in pigmentation. The effects of α-MSH on pigmentation are mediated by the MC1-R expressed specifically on the surface of melanocytes. Similarly the MC2-R is involved in the regulation of adrenal steroidogenesis by ACTH. However, given the complexity of expression of the MC3, MC4, and MC5 receptors, it has not been possible to identify any simple correlation between these receptors and the reported biological activities of the melanocortin peptides. Consequently, potent and receptor specific agonists and especially antagonists would be extremely valuable tools for the determination of the physiological roles of the MC3, MC4, and MC5 receptors.

Though the extensive structure-activity relationships mentioned above have provided much information on agonist activity related to pigmentary effects (see, for example, refs. (O. Donohue and Dorsa, 1982; Hruby et al., 1984; Eberle, 1988; Hadley, 1988; Hruby et al., 1993; Vaudry and Eberle, 1993)), until recently there have been only a few reports (Al-Obeidi et al., 1989; Sawyer et al., 1989; al-Obeidi et al., 1990; Sawyer et al., 1990; Jayawickreme et al., 1994) on the development of α-MSH antagonists. We report here on the discovery of two highly potent and selective antagonists for certain amphibian MC1 receptors and for the mammalian neural MC3 and MC4 receptors.

Results

Design and Synthesis. The antagonists reported here are based on the super potent and super prolonged acting cyclic lactam-containing agonist

Ac-Nle^4-c[Asp^5,D-Phe^7,Lys^{10}]α-MSH-(4-10)-NH_2. Structure-activity and conformation-activity (Cody et al., 1988; Al-Obeidi et al., 1989; Al-Obeidi et al., 1989) studies have led us to propose a bioactive conformation for α-MSH at the classical pigment cell receptor (Nikiforovich et al., 1992; Sharma et al., 1993). These studies indicate that the side chain residues of His^6, Phe^7, Arg^8, and Trp^9 are critical for agonist activity. Using strategies we have previously suggested for peptide hormone and neurotransmitter antagonist development (Hruby, 1992), we have sought ways to disrupt the proposed bioactive conformation necessary for transduction while maintaining strong binding to the inactive form of the receptor. One of these approaches has involved modification of the critically important Phe^7 residue by a variety of bulky aromatic amino acid residues at this position. We report here that substitution of D-2'-naphthylalanine (D-Nal-(2)) and D-*p*-iodophenylalanine in position 7 of the potent cyclic agonist analogue Ac-Nle^4-c[Asp^5,D-Phe^7,Lys^{10}]α-MSH-(4-10)-NH_2 produced potent antagonist analogues at certain melanocortin receptors.

Synthesis of the peptide analogues **1-4** (**Table 3.1**) was accomplished by solid-phase methods of peptide chemistry similar to those previously reported for the synthesis of Ac-Nle^4-c[Asp^5,D-Phe^7,Lys^{10}]α-MSH-(4-10)-NH_2 using an automatic peptide synthesizer. Briefly, the synthesis was accomplished on a *p*-methylbenzhydrylamine resin using an N^{α}-Boc strategy and via cyclization of the macrocyclic lactam rings on the solid support using (benzotriazol-1-yloxy)tris(dimethylamino)phosphonium hexafluorophosphate (BOP) reagent in the presence of diisopropylethylamine as described previously (Al-Obeidi et al., 1989). The cyclic, partially protected peptide was deprotected and cleaved from the resin by treatment with HF-anisole for 45 min. at 0 °C (Al-Obeidi et al., 1989).

The resulting crude peptides were purified by reversed-phase HPLC and characterized by fast atom bombardment mass spectrometry and amino acid analysis. Purity was assessed by analytical RP-HPLC and thin layer chromotography (TLC) in three different solvent systems (see the Experimental Section for details).

Biological Assay Methods. The analogues were assayed for agonist and antagonist activity using the classical frog skin (*Rana pipiens*) (Shizume et al., 1954) and, in a few cases, the lizard skin (*Anolis carolinensis*) (Castrucci et al., 1989) bioassays. The analogues also were assayed for agonist and antagonist activities at cloned mammalian melanocortin receptors using a newly developed cAMP-dependent colorimetric β-galactosidase assay (Chen et al., 1995) (see the Experimental Section for details). This assay used colonel 293 cell lines expressing human MSH receptor (hMC1-R), human MC3 receptor, human MC4 receptor, and mouse MC5 receptor which were transfected with a CRE-β-galactosidase construct using a $CaPO_4$ method (Chen and Okayama, 1987) (see the Experimental Section for details). Antagonist p*A*2 values in all assays were determined using the method of Schild (Schild, 1947).

The results for the *R. pipiens*, human, and mouse MSH (MC1) receptors for the four D-Phe7-substituted analogues of Ac-Nle^4-c[Asp^5,D-Phe^7,Lys^{10}]α-MSH-(4-10)-NH_2, namely, the D-Phe(pF)^7, D-Phe(pCl)^7, D-Phe-(pI)^7, and D-Nal(2)^7 analogues **1-4**, respectively, are given in **Table 3.1**. The comparative results for the four mammalian melanocortin receptors are given in **Table 3.2**.

The analogue Ac-Nle^4-c[Asp^5,D-Phe(pI)^7,Lys^{10}]α-MSH-(4-10) (**3**; **Table 3.1**) has only minimal agonist activity in the frog skin (*R. pippins*) assay but, as shown in **Figure 3.1**, is a potent inhibitor of the biological response of α-MSH.

Evaluation of the dose-response displacement curves (**Figure 3.1**) showed that **3** was an exceptionally potent antagonist analogue (pA_2 = 10.3, **Table 3.1**) in this *in vitro* melanocortin 1 receptor assay. Interestingly, the analogue was a potent agonist (EC_{50} = 0.60 nM, data not shown) in the lizard (*A. carolinensis*) skin assay, a highly potent agonist at the human MC1-R (EC_{50} = 55 pM, **Table 3.1**), and a modestly potent agonist at the mouse MC1-R (EC_{50} = 0.19 nM, Table 1). The cyclic analogue Ac-Nle^4-c[Asp^5,D-Nal(2)^7,Lys^{10}]α-MSH-(4-10) (**4**) which has the bulky aromatic amino acid D-Nal(2) in position 7 also exhibited potent antagonist activity in the frog skin MC1-R assay ($pA_2 \geq 10.5$, Table 1). Interestingly, the D-*p*-fluorophenylalanine- and D-*p*-chlorophenylalanine-containing analogues **1** and **2** (**Table 3.1**) were both potent agonists at all melanocortin 1 receptors.

In the frog skin bioassay, it was noted that the antagonist activity of both **3** and **4** was prolonged in a dose-dependent manner. The antagonist effects of both analogues can be blocked by pretreating the frog skin with the potent prolonged acting agonist [Nle^4-D- Phe^7]α-MSH. Concentrations of the antagonists at 10^{-6}-10^{-7} M generally produced an irreversible antagonism in that, following removal of analogues from the assay medium, subsequent challenges with α-MSH failed to activate frog MC1 receptor for several hours after removal of the antagonists. The antagonism of frog skin MC1 receptor was specific for α-MSH since the skins would still maximally darken in response to theophylline (a phosphodiesterase inhibitor). These observations may prove of great importance if any of these antagonists were to prove to be of clinical /physiological usefulness.

A newly described cAMP-dependent colorimetric β-galactosidase assay (Chen et al., 1995) was used to determine the agonist and antagonist activities of the new cyclic lactam derivatives of α-MSH at cloned mammalian melanocortin receptors. This assay utilizes a β-galactosidase reporter gene fused to a cAMP-regulated promoter to detect changes in intracellular cAMP downstream of receptor activation and was useful in these studies since it has been shown that all the melanocortin receptors couple to the effector adenylyl cyclase (Chhajlani and Wikberg, 1992; Mountjoy et al., 1992; Chhajlani et al., 1993; Gantz et al., 1993a; Gantz et al., 1993b; Roselli-Rehfuss et al., 1993; Barrett et al., 1994; Desarnaud et al., 1994; Gantz et al., 1994a; Griffon et al., 1994; Labbe et al., 1994; Mountjoy et al., 1994).

Modification of D-phenylalanine^7 at the para position or substitution of the phenyl group with naphthyl group (compound **4**, **Table 3.1**) had little effect on agonist activity of the compounds at the human MSH receptor (hMC1-R) or mouse MC5 receptor (**Figure 3.2**). In contrast, replacement of the D-Phe^7 with D-Phe(pI)^7 dramatically reduced agonist activity at the MC3 and MC4 receptors (**Figure 3.2**). Both compounds are partial agonists with greatly increased EC_{50}s (**Table 3.2**). Interestingly, the D-Phe(pCl)^7-substituted analogue **2** was a full agonist and actually was more potent than [Nle^4-D-Phe^7]α-MSH at every receptor except the hMC3-R. The D-Phe(pF)^7-substituted analogue **1** likewise was a very potent full agonist in all assays (**Table 3.2, Figure 3.2**).

The two compounds acting as weak partial agonists at the MC3-R and MC4-R (analogues **3** and **4**) were then examined for antagonist activity at these receptors (**Figure 3.3**). As can be seen, the D-Nal(2)^7-substituted cyclic lactam analogue **4** is a potent antagonist of the MC3-R and MC4-R, with pA_2 values of

8.3 and 9.3, respectively (**Table 3.2**). Very little agonist activity is seen with these compounds at the hMC4-R. In contrast, the *p*-iodo-substituted compound **3** is also a potent antagonist but retains significant partial agonist activity, stimulating cAMP-dependent β-galactosidase activity to 50% of maximal levels at the hMC4-R and hMC3-R as well (**Figure 3.3**).

Competition binding experiments (see the Experimental Section for details) were performed to determine if iodination of the phenylalanine aromatic ring or replacement of the phenyl ring with a naphthyl ring has any effect on the affinity of the cyclic lactam compounds for the MC3 and MC4 receptors (**Figure 3.4**, **Table 3.3**). No significant alteration in IC_{50} values was observed relative to those calculated for [Nle^4,D-Phe^7]α-MSH.

Discussion

These exciting and intriguing results provide new insights into antagonist structure-activity relationships for melanocortin receptors and point to different requirement for antagonist activity at different pigmentary receptors in different species and at different melanocortin receptors in the same species. In previous studies from our laboratory, we demonstrated that Ac-[D-Trp^7,D-Phe^{10}]α-MSH-(7-10)-NH_2 was a very weak antagonist in both the frog skin and lizard shin melanocortin receptor assays (pA_2 = 4.8 and 5.7, respectively), and other closed related analogues were either weak agonists or weak antagonists but only at one of the two receptors (Sawyer et al., 1989; Sawyer et al., 1990). In another study, the linear 4-10 α-MSH analogue Ac-Nle-Asp-Trp-D-Phe-Nle-Trp-Lys-NH_2 was found (al-Obeidi et al., 1990) to be an antagonist in the frog skin assay (pA_2 = 8.4) but was active in the lizard skin assay only as an agonist. Interestingly, the

corresponding cyclic lactam analogue of the above linear peptide Ac-Nle^4-c[Asp^5,Trp^6,D-Phe^7,Nle^8,Lys^{10}]α-MSH-(4-10)-NH_2, was a weak agonist in the frog skin assay (EC_{50} = 0.1 μM) (al-Obeidi et al., 1990). Very recently Jayawickreme et al. (Jayawickreme et al., 1994) reported the discovery of other α-MSH antagonists for the *Xenopus laevis* MC1 receptor using a library approach and an assay using cultured *X. Laevis* melanophores and cAMP accumulation as the bioassay. Several antagonists with IC_{50} values in the range of 5 μM-11 nM were obtained. Apparently no effort was made to assess partial agonist/antagonist activity in this assay. The nonapeptide H-Met-Pro-D-Phe-Arg-D-Trp-Phe-Lys-Pro-Val-NH_2 was the most potent inhibitor (IC_{50} = 11 nM), which would correspond to a pA_2 value of ca. 8 if the assay conditions represent an equilibrium. At this time it is difficult to make any general statements about what substitutions in α-MSH will lead to antagonist activities of the MSH receptors. Indeed it is extremely intriguing and quite unusual to our knowledge that an analogue of a native hormone such as **3** and **4** would be such a potent antagonist at one physiological receptor in one species (in this case the frog) but a potent agonist in other species (the human and mouse MC1 receptors) (**Table 3.1**). However, this should provide a very useful insight for the future. Obtaining the structure of the α-MSH receptor (MC1-R) for the frog and lizard should provide key insights into structural requirements for agonist vs antagonist activity in these receptors and greatly aid in the development of a potent antagonist for the human MC1 receptor.

Equally intriguing are the antagonist activities for the new analogues at the human MC3 and human MC4 receptors. The potent and reasonably selective antagonist potencies for the D-Nal (2)^7 analogue **4** (**Figure 3.3**, **Table 3.2**) and

the partial agonist, yet potent antagonist, properties for the D-Phe(pI)^7 analogue **3** at the hMC4 receptor and the hMC3 receptor, respectively, should prove to be very useful for further design. Though it is not possible with the presently limited group of analogues to provide a model for a particular approach to antagonist design or receptor selectivity, this work suggests that large stereoelectronic steric modifications in the message sequence (His-Phe-Arg-Trp) of a melanotropin can provide potent antagonist analogues for the MC3 and MC4 receptors.

As this manuscript was being written, Adan et al. (Adan et al., 1994) reported on the antagonist properties for certain linear ACTH-(4-10) analogues using rat MC3, human MC4, and ovine MC5 receptors transfected in HEK 293 cells. The analogues had modifications in the 6-10 positions of ACTH-(4-10). pA_2 values of <6-8.6 were reported, with the analogue H-Met-Glu-His-Phe-Pro-Gly-Pro-OH ([Pro^{8,10},Gly^9]ACTH-(4-10)) being the most potent, with its most potent antagonist activity at the MC4 receptor (pA_2 = 8.6) (Adan et al., 1994). Interestingly, the L-*p*-iodophenylalanine-containing linear analogue H-Met-Glu-His-Phe(pI)-Arg-Trp-Gly-OH was reported to have good antagonist activity (pA_2 = 7.4-8.4) at all three melanocortin receptors investigated. No activities at melanocortin 1 receptors were reported.

In summary, the results presented here demonstrate that modifications of the phenyl ring of the D-Phe^7 residue of a cyclic lactam derivative of α-MSH-(4-10) that retain aromatic character can result in melanocortin receptor antagonists with high potency and specificity. The *in vivo* stability and efficacy of the patent cyclic lactam derivative Ac-Nle^4-c[Asp^5,D-Phe^7,Lys^{10}]α-MSH-(4-10)-NH_2 in the introduction of pigmentation (Al-Obeidi et al., 1989; Al-Obeidi et al., 1989; Johnson et al., 1994) suggest that these antagonists may be very useful for

probing the proposed physiological functions of the MC3 and MC4 receptors (Chhajlani and Wikberg, 1992; Labbe et al., 1994; Low, 1994). We do not yet understand why the modifications tested antagonize the mammalian MC3 and MC4 receptors while retaining full agonist activity at the mammalian MC1 and MC5 receptors. Nor do we understand why they antagonize the frog MC1-R while having full agonist activity at the mammalian MC1-R. Nonetheless, the results reported here suggest that it should be possible to obtain potent and highly selective ligands for different melanocortin receptor types as well as for the subtypes of the same receptor that apparently are found in different species. In addition, analogue **3** can be obtained in its radioiodinated form by a technique reported earlier by us (Sharma et al., 1991), and this could serve as a useful tool in various biological studies. Though an interesting beginning has been made, much more exploration of structure-activity and conformation-activity relationships is needed to develop predictive insights into the differential requirements for the various melanocortin receptors.

Materials and Methods

General Methods for Peptide Synthesis and Purification.

All peptides were synthesized by the solid-phase method of peptide synthesis using procedures similar to those used for the synthesis of Ac-Nle^4-c[Asp^5,D-Phe^7,Lys^{10}]α-MSH-(4-10)-NH_2 and related analogues. (Al-Obeidi et al., 1989) p-Methylbenzhydrylamine (pM-BHA) resin (0.35 mmol/g) was used as the solid support using an N^{α}-BOC protection strategy and an orthogonal side chain protection strategy (Al-Obeidi et al., 1989; Hruby et al., 1990) that allowed cyclization of the macro-cyclic lactam rings on the solid support. N^{α}-BOC-

protected amino acids were purchased from Bachem Inc. (Torrance, CA) or prepared by standard literature procedures. The reactive side chain groups were protected as follows: Lys with Fmoc, Asp with OFm, His with (benzyloxy)methyl (BOM), Arg with tosyl, and Trp with formyl. All reagent and solvents were ACS grade or better and used without further purification except as noted. Following assembly on the solid support as described below, the peptides were cleaved from the resin with anhydrous HF (10 mL/g of resin) in the presence of 10% anisole at rapidly by vacuum distillation and the resin filtered off and washed with ether (2 x 25 mL). The crude peptide was dissolved into glacial acetic acid (2 x 30 mL) and 30% aqueous acetic acid fractions were lyophilized, and the crude peptide was purified by reversed-phase preparative HPLC (RP-HPLC) on a C18-bonded silica gel column (Vaydac 218TP 1010, 1.0 x 25 cm) eluted with a linear acetonitrile gradient (20-40%) with a constant concentration of 0.1% aqueous trifluoroacetic acid. The separation was monitored at 280 nm with a UV absorbance detector. The fractions corresponding to the desired analogue were collected, and the combined fractions were lyophilized to give the final product as a white powder. The purity of the final products was checked by thin layer chromatography in at least three solvent systems and by RP-HPLC in two different gradient systems with UV monitoring at 280 and 223 nm (see **Table 3.4** for details of the solvent systems and gradient systems used). The structure of the pure peptides were confirmed by fast atom bombardment (FAB) mass spectrometry (**Table 3.4**) and amino acid analyses which were consistent with the expected values in all cases. Optical rotations were taken (**Table 3.4**). Amino acid analyses were performed on a 42017 ABI amino acid analyzer following hydrolysis at 160 °C in propionic acid which destroys tryptophan. The unusual

amino acids were not determined by the Biotechnology Facility (University of Arizona)due to its policy and excessive costs. α-MSH was purchased from Bachem.

Ac-[Nle^4,D-Phe^7]α-MSH. The title compound was synthesized by standard solid-phase methods, purified by methods previously reported, and identical in all respects with the compound previously synthesized (Sawyer et al., 1980).

Ac-Nle^4-c[Asp^5,D-Phe(pF)^7,Lys^{10}]α-MSH-(4-10)-NH$_2$ (1, SHU9128). The title compound was prepared using methods similar to those previously reported for cyclic lactam analogues of α-MSH-(4-10) (Al-Obeidi et al., 1989; Al-Obeidi et al., 1989) with cyclization on the solid support. The protected peptide resin to the title compound was prepared from 1.5 g of pMBHA resin (0.35 mmol of NH_2/g of resin) by first coupling N^{α}-BOC-Lys(N^{ε}-FMOC) to the resin. The following amino acids were than added to the growing peptide chain by stepwise addition of N^{α}-BOC-Trp (N^{i}-For), N^{α}-BOC-Arg(N^{G}-Tos), N^{α}-BOC-D-Phe(pF), N^{α}-BOC-His(N^{π}-BOM), N^{α}-BOC-Asp(β-OFm), and N^{α}-BOC-Nle using standard solid phase methods. Each coupling reaction was achieved using a 3-fold excess of DIC and a 2.4-fold excess of HOBt after coupling the last amino acid. The N^{ε}-FMOC and β-OFm protecting groups were removed by treating the N^{α}-BOC-protected peptide resin with 20% piperidine in NMP for 30 min. The peptide resin was washed with DMF (3 x 40 mL), dichloromethane (DCM) (3 x 40 mL), and 10% diisopropylethylamine (DIEA) (3 x 40 mL) and them suspended in 15 mL of NMP and mixed with 6-fold excess of BOP reagent in the present of a 8-fold excess of DIEA for 2 h. The coupling was repeated twice if needed until the resin gave a negative ninhydrin test (Kaiser et al., 1970). Then the N^{α}-BOC

protecting group was removed in the usual manner with 50% TFA in DCM. The amino group was neutralized with 10% DIEA in DCM and acetylated with 25% acetic anhydride in DCM for 20 min. The peptide resin was cleaved in 15 mL of anhydrous HF as outlined above. The HF-anisole and dithioethane were removed rapidly by vacuum distillation at 4 °C. The residue was washed with ethyl ether (2 x 25 mL) and the cleaved peptide dissolved in acetic acid (2 x25 mL) and 30% aqueous acetic acid (2 x 30 mL). The pooled acetic acid and aqueous phase fractions were lypophilized to give a white powder that was purified by preparative HPLC on a C18-bonded silica gel column (Vydac 218TP 1010, 1.0 x 25 cm) eluted with a linear gradient of acetonitrile (20-40%) in aqueous 0.1% trifluoroacetic acid (v/v). The purification was monitored at 280 nm, and the fractions corresponding to the major peak were collected, combined, and lyophilized to give the title compound **1** as a pure (>98%) whit powder. Analytical data are given in **Table 3.4**.

Ac-Nle^4-c[Asp^5,D-Phe(pCl)^7,Lys^{10}]α-MSH-(4-10)-NH$_2$ (2, SHU9203). The title compound was prepared in a manner very similar to that reported above for analogue **1** except that Na-BOC-D-Phe-(pCl) was added to the growing peptide chain in the appropriate sequence. The compound was purified as before for **1** to give **2** as a white powder. Analytical data are given in **Table 3.4**.

Ac-Nle^4-c[Asp^5,D-Phe(pI)^7,Lys^{10}]α-MSH-(4-10)-NH$_2$ (3, SHU8914). The title compound was prepared in a manner very similar to that reported above for analogue **1** except that Na-BOC-D-Phe-(pI) was added to the growing peptide chain in the appropriate sequence. The compound was purified as before for **1** to give **3** as a white powder. Analytical data are given in **Table 3.4**.

Ac-Nle^4-c[Asp^5,D-Nal(2)^7,Lys^{10}]α-MSH-(4-10)-NH$_2$ (4, SHU9119). The title compound was prepared in a manner very similar to that reported above for analogue **1** except that N$^{\alpha}$-BOC-D-Nal(2) was added to the growing peptide chain in the appropriate sequence. The compound was purified as before for **1** to give **4** as a white powder. Analytical data are given in **Table 3.4**.

General Biological Methods. All products for cell culture were purchased from Gibco-BRL (Grand Island, NY). $CaCl_2$, NaCl, and Na_2HPO_4 were purchased from Mallinckrodt Chemical (Paris, KN). Triton X-100, *o*-nitrophenyl-β-D-galactopyranoside (ONPG), isobutylmethylxanthine, an bovine serum albumin (BSA) were purchased from Sigma (St. Louis, MO). G250 protein reagent concentrate and 2-mercaptoethanol were purchased from Bio-Rad (Hercules, CA). β-Galactosidase activity was measured and normalized by protein concentration in each well of a 96-well plate. The 96-well plate spectrophotometer used to monitor β-galactosidase activity at 405 nm and protein concentration at 595 nm was from Molecular Devices (Sunnyvale, CA).

Bioassays. Bioassays using frog (*R. Pipiens*) and lizard (*A. carolinensis*) skins were performed by published procedures (Shizume et al., 1954; Huntington and Hadley, 1974; Castrucci et al., 1984). In these bioassays, skins become dark as a result of melanin granule dispersion within melanocytes in response to a melanotropin. This darkening response can be conveniently monitored by photo reflectance methods. The potency of each peptide was determined from log dose-response curves comparing the melanotropic activity of the analogues with that of the native hormone, α-MSH. Competitive antagonist activity was measured by constructing a dose-response curve corresponds to antagonism. The inhibition potency (pA_2 values) was determined by the method of Schild (Schild, 1947).

β-galactosidase Activity Assay. Clonal 293 cell lines expressing the human MSH receptor (hMC1-R), human MC3 receptor, human MC4 receptor, and mouse MC5 receptor were transfected with a pCRE/β-galactosidase construct using a $CaPO_4$ method (Chen and Okayama, 1987); 4 μg of pCRE/β-gal DNA was used for transfection of a 10 cm dish of cells. On 15-24 h posttransfection, cells were split into 96-well plates with 20,000-30,000 cells/well and incubated at 37 °C in a 5% CO_2 incubator until 48 h posttransfection. Cells were then stimulated with different α-MSH analogues diluted in stimulation medium (Dulbecco's modified Eagle's medium containing 0.1 mg/ml bovine serum albumin and 0.1 mM isobutylmethylxanthine) for 6 h at 37 °C in a 5% CO_2 incubator. Agonist activity was measured by stimulating cells with varying concentrations of α-MSH, Ac-[Nle^4,D-Phe^7]α-MSH, and cyclic analogues **1-4** (table 1). Antagonist activity was measured by stimulating MC3 and MC4 receptor cell lines with varying concentrations of α-MSH or α-MSH plus varying concentrations of the compound **3** or **4**. After stimulation, cells were lysed in 50 μl of lysis buffer (250 mM Tris-HCl, pH 8.0, 0.1% Triton X-100), frozen, thawed, and then assayed for β-galactosidase activity as described (Chen et al., 1995). Data represent means and standard deviations from triplicate data points, and curves were fitted by nonlinear regression using GraphPad Prism software. Antagonist pA_2 values were determined using the method of Schild (Schild, 1947).

Competition Binding Assay. Cell lines expressing the hMC3-R or hMC4-R were plated at 1 x 10^6 cells/well in 24-well plates. Prewarmed PBS-BSA solution (1 mg/ml BSA in PBS solution) containing 3.1 x 10^{-10} ^{125}I-labeled [Nle^4,D-Phe^7]α-MSH (100,000 cpm) and different concentrations of Ac-[Nle^4,D-Phe^7]α-

MSH-NH_2, Ac-Nle^4-c[Asp^5,D-$Nal(2)^7$,Lys^{10}]α-MSH-(4-10)-NH_2, or Ac-Nle^4-c[Asp^5,D-$Phe(pI)^7$,Lys^{10}]α-MSH-(4-10)-NH_2 was added to each well. Cells were incubated for 30 min. at 37 °C in a 5% CO_2 incubator, washed twice with PBS-BSA at 37 °C, lysed with 500 µl of 0.5 N NaOH, and counted with a γ-counter. Nonspecific binding, determined as the amount of radioactivity bound at 5 x 10^{-6} M cold [Nle^4,D-Phe^7]α-MSH, was 3-5% of the total counts bound. Data represent means and standard deviations from duplicate data points and were analyzed using GraphPad Prism software.

Acknowledgment. This research was supported by grants from the U.S. Public Health Service: DK 17420(V.J.H.) and DK 44239 and HD 30236 (R.D.C.). we thank Carrie Haskell-Luevano for many helpful discussions.

Figure Legends.

Figure 3.1. Demonstration that Ac-Nle^4-c[Asp^5,D-Phe(pI)^7,Lys^{10}]α-MSH-(4-10)-NH_2 (**3, SHU8914**) is a potent antagonist of α-MSH in the frog skin MC1 receptor assay system. Antagonism of the dose-response curve of α-MSH by 10^{-9} (Δ), 10^{-8} (▲) and 10^{-7} (□) M antagonist **3** is demonstrated by the rightward shift of the dose-response curve of α-MSH.

Figure 3.2. Effect of D-Phe^7 modifications and substitution on the agonist activity of Ac-Nle^4-c[Asp^5,D-Phe^7,Lys^{10}]α-MSH-(4-10)-NH_2. Cell lines expressing the human MC1, human MC3 , human MC4, and mouse MC5 receptors were incubated with varying concentrations of each of the analogues shown. Agonist activity was determined as a function of cAMP-dependent β-galactosidase activity. NDP-α-MSH is [Nle^4,D-Phe^7]α-MSH-NH_2. Analogue 1 (SHU9128), Ac-Nle^4-c[Asp^5,D-Phe(pF)^7,Lys^{10}]α-MSH-(4-10)-NH_2; Analogue 2 (SHU9203), Ac-Nle^4-c[Asp^5,D-Phe(pCl)^7,Lys^{10}]α-MSH-(4-10)-NH_2 ; Analogue 3 (SHU8914), Ac-Nle^4-c[Asp^5,D-Phe(pI)^7,Lys^{10}]α-MSH-(4-10)-NH_2 ; Analogue 4 (SHU9119), Ac-Nle^4-c[Asp^5,D-Nal(2)^7,Lys^{10}]α-MSH-(4-10)-NH_2. **3.2a**, hMC1-R; **3.2b**, hMC3-R; **3.2c**, hMC4-R; **3.2d**, mMC5-R.

Figure 3.3. Dose-response curves for antagonism of the MC3 and MC4 receptors by of Ac-Nle^4-c[Asp^5,D-Nal(2)^7,Lys^{10}]α-MSH-(4-10)-NH_2 (**4**, SHU9119) and Ac-Nle^4-c[Asp^5,D-Phe(pI)^7,Lys^{10}]α-MSH-(4-10)-NH_2 (**3**, SHU8914). Cells

expressing the MC3 and MC4 receptors were stimulated with varying concentrations of α-MSH from 0 to 10^{-6} M as indicated on the χ axis, with or without the analogues indicated. Agonist activity was determined as a function of cAMP-dependent β-galactosidase activity. **3.3a**, SHU9119 on hMC4-R; **3.3b**, SHU8914 on hMC4-R; **3.3c**, SHU9119 on hMC3-R; **3.3d**, SHU8914 on hMC3-R.

Figure 3.4. Competition of ^{125}I-labeled Ac-[Nle^4,D-Phe^7]α-MSH binding to the MC3 and MC4 receptors by Ac-Nle^4-c[Asp^5,D-Nal(2)^7,Lys^{10}]α-MSH-(4-10)-NH_2 (**4**, SHU9119) and Ac-Nle^4-c[Asp^5,D-Phe(pI)^7,Lys^{10}]α-MSH-(4-10)-NH_2 (**3**, SHU8914). Cell lines expressing the MC3 and MC4 receptors were coincubated with ^{125}I-labeled Ac-[Nle^4,D-Phe^7]α-MSH and varying concentrations of the analogues shown. Data indicate specific binding following the subtraction of nonspecific from total counts bound. NDP-α-MSH is [Nle^4,D-Phe^7]α-MSH-NH_2. **3.4a**, hMC3-R; **3.4b**, hMC4-R.

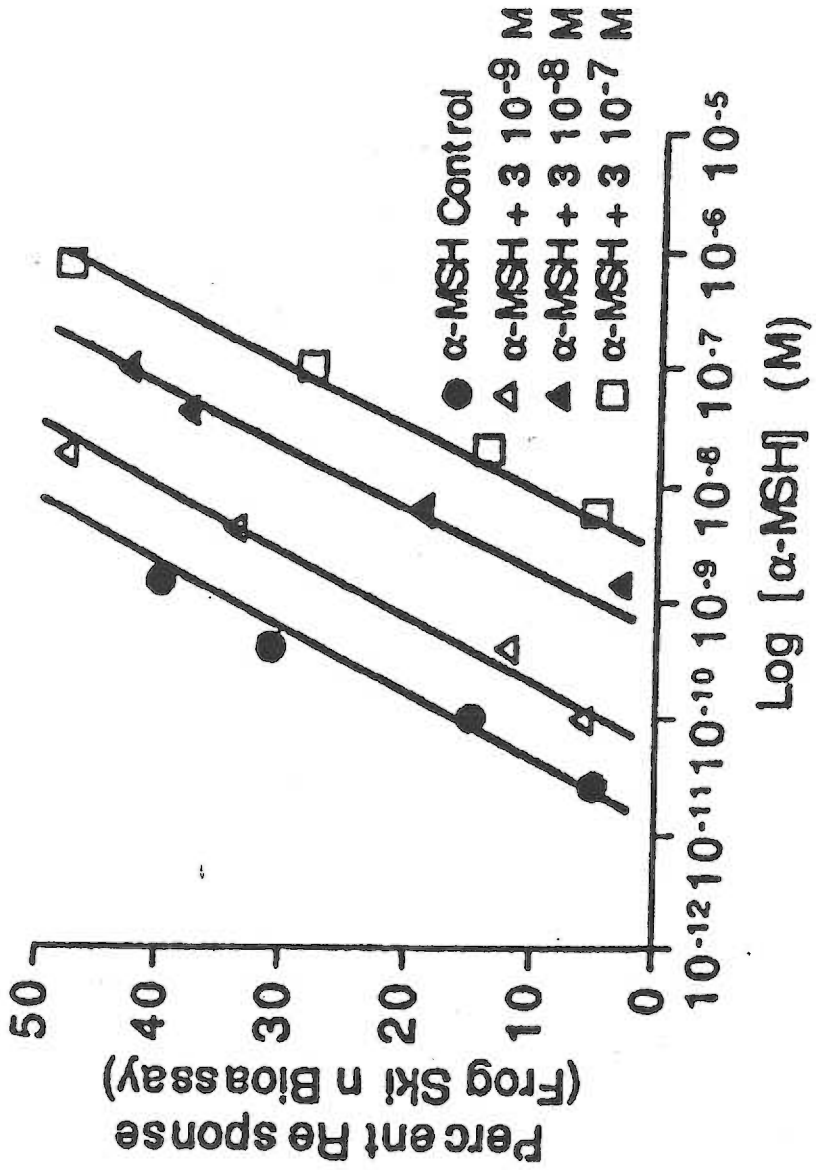
Percent Response
(Frog Skin Bioassay)
50
40
30
20
10
0
10-12 10-11 10-10 10-9 10-8 10-7 10-6 10-5
Log [α-MSH] (M)
α-MSH Control
α-MSH + 3 10-9 M
α-MSH + 3 10-8 M
α-MSH + 3 10-7 M

Figure 3.1.

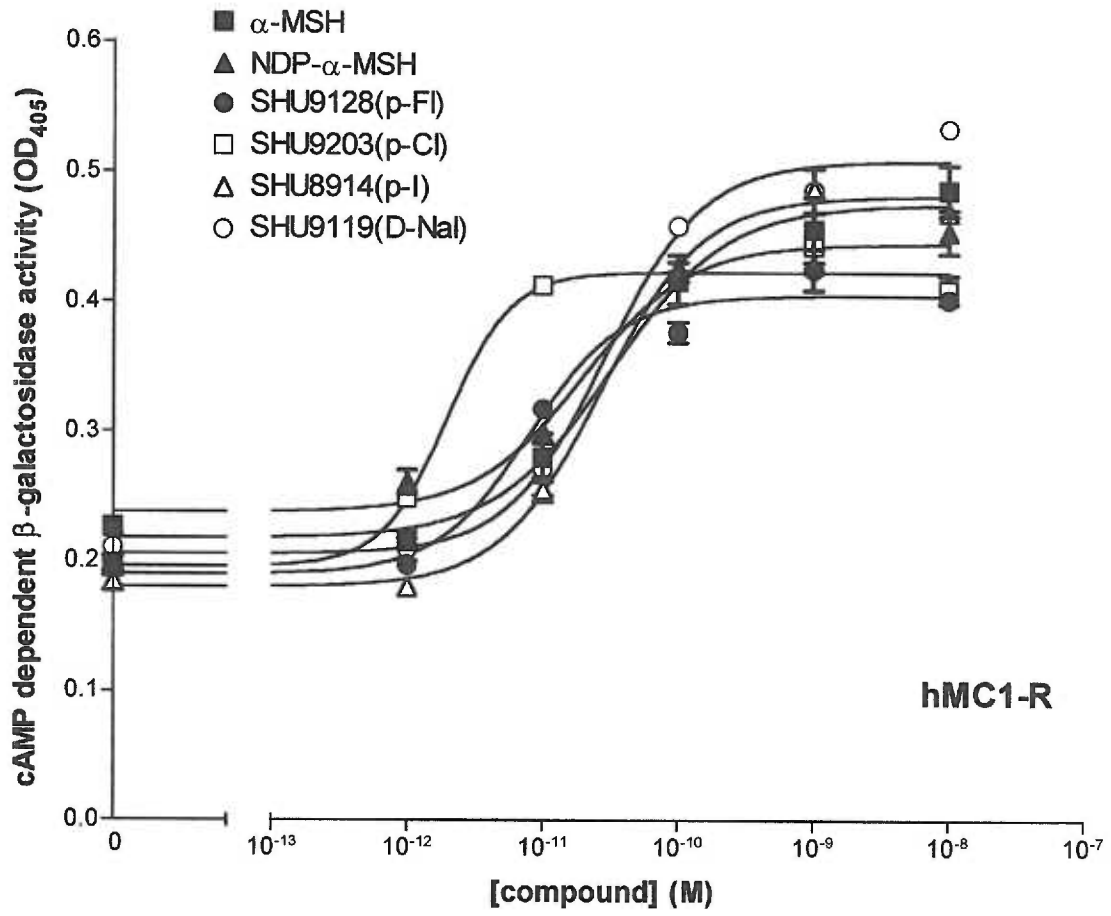

Figure 3.2a (hMC1-R)

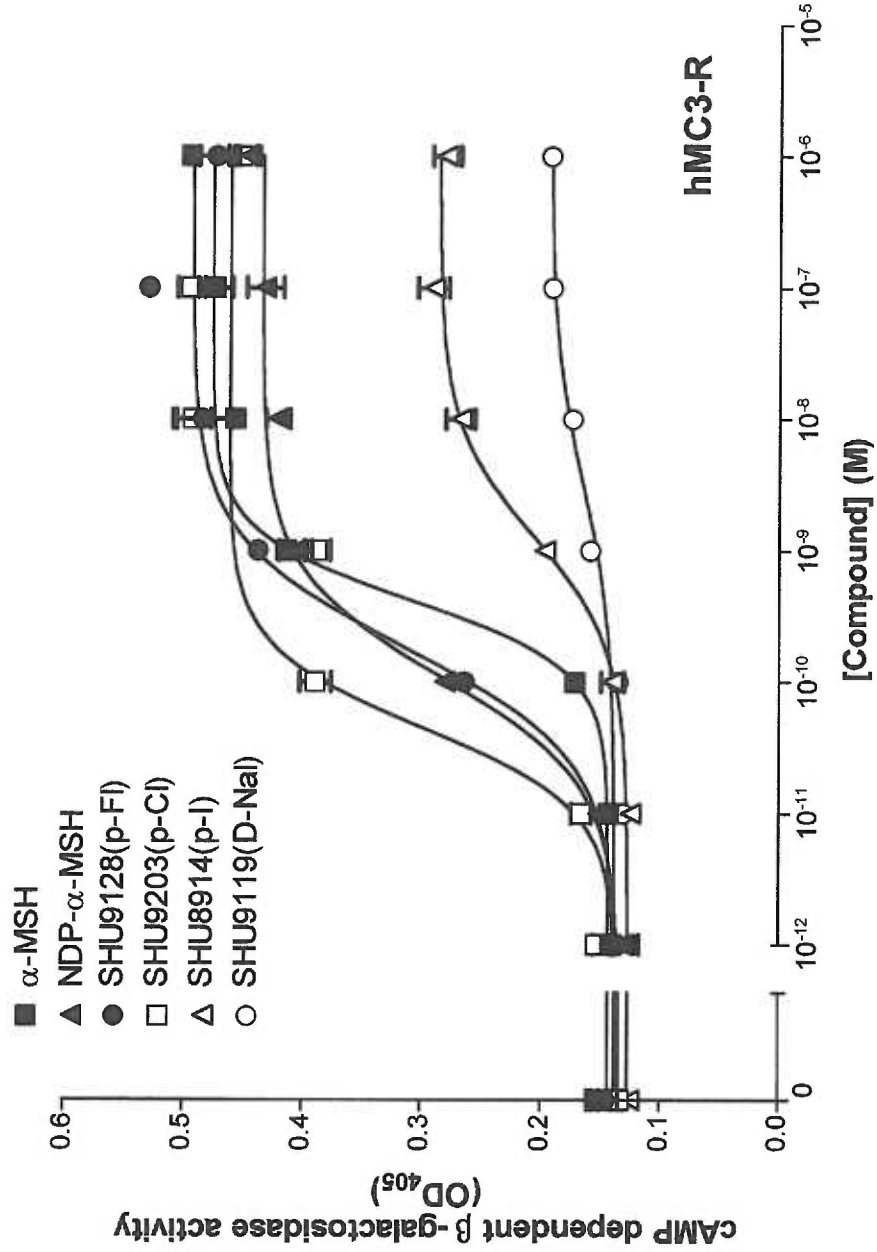

Figure 3.2b (hMC3-R)

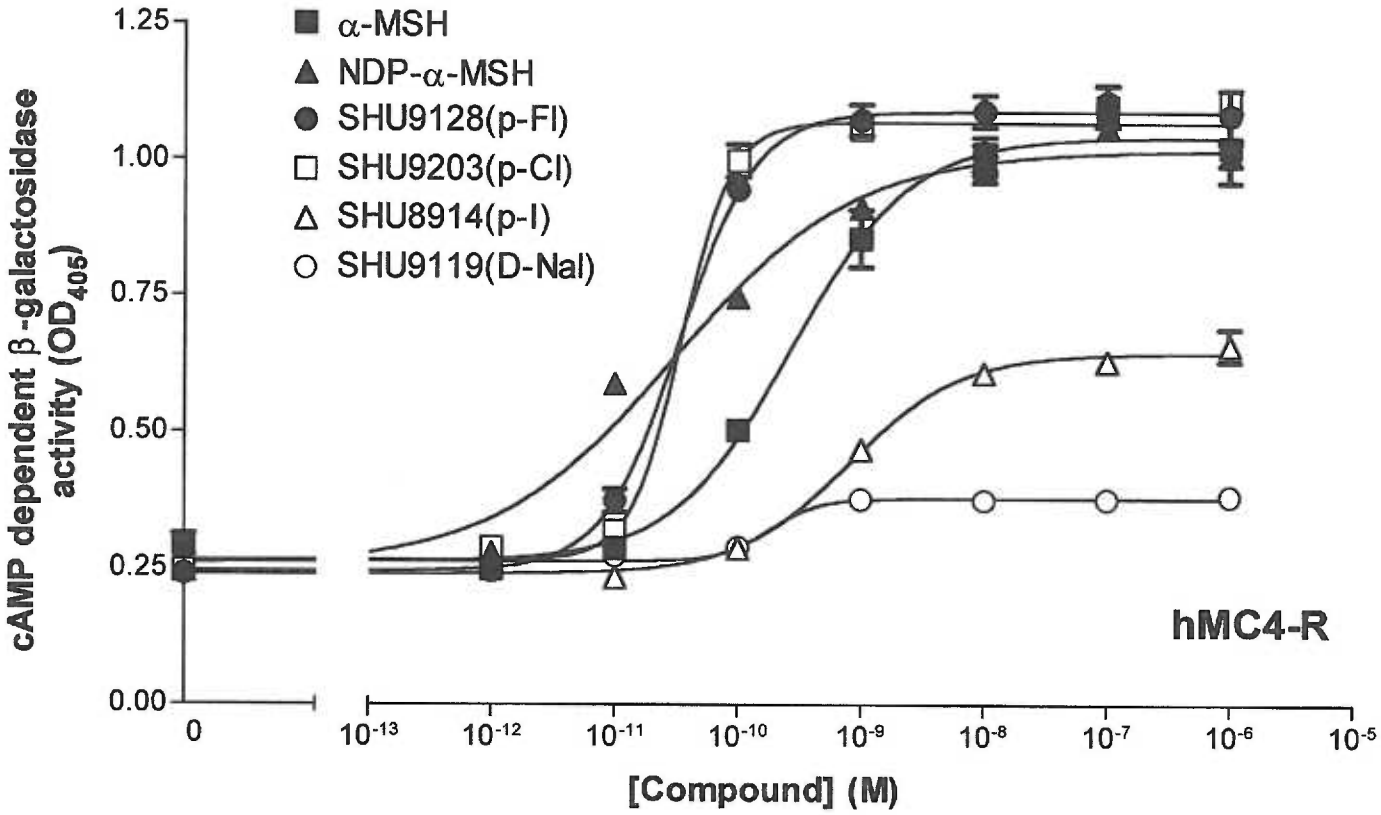

Figure 3.2c (hMC4-R)

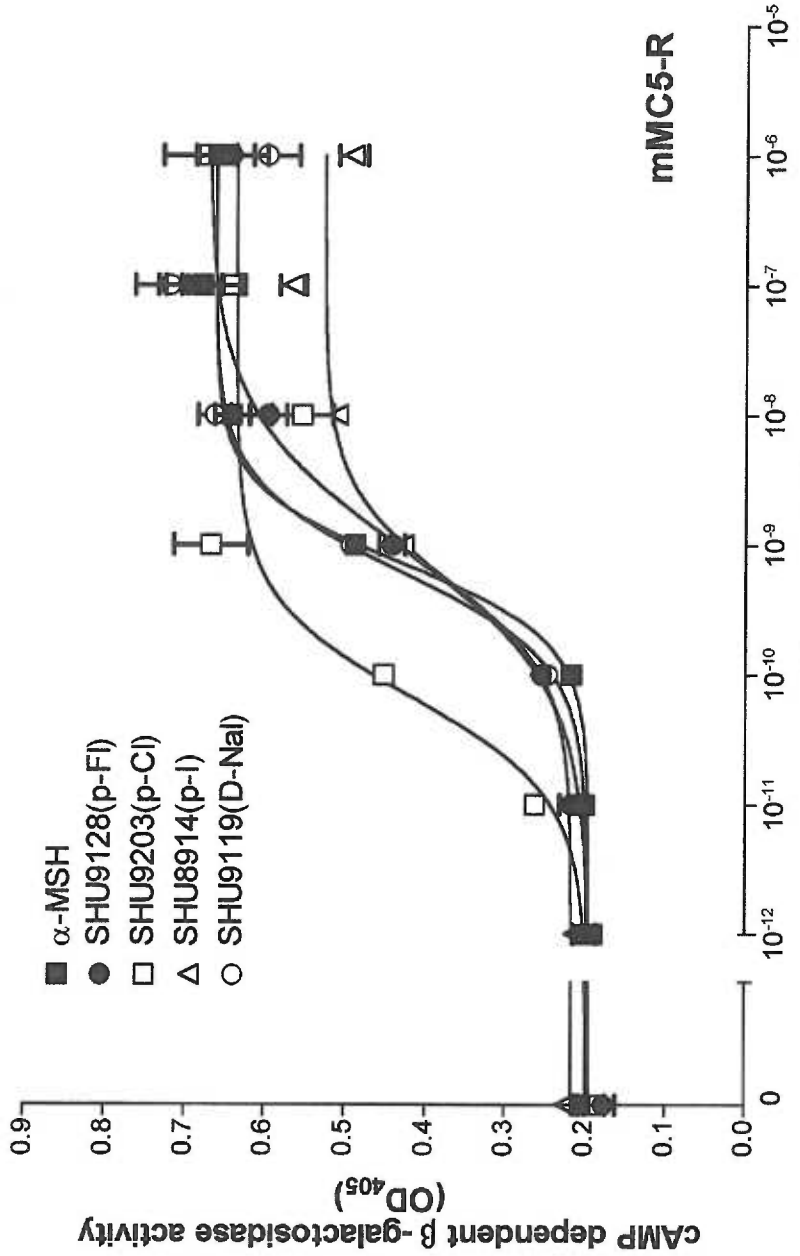

Figure 3.2d (mMC5-R)

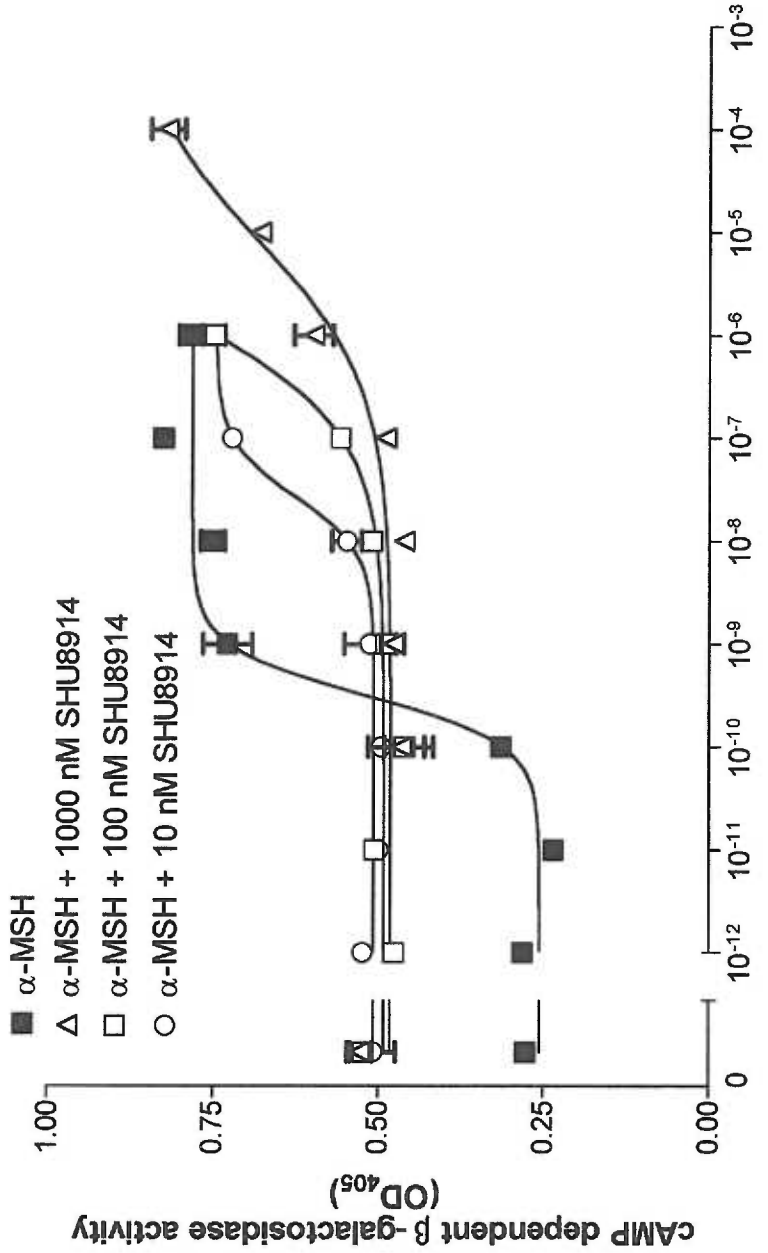

Figure 3.3b (hMC4-R)

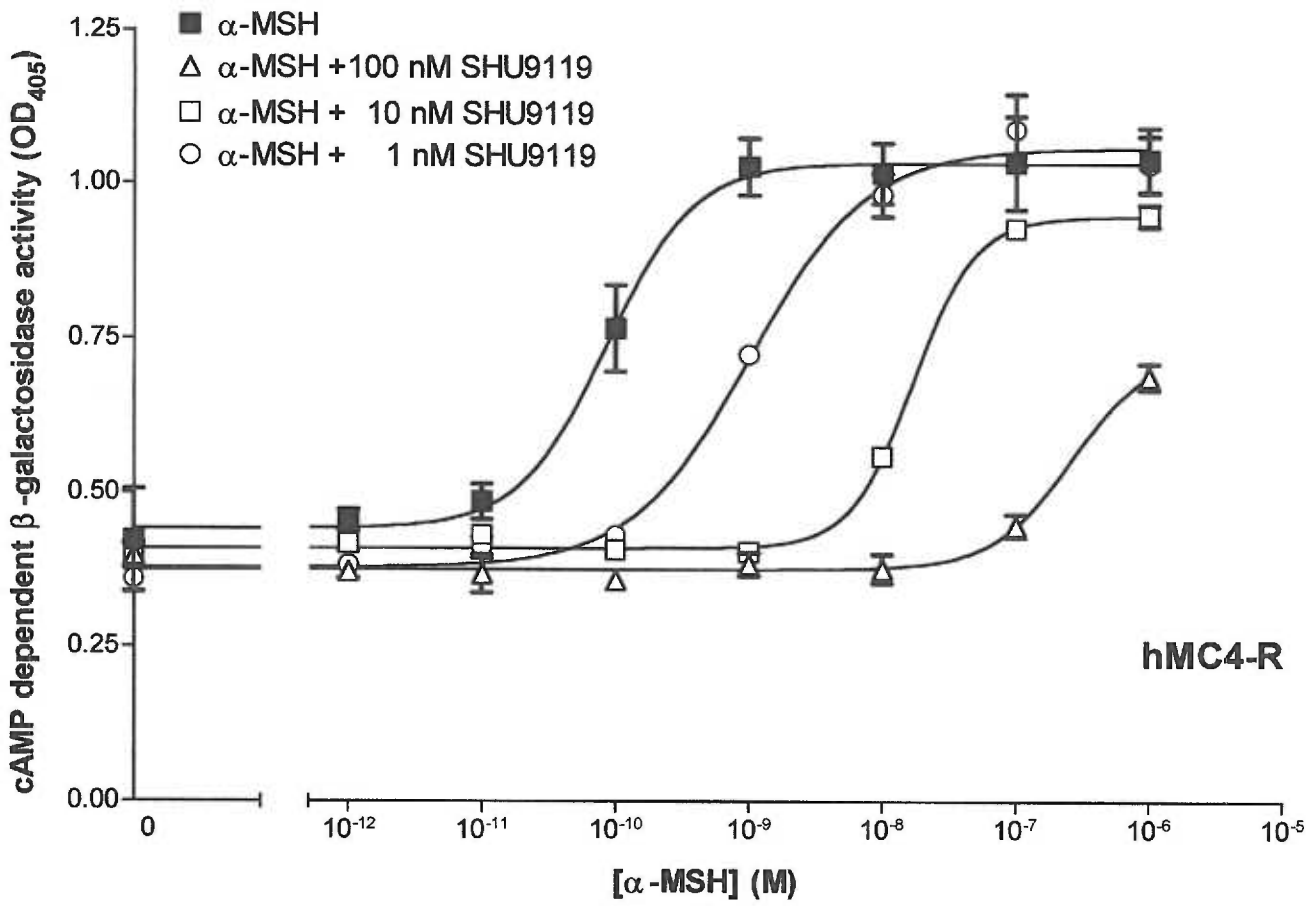

Figure 3.3a (hMC4-R)

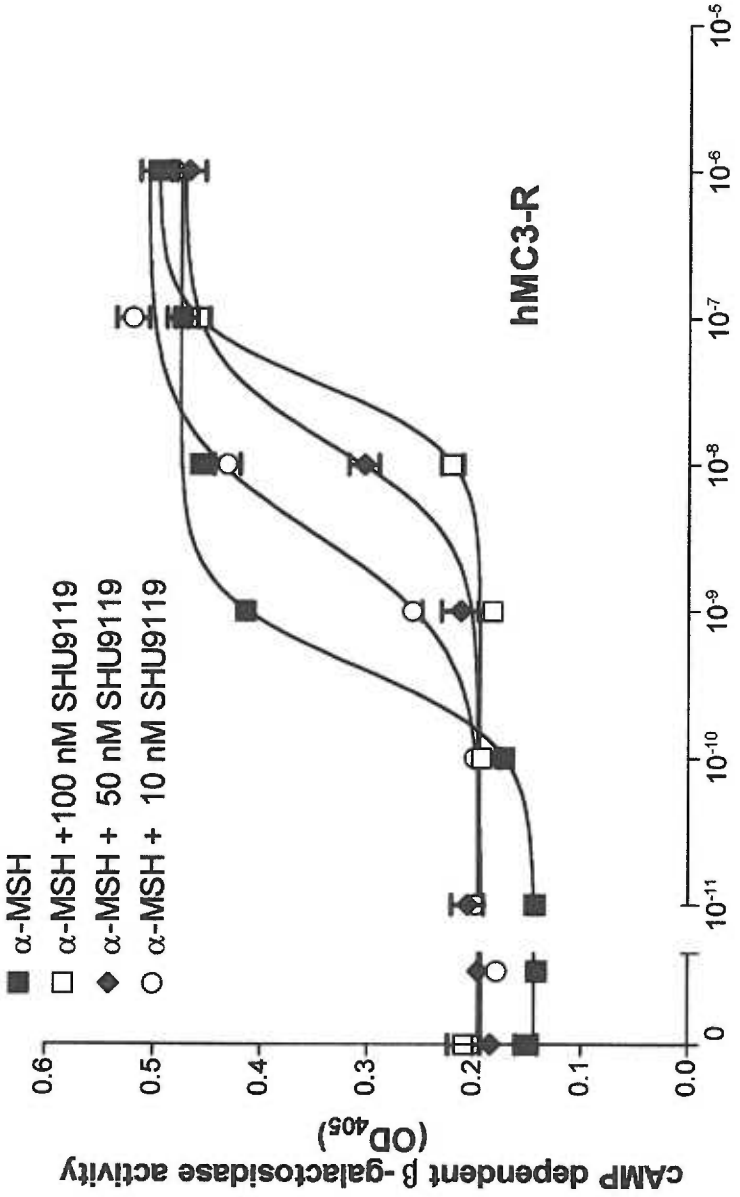

Figure 3.3c (hMC3-R)

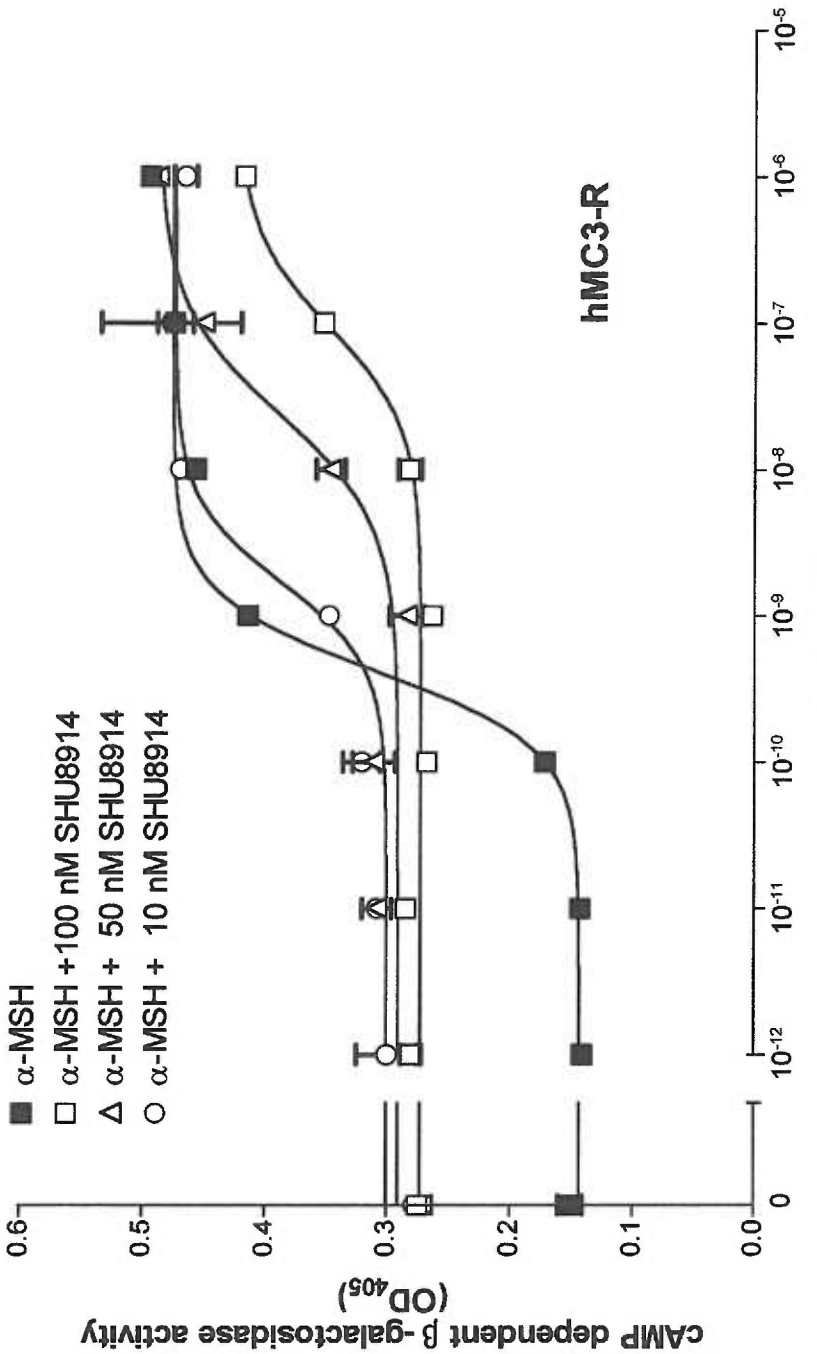

Figure 3.3d (hMC3-R)

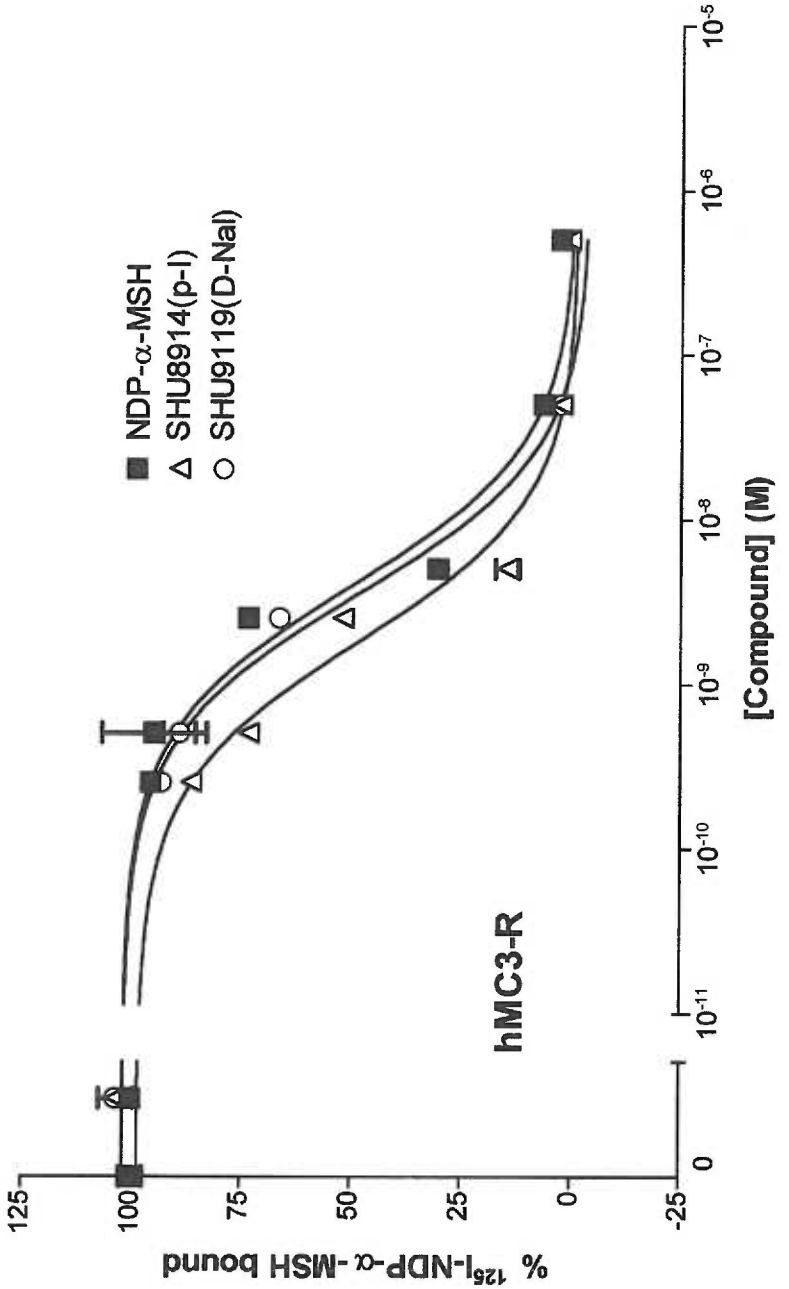

Figure 3.4a (hMC3-R)

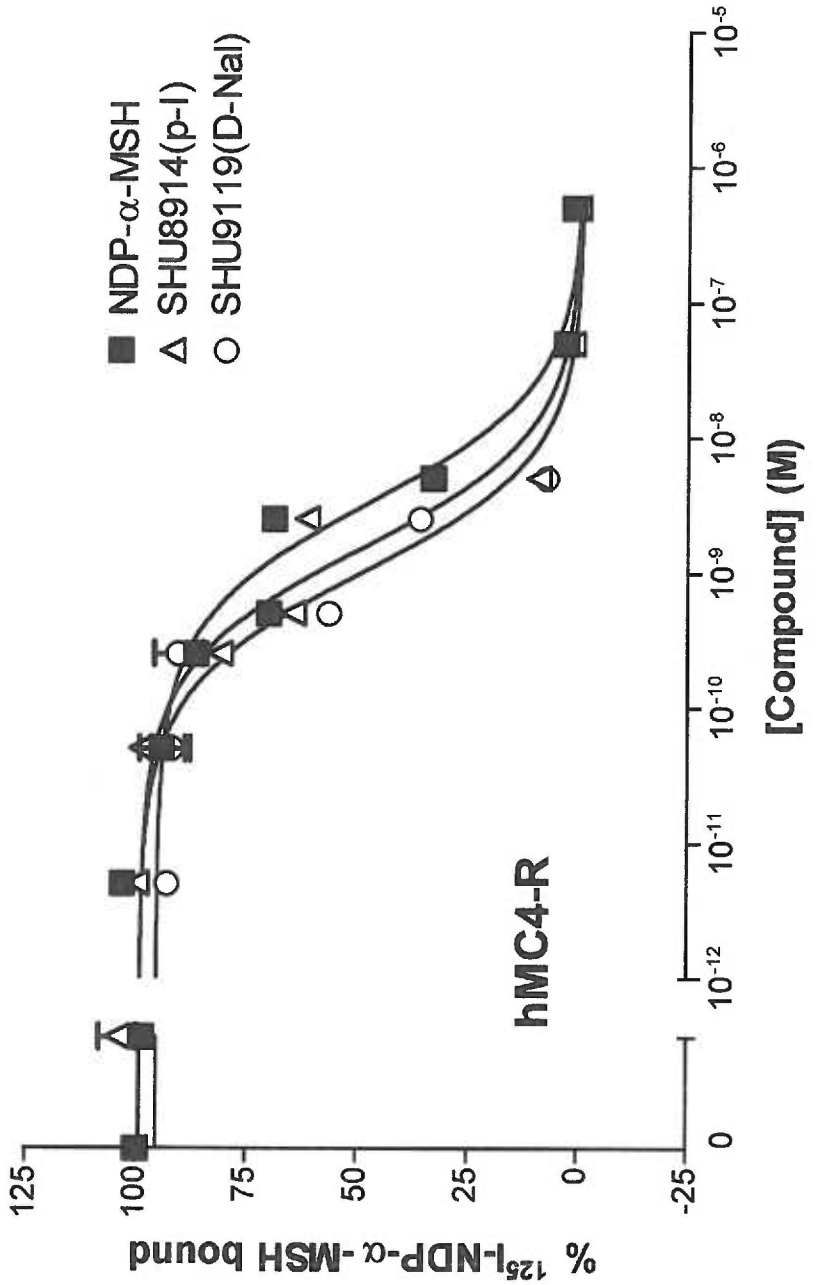

Figure 3.4b (hMC4-R)

Table 3.1. Agonist and antagonist activities of cyclic melanotropin analogues at various MC-1 receptors

Compound	EC_{50} Values (nM)		
	Frog skin assay	mMC1-R assay	hMC1-R assay
α-MSH	0.10 ± 0.03	1.3 ± 1.4	0.091 ± 0.070
1, Ac-Nle^4-c[Asp^5,D-Phe(pF)^7,Lys^{10}]α-MSH-(4-10)-NH_2[a] (SHU9128)	0.10 ± 3.5	0.026 ± 0.010	0.016 ± 0.003
2, Ac-Nle^4-c[Asp^5,D-Phe(pCl)^7,Lys^{10}]α-MSH-(4-10)-NH_2 (SHU9203)	2.0 ± 0.8	0.0095 ± 0.0053	0.005 ± 0.004
3, Ac-Nle^4-c[Asp^5,D-Phe(pI)^7,Lys^{10}]α-MSH-(4-10)-NH_2 (SHU8914)	Antagonist $pA_2 = 10.3$	0.19 ± 1.3	0.055 ± 0.031
4, Ac-Nle^4-c[Asp^5,D-Nal(2)^7,Lys^{10}]α-MSH-(4-10)-NH_2 (SHU9119)	Antagonist $pA_2 \geq 10.5$	0.039 ± 0.029	0.036 ± 0.012

[a] The complete structure of 1 is Ac-Nle^4-Asp-His-D-Phe(pF)^7-Arg-Trp-Lys^{10}-NH_2. Compound **2-4** are the same except for the amino acid in the 7-position.

Table 3.2. EC_{50} values (pM) for D-Phe^7-substituted Ac-Nle^4-c[Asp^5,D-Phe^7,Lys^{10}]α-MSH-(4-10)-NH_2 analogues at the different melanocortin receptors

	EC_{50} values (nM)			
	hMC1-R	hMC3-R	hMC4-R	mMC5-R
α-MSH	91 ± 69	669 ± 355	210 ± 57	807 ± 125
[Nle^4,D-Phe^7]α-MSH-NH_2	23 ± 7	132 ± 31	17 ± 18	ND[a]
1, SHU9128 (pF)	16 ± 3	191 ± 9	19 ± 14	1360 ± 549
2, SHU9203 (pCl)	5 ± 4	63 ± 26	18 ± 14	117 ± 70
3, SHU8914 (pI)	55 ± 31	1134 ± 197	573 ± 357	684 ± 227
		Partial Agonist	Partial Agonist	Partial Agonist
		$pA_2 = 8.3$	$pA_2 = 9.7$	
4, SHU9119 (D-Nal(2))	36 ± 12	2813 ± 575	No Activity	434 ± 260
		Partial Agonist	Antagonist	Full Agonist
		$pA_2 = 8.3$	$pA_2 = 9.3$	

[a] ND = Not determined.

Table 3.3. IC_{50} values (nM) for Phe^7-substituted Ac-Nle^4-c[Asp^5,D-Phe^7, Lys^{10}]α-MSH-(4-10)-NH_2 analogues

	hMC3-R	hMC4-R
[Nle^4,D-Phe^7]α-MSH	3.8	3.6
3, SHU8914 (pI)	1.8	2.5
4, SHU9119 (D-Nal(2))	3.3	1.8

Table 3.4. Analytical properties of new cyclic α-melanotropin peptides used in this study

Compd	$[\alpha]^{22}_{589}$ in 10% HOAc (deg)	TLC R_1 values			HPLC[b] K'	FAB-MS,[g] M + H found (calcd)
		A	B	C		
1	-27.6 (c 0.023)	0.82	0.04	0.69	5.71[c] 6.71[d]	1042.5 (1042.1)
2	-41.8 (c 0.038)	0.80	0.05	0.69	4.42[c] 3.11[e]	1059.9 (1058.6)
3	-45.4 (c 0.032)	0.84	0.02	0.68	6.83[c] 8.14[f]	1151 (1150.1)
4	-65.2 (c 0.018)	0.79	0.01	0.65	7.28[c] 9.59[f]	1075 (1075.3)

[a] Solvent systems: (A) 1-butanol/HOAc/pyridine/H_2O(5:1:5:4), (B) EtOAc/pyridine/HOAc/H_2O (5:5:1:3), (C) 1-butanol/HOAc/H_2O(4:1:5). [b] Analytical HPLC performed on a C18 column (Vydac 218TP 104) using a gradient of acetonitrile in 0.1% aqueous TFA in 30 min at 1.5 mL/min. The following gradients were used. [c] 20-40% acetonitrile in 30 min. [d] 20-30% acetonitrile in 30 min. [e] 25-35% acetonitrile in 30 min. [f] 10-40% acetonitrile in 30 min. [g] Fast atom bombardment mass spectrometry.

Chapter 3 Appendix

Before our studies on the MSH analogues characterized in chapter 3, initial experiments were carried out on additional series of analogues. The structures of these analogues are shown in **Table 3A.1**. Limited data points were tested for these 9 MSH analogues on rMC3-R, hMC4-R and mMC5-R. Different receptors were stimulated with a series concentrations of α-MSH in the absence and presence of these analogues at 100 nM concentration. Five different concentrations of α-MSH were tested, including 10^{-12} M, 10^{-10} M, 10^{-8} M, 10^{-7} M and 10^{-6} M. The agonist activities can be seen when the analogues are used in the absence of α-MSH.

The effects of these analogues on rMC3-R are shown in **Figure 3A.1**. Analogue SHU-9119 showed only minimum activity as an agonist, while 100 nM SHU-9119 can antagonize stimulation of rMC3-R until 10^{-7} M α-MSH concentration was reached (**Figure 3A.1b**). In addition, SHU-9005 showed partial agonist activity at 100 nM concentration, meanwhile the same concentration can also antagonize the stimulation of rMC3-R until 10^{-7} α-MSH concentration was reached (**Figure 3A.1a**). These indicated that in case of antagonist activities, SHU-9119 is a better antagonist than SHU-9005 on the rMC3-R. The other analogues tested are all agonists of the rMC3-R (**Figure 3A.1**) except that SHU-9403 appears to exhibit neither agonist nor antagonist activity on the rMC3-R (**Figure 3A.1b**).

Different pharmacological profiles of these analogues were observed on the hMC4R (**Figure 3A.2**) and mMC5R (**Figure 3A.3**) in comparison to the rMC3R, which indicated receptor-ligand interaction is unique for each individual receptor, though they are from same receptor family and have high homology. SHU-9005, a mixed agonist of the rMC3-R, appeared to be a full agonist for hMC4-R (**Figure 3A.2a**) and mMC5-R (**Figure 3A.3a**). SHU-9119, a good antagonist of the rMC3-R, showed as a better antagonist of the hMC4-R(**Figure 3A.2b**), and as an agonist on the mMC5-R (**Figure 3A.3b**). Both results are consistent with our results in chapter 3, which showed SHU-9119 is 10 times potent on hMC4-R than on hMC3-R with a pA_2 value of 9.3 and 8.3, respectively, and a full agonist of the mMC5-R with an EC_{50} value of $0.43 \pm 0.26 \times 10^{-9}$ M (**Table 3.2**). Although SHU-9403 showed no activities at the rMC3-R, it functioned as a partial agonist of the hMC4-R (**Figure 3A.2b**). All the other analogues are agonists of the hMC4-R (**Figure 3A.2**).

Of all the analogues tested on the mMC5-R, only three of them showed agonist activities, including SHU-9005, SHU-9010 (**Figure 3A.3a**), and SHU-9119 (**Figure 3A.3b**). All the other analogues appeared to exhibit neither agonist nor antagonist activity (**Figure 3A.3b**). The two analogues with full agonist activities at the mMC5-R, SHU-9005 and SHU-9010, are both 13mers, and bigger than the other heptapeptide analogues tested. Combined with the result that SHU-9119, which has a bulky aromatic substitution at position 7, also showed agonist activity, the pocket for ligand entry and activation of the mMC5-R is probably bigger and more flexible than that of the MC3-R or MC4-R.

Figure legends

Figure 3A.1 Effects of MSH analogue on the activation of rMC3-R.

a. The rMC3-R was stimulated with series concentrations of α-MSH, as shown in the X axis in the absence (α-MSH alone) or presence of 100 nM SHU-9005, 9010, 9107, and 9108. **b**. The rMC3-R was stimulated with series concentrations of α-MSH, as shown in the X axis in the absence (α-MSH alone) or presence of 100 nM SHU-9109, 9119, 9306, 9403, and CHL-1-94. See **chapter 3** for methods.

Figure 3A.2 Effects of MSH analogue on the activation of hMC4-R.

a. The hMC4-R was stimulated with series concentrations of α-MSH, as shown in the X axis in the absence (α-MSH alone) or presence of 100 nM SHU-9005, 9010, 9107, and 9108. **b**. The hMC4-R was stimulated with series concentrations of α-MSH, as shown in the X axis in the absence (α-MSH alone) or presence of 100 nM SHU-9109, 9119, 9306, 9403, and CHL-1-94. See **chapter 3** for methods.

Figure 3A.3 Effects of MSH analogue on the activation of mMC5-R.

a. The mMC5-R was stimulated with series concentrations of α-MSH, as shown in the X axis in the absence (α-MSH alone) or presence of 100 nM SHU-9005, 9010, 9107, and 9108. **b**. The mMC5-R was stimulated with series concentrations of α-MSH, as shown in the X axis in the absence (α-MSH alone) or presence of 100 nM SHU-9109, 9119, 9306, 9403, and CHL-1-94. See **chapter 3** for methods.

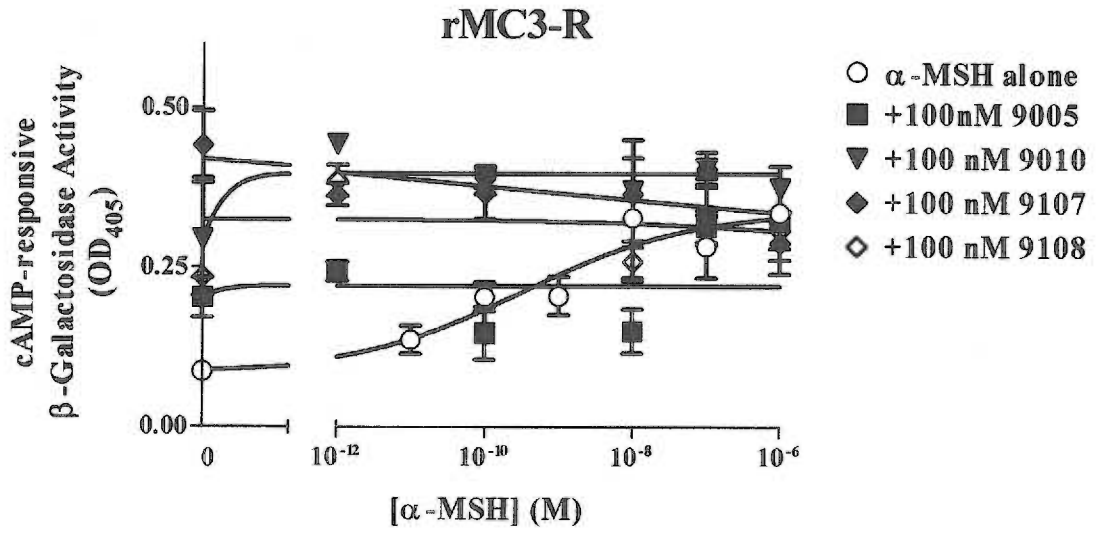

Figure 3A.1a

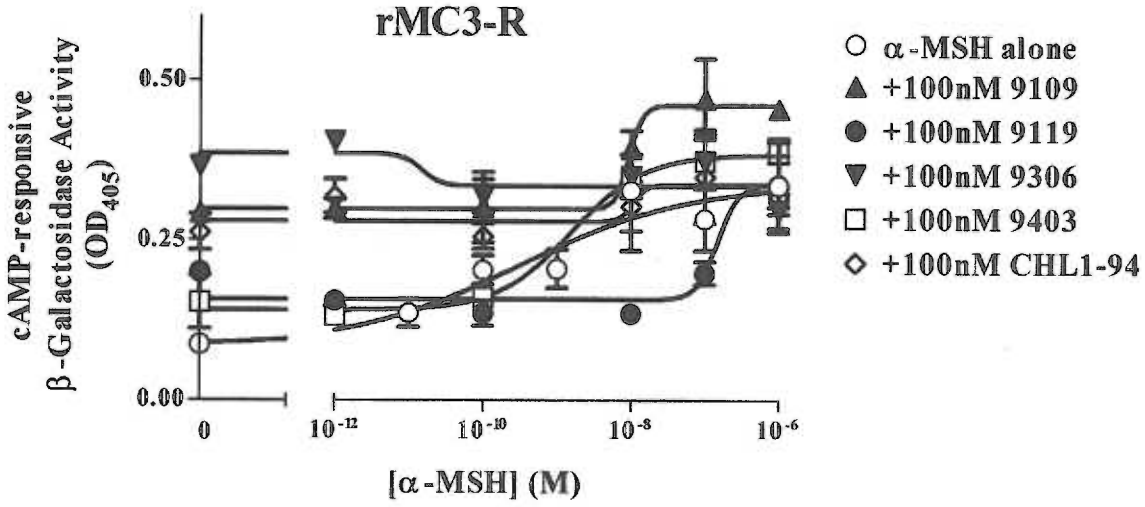

Figure 3A.1b

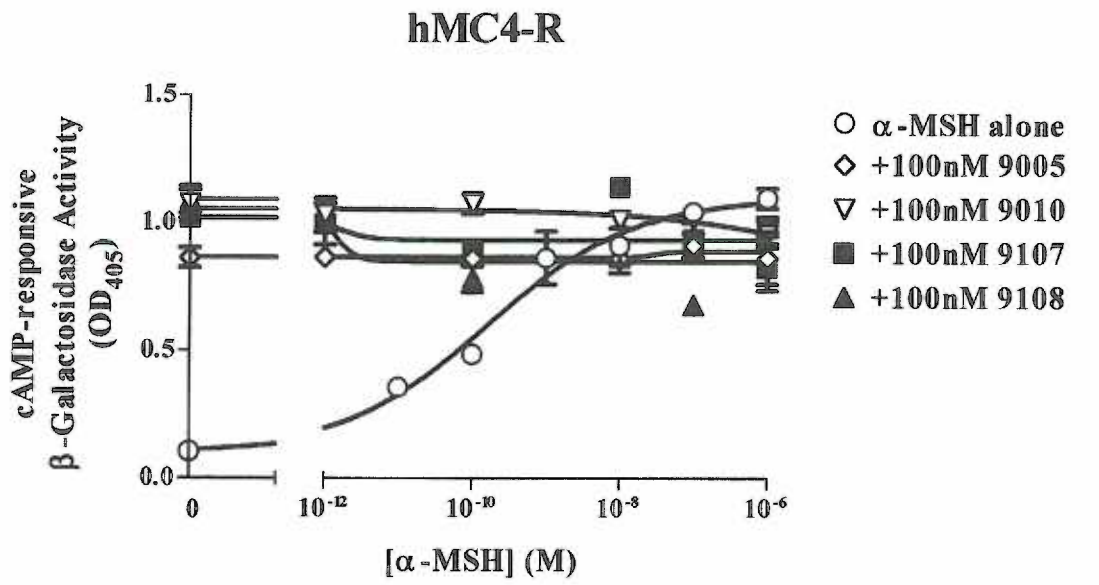

Figure 3A.2a

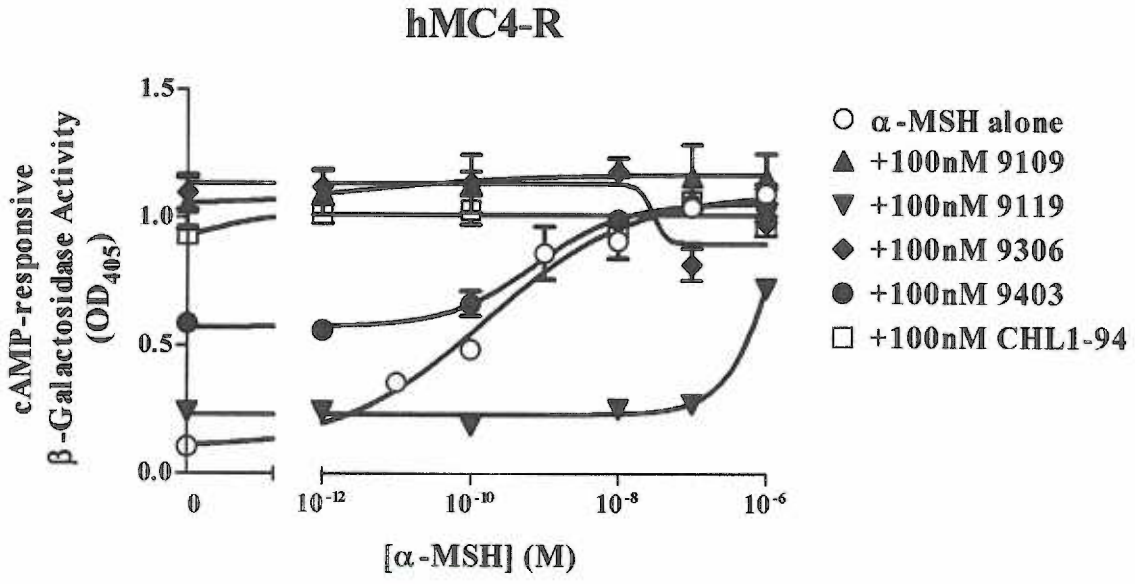

Figure 3A.2b

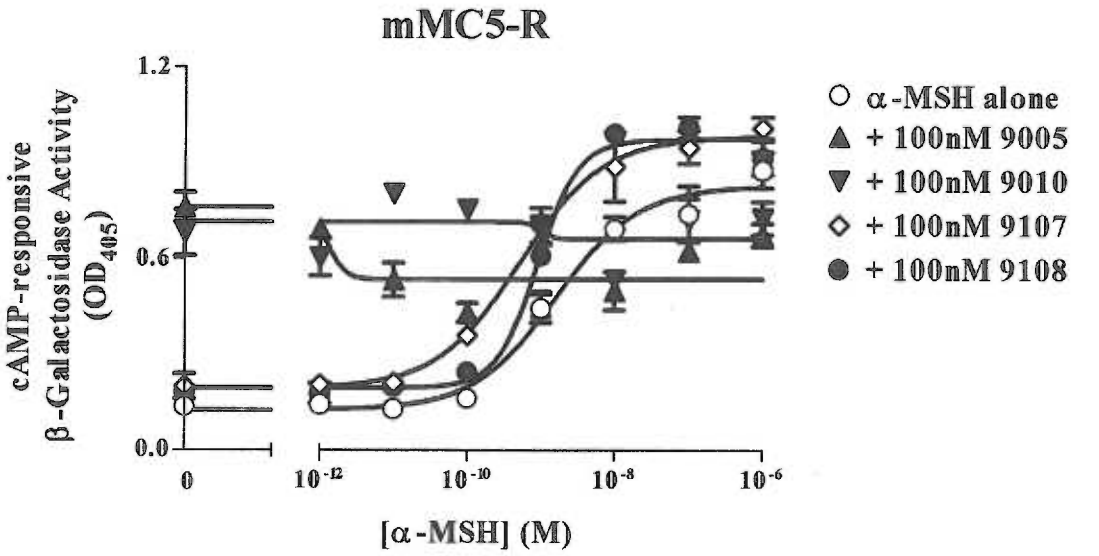

Figure 3A.3a

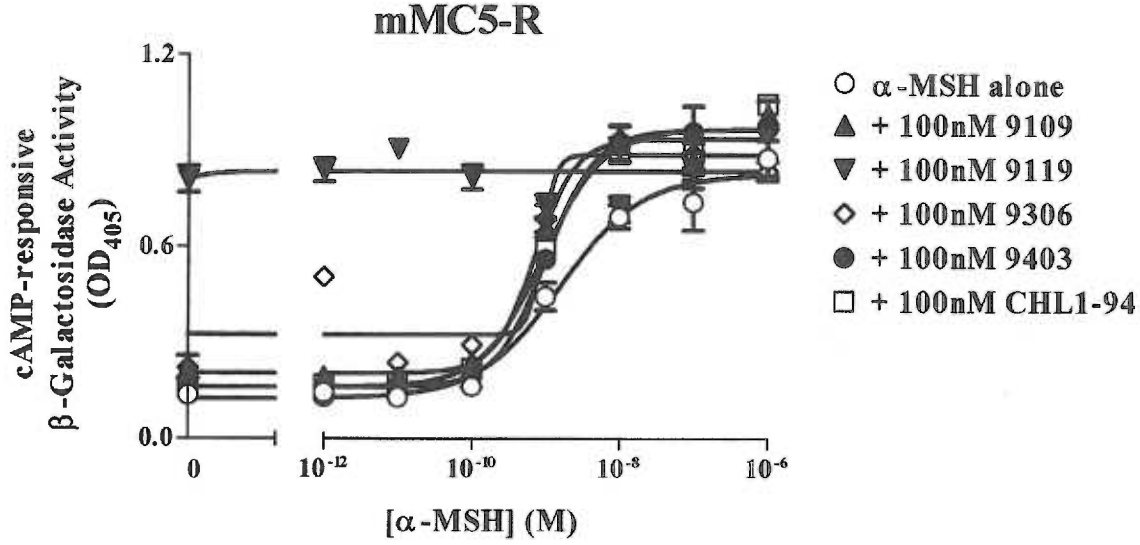

Figure 3A.3b

Table 3A.1 Structure of Melanotropin Analogues

Sample code	Structure	
SHU-9005	Ac-Ser-Tyr-Ser-Nle-Glu-His-D-(p-I)Phe-Arg-Trp-Gly-Lys-Pro-Val-NH_2	
SHU-9010	Ac-Ser-Tyr-Ser-Nle-Glu-His-D-Phe-Arg-Trp-Gly-Lys-Pro-Val-NH_2 (Lys-Arg)	
SHU-9107	Ac-Nle-Asp-His-D-Phe-Arg-Trp-Sar-Lys-NH_2	
SHU-9108	Ac-Nle-Asp-His-D-Phe-Arg-Trp-Aib-Lys-NH_2	
SHU-9109	Ac-Nle-D-Asp-His-D-Phe-Arg-Trp-Ala-Lys-NH_2	
SHU-9119	Ac-Nle-Asp-His-D-Nal-Arg-Trp-Lys-NH_2	
SHU-9306	Tyr-Glu-His-D-Phe-Arg-Trp-Gly-Lys-Pro-Val	[(Tyr^4,D-Phe^7)-$ACTH_{4-13}$]
SHU-9403	His-D-Phe-Lys-Trp-NH_2	
CHL-1-94	Ac-Cys-Asp-His-D-Phe-Arg-Trp-Cys-Lys-NH_2	

" ⌐¬ " indicates covalent bond between two residues. Sar represents N-methyl-glycine, Aib represents amino-buteric acid. Underlined sequence is the pharmacophore or modifications of pharmacophore of α-MSH.

Chapter 4

A Non-epistatic Interaction of *Agouti* and *Extension* in the Fox, *Vulpes vulpes*

Dag Inge Våge[1], Dongsi Lu[2,4], Helge Klungland[1], Sigbjørn Lien[1], Stefan Adalsteinsson[3] and Roger D. Cone[2]

[1]Department of Animal Science, Agricultural University of Norway, P.O. Box 5025, N-1432 Ås, Norway.

[2]Vollum Institute for Advanced Biomedical Research, Oregon Health Sciences University, Portland, Oregon 97201, USA.

[3]The Nordic Gene Bank for Farm Animals, Agricultural University of Norway, P.O. Box 5025, N-1432 Ås, Norway.

[4]Department of Cell and Developmental Biology, Oregon Health Sciences University, Portland, Oregon 97201, USA

Published in Nature Genetics, Vol. 15, No.3, 311-315 (1997)

Abstract

Agouti and *extension* are two genes that control the production of yellow-red (phaeomelanin) and brown-black (eumelanin) pigments in the mammalian coat (Searle, 1968). *Extension* encodes the melanocyte-stimulating hormone receptor (MC1-R) (Robbins et al., 1993; Klungland et al., 1995) while *agouti* encodes a peptide antagonist of the receptor (Bultman et al., 1992; Miller et al., 1993; Lu et al., 1994). In the mouse, *extension* is epistatic to *agouti* (Bateman, 1961; Wolff et al., 1978), hence dominant mutants of the MC1-R encoding constitutively active receptors are not inhibited by the agouti antagonist, and animals with dominant alleles of both loci remain darkly pigmented. In the fox the proposed *extension* locus is not epistatic to the agouti locus (Ashbrook, 1937; Adalsteinsson et al., 1987). We have cloned and characterized the MC1-R and the *agouti* gene in coat color variants of the fox (*Vulpes vulpes*). A constitutively activating C125R mutation in the MC1-R was found specifically in darkly pigmented animals carrying the Alaska Silver allele (E^A). A deletion in the first coding exon of the *agouti* gene was found associated with the proposed recessive allele of *agouti* in the darkly pigmented Standard Silver fox (*aa*). Thus, as in the mouse, dark pigmentation can be caused by a constitutively active MC1-R, or homozygous recessive status at the *agouti* locus. Our results, demonstrating the presence of dominant *extension* alleles in

foxes with significant red coat coloration, suggest the ability of the fox agouti protein to counteract the signalling activity of a constitutively active fox MC1-R.

Results and Discussion

Two different alleles each at the proposed *extension* (*E, E^A*) and *agouti* (*A, a*) loci result in nine possible genotypes and five distinct coat color phenotypes in the fox (Ashbrook, 1937; Adalsteinsson et al., 1987) (**Figure 4.1**). This assignment of *agouti* and *extension* loci parallels that for the mouse and implies that the absence of any significant phaeomelanin pigment in the dark Silver foxes results from the presence of dominant *extension* locus alleles, or the absence of functional agouti protein. In the mouse (Robbins et al., 1993) and cattle (Klungland et al., 1995), dominant *extension* locus alleles encode mutant forms of the MC1-R that have constitutive activity. To determine the molecular identity of the *agouti* and *extension* loci in the fox, we isolated the entire MC1-R coding sequence by PCR and directly sequenced it from 17 foxes representing a variety of coat color phenotypes. We found polymorphisms in six different positions, however only one change, C125R, correlated perfectly with the proposed dominant *extension* allele responsible for the darkly pigmented Alaska phenotype (**Figure 4.2a**). We cloned a cDNA spanning the majority of agouti coding sequence from the Red fox using degenerate oligonucleotides based on the mouse and human agouti sequence. Subsequent PCR cloning of agouti cDNAs from both the Red and Standard Silver fox demonstrated the presence of a 166 nucleotide deletion in the Standard Silver fox cDNA, spanning the second exon (**Figure 4.2b**). This deletion removes the start codon and entire signal peptide, thus likely ablating the production of functional agouti protein.

We analyzed the C125R mutation for cosegregation with the darkly pigmented Alaska phenotype in 88 animals from six commercial farms in Norway using a PCR polymorphism test that detects the creation of a Bsa JI restriction site (**Figure 4.3a**). Southern hybridization of the *agouti* locus was performed using a 1,300-bp probe from the intron between exons 2 and 3 from the fox (**Figure 4.3b**). We found the C125R mutation in all 34 animals classified as Cross foxes, which are obligatory carriers of the dominant E^A allele (**Figure 4.3c**). Southern hybridization with the agouti probe demonstrated a 1.2-kb deletion of genomic sequences spanning the entire second exon and approximately 1 kb of the first and second introns in animals containing the proposed *a* allele. We found a smaller 2.5-kb *Taq*$^{\alpha}$I fragment of the agouti gene reflective of this deletion in all 30 Smoky Red and Blended Cross foxes classified phenotypically as carriers of a recessive *agouti* allele (*a*), while all Red foxes were homozygous for *A*, containing only the 3.7-kb *Taq*$^{\alpha}$I fragment. All 19 Silver foxes that were not E^AE^A were homozygous for the *a* allele, as we predicted (**Figure 4.3c**).

As the C125R change was the only mutation that was completely associated with the Alaska phenotype, this mutation was introduced by *in vitro* mutagenesis into the same position (aa123) of the highly conserved mouse MC1 receptor (85 % amino acid identity) for pharmacological analysis. MC1-R (C123R), when expressed in the 293 cell system, was found to activate adenylyl cyclase to levels from 25-90% maximal levels, in the absence of any hormone stimulation (**Figure 4.4a**). Competition binding studies using ^{125}I-NDP-α-MSH

showed that the MC1-R (C123R) is expressed at very low copy number (<300/cell) (**Figure 4.4b**), perhaps due to a potent downregulation of this constitutively active receptor. Ligand binding to the C123R receptor was reproducible, however, and suggested that the receptor retains a high affinity for ligand (**Figure 4.4c**, $IC_{50} = 1.14 \pm 0.24 \times 10^{-9}$ M). The full length wild type fox MC1-R was transiently expressed in Cos-1 cells, and appeared to couple normally to adenylyl cyclase, as measured by analysis of intracellular cAMP concentrations, with an EC_{50} of 1.6×10^{-9} M (**Figure 4.4d**), comparable to the value reported for the mouse MC1-R (2.0×10^{-9} M) (Mountjoy et al., 1992) . While constitutive activity of E^A allele of the fox MC1-R was seen in some experiments, the result could not be reliably reproduced. Competition binding experiments demonstrated that this was due to extremely low levels of expression of the E^A allele in heterologous cells, in contrast with the significant number of high affinity binding sites seen after transfection of the *E* allele (**Figure 4.4e**). This result is consistent with the potent downregulation seen with constitutive activation of the mouse MC1-R (**Figure 4.4b** and (Cone et al., 1996)), and has been reported for the K296E allele of rhodopsin (Li et al., 1995).

Our results allow a detailed interpretation of fox coat color phenotypes resulting from *extension* and *agouti* . Red coat color in cattle (Klungland et al., 1995) and the red guinea pig (Cone et al., 1996) result from homozygosity of defective alleles of the MC1-R. Polymorphisms in the MC1-R have also been reported at high frequency in association with light skin or red hair in man (Valverde et al., 1995; Koppula et al., 1997). In contrast, we observed no

deletions or deleterious mutations in the MC1-R in DNA from the Red fox (*EEAA*) sequenced in our study. This allele of the receptor appeared normal in functional expression assays in tissue culture (**Figure 4.4d**), and *in vivo*, based on the eumelanin found around the ears, tail, and feet in this animal (**Figure 4.1a**). These observations demonstrate that red coat color results from inhibition of the MC1-R by the product of the *A* allele of *agouti*.

The deletion of agouti exon 2 coding sequences that we found in the Standard Silver fox is very likely to result in the absence of functional agouti protein. In the complete absence of agouti in the Standard Silver fox (*EEaa*), we found only eumelanin, identical phenotypically to what is observed due to constitutively active MC1-R in the Alaska Silver fox (**Figure 4.1e**). When two constitutively active MC1-Rs are found, such as in the Alaskan Silver (E^AE^AAA), Sub-Alaskan Silver (E^AE^AAa) , or Double Silver fox (E^AE^Aaa) primarily eumelanin is found. In striking contrast to the mouse, however, we found that heterozygosity of the dominant *extension* allele E^A is not sufficient to override inhibition of eumelanin production by *agouti*. One wild type *agouti* allele (**Figure 4.1d**) produces significant red pigment around the flanks, midsection, and neck in the Blended Cross fox (E^AEAa). While we can not exclude the possibility that very high levels of agouti expression block the small component of ligand stimulated receptor activity seen, for example, at 10^{-6} to 10^{-7} M doses of hormone (**Figure 4.4a**), our results suggest an interaction between *extension* and *agouti*

distinct from the epistasis seen in the mouse, two hypotheses are proposed to explain this finding.

In the recently proposed allosteric ternary complex model (Lefkowitz et al., 1993), G-protein coupled receptors are in equilibrium between the inactive (R) and active (R*) states, even in the absence of ligand . In contrast to the classical competitive antagonist which binds equally well to R and R* and acts by blocking ligand binding, inverse agonists, recently verified experimentally (Samama et al., 1994), bind preferentially to R and thus shift the receptor equilibrium in the direction of the inactive state. While the mouse agouti protein behaves like a classical competitive antagonist, it is possible that the fox protein is an inverse agonist and can inhibit the constitutively active E^A allele of the MC1-R. A second hypothesis would invoke another target of agouti action on the melanocyte in addition to the MC1-R (Lu et al., 1994; Blanchard et al., 1995). In support of this idea, the agouti peptide has been found to increase intracellular Ca^{2+} in a muscle cell line via a mechanism that may not involve melanocortin receptor antagonism (Zemel et al., 1995).

Our results also elaborate on the molecular mechanism by which dominant MC1-R alleles are created. Constitutive activation of the MC1-R in the darkly pigmented *sombre* mouse results from mutation of a glutamic acid at position 92 (aa 94 in the fox) to a lysine in transmembrane domain two, presumably disrupting an intramolecular bond that constrains the receptor in an inactive conformation (Robbins et al., 1993). Identification of the activating C125R mutation in the fox implies either a direct role of this cysteine in constraining the

receptor, or an indirect effect in which the introduced arginine creates a strong electrostatic interaction with aspartic acid residues one or two turns of the α-helix above at positions 117, and 121, disrupting the ability of one or both of these residues to hydrogen bond. For example, an internal constraint consisting of a hydrogen bond between D117 and E94 could be disrupted by insertion of a positive charge at either position 94 or 125 and would provide a common mechanism for the naturally occurring constitutive activation of the *sombre* mouse and Alaska fox MC1 receptors.

Methods

Animals. Blood and tissue samples from animals described in this study were collected for the preparation of genomic DNA from six commercial farms in Norway. Alaska Cross fox or Blended Cross fox animals, derived from 11 independent sibships, were classified as carriers of the Alaska allele E^A, while the Smoky Red and Blended Cross fox animals were classified as carriers of the recessive *agouti* allele *a*.

Oligonucleotides. All sequences are given in the 5' - 3' direction. E signifies extension locus primers while A signifies agouti. Engineered restriction sites are underlined.

E1: ctcctcgag(acgt)cttct(acgt)ggttc(acgt)ct(acgt)aa(ct)tc (forward primer)

E2: cagaattcggaa(ag)ta(gt)atga(ag)ggggtc (reverse primer)

E5: caagaaccgcaacctgcact (forward primer)

E8: aggctggataccatagaacc (reverse primer)

E9: ccgtcgggaatggacacctcc (reverse primer)

E10: gcacctctcactcatggtcct (forward primer)

E11: tgggaattcgccagcttgaagtgaggggtg (reverse primer)

E12: caagaattccctcaccctcatcatctgcaa (forward primer)

E13: aactgagcgagacacctgagg (forward primer)

E14: ccccagtcacaggggtatcaa (reverse primer)

BAM E13: ggcggatccaactgagcgagacacctgagg (forward primer)

R1 E14: ctgcaaggaattcccccagtcacaggggtatca (reverse primer)

A1: (acgt)aaggaggcttcgatgaagaa (exon 4, forward primer)

A2: tcagcagttgagg(acgt)tgag(agct)ac (exon 4, reverse primer)

A3: (agct)cgctgaacaagaaatccaa(ag) (exon 3, forward primer)

A4: aagaagcggcactggcagga (exon 4, reverse primer)

A5: gtctccctgtgcttcctcac (exon 2, forward primer)

A6: ccgcctcttttctgctgatc (exon 3, reverse primer)

A7: ttgcagctgttgcgagtggc (exon 4, reverse)

A8: cacaggctgagcattgag (exon 1, forward)

ME1: atccgtggctccatggtgtcc (forward primer)

ME2: gagcacgtcaatgaggttgtc (reverse primer)

Cloning of the fox MC1-R. The degenerate primers E1 and E2 were used to amplify a 832 bp fragment of the fox MC1-R (primers not included), corresponding to position 509-1340 in the human cDNA sequence. Each PCR reaction was carried out in a total volume of 100 ml, containing 500 ng genomic DNA, 200 pmol of E1 and 100 pmol of E2, 200 μM of each dNTP, Vent buffer (BioLabs) and 2U Vent DNA polymerase. Genomic DNA was denatured for 3 min at 94°C and PCR was run for 35 cycles at 94°C for 1 min, 52°C for 1 min, and 72°C for 1 min. Amplified DNA was separated in a 1% agarose gel, and the band of expected length was cut out, reamplified at 55°C, digested with Xho I and

EcoR I, cloned into pBLUESCRIPT II KS (Stratagene Inc.) and sequenced according to standard protocols.

The 832bp probe was then used as a probe to clone the entire fox MC1-R. 0.8 μg Red fox genomic DNA (*EE*) was digested with 0.6 units of Tsp 509I at 65°C for 1 hour. The digestion products were purified with phenol/ chloroform method. 100 ng of the purified genomic DNA fragments were ligated to 1 μg of the EcoRI predigested ZAP Express vector (Stratagene Cloning Systems) at 12°C overnight. ZAP ExpressTM Predigested Gigapack®III Gold Cloning Kit (Stratagene Cloning Systems) was used to package the ligation products into the Rec A- E. coli host strain XL1-Blue MRF' cells. This library was probed with a partial sequence of the fox MC1-R amplified as described above. In vivo excision of the pBK-CMV phagemid vector from the ZAP express vector of the positive clone was done as described [ZAP ExpressTM Predigested Gigapack®III Gold Cloning Kit (Stratagene Cloning Systems)]. Sequencing of the complete fox receptor allowed the determination of amino and carboxyl-terminal sequences; the presence of two additional amino acids in the amino terminal extracellular domain of the fox receptor results in a two amino acid discordance in numbering the fox and mouse receptor residues.

PCR-amplification and direct sequencing of the MC1-R. Based on the complete sequence of the fox MC1-R clone, primers E13 and E14 were designed to amplify the entire coding region to look for polymorphisms in a large number

of coat color variants. The fox genomic DNA from animals representing three of the five phenotypes (Red fox, Alaska Cross fox, and Alaska Silver fox) were amplified. Each PCR reaction was carried out in a total volume of 50 µl, containing 250 ng genomic DNA, 1 µM of each primer, 400 µM of dNTP mix and standard buffer conditions. 1 U of Vent DNA polymerase (NEB) was added after denaturing the genomic DNA at 96°C for 5 min. PCR was run for 30 cycles at 94°C for 45 sec, 64°C for 45 sec, and 72°C for 70 sec, then run for another 7 min at 72°C. The PCR products were purified by QIAquick PCR purification Kit (QIAGEN) and then used for sequencing by an ABI model sequencer. 5 to 7 µl of the PCR product was used for each sequencing reaction. Primers E9, E10, E11, and E12 were used to generate the complete 951 nucleotide coding sequence from each clone.

MC1-R Restriction length polymorphism. PCR amplifications were carried out with primers E5 and E8 in a volume of 20 µl containing 50 ng genomic DNA, 10 pmol of each primer, 200 µM dNTP, standard buffer conditions and 1 U Taq polymerase. Genomic DNA was denatured for 3 min. at 94°C, and PCR run for 35 cycles at 94°C for 30 sec., 58°C for 30 sec., and 72°C for 30 sec. Ten µl of the PCR-product was digested with 2.5 U Bsa JI for 2 hours at 37°C in a 15 µl reaction. Digested DNA was separated on a 4% agarose gel. When the wild type allele is present, the initial 204 bp PCR fragment is cut into fragments of 123 bp and 81 bp respectively by the restriction enzyme Bsa JI . If the mutant allele is

present, the 81 bp fragment is further cut into fragments of 58 bp and 23 bp (**Figure 4.3a**).

Cloning of the fox *agouti* and RFLP analysis. Most of the exon 3 and exon 4 coding region of the fox agouti gene was amplified by two different sets of primers (A1/A2 and A3/A4) designed based on the reported mouse (Bultman et al., 1992; Miller et al., 1993) and human (Wilson et al., 1995) sequences. Poly A+ RNA was isolated from dorsal skin of the Red fox and the Standard Silver fox using a mRNA Direct Kit (Dynal), and approximately 170 ng mRNA was used for cDNA synthesis (Clontech Laboratories, Inc.). The resulting cDNA was diluted into 50 µl, and 5 µl used for each PCR reaction. The 30 µl reactions contained 30 pmol of each primer, 200 µM dNTPs, standard buffer conditions, and 1.5 U Taq polymerase. cDNA was denatured for 3 min. at 94°C, and PCR run for 40 cycles at 94°C for 15 sec., 55°C (A1/A2) or 60°C (A3/A4) for 15 sec., and 72°C for 30 sec. Bands of the expected size were excised from an agarose gel, reamplified under identical conditions, and sequenced directly, or after insertion into the pCRII cloning vector (Invitrogen).

The 5' region of the agouti cDNA was amplified by using a 5' RACE kit (GibcoBRL). Primer A4 was used for gene specific cDNA synthesis, and antisense primers A7 and A6 were used for nested PCR. The annealing temperatures were 59°C and 63°C in the first and second nested reactions, respectively. Bands of the expected size were excised from an agarose gel and

sequenced directly. The exon 1 primer A8, designed based on this sequence, was subsequently used together with primer A7, derived from the 3' end of exon 4, for amplifying and comparing cDNAs from the Red and Silver foxes, using conditions above, with an annealing temperature of 60°C.

Primers A5 and A6 were used for amplification of the second intron. PCR conditions were identical to those above, except that the annealing temperature was changed to 62°C, extension time to 90 sec, and number of cycles to 35. The resulting 1.3kb fragment was directly sequenced and shown to contain exon 2 sequence at its 5' end. This fragment was subsequently used as a probe in Southern analysis of the agouti gene.

In vitro mutagenesis. The C125R mutation was introduced into the mouse MC1 receptor coding sequence by polymerase chain reaction. Two oligonucleotides, ME1 and ME2 were designed end to end to hybridize to opposite strands and amplify an entire pBS plasmid (Stratagene) containing the complete MC1-R coding sequence. One oligonucleotide contained the sequence necessary to introduce the C123R change. Following PCR using Vent Polymerase (NEB), linear DNAs were purified by agarose gel electrophoresis, ligated and clonally isolated. The entire MC1-R coding sequence was determined using an ABI model 373 sequencer to verify that only a single amino acid change (C123R in the mouse) was present.

Mouse MC1-R expression. The mutated MC1-R (C123R) was subcloned into the pcDNA III vector (Invitrogen) for expression studies. The MC1 receptor couples through Gs to activation of adenylyl cyclase and subsequent elevation of intracellular cAMP. The ability of MC1-R (C123R) to elevate intracellular cAMP was measured following stable transfection into the human 293 cell line using a cAMP-dependent β-galactosidase assay described in detail previously (Chen et al., 1995). In this assay, a cAMP responsive enhancer element (CRE) fused to the β-galactosidase gene is used as a colorimetric assay of intracellular cAMP concentrations. Briefly, stable 293 cells expressing the wild type mMC1-R or mMC1-R (C123R) were transiently transfected with a pCRE/β-galactosidase construct using a $CaPO_4$ method (Chen and Okayama, 1987). 4 μg of pCRE/β-galactosidase DNA was used for transfection of a 10 cm dish of cells. After 15 to 24 hours, cells were split into 96-well plates with 20,000 to 30,000 cells per well and incubated at 37^0C in a 5% CO_2 incubator until 48 hours post transfection. Cells were then stimulated with different concentrations of α-MSH or Nle^4-D-Phe^7-α-MSH (NDP-α-MSH) in stimulation medium (Dulbecco's modified Eagle's medium containing 0.1 mg/ml bovine serum albumin and 0.1 mM isobutylmethylxanthine) for 6 hours at 37°C in a 5% CO_2 incubator. After stimulation, cells were lysed in 50 ml lysis buffer (250 mM Tris-HCl, pH 8.0, 0.1% Triton X-100), frozen and thawed, and then assayed for β-galactosidase activity as described (Solca et al., 1989). Data represent means and standard error from triplicate data points and curves were fitted by nonlinear regression using Prism

software (Graphpad). For competition binding experiments 293 cells stably expressing the wild-type or C123R mutation of the mouse MC1-R were incubated for 1hr at room temperature with 1nM ^{125}I-Nle^4, D-Phe^7-α-MSH (approx. 800 Ci/mMol., prepared as described (Felgner et al., 1994), and varying concentrations of cold Nle^4, D-Phe^7-α-MSH. Cells were washed twice with cold PBS, lysed, and counted in a γ-counter. Non-specific binding was determined as the counts remaining in the presence of 1 μM Nle^4, D-Phe^7-α-MSH. Data indicate the mean and standard deviation of duplicate determinations, and curves were fitted using Prizm (Graphpad Software). Data is displayed as total counts or % maximal binding.

Fox MC1-R expression. The coding region of the fox extension locus, E and EA, amplified by BAM E13 and R I E14 were subcloned into pcDNA III vector (Invitrogen) for expression studies. The ability of the fox MSH receptor to elevate intracellular cAMP was measured following transient transfection into Cos 1 cell line using cAMP RIA assay (NEN). The transient transfection was carried out by electroporation method (Bio-rad). Immediately after the electroporation, cells were split into 24 -well plate with approximately 200,000 cells per well as counted before the electroporation. RSV-luciferase construct was co-transfected with the receptor to control for the transfection efficiency. Data represent means and standard deviation from duplicate data points and curves were fitted by nonlinear regression using Prism software (Graphapad).

Competition binding experiments with the fox MC1-R were performed as described above for the mouse receptor.

GenBank accession number. Fox MC1-R: X90844, Fox agouti: Y09877

Acknowledgments

We are grateful to the Norwegian Fur Breeders' Association (DIV) and National Institutes of Health (RDC, AR42415) for financial support. We also thank Prof. Einar J. Einarsson for providing the color pictures in **Figure 4.1**.

Figure Legends

Figure 4.1 Coat color phenotypes in the fox, *Vulpes vulpes*. The nine genotypes resulting from alleles at the extension and agouti loci result in five coat color phenotypes, (**a**) Red *EEAA* , (**b**) Smoky Red *EEAa*, (**c**) Gold or Alaska Cross $EE^{A}AA$, (**d**) Silver or Blended Cross $EE^{A}Aa$, and (**e**) Silver *EEaa*, $E^{A}Eaa$,$E^{A}E^{A}aa$,$E^{A}E^{A}Aa$, or $E^{A}E^{A}AA$. The five genotypes producing the Silver coat color phenotype are termed, corresponding to the genotypic order listed above, Standard Silver, Sub-standard Silver, Double Silver, Sub-Alaska Silver, and Alaska Silver.

Figure 4.2 Sequence variants of the fox MC1 receptor and agouti peptide. (**a**) Amino acid sequence of the Red fox MC1-R. Polymorphisms present in both the E and EA alleles are indicated as multiple amino acids within a circle, while the C125R change uniquely associated with the E^{A} allele is indicated with an arrow. Shading indicates residues shared by both the mouse and fox receptors, with the first residue indicating the conserved amino acid, where relevant. The nucleotide sequence of the fox MC1-R is available under the Genbank accession numbers X90844. All known constitutively active variants demonstrated previously in mice (Robbins et al., 1993) and cattle (Klungland et al., 1995) are also indicated. (**b**) Nucleotide and amino acid sequence of the Red fox agouti peptide. Nucleotides deleted in the comparable cDNA from the Standard Silver fox are

boxed. Residues that differ in the mouse agouti sequence are indicated below the fox sequence; XXX indicates nucleotides deleted in the mouse cDNA, and --- indicates comparable fox nucleotides absent from the mouse sequence. The existing fox cDNA clones terminate 6 amino acid residues before the end of the comparable coding sequence of the mouse gene. Arrows indicate the position of introns in the mouse agouti gene; the precise intron locations in the fox gene have only been determined for the second intron. Nucleotide and amino acid sequence is available under the Genbank accession number Y09877.

Figure 4.3 RFLP analysis of the fox *extension* and *agouti* loci. (**a**) Agarose gel analysis of RFLP products of the MC1-R. Lane 1: jX174 digested with HaeIII. Lanes 2-4: Red fox (*EE*), Alaska Cross fox (E^AE), and Alaska Silver fox (E^AE^A). Molecular sizes are shown to the right. DNA is amplified by primers E5 and E8 and digested with BsaJI. The C125R change creates a new BsaJI site in the 81bp fragment, reducing it to fragments of 23 and 58 bp. (**b**). Southern hybridization analysis of agouti gene structure. Lanes correspond to Taqa I-cut genomic DNA from (left to right) the Red fox (*AA*), Smoky Red fox (*Aa*), and Standard Silver fox (*aa*) probed with sequence from intron 2 of the agouti gene. (**c**) Distribution of extension and agouti alleles among the five coat color phenotypes of the fox. C125 alleles of the MC1-R were scored as *E* while R125 alleles were scored as E^A. The deleted 2.5kb form of the agouti gene was scored as the a allele while the 3.7kb form was scored as *A*. Experimental data fit the proposed theory with one exception. More than 50% of the animals phenotyped as Alaska Cross Foxes

(*EE^{A}AA*)were heterozygous *Aa*, due to the difficulty in distinguishing this animal phenotypically from the Blended Cross fox (*EE^{A}Aa*).

Figure 4.4 Pharmacological properties of a mouse MC1-R containing the C123R mutation, and the *E* and *E^A* alleles of the fox MC1-R. (**a**) Constitutive activation of adenylyl cyclase by a mouse MC1-R containing the Alaska Silver fox (C123R) mutation. Wild type and mutant MC1 receptors were assayed by analyzing their ability to activate expression of a cAMP-responsive β-galactosidase fusion gene. Cells stably expressing each receptor and transiently expressing the fusion construct were stimulated for 6 hours with medium alone or with medium containing increasing concentrations of α-MSH , and β-galactosidase concentrations determined. Data points are the mean of triplicate determinations divided by maximal levels achieved by forskolin stimulation to normalize for transfection efficiency, and error bars represent standard deviation. Forskolin-stimulated levels of β-galactosidase activity, normalized to total cell protein were comparable in wild type (OD405nm/OD595nm=2.4) and mutant receptor transfected cells (OD405nm/OD595nm=2.2), indicating similar transfection efficiencies. (**b & c**) Competition binding studies of the mouse C123R mutant of the MC1-R. Cells permanently transfected with the wild type or C123R mutant of the mMC1-R were incubated for one hour with ^{125}I-Nle^4, D-Phe^7-α-MSH and the amounts of cold NDP-α-MSH shown. Following washing, specific counts were determined by subtracting the residual counts remaining after incubation in

the presence of 10^{-6} M cold NDP-α-MSH. Non-specific counts bound were 12% of total counts for the wild-type receptor and 69% of total counts for the C123R mutant. Data are displayed as total specific counts bound (**b**) or as a percentage of maximal specific counts bound (**c**). Data points indicate means of duplicate determinations and bars indicate standard deviation. (**d**) Coupling of the wild type fox (*E*) MC1-R to adenylyl cyclase. The fox MC1-R was transiently expressed in Cos cells and stimulated with the concentrations of α-MSH shown. Intracellular cAMP concentrations were determined by RIA. Data shown indicates mean and standard deviation from three determinations. (**e**) Lack of functional expression of the EA allele of the fox MC1-R. Competition binding experiments using 293 cells stably transfected with the receptors indicated were performed as described in b & c above. Non-specific binding was determined in the presence of 10^{-5} M α-MSH, and was 3.5% of total counts bound. Data represents the mean and standard deviation from duplicate determinations.

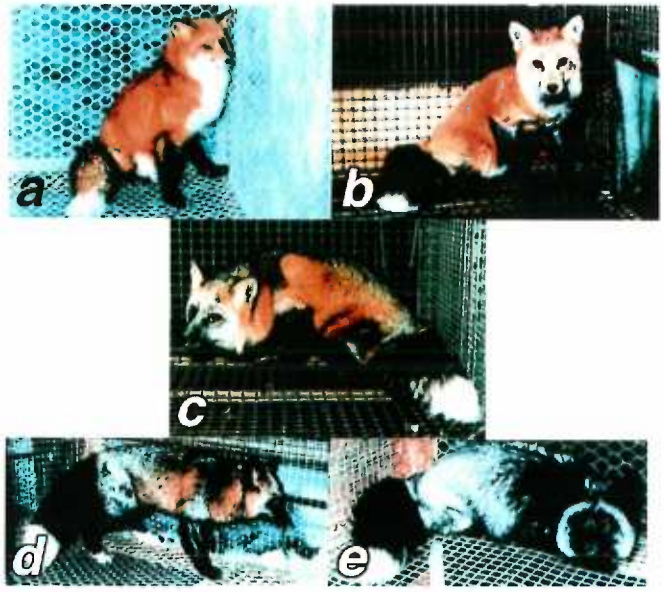

Figure 4.1 Coat Color Phenotypes in the Fox, *Vulpes vulpes*

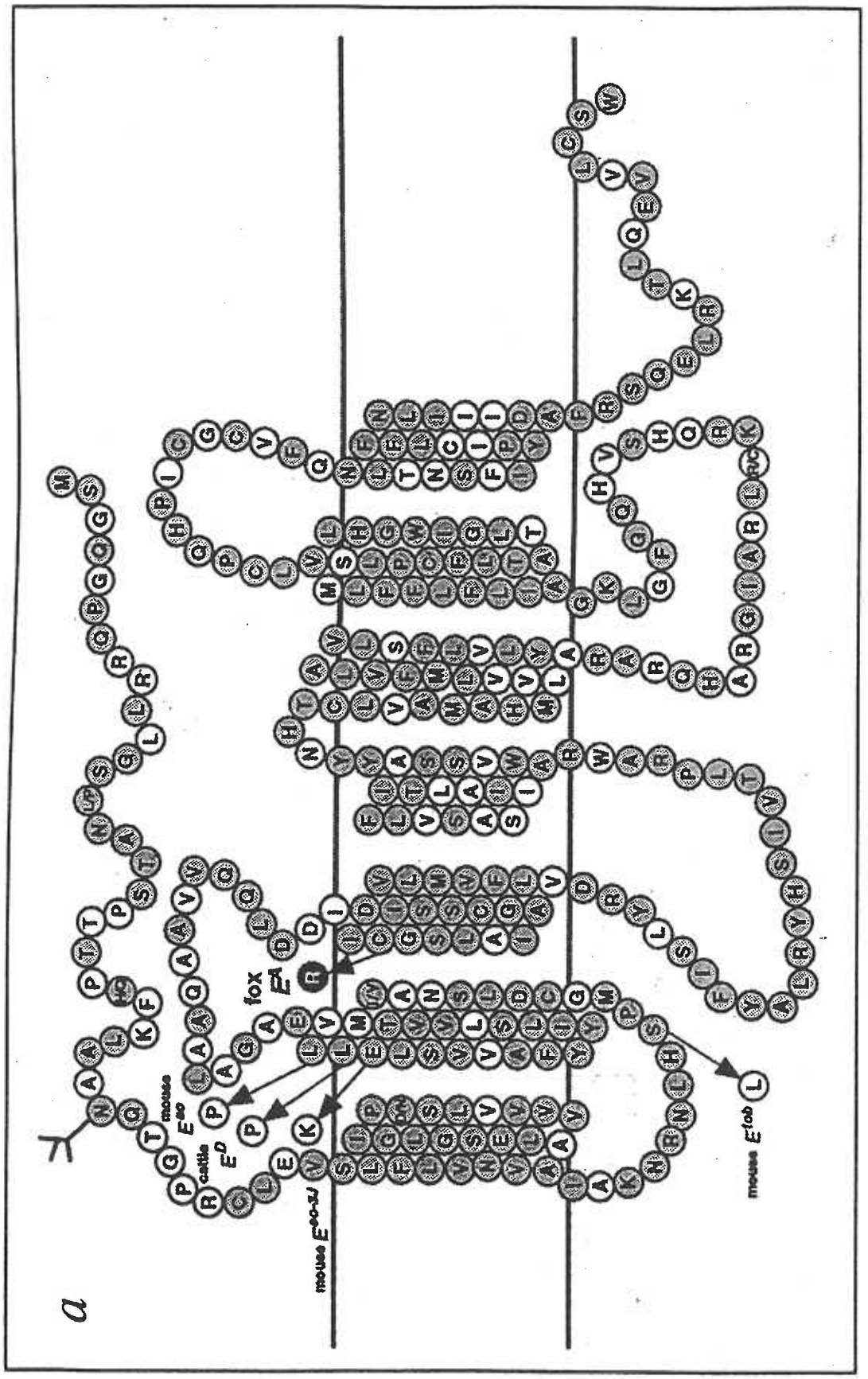

Figure 4.2a

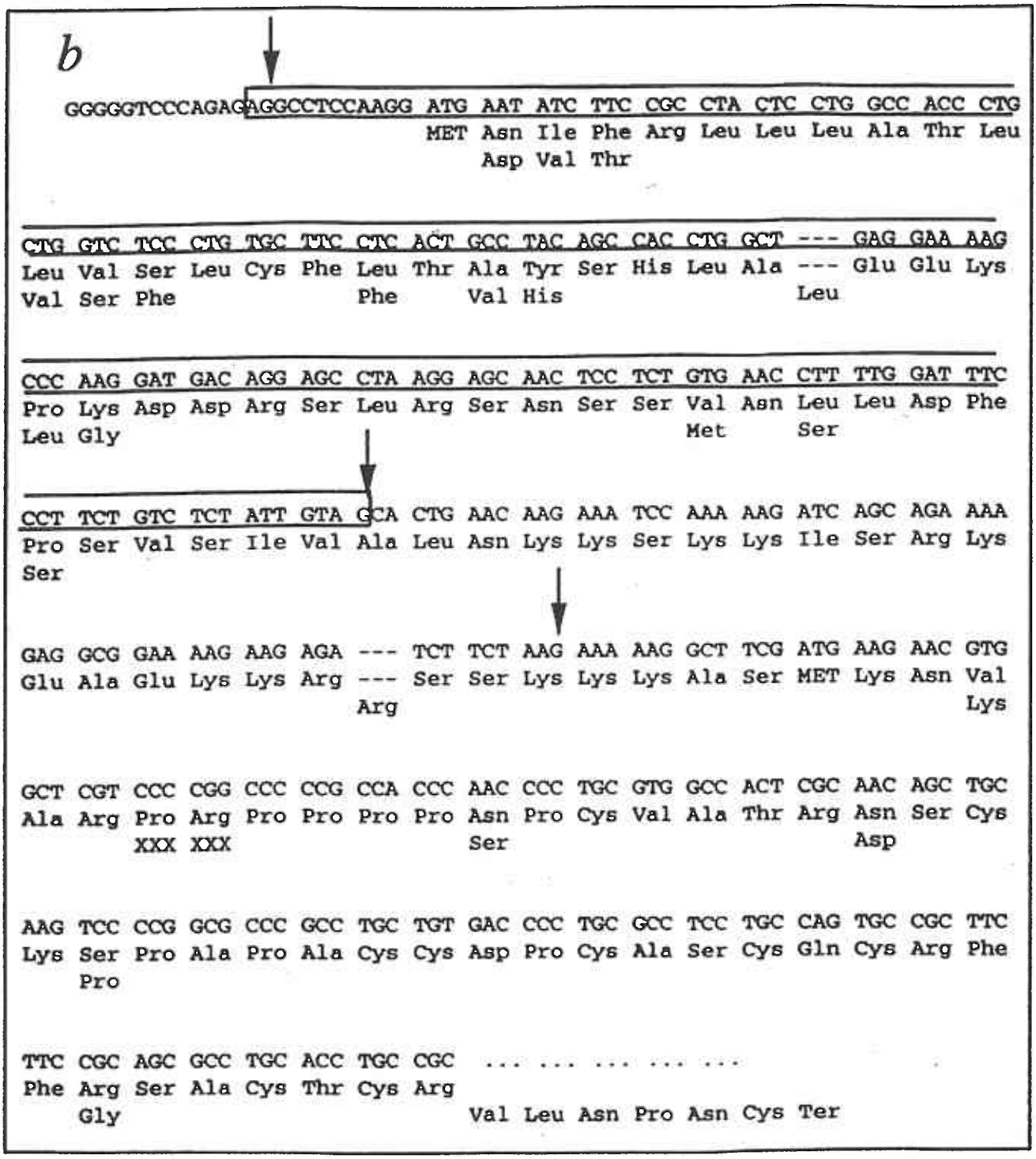
b
GGGGGTCCCAGAGAGGCCTCCAAGG ATG AAT ATC TTC CGC CTA CTC CTG GCC ACC CTG
MET Asn Ile Phe Arg Leu Leu Leu Ala Thr Leu
Asp Val Thr
CTG GTC TCC CTG TGC TTC CTC ACT GCC TAC AGC CAC CTG GCT --- GAG GAA AAG
Leu Val Ser Leu Cys Phe Leu Thr Ala Tyr Ser His Leu Ala --- Glu Glu Lys
Val Ser Phe Phe Val His Leu
CCC AAG GAT GAC AGG AGC CTA AGG AGC AAC TCC TCT GTG AAC CTT TTG GAT TTC
Pro Lys Asp Asp Arg Ser Leu Arg Ser Asn Ser Ser Val Asn Leu Leu Asp Phe
Leu Gly Met Ser
CCT TCT GTC TCT ATT GTA GCA CTG AAC AAG AAA TCC AAA AAG ATC AGC AGA AAA
Pro Ser Val Ser Ile Val Ala Leu Asn Lys Lys Ser Lys Lys Ile Ser Arg Lys
Ser
GAG GCG GAA AAG AAG AGA --- TCT TCT AAG AAA AAG GCT TCG ATG AAG AAC GTG
Glu Ala Glu Lys Lys Arg --- Ser Ser Lys Lys Lys Ala Ser MET Lys Asn Val
Arg Lys
GCT CGT CCC CGG CCC CCG CCA CCC AAC CCC TGC GTG GCC ACT CGC AAC AGC TGC
Ala Arg Pro Arg Pro Pro Pro Pro Asn Pro Cys Val Ala Thr Arg Asn Ser Cys
XXX XXX Ser Asp
AAG TCC CCG GCG CCC GCC TGC TGT GAC CCC TGC GCC TCC TGC CAG TGC CGC TTC
Lys Ser Pro Ala Pro Ala Cys Cys Asp Pro Cys Ala Ser Cys Gln Cys Arg Phe
Pro
TTC CGC AGC GCC TGC ACC TGC CGC ... ...
Phe Arg Ser Ala Cys Thr Cys Arg
Gly Val Leu Asn Pro Asn Cys Ter

Figure 4.2b

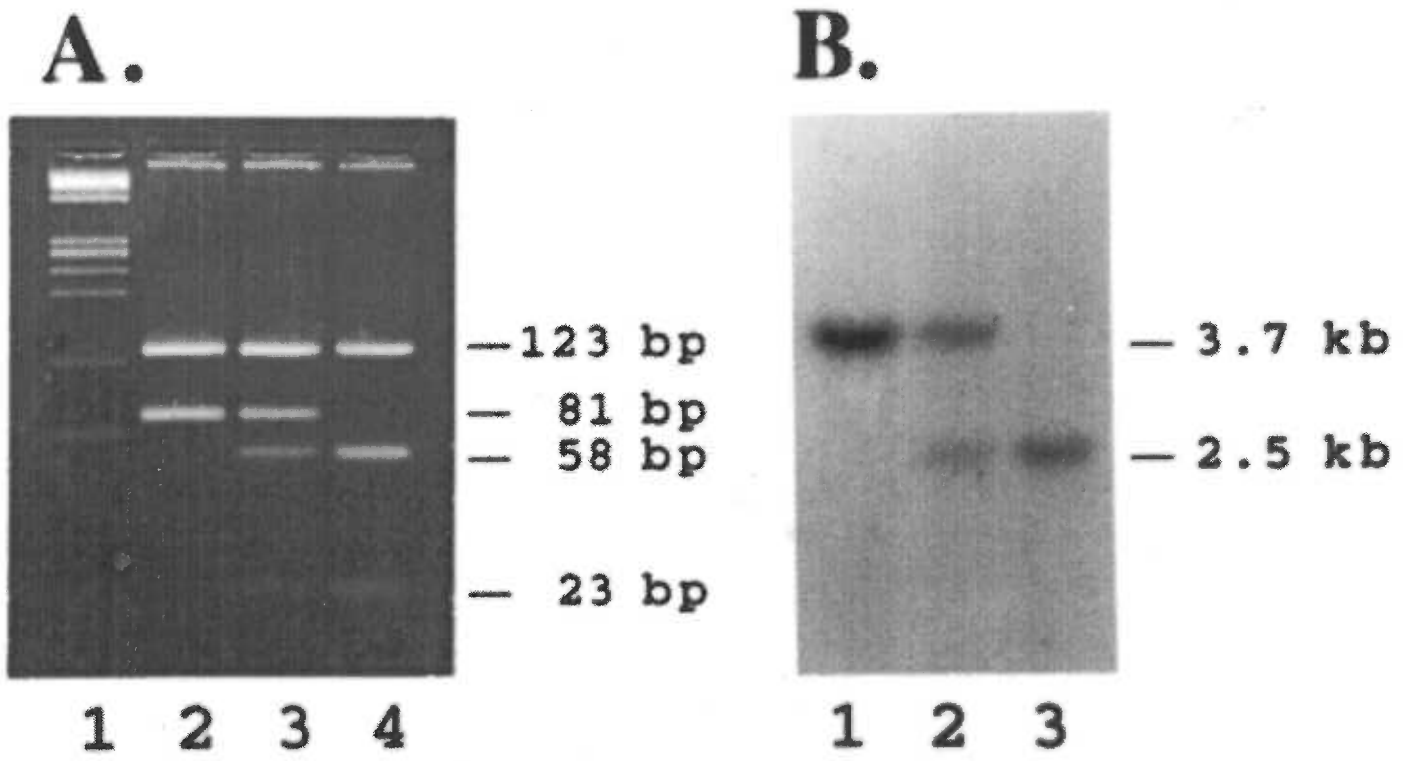

Figure 4.3a-b. RFLP Analysis of the Fox *Extension* and *Agouti* Loci.

GENOTYPE	PHENOTYPE				
	Red Fox	Smoky Red Fox	Alaska Cross Fox	Blended Cross Fox	Silver Fox
EEaa					12
EE^{A}aa					7
E^{A}E^{A}aa					0
E^{A}E^{A}AA					1
E^{A}E^{A}Aa					0
EE^{A}Aa			16	3	
EE^{A}AA			15		
EEAa		27			
EEAA	7				

Figure 4.3c

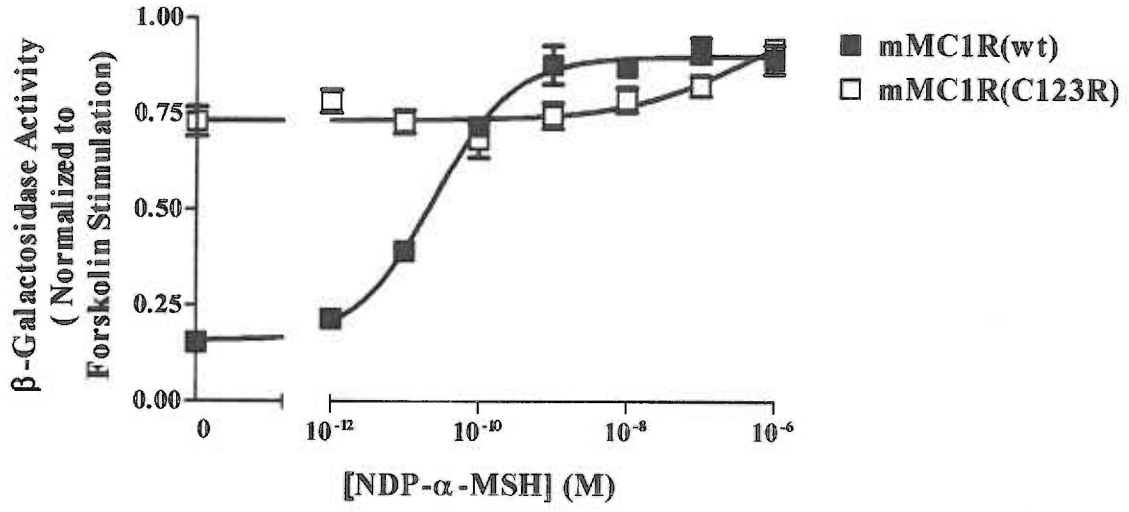
β-Galactosidase Activity
(Normalized to
Forskolin Stimulation)
1.00
0.75
0.50
0.25
0.00
0
10-12
10-10
10-8
10-6
[NDP-α-MSH] (M)
mMC1R(wt)
mMC1R(C123R)

Figure 4.4a

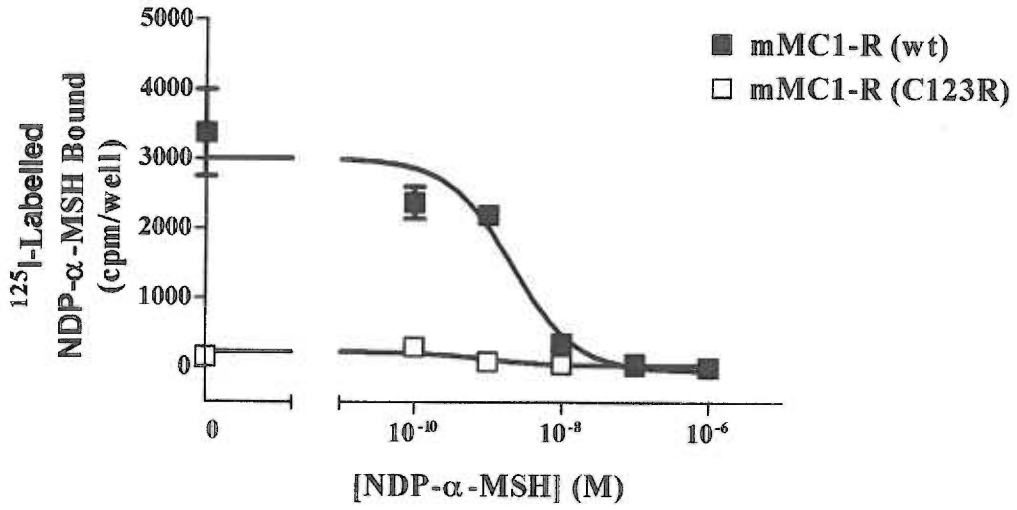

Figure 4.4b

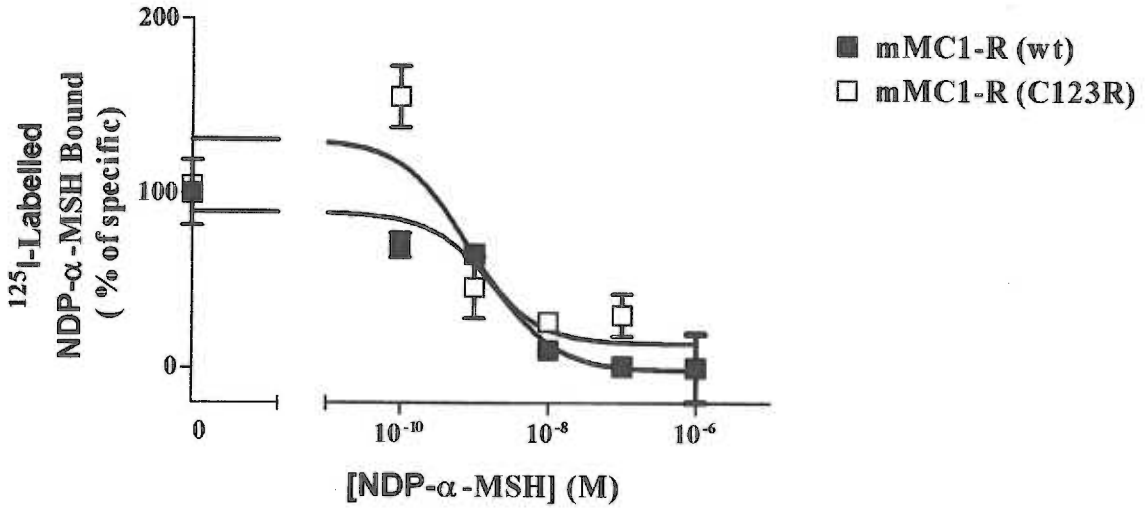

Figure 4.4c

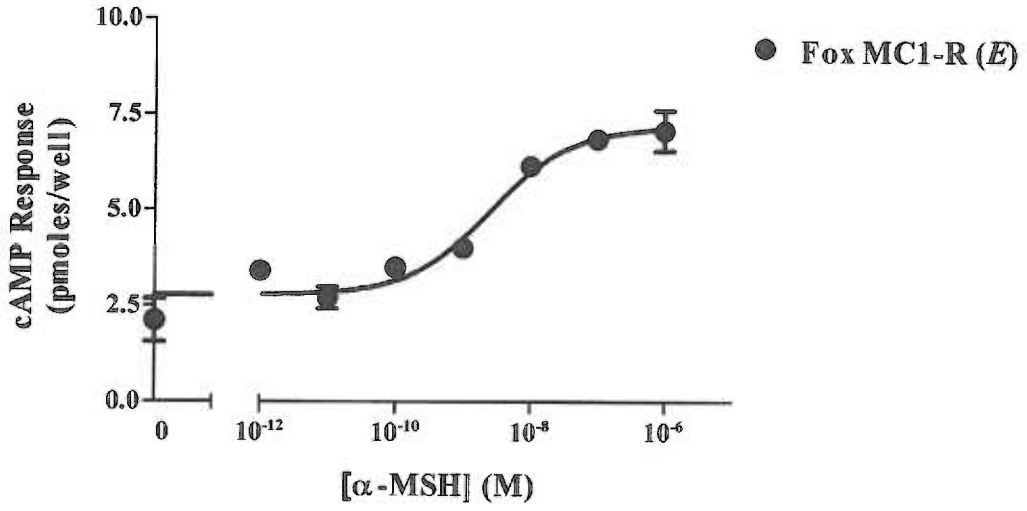

Figure 4.4d

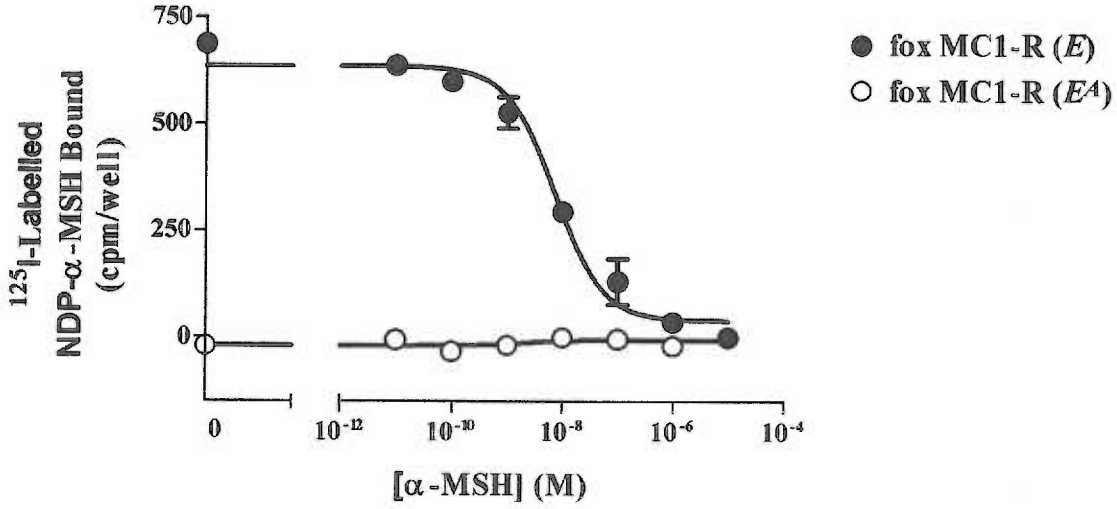

Figure 4.4e

Chapter 5

A Ligand-Mimetic Model for Constitutive Activation of the Melanocortin-1 Receptor

Dongsi Lu, Dag Inge Vage, and Roger D. Cone

The Vollum Institute for Advanced Biomedical Research (D.L., R.D.C.)
Oregon Health Sciences University
Portland, OR 97201

Department of Animal Science (D.I.V.)
Agricultural University of Norway
P.O. Box 5025
N-1432 As, Norway

Roger D. Cone
Vollum Institute for Advanced Biomedical Research
3181 S.W. Sam Jackson Park Road
Portland, OR 97201
ph. 503 494-4668
fax 503 494-4534
email: cone@ohsu.edu

running title: Model for activation of the MC1-R

ABSTRACT

Dark coat color in the mouse and the fox has been demonstrated to result from constitutively activated melanocortin-1 receptors. Receptor mutations in the mouse (E92K, L98P), cow (L99P), fox (C125R) and sheep (D119N) cluster near the membrane/extracellular junctions of the second and third transmembrane domains. This negatively charged domain, which includes D115, is a likely site of electrostatic interaction with an essential arginine residue in the ligand. We show here that for the transmembrane residues E92, D119, and C125, conversion to a basic residue is required for constitutive activation of the receptor. The acidic residue D119 is required for high affinity ligand binding. Furthermore, these constitutively activating mutations result in greatly reduced agonist efficacy and affinity, in contrast with many of the mutations of this type in other receptors that increase agonist affinity. Therefore, we propose that the E92K, L98P, and C125R mutations do not activate the receptor by directly disrupting intramolecular constraints on formation of the active high affinity state, R*, but rather by mimicking the insertion of a basic residue that also occurs during ligand binding, thereby decreasing ligand binding affinity.

INTRODUCTION

The melanocyte-stimulating hormone receptor (MSH-R or MC1-R) regulates the eumelanin/phaeomelanin switch in melanocytes, controlling the relative amount of yellow-red phaeomelanin and brown-black eumelanin pigments ultimately deposited in skin and hair (Cone et al., 1996). The MC1-R couples through Gs to adenylyl cyclase to stimulate tyrosinase, the rate limiting enzyme in the synthesis of both classes of melanin pigments (Hearing and Jimenez, 1987; Hearing and Tsukamoto, 1991). For reasons that are not yet understood, basal levels of tyrosinase expression lead largely to phaeomelanin synthesis while elevated levels of tyrosinase, resulting from α-MSH stimulation of melanocytes, diverts intermediates primarily along the eumelanin synthetic pathway (Hearing, 1987; Hearing and Jimenez, 1987; Hearing and Tsukamoto, 1991).

Two genetic loci known to regulate the eumelanin/phaeomelanin switch are *agouti* and *extension*, and most domesticated animals have multiple alleles at each of these loci (Searle, 1968). The *agouti* and *extension* alleles in concert determine the distribution of phaeomelanin and eumelanin, both along each hair shaft as well as spatially along the coat of the animal. Dominant alleles at *extension* result in dark brown or black coat color while animals homozygous for recessive alleles have yellow or red coats; the opposite is true for *agouti* alleles. The identification of the MC1-R as the *extension* locus in the mouse led to the finding that a point mutation, E92K, in the dominant allele, $E^{So\text{-}3J}$, resulted in a receptor that was

constitutively active, defined as being able to significantly elevate adenylyl cyclase activity in the absence of ligand (Robbins et al., 1993). A second dominant allele, E^{tob} (L69S), found in the wild tobacco mouse appeared to produce a hyperactive receptor that could yield greater levels of cyclase activity when exposed to the same ligand concentrations as the wild type receptor. A third allele (E^{so}, L98P) was found in an independent occurence of the Sombre phenotype, and also produces a constitutively active receptor (Cone et al., 1996). More recently, a second constitutively active MC1-R has been characterized in the red fox, *Vulpes vulpes* (Vage et al., 1997). In this animal, a C125R change in the third membrane spanning domain produces the dark black morph, known as the Alaska silver fox. Additional dominant mutations in the MC1-R have now been reported in cattle (Klungland et al., 1995), and in chickens (Takeuchi et al., 1996), however these mutations have not yet been characterized pharmacologically.

Constitutively active G protein-coupled receptors (GPCRs) were first identified in chimeras of the α_1- and β_2-adrenergic receptors (Cotecchia et al., 1990). Ultimately, this effect was mapped to residues at the C-terminal end of the third intracellular loop, and in particular, the replacement of an alanine at position 293 with any other residue was found to increase the basal activity of the receptor and enhance the affinity for ligand as much as 100 fold (Kjelsberg et al., 1992). Following the identification of naturally occurring constitutively active MC1 and rhodopsin molecules, activating mutations in GPCRs were found to be

responsible for a diverse array of inherited as well as somatic genetic disorders including hyperfunctioning thyroid adenomas (Parma et al., 1993; Porcellini et al., 1995; Van Sande et al., 1995), autosomal dominant hyperthyroidism (Tonacchera et al., 1996; Tonacchera et al., 1996; Vassart et al., 1995), familial precocious male puberty (Laue et al., 1995; Shenker et al., 1993; Yano et al., 1995), metaphyseal chondrodysplasia (Schipani et al., 1995), familial hypoparathyroidism (Pollak et al., 1994; Tominaga and Takagi, 1996), and congenital night blindness (Dryja et al., 1993; Rao et al., 1994).

While constitutively activating mutations have been found in virtually all domains of the GPCR, some mechanistic similarities are commonly found. Many constitutively active receptors demonstrate a higher affinity for agonist and lower EC_{50} for further activation (Shenker et al., 1993; Van Sande et al., 1995). In some cases the increased affinity for agonist, but not antagonist, was dramatic (Ren et al., 1993), and the correlation between agonist efficacy and increased affinity for constitutively active mutants (Samama et al., 1993) led to a proposed modification of the ternary complex model for GPCR activation (DeLean et al., 1980). The established model holds that agonist binding stabilizes the active conformation (RG*) of the receptor in a complex with G protein while antagonists typically bind equally well to R and R*. Based on the identification and characterization of constitutively active GPCRs, an extended or "allosteric ternary complex" model was proposed in which receptor, independent of ligand binding, is in equilibrium between an inactive and active conformation (Lefkowitz et al., 1993).

Mutations that constitutively activate receptors are proposed to disrupt internal constraints in the receptors, make the receptors less conformationally constrained (Gether et al., 1995), and therefore decrease the energy required to reach the R* state. The model thus explains the increased affinity of agonists for constitutively active receptors, even in the absence of G protein, since constitutive activation results in a higher percentage of receptors in the high affinity R* state.

The two constitutively activating mutations of the mMC1-R, an E92K change near the extracellular margin of the second transmembrane domain and an L98P change approximately two turns in the α-helix above E92 were predicted to activate the receptor by directly disrupting an internal constraint resulting from an electrostatic interaction between E92 and another unidentified residue (Robbins et al., 1993). The L98P was predicted to alter the constraint involving E92 by disrupting the α-helical structure of the second transmembrane domain in which E92 was found. A similar model was proposed for a K296E mutation found in the seventh membrane spanning domain of rhodopsin in a family with retinitis pigmentosa (Robinson et al., 1992). This mutation, which occurs at the site of covalent attachment of the retinal chromophore, was found to produce an opsin that was capable of fully activating transducin in the absence of light or retinal. Twelve different amino acid substitutions at this position have been examined, and only the basic lysine or arginine residues prevent constitutive activation of the receptor (Cohen et al., 1993). Furthermore, a glutamic acid at position 113 is generally accepted as a counterion of the Schiff base linkage

between K296 and retinal (Nathans, 1990; Sakmar et al., 1989), and mutagenesis of this glutamic acid residue to a Gln also constitutively activates rhodopsin (Robinson et al., 1992).

Remarkably, however, in contradiction to the allosteric ternary complex model the E92K, L98P, and C125R mutations that constitutively activate the MC1-R activate basal receptor activity but dramatically lower agonist affinity and efficacy. We show here that these mutations do not directly disrupt internal constraints favoring the inactive receptor conformation. Rather, these constitutively activating mutations cluster in a negatively charged domain of the receptor predicted to interact electrostatically with an arginine residue in the agonist that is required for high affinity binding. We demonstrate that introduction of a basic residue in this region of the receptor is essential for constitutive activation, and propose that these mutations activate the receptor by ligand-mimicry.

RESULTS

Insertion of a Basic Residue at Position 92 is Required for Constitutive Activation of the Sombre Mouse Allele ($E^{So\text{-}3J}$)

To understand the mechanism of constitutive activation of the MC1-R, in vitro mutagenesis was performed at a number of positions in the receptor identified as activating positions in the mouse (E92, L98P), fox (C125), and sheep (D119), and at a conserved position, D115, in this same domain (**Figure 5.1**). Agonist efficacy was determined using the native peptide ligand, α-MSH, and a synthetic ligand, NDP-α-MSH, which has a higher affinity for receptor.

Glutamic acid 92 of the murine MC1-R was mutated to alanine, aspartate, lysine, glutamine and arginine to determine requirements at this position for constitutive activation. All changes in position 92 increased the EC_{50} for activation of the mutant receptors by either α-MSH or NDP-α-MSH (**Fig. 5.2A-B and Table 5.1**). Only introduction of a basic lysine or arginine at this position resulted in constitutively active receptors. Both receptors containing basic residues at position 92 showed elevated basal cAMP-responsive β-galactosidase activity, even in the absence of hormone stimulation. The basal level of the E92K mutant receptor was about 30% to 50% of the maximal stimulation level of the wild type receptor achieved by treatment with 10^{-6} M α-MSH or NDP-α-MSH. However, the E92K mutant receptor could be fully activated by NDP-a-MSH to levels

comparable to the wild type receptor. The basal activity of the E92R mutant was about 60% to 90% of the maximal stimulation level of the wild type receptor, and the mutant receptor was not further activated by NDP-α-MSH.

Competition binding studies (**Fig. 5.2C-D and Table 5.1**) demonstrated that IC_{50} values for the E92A (1.07±0.53 nM) and E92D (8.05±4.34 nM) mutant receptors remained similar to the wild type (0.79±0.48 nM). However, IC_{50} values for the E92K and E92Q mutants were increased to 423±226 nM and 3230±1930 nM, respectively. Binding to the E92R mutant receptor could not be detected. Mutations at this position also dramatically lowered the amount of ligand binding detected in competition studies (**Fig. 5.2C**), whether as a consequence of a reduction in receptor affinity (E92K), receptor number (E92A), or perhaps both. Scatchard analysis (**Fig. 5.2E**) supported the competition binding data, and indicated a 10-fold increase in *K*d for the E92K receptor (6.41 ±2.52nM versus 0.62±0.3 for the wild type).

Insertion of a Proline Residue Adjacent to E92 Constitutively Activates the MC1-R in Cattle (E^D) and in an Independent Occurrence of the *Sombre* Mouse (E^{so})

Two proline insertion events, L98P in an independent occurence of the *Sombre* phenotype in mice (Robbins et al., 1993), and L99P in black Icelandic Cattle (Klungland et al., 1995) have been found to be linked to dominant MC1-R alleles.

Preliminary data demonstrated that the murine L98P receptor was constitutively active (Cone et al., 1996). The L98P receptor has a basal activity equal to 30% to 50% of the maximal stimulation level of the wild type receptor (**Fig. 5.3A-B and Table 5.2**). The L98P mutant receptor can be slightly activated by α-MSH, and nearly fully activated by NDP-α-MSH. Similar to the E92K and E92R mutants, the L98P mutant demonstrates constitutive activity and an increase in EC_{50} from 0.016±0.005 nM to 3.27±0.19 nM. The IC_{50} for the L98P mutant receptor (301±54 nM) was also 100 fold higher than the wild type receptor (**Fig. 5C-D and Table 5.2**).

While the L99P change in the bovine receptor was not characterized pharmacologically, it might be expected to behave similarly to the murine L98P mutation. To test the limits of the domain in which a proline insertion will constitutively activate the receptor, an E100P mutation was also constructed and tested pharmacologically. This mutant was found to be very similar to the wild type receptor, with comparable EC_{50} and IC_{50} values (**Fig. 5.3A-D and Table 5.2**).

Mutation of Conserved Basic Receptor Residues H183, H258, and K276 Does Not Constitutively Activate the MC1-R

An hypothesis for constitutive activation of rhodopsin is that an ionic bridge between K296 and E113 constrains the receptor in an inactive conformation,

since removal of the charge at either position will activate the receptor in the absence of light or retinal (Cohen et al., 1992; Robinson et al., 1992). The requirement of a basic residue at position 92 for constitutive activation, rather than simple ablation of the negative charge, argues against a similar model for the MC1-R. Nevertheless, to test for basic residues that might stabilize the receptor via an electrostatic interaction with E92 we mutagenized all three conserved basic residues that might be in a position to interact with this residue. In theory, disruption of such a residue should also result in a constitutively active receptor.

The three residues, H183, H258 and K276 were mutagenized to negative charged residues, as well as to other amino acids, however no constitutive activation resulted (**Fig. 5.4A-B** and **Fig. 5.5A-B**). The EC_{50} for NDP-α-MSH stimulation was unchanged for the receptor with a H258E change while the EC_{50} for α-MSH stimulation was significantly increased. Introduction of isoleucine or tryptophan at this position increased the EC_{50} for NDP-α-MSH stimulation by 5 and 20-fold, respectively, and made the receptor nearly resistant to α-MSH stimulation. All three mutations decreased the IC_{50} for competition binding of NDP-α-MSH by 100-fold or more (**Table 5.3**). Quite differently, the H183E and K276E mutant receptors showed wild-type activation and binding properties. The two other K276 mutant receptors, K276A and K276L, showed about a 10 fold increase in EC_{50} for α-MSH stimulation but no change in the EC_{50} for NDP-α-MSH and no change in the IC_{50} (**Table 5.3 and 5.4**). Thus, removal of potentially basic

residues at positions 183, 258, and 276 not only does not activate the receptor, but suggests these residues have no major role in ligand binding or activation.

Insertion of a Basic Residue at Position 123 is Required for Constitutive Activation of the Alaskan Silver Fox Allele (E^A)

Recently, a mutation of a conserved cysteine at position 125 (equivalent to C123 in the mouse) to an arginine has been found to be associated with a dominant *extension* locus allele responsible for dark coat color seen in the Alaska Silver fox (Vage et al., 1997). The C123 residue is found in the middle of transmembrane domain III, and was analyzed in a similar fashion to the E92 position. This residue was mutagenized from a non-charged polar residue to a non-polar residue of similar size (alanine), an acidic residue (glutamate), and two basic residues (lysine and arginine). In parallel with the E92 position, only the insertion of a lysine or arginine at this position were found to constitutively activate the receptor (**Fig. 5.6A-B**). C123K and C123R changes both constitutively activated the receptor to about 30% to 40% of the maximal stimulation level. These four mutations have wild type IC_{50}s for ligand binding (**Fig. 5.6C-D and Table 5.5**), indicating that C123 is not directly involved in ligand binding. Since the C123A change had no effect on ligand binding or activation of the receptor, it can be inferred that the disulfide bonding capability of the cysteine plays no detectable role in ligand binding or receptor activation . Interestingly, this position behaved very similarly to the E92 position, in that constitutive activation resulting from the

insertion of a basic residue greatly decreased the effectiveness of both α-MSH and NDP-α-MSH in further activation of the receptor (**Fig. 5.2A-B**).

Mutagenesis of Either of Two Closely Spaced Aspartates (D115 & D119) Leads to Constitutive Activation, With the Latter Change Being Associated With a Dominant Extension Allele in the Sheep (E^D)

Independent of any genetic data implying a role in constitutive activation, *in vitro* mutagenesis studies were carried out on two aspartate residues, D115 and D119, located near the junction between the presumed second extracellular loop and transmembrane domain III. With E92 apparently not involved in ligand binding, these two residues are the only other conserved acidic residues in a position to interact electrostatically with the arginine residue in the H-F-R-W pharmacophore of ligand a-MSH. Midway through the study, it was learned that the D119N change is associated, together with a M71K change, with a dominant *extension* locus allele in the sheep (DIV, unpublished data). The D119 position was mutagenized to three different amino acids, lysine, asparagine, and valine. In parallel with the E92 and C123 positions, elevated basal level of cAMP-response β-galactosidase activity equivalent to about 20% to 40% of the maximal stimulation level of the mMC1-R, was only seen following the insertion of a basic residue at this position (**Fig. 5.7A-B, Table 5.6**). Likewise, neither one of the three mutant receptors could be activated by α-MSH, while all three were activated by NDP-α-MSH at greatly reduced efficacy . In contrast with changes

at E92 and C123, all three D119 variants demonstrated a 10-100 fold increase in IC_{50} values for competition of NDP-α-MSH binding in comparison with the wild-type receptor, implying a contribution of D119 in high affinity ligand binding (**Fig. 5.7C-D and Table 5.6**).

The D115 was mutagenized to three different amino acids, glutamate, lysine and valine. In contrast to positions 92, 123, and 119, at which basic residues appear to be required for constitutive activation, any replacement of the aspartate at position 115 elevated the basal activity of the receptor (**Fig. 5.8A-B**). In fact, even replacement of the aspartate with glutamate constitutively activated the receptor, demonstrating the importance of the size of the residue as well as the charge. Constitutive activation by mutations at this position did not appear to be consistently associated with a reduction in ligand efficacy, since, for example, the EC_{50}s for activation of the D115 and D115K receptors by NDP-α-MSH were comparable (**Table 5.7**). While D115E had an affinity for ligand comparable to the wild type receptor, replacement of the negative charge with either valine or lysine produced a 2.5 and 100-fold increase in IC_{50}, respectively (**Fig. 5.8C-D and Table 5.7**).

An M71K Mutation, Found Near the Intracellular Half of Transmembrane Domain 2 of the E^D Allele of the Sheep, Has Constitutive Activity Independent of the D119N Mutation

The M71K and D119N mutations appear to coexist in the E^D allele of the sheep MC1-R (D.I.V., unpublished data). As mentioned above, the D119N mutation alone in the context of the mouse MC1-R did not constitutively activate the receptor. Consequently, we tested the effect of M71K alone, and M71K plus D119N together in the mMC1-R. The M71K change alone potently activated the MC1-R to approximately 40% of maximal levels (**Fig. 5.9A-B**). Additionally, this receptor could be further activated to maximal levels by either α-MSH or NDP-α-MSH with EC_{50}s 10- and 50-fold higher than the wild type receptor, respectively. The IC_{50} for the M71K receptor was approximately four times lower than that of the wild type receptor (**Table 5.8**).

Introduction of the D119N change back into the M71K single mutant resulted in a receptor with properties more reminiscent of the E92K and C123R mutations. The addition of the D119N change reduced the extent of constitutive activation of the receptor, reduced the efficacy of NDP-α-MSH 4-fold, and reduced the efficacy of a-MSH to undetectable levels.

Removal of All Three Acidic Residues, E92, D115, and D119, Still Yields a Constitutively Active Receptor

Insertion of a positive charge in the second or third membrane spanning domain could be argued to create an electrostatic interaction between the two membrane spanning domains that results in a partially active receptor conformation. To test this hypothesis, we constructed four different receptors with two or three basic residue substitutions. Even when all three conserved acidic residues, E92, D115, and D119, are replaced with lysines, the receptor remains constitutively activated. Thus, once insertion of a single basic residue occurs, removal of the remaining acid residues does not inactivate the receptor. The most potent constitutive activation appeared to occur when both transmembrane domains 2 and 3 were replaced with a single basic residue each. Additionally, insertion of multiple basic residues appeared to remove responsiveness even to the potent NDP-α-MSH ligand (**Fig. 5.10A-B**).

DISCUSSION

Introduction of a basic residue near the extracellular face of transmembrane domains 2 and 3 is one mechanism for constitutive activation of the MC1-R

The E92K mutation in the $E^{so\text{-}3J}$ allele of the murine MC1-R was originally proposed to constitutively activate the receptor by disrupting an intramolecular electrostatic interaction that constrained the receptor in an inactive conformation (Robbins et al., 1993), in parallel with the constraint demonstrated to exist between K296 and E113 of rhodopsin (Robinson et al., 1992). The data presented here argue strongly against this original model.

First, if the glutamic acid residue at position 92 is essential for the formation of an electrostatic interaction that constrains the receptor in an inactive conformation, then any change that removes the negative charge at this position should cause constitutive activation of the MC1-R. However, only the insertion of a lysine or arginine at this position activated the receptor, while alanine, aspartate, isoleucine, and glutamate did not (**Fig. 5.2**). Second, we were unable to find any conserved basic residues in the receptor that could serve as a potential counterion for E92 (**Fig. 5.4 and 5.5**). His183, His258 and Lys276, the only basic residues in or adjacent to the extracellular half of the transmembrane domains, were mutagenized to test their potential as counterions. The His183 is conserved in both MC1-R and MC2-R, the His 258 is conserved in all five melanocortin

receptors, and the K276 is unique for the MC1-R. If any of these basic residues interact electrostatically with the glu 92 then removing the positive charge at these positions should produce a pharmacological phenotype similar to E92K. Seven mutations were made at these three positions and none of them caused constitutive activation of the MC1-R. Interestingly, the IC_{50} of all three mutations of His 258 increased dramatically compared to the wild type receptor, indicating that this residue might be involved in the binding pocket of the receptor. All other mutations at either His 183 or Lys 276 positions did not cause significant functional changes of the receptor. These observations excluded both residues from playing important roles in ligand receptor interaction.

Remarkably, two additional residues were identified with properties very similar to E92. C125R is a mutation found as a dominant allele of the MC1-R in the darkly pigmented Alaska silver (Vage et al., 1997). When this mutation was introduced into the mMC1-R (C123R), the receptor was constitutively activated. In order to find out the mechanism of this mutation, more mutations encoding a variety of amino acid residues at the same position were constructed (**Fig. 5.6A-B**). Again, only changes to lysine or arginine resulted in constitutive activation. A change from cysteine to alanine resulted in a receptor that was identical to the wild type, suggesting that the disulfide bonding capability of the cysteine does not play a role in ligand binding or receptor activation. Surprisingly, all four mutant receptors have similar IC_{50}s to the wild type receptor,

even though the total binding of ^{125}I-NDP-α-MSH to the C123R receptor is significantly decreased (**Fig. 5.6C-D**).

The D115 and D119 share a common feature with E92, being the only conserved negative charges in the extracellular half of the transmembrane bundles. This observation led us to investigate the role of these residues in MC1-R function. Similar to the effects seen at E92 and C123, only the introduction of a positive charge at D119 caused constitutive activation of the receptor (**Fig 5.7A-B**).. While this study was in progress, a D119N change was identified that correlated with a dominant *extension* locus allele in the black Norwegian sheep (DIV, unpublished data). This allele also contained an M71K change, which is described in more detail below.

Identification of D119 as a potential component of the ligand binding site

Glu 92, asp 115, and asp 119 are conserved in all five melanocortin receptors and are the only conserved acidic residues existing in the presumed exterior part of the transmembrane domains that would thus be in a position to readily interact as counterions with the essential arginine residue in the H-F-R-W pharmacophore of α-MSH (Eberle, 1988). Two independent modeling studies of the MC1-R have identified this negatively charged domain as part of the ligand binding pocket (Frandberg et al., 1994; Haskell-Luevano et al., 1995; Haskell-Luevano et al.,

1996). Introduction of non-basic residues at positions 92 and 115 had no effect on the affinity of ligand binding as assessed in competition binding studies. In contrast, All three D119 variants constructed demonstrated a 10-100 fold lower affinity for NDP-α-MSH, pointing to this residue as a likely site of electrostatic interaction for arg8 of ligand (**Fig. 5.7C-D**).

Constitutive activation via mutations in the negative charge domain reduces ligand affinity and ligand efficacy

Generally, constitutively activating mutations in GPCRs have been found to have increased affinity for, and increased sensitivity to, agonist (Klebig et al., 1995; Ren et al., 1993; Samama et al., 1993; Shenker et al., 1993; Van Sande et al., 1995). Furthermore, the degree of constitutive activity is proportional to the increase in ligand affinity and efficacy. Surprisingly, the opposite was the case for activating mutations at E92, C123, and D119. Insertion of basic residues at these positions uniformly decreased apparent affinity for α-MSH and NDP-α-MSH, and greatly decreased the efficacy of these agonists (**Figs. 5.2, 5.6, 5.7**). Scatchard analysis of one mutation, E92K, demonstrated a 10-fold decrease in affinity of the receptor for NDP-α-MSH from 0.62nM to 6.4nM (**Fig 5.2E**). In some cases, agonist efficacy could only be demonstrated with the use of the superpotent agonist NDP-α-MSH.

Two proline mutations near the extracellular margin of the second membrane spanning domain have also been found associated with dominant *extension* locus alleles, L98P in the sombre mouse (Cone et al., 1996; Robbins et al., 1993), and L99P in darkly pigmented cattle (Klungland et al., 1995). The L98P receptor showed the same pharmacological properties as the E92K, C123R, and D119K mutant receptors (**Figs. 5.3, 5.2, 5.6, and 5.7**). These data suggest that the packing of the second and third transmembrane domains is critical for activation of the MC1-R, and that insertion of basic residues at E92, C123, and D119, or insertion of prolines near the extracellular margin of the second membrane spanning domain may be alternative ways to accomplish this. A proline introduced in position 100 of the receptor had no effect on receptor function, suggesting that this residue may be just outside the a-helical transmembrane domain (**Fig. 5.3 and Table 5.2**).

Replacement of all three acidic residues from the negatively charged ligand binding domain still constitutively activates the MC1-R

Given the potential proximity of E92, D115, and D119 in space, it is possible that significant repulsion results between TM2 and TM3. Introduction of positive charge by mutagenesis or by ligand binding could thus reduce this repulsion between the transmembrane domains as part of the conformational change involved in forming R*. To test this hypothesis, receptors were constructed in which multiple positive charges were introduced. Both the E92K/D115K and

E92K/C123R double mutant receptors have basal levels of cAMP-dependent β-galactosidase activity which are greater than that of either mutation alone, suggesting that addition of positive charge constitutively activates the receptor via independent and additive mechanisms (**Fig. 5.10**). Furthermore, even replacement of all three conserved acidic residues, E92, D115, and D119, with lysines produces a constitutively active receptor that has now lost any detectable responsiveness, even to the superpotent ligand NDP-α-MSH (**Fig 5.10**). These data make it difficult to support a model in which a specific interaction between the negatively charged residues in transmembrane domains 2 and 3 is disrupted in process of constitutive activation. Rather, the mutations may be independently altering the structures of the TM2 and TM3 helices.

Alternative mechanisms for constitutive activation of the MC1-R

Our results suggested the involvement of a novel mechanism for the constitutive activation of the MC1 receptor by the D119 and M71 mutations. In contrast to other mutations in the negatively charged ligand binding domain, at which basic residues are required for constitutive activation, replacement of the aspartate at D115 with any other residue will cause constitutive activation (**Fig. 5.8**). This observation tends to suggest that the D115 may be involved in an electrostatic interaction or hydrogen bond that may serve to constrain the receptor in an inactive conformation. It is possible, however, that D115 is not in a transmembrane milieu, but rather in the first extracellular loop. As such, the

constraining interaction may involve residues in this or other extracellular loops that have not yet been studied. Additionally, constitutively activating mutations at this position did not consistently decrease ligand affinity or efficacy, suggesting a different mechanism of action from the L98P, E92K, C123R, and D119K mutations.

The M71K mutant receptor showed a unique profile compared to mutations in the negatively charged ligand binding domain (**Fig. 5.9**). The efficacy and affinity of α-MSH appeared to be slightly increased. Considering the specific location of this mutation near the first intracellular loop, this mutation is most likely having a more direct effect on the interaction on the stability of the R*G complex. Consequently, this receptor appears pharmacologically like those that stabilize R* thus increasing apparent affinity for agonist, as a consequence of mutations that are not proximal to the ligand binding site.

Ligand-Mimetic Models for Constitutive Activation of the MC1-R

According to the ternary allosteric complex model, all constitutively activating mutations of the GPCRs should have a reduction in the energy barrier that must be overcome in the R to R* transition (Lefkowitz et al., 1993; Samama et al., 1993). This transition may actually have many states, however, as is indicated in biophysical studies of rhodopsin (for review see Rao and Oprian, 1996), as the information resulting from ligand binding is transferred across the receptor to

intracellular domains that couple with heterotrimeric G protein to catalyze GDP release. This may be reflected in multiple mechanisms of constitutive activation as reported here for the MC1-R, from alterations very proximal to ligand binding to those proximal to G protein coupling.

Early studies of adrenergic receptors identified several residues in the third intracellular loop, known to be a region involved in G protein coupling (Cotecchia et al., 1990), that enhanced the basal activity while also demonstrating increasing agonist affinity and efficacy (Cotecchia et al., 1990; Ren et al., 1993; Samama et al., 1993). Many subsequent activating mutations characterized in the TSH-R (Cotecchia et al., 1990; Ren et al., 1993; Samama et al., 1993; Van Sande et al., 1995) and LH-R (Shenker et al., 1993), share this property, and it has been suggested that increased agonist affinity is a hallmark of constitutive activation. However this did not take into account the possibility of mutations that would be more proximal to ligand binding, decreasing the energy barrier to R* by directly mimicking the conformational effects of ligand binding and disrupting a component of high affinity ligand binding in the process. We show that several of the mutations that constitutively activate the MC1-R fall into this class.

We characterize here a domain of the MC1-R containing a series of residues, E92, L98, C123, D119, and D115. These residues may, according to modeling studies (Frandberg et al., 1994; Haskell-Luevano et al., 1995; Haskell-Luevano et al., 1996), be spatially juxtaposed. One member of this group, D119, is required for

high affinity ligand binding. Only introduction of a positive charge at E92, C123, and D119 in the transmembrane domains will produce constitutive activation, and reduced ligand affinity and efficacy is a hallmark of this activation. Consequently, we propose that constitutive activation is occurring by ligand mimicry (**Fig. 5.11**). The arginine residue at position 8 of α-MSH, essential for high affinity ligand binding, normally binds in this pocket, interacting primarily with D119, and replacement of E92, C123, or D119 with a basic residue can mimic the effects of ligand arginine on receptor conformation.

We were not able to confirm, however, that introduction of a positive charge into the arginine binding pocket released a specific horizontal receptor constraint involving molecular interactions between E92, D119, and D115. An example of such a constraint would be the electrostatic interaction between K296 and E113 of rhodopsin, which can be similarly disrupted to activate the receptor either by non-specific mutagenesis of either residue or photon- induced conformational changes in the covalently attached chromophore retinal (Robinson et al., 1992). Substitution of negatively charged residues with lysines in each transmembrane domain 2 and 3 appeared to be additive, and even substitution of all three acidic residues produced a constitutively active receptor, suggesting that the relative degree of electrostatic attraction or repulsion of TM domains 2 and 3 is not a critical factor in receptor activation. Consequently, we propose that one effect of ligand binding, mimicked by insertion of one or more positive charges at the extracellular junction of TM domains 2 and 3, may be the direct transmission of a

conformational change along the TM2 and TM3 a-helical bundles. This could be envisioned as a release from a vertical constraint imposed on the TM a-helical domains, perhaps by interaction of the charged E92, D119, and D115 residues with the negatively charged lipid head groups at the junctions of the membrane with the aqueous intracellular and extracellular milieu. This information could be transmitted across the membrane in a fashion that ultimately effects the environment of the conserved E/DRY sequence at the beginning of second intracellular loop, Significant evidence exists for rhodopsin (Rao and Oprian, 1996) as well as the α1-adrenergic receptor (Scheer et al., 1996) that the protonation state of the glutamic/aspartic acid is dramatically affected by local changes in the milieu, and the protonation state of this residue in turn appears to have a critical impact on G protein coupling. Mutations in the MC1-R TM2 may indirectly affect protonation state of the aspartic acid by altering the positioning of TM2 residues, such as M71 and D81 of the MC1-R, since comparable residues in the adrenergic receptors (Scheer et al., 1996) and rhodopsin (Rao and Oprian, 1996) are known to be involved in the formation of a polar pocket that affects the protonation state of the TM3 aspartate. Mutations in TM3 could directly alter the lipophilic environment of the DRY sequence by altering the packing of this α -helix.

Acknowledgments

This work was supported by a grant from the National Institutes of Health (RDC, AR42415), and the Norwegian Fur Breeder's Association (DIV).

MATERIALS and METHODS

Site-Directed Mutagenesis

Polymerase chain reaction (PCR) was used to make single amino acid changes in different regions of the mMC1-R. The PBS vector (Strategene) containing the wild type mMC1-R coding region was amplified using Vent^{TM} DNA polymerase (NEB) with two adjacent primers designed to hybridize to opposite strands. One primer contains the designed mutation and the other is complementary to the wild type receptor. A portion of agarose gel-purified PCR product was phosphorylated and self-ligated. A single colony was selected following transformation. The mutations, as well as the remainder of the mMC1-R, were confirmed by sequencing using an ABI model sequencer.

Receptor Expression

The Bam HI-Sal I fragments from the wild type mMC1-R and different mMC1-R mutants were cloned into the expression vector pCDNA 3 (Invtrogen). Human embryonic kidney 293 cells were transfected with 20 ug DNA of each construct using the calcium phosphate method (Chen and Okayama, 1987). Selection began 72 hours post-transfection in Dulbecco's modified Eagle's medium containing 10% newborn calf serum and 1 mg/ml geneticin.

β-Galactosidase Activity Assay

HEK 293 stable cell lines expressing the wild type mMC1 receptor and different mutants were transfected with a pCRE/β-galactosidase (pCRE/β-gal) construct using the calcium phosphate method (Chen and Okayama, 1987). 4 μg of pCRE/b-gal DNA was used for transfection of a 10 cm dish of cells. At 15 to 24 hours post-transfection, cells were split into 96-well plates with 20,000 to 30,000 cells per well and incubated at 37^0C in a 5% CO_2 incubator until 48 hours post-transfection. Cells were then stimulated with different concentrations of α-MSH and Ac-[Nle^4,D-Phe^7]-α-MSH (NDP-α-MSH) diluted in stimulation medium (Dulbecco's modified Eagle's medium containing 0.1 mg/ml bovine serum albumin and 0.1 mM isobutylmethylxanthine) for 6 hours at 37^0C in a 5% CO_2 incubator. The cells were also stimulated by Forskolin (10 μM) to normalize for transfection efficiency. After stimulation, cells were lysed in 50 ml lysis buffer (250 mM Tris-HCl, pH8.0, 0.1% Triton X-100), frozen and thawed, and then assayed for b-galactosidase activity as described (Chen et al., 1995). β-galactosidase activity was normalized both to protein concentrations and to forskolin (10 μM) stimulated level. Data represent means and standard deviation from triplicate data points and curves were fitted by nonlinear regression using Prism software (Graphapad).

Ligand Binding

Competition binding experiments were performed on stable cell lines containing the wild or mutant receptors. Those cells were plated at 5 X 10^6 cells per well to a 24-well plate in the day before the binding experiment performed. The cells were then incubated for 45 minutes at room temperature in binding medium (1 mg/ml BSA in Ca++/Mg++ PBS) containing 30-100,000 cpm of ^{125}I-NDP-α-MSH per well. Series concentrations of unlabelled NDP-α-MSH were used to compete with the labeled NDP-α-MSH. Controls of non-specific binding contain 1 or 10 μM of unlabelled NDP-α-MSH. After 45 minutes of incubation, the medium was aspirated and the cells were washed once with 1 ml of BSA/PBS (1mg/ml BSA in Ca++/Mg++ PBS) per well. Later, 0.5 ml of Gibco's versin was used to transfer cells to test tubes for counting radioactivity. Data represent means and standard deviation from duplicate data points and curves were fitted by nonlinear regression using Prism software (Graphapad).

Figure legends

Figure 5.1 Amino acid sequence variants of the melanocortin 1 receptors. Naturally occurring mutations from different species are indicated with arrows, and the species involved are indicated. The positions of these residues are shown as the homolog residues in the mouse MC1-R . The inset pictures show the phenotypes of animals with wild type *extension* allele(s) and with dominant *extension* allele(s) in the mouse, fox and cattle.

Figure 5.2 Pharmacology of the E92 mutants of the mMC1-R. **A-B**, Constitutive activation of the E92K and E92R mutant receptors. Wild type and E92 mutant MC1 receptors were assayed by analyzing their ability to activate expression of a cAMP-induced β-galactosidase fusion gene. Cells stably expressing each receptor and transciently expressing the fusion construct were stimulated for 6 h with medium alone, 10 μM forskolin, or increasing concentrations of α-MSH (**A**), or NDP-α-MSH (**B**), then β-galactosidase concentrations were determined. Data points represent means of triplicate determinations divided by maximal levels of β-galactosidase activity achieved by 10 μM forskolin stimulation to normalize for transfection efficiency, and error bars indicate standard deviations. **C, D**, Competition binding studies of the mouse E92 mutants of the MC1-R along with the wild type. Different concentrations of cold NDP-α-MSH are used to compete with the ^{125} I-NDP-α-MSH. Nonspecific binding is determined as the counts bound in the presence of 10^{-5} M cold NDP-α-

MSH. Data are displayed as total specific counts bound (**C**) or as a percentage of maximal specific counts bound (**D**). Data points represent means of duplicate determinations and bars indicate standard deviations. **E**, Scatchard analysis shows that the mouse E92K mutant of the MC1-R has ten fold higher K_D value than the wild type receptor, indicating the reduced binding affinity of the E92K mutant of the MC1-R for the ligand. Inset shows the enlarged curve for E92K mutant of the MC1-R. K_d values were 6.41 $\pm$ 2.52 nM for E92K, and 0.62 $\pm$ 0.30 nM for wild type MC1 receptor.

Figure 5.3 Pharmacology of the Proline mutants of the mMC1-R. **A-B**, Constitutive activation of the L98P mutant receptor. Wild type and Proline mutant MC1 receptors were assayed by analyzing their ability to activate expression of a cAMP-induced β-galactosidase fusion gene. Cells stably expressing each receptor and transciently expressing the fusion construct were stimulated for 6 h with medium alone, 10 μM forskolin, or increasing concentrations of α-MSH (**A**), or NDP-α-MSH (**B**), then β-galactosidase concentrations were determined. Data points represent means of triplicate determinations divided by maximal levels of β-galactosidase activity achieved by 10 μM forskolin stimulation to normalize for transfection efficiency, and error bars indicate standard deviations. **C, D**, Competition binding studies of the mouse Proline mutants of the MC1-R along with the wild type. Different concentrations of cold NDP-α-MSH are used to compete with the ^{125} I-NDP-α-MSH. Nonspecific

binding is determined as the counts bound in the presence of 10^{-5} M cold NDP-α-MSH. Data are displayed as total specific counts bound (**C**) or as a percentage of maximal specific counts bound (**D**). Data points represent means of duplicate determinations and bars indicate standard deviations.

Figure 5.4 Pharmacology of the histidine mutants of the mMC1-R. **A-B**, Non of the histidine mutants are constitutive activated. Wild type and Histidine mutant MC1 receptors were assayed by analyzing their ability to activate expression of a cAMP-induced β-galactosidase fusion gene. Cells stably expressing each receptor and transciently expressing the fusion construct were stimulated for 6 h with medium alone, 10 μM forskolin, or increasing concentrations of α-MSH (**A**), or NDP-α-MSH (**B**), then β-galactosidase concentrations were determined. Data points represent means of triplicate determinations divided by maximal levels of β-galactosidase activity achieved by 10 μM forskolin stimulation to normalize for transfection efficiency, and error bars indicate standard deviations. **C, D**, Competition binding studies of the mouse Histidine mutants of the MC1-R along with the wild type. Different concentrations of cold NDP-α-MSH are used to compete with the ^{125}I-NDP-α-MSH. Nonspecific binding is determined as the counts bound in the presence of 10^{-5} M cold NDP-α-MSH. Data are displayed as total specific counts bound (**C**) or as a percentage of maximal specific counts bound (**D**). Data points represent means of duplicate determinations and bars indicate standard deviations.

Figure 5.5 Pharmacology of the K276 mutants of the mMC1-R. **A-B**, Non of the K276 mutants are constitutive activated. Wild type and K276 mutant MC1 receptors were assayed by analyzing their ability to activate expression of a cAMP-induced β-galactosidase fusion gene. Cells stably expressing each receptor and transciently expressing the fusion construct were stimulated for 6 h with medium alone, 10 μM forskolin, or increasing concentrations of α-MSH (**A**), or NDP-α-MSH (**B**), then β-galactosidase concentrations were determined. Data points represent means of triplicate determinations divided by maximal levels of β-galactosidase activity achieved by 10 μM forskolin stimulation to normalize for transfection efficiency, and error bars indicate standard deviations. **C, D**, Competition binding studies of the mouse K276 mutants of the MC1-R along with the wild type. Different concentrations of cold NDP-α-MSH are used to compete with the ^{125}I-NDP-α-MSH. Nonspecific binding is determined as the counts bound in the presence of 10^{-5} M cold NDP-α-MSH. Data are displayed as total specific counts bound (**C**) or as a percentage of maximal specific counts bound (**D**). Data points represent means of duplicate determinations and bars indicate standard deviations.

Figure 5.6 Pharmacology of the C123 mutants of the mMC1-R. **A-B**, Constitutive activation of the C123R and C123K mutant receptors. Wild type and C123 mutant MC1 receptors were assayed by analyzing their ability to activate expression of a cAMP-induced β-galactosidase fusion gene. Cells stably

expressing each receptor and transciently expressing the fusion construct were stimulated for 6 h with medium alone, 10 μM forskolin, or increasing concentrations of α-MSH (**A**), or NDP-α-MSH (**B**), then β-galactosidase concentrations were determined. Data points represent means of triplicate determinations divided by maximal levels of β-galactosidase activity achieved by 10 μM forskolin stimulation to normalize for transfection efficiency, and error bars indicate standard deviations. **C, D**, Competition binding studies of the mouse C123 mutants of the MC1-R along with the wild type. Different concentrations of cold NDP-α-MSH are used to compete with the ^{125}I-NDP-α-MSH. Nonspecific binding is determined as the counts bound in the presence of 10^{-6} M cold NDP-α-MSH. Data are displayed as total specific counts bound (**C**) or as a percentage of maximal specific counts bound (**D**). Data points represent means of duplicate determinations and bars indicate standard deviations.

Figure 5.7 Pharmacology of the D119 mutants of the mMC1-R. **A-B**, Constitutive activation of the D119K mutant receptor. Wild type and D119 mutant MC1 receptors were assayed by analyzing their ability to activate expression of a cAMP-induced β-galactosidase fusion gene. Cells stably expressing each receptor and transciently expressing the fusion construct were stimulated for 6 h with medium alone, 10 μM forskolin, or increasing concentrations of α-MSH (**A**), or NDP-α-MSH (**B**), then β-galactosidase concentrations were determined. Data points represent means of triplicate

determinations divided by maximal levels of β-galactosidase activity achieved by 10 μM forskolin stimulation to normalize for transfection efficiency, and error bars indicate standard deviations. **C, D**, Competition binding studies of the mouse D119 mutants of the MC1-R along with the wild type. Different concentrations of cold NDP-α-MSH are used to compete with the ^{125} I-NDP-α-MSH. Nonspecific binding is determined as the counts bound in the presence of 10^{-5} M cold NDP-α-MSH. Data are displayed as total specific counts bound (**C**) or as a percentage of maximal specific counts bound (**D**). Data points represent means of duplicate determinations and bars indicate standard deviations.

Figure 5.8 Pharmacology of the D115 mutants of the mMC1-R. **A-B**, Constitutive activation of the D115 mutant receptors. Wild type and Proline mutant MC1 receptors were assayed by analyzing their ability to activate expression of a cAMP-induced β-galactosidase fusion gene. Cells stably expressing each receptor and transciently expressing the fusion construct were stimulated for 6 h with medium alone, 10 μM forskolin, or increasing concentrations of α-MSH (**A**), or NDP-α-MSH (**B**), then β-galactosidase concentrations were determined. Data points represent means of triplicate determinations divided by maximal levels of β-galactosidase activity achieved by 10 μM forskolin stimulation to normalize for transfection efficiency, and error bars indicate standard deviations. **C, D**, Competition binding studies of the mouse D115 mutants of the MC1-R along with the wild type. Different concentrations

of cold NDP-α-MSH are used to compete with the ^{125} I-NDP-α-MSH. Nonspecific binding is determined as the counts bound in the presence of 10^{-5} M cold NDP-α-MSH. Data are displayed as total specific counts bound (**C**) or as a percentage of maximal specific counts bound (**D**). Data points represent means of duplicate determinations and bars indicate standard deviations.

Figure 5.9 Pharmacology of the M71 mutants of the mMC1-R. **A-B**, Constitutive activation of the M71K mutant receptors. Wild type and Proline mutant MC1 receptors were assayed by analyzing their ability to activate expression of a cAMP-induced β-galactosidase fusion gene. Cells stably expressing each receptor and transciently expressing the fusion construct were stimulated for 6 h with medium alone, 10 μM forskolin, or increasing concentrations of α-MSH (**A**), or NDP-α-MSH (**B**), then β-galactosidase concentrations were determined. Data points represent means of triplicate determinations divided by maximal levels of β-galactosidase activity achieved by 10 μM forskolin stimulation to normalize for transfection efficiency, and error bars indicate standard deviations. **C, D**, Competition binding studies of the mouse M71 mutants of the MC1-R along with the wild type. Different concentrations of cold NDP-α-MSH are used to compete with the ^{125} I-NDP-α-MSH. Nonspecific binding is determined as the counts bound in the presence of 10^{-5} M cold NDP-α-MSH. Data are displayed as total specific counts bound (**C**) or as a percentage of maximal specific counts bound (**D**). Data points represent means of duplicate determinations and bars indicate standard deviations.

Figure 5.10 Pharmacology of the double and triple mutants of the mMC1-R. **A-B**, Constitutive activation of the double and triple mutant receptor. Wild type and double and triple mutant MC1 receptors were assayed by analyzing their ability to activate expression of a cAMP-induced β-galactosidase fusion gene. Cells stably expressing each receptor and transciently expressing the fusion construct were stimulated for 6 h with medium alone, 10 μM forskolin, or increasing concentrations of α-MSH (**A**), or NDP-α-MSH (**B**), then β-galactosidase concentrations were determined. Data points represent means of triplicate determinations divided by maximal levels of β-galactosidase activity achieved by 10 μM forskolin stimulation to normalize for transfection efficiency, and error bars indicate standard deviations.

Figure 5.11 Ligand-mimetic model of the constitutive activation of the mouse MC1-R. Interaction **a** included interactions between the residues in the transmembrane domain II or III, and then to the DRY sequence in N-terminal of the second intracellular loop. Interaction **b** involved the connection between D82 of the second transmembrane domain and the DRY sequence mentioned above.

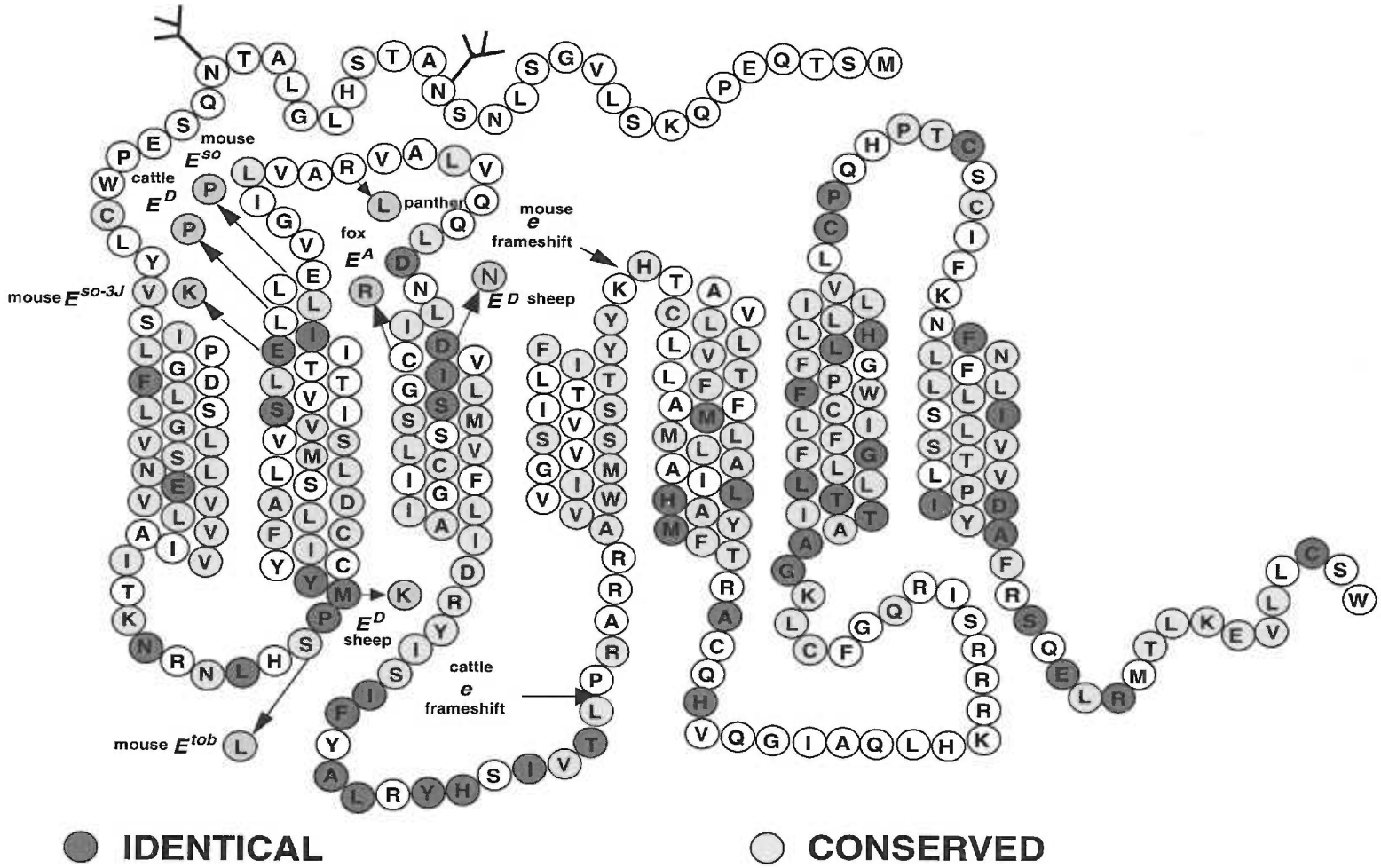

Figure 5.1 Amino Acid Sequence Variants of the Melanocortin 1 Receptor

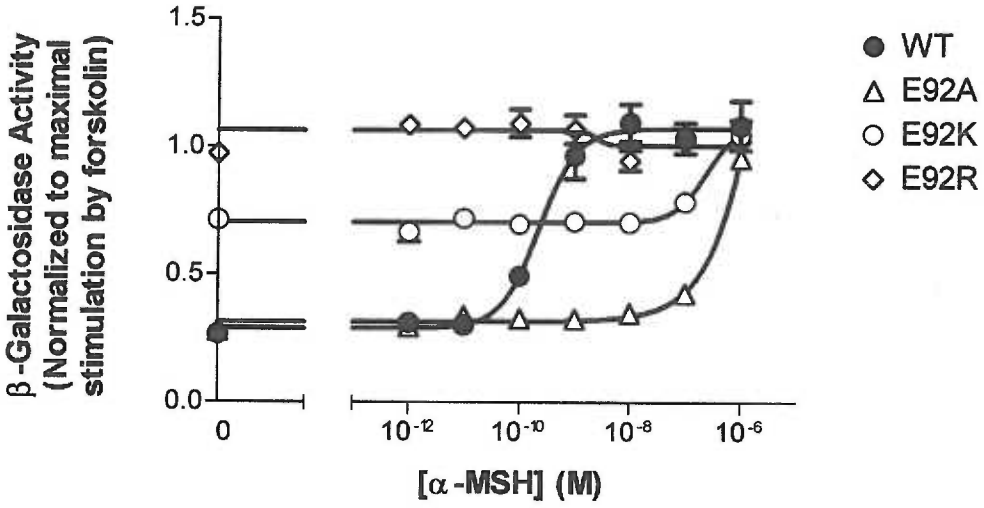

Figure 5.2A

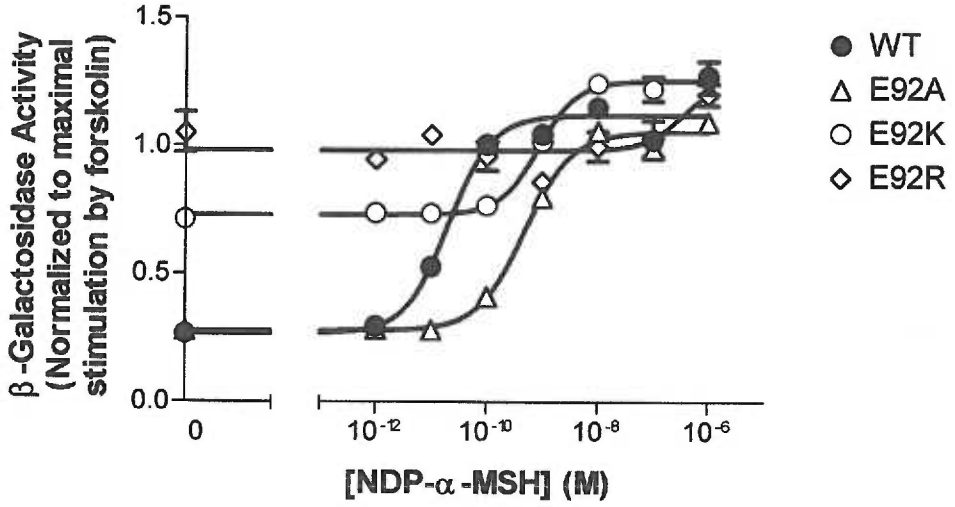

Figure 5.2B

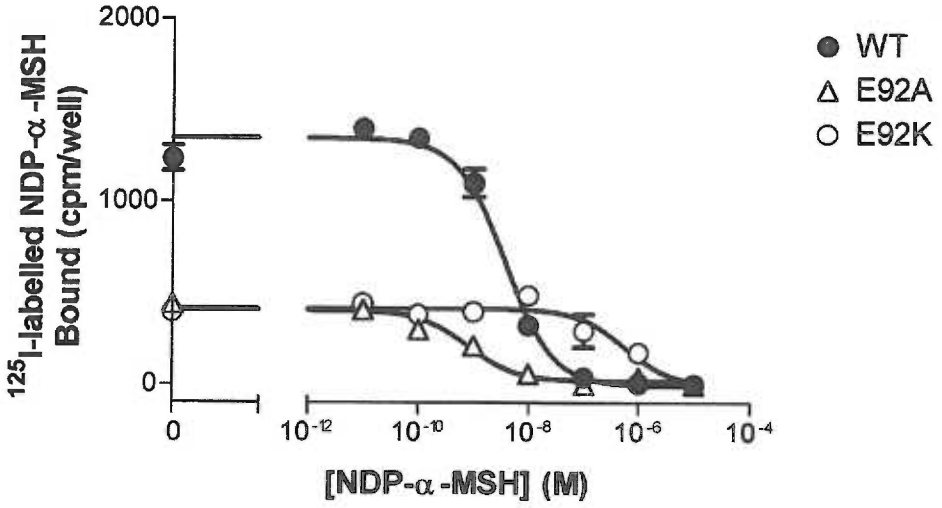

Figure 5.2C

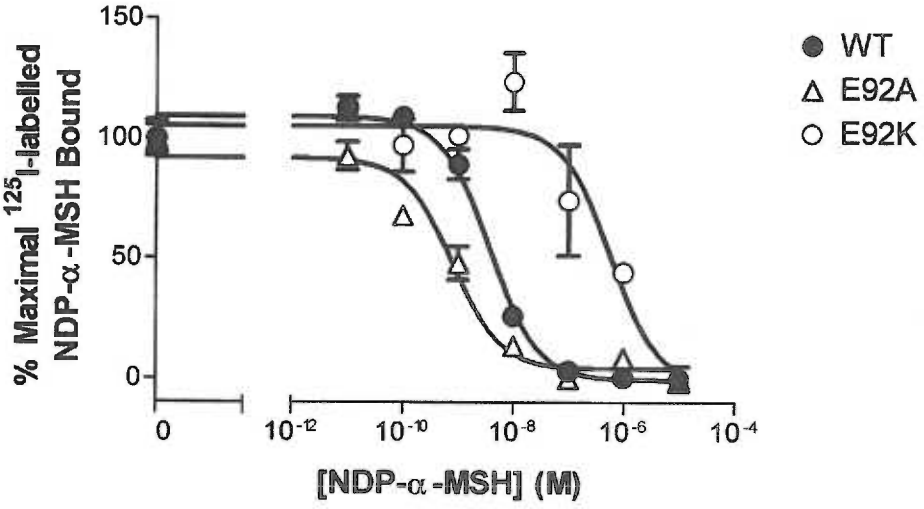

Figure 5.2D

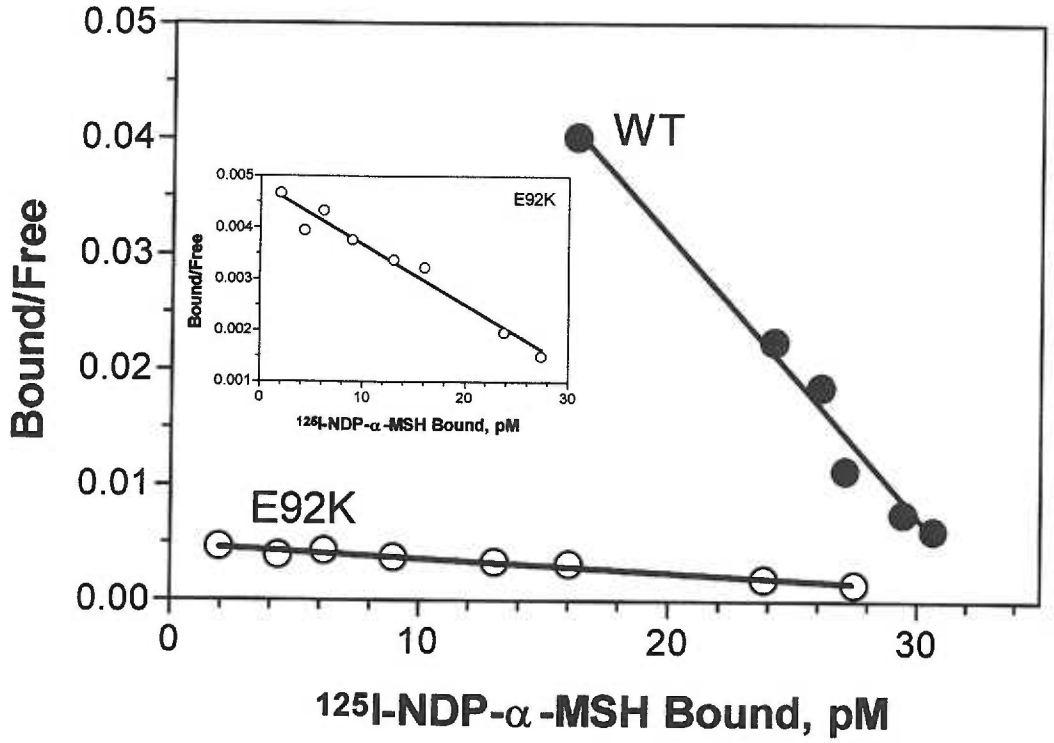
0.05
0.04
0.03
0.02
0.01
0.00
Bound/Free
0
10
20
30
125I-NDP-α-MSH Bound, pM
WT
E92K
0.005
0.004
0.003
0.002
0.001
Bound/Free
E92K
0
10
20
30
125I-NDP-α-MSH Bound, pM

Figure 5.2E

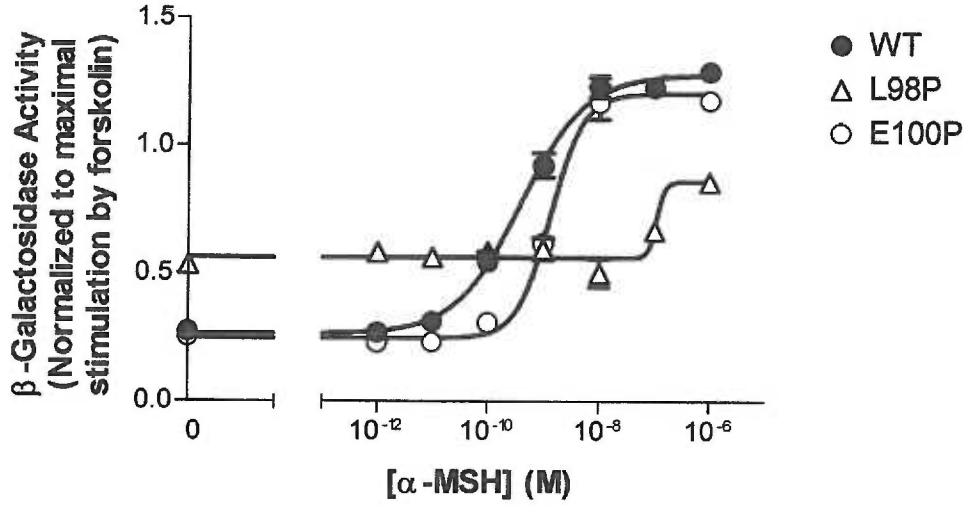

Figure 5.3A

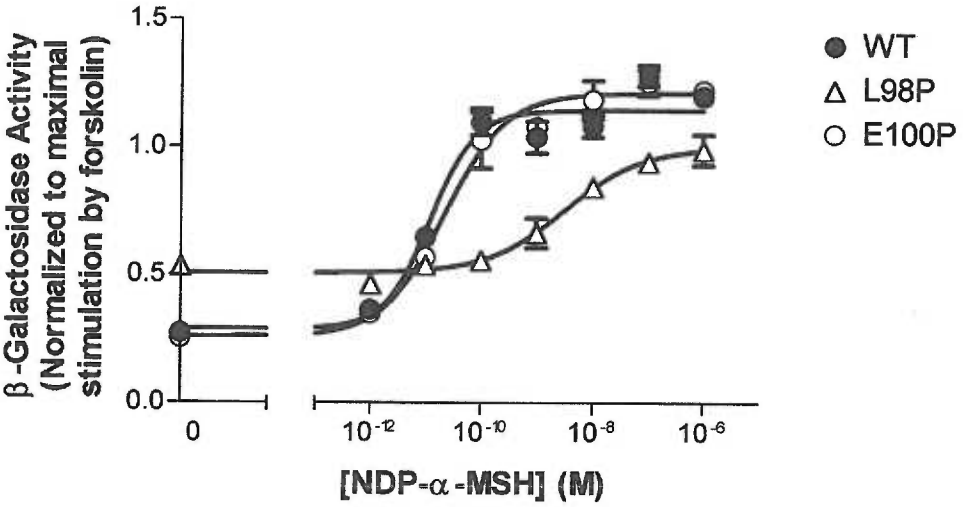

Figure 5.3B

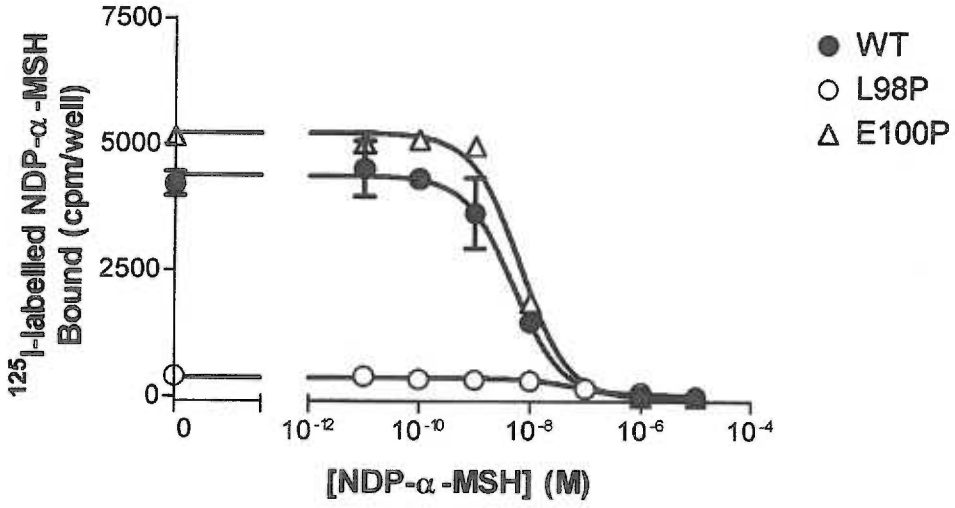

Figure 5.3C

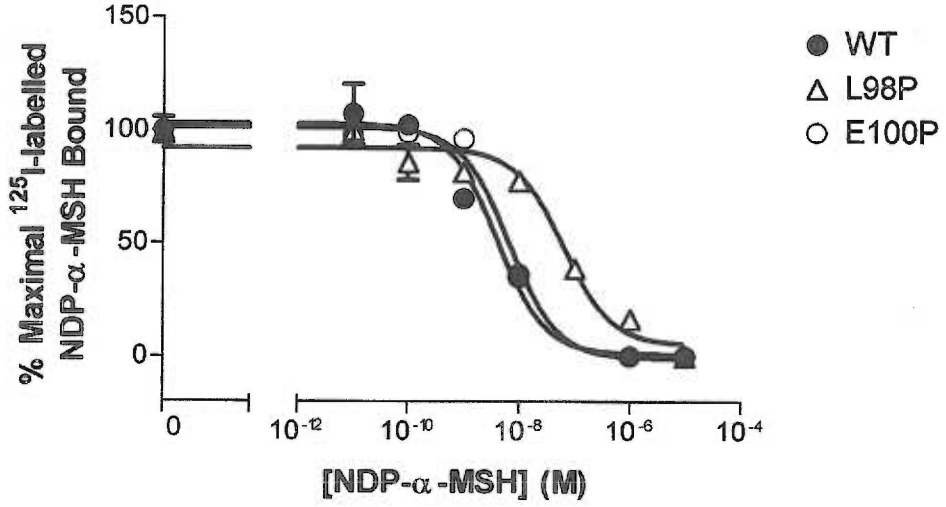

Figure 5.3D

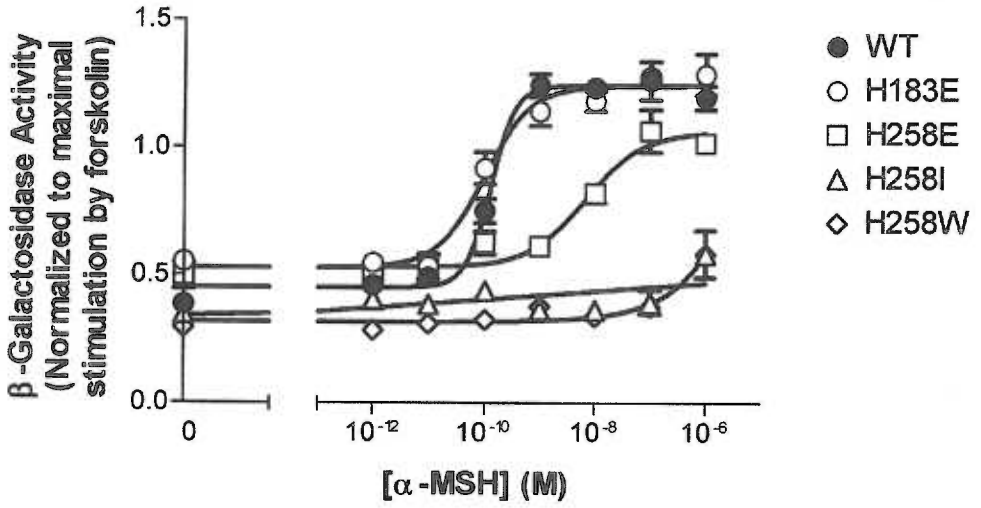

Figure 5.4A

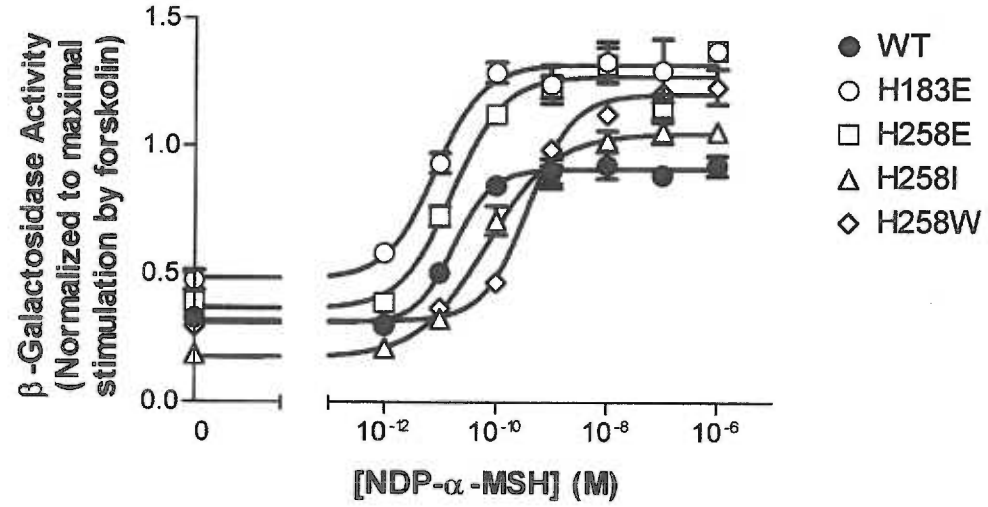

Figure 5.4B

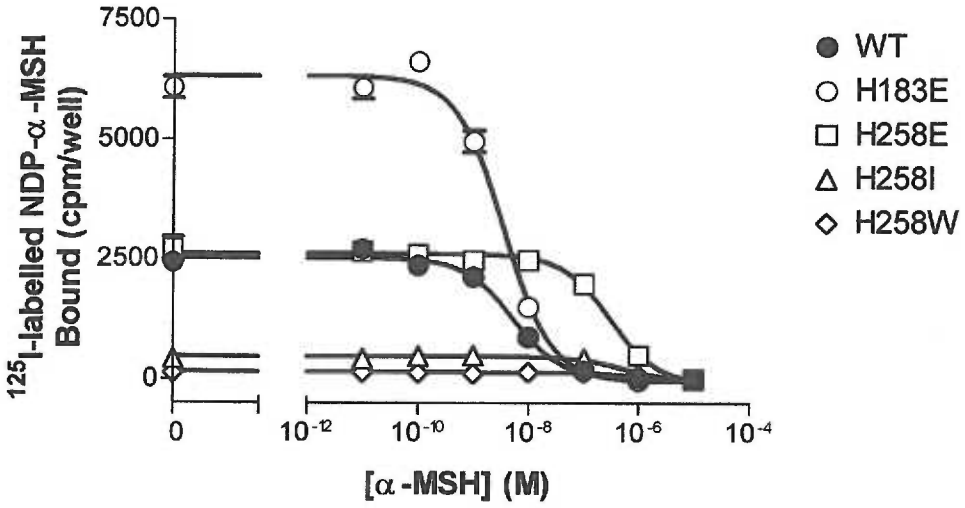

Figure 5.4C

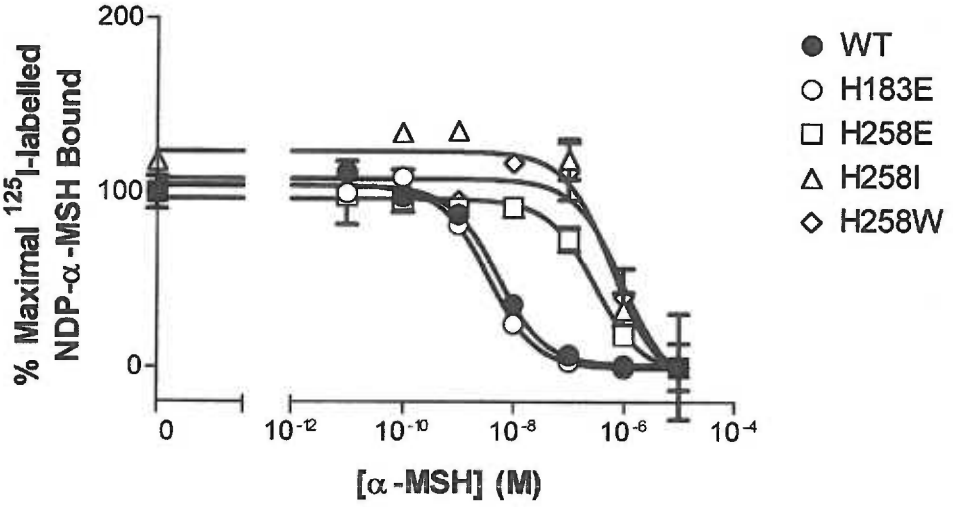

Figure 5.4D

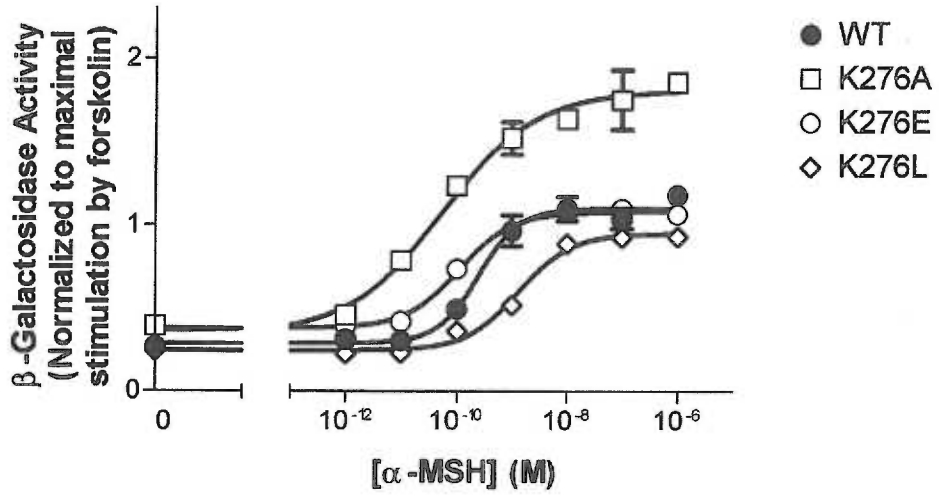

Figure 5.5A

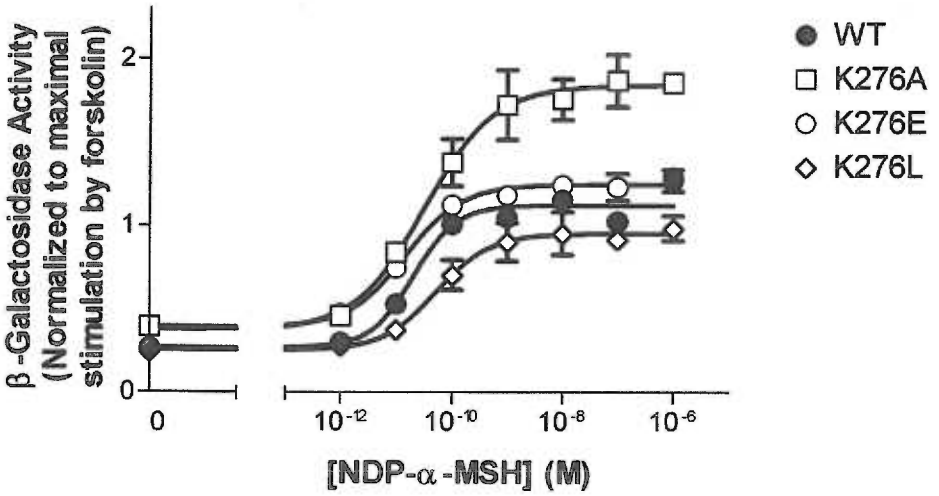

Figure 5.5B

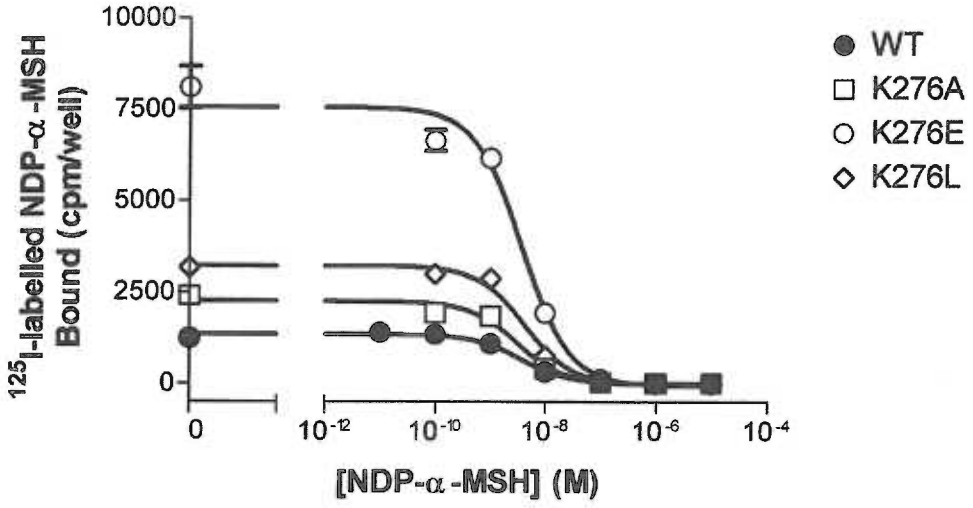

Figure 5.5C

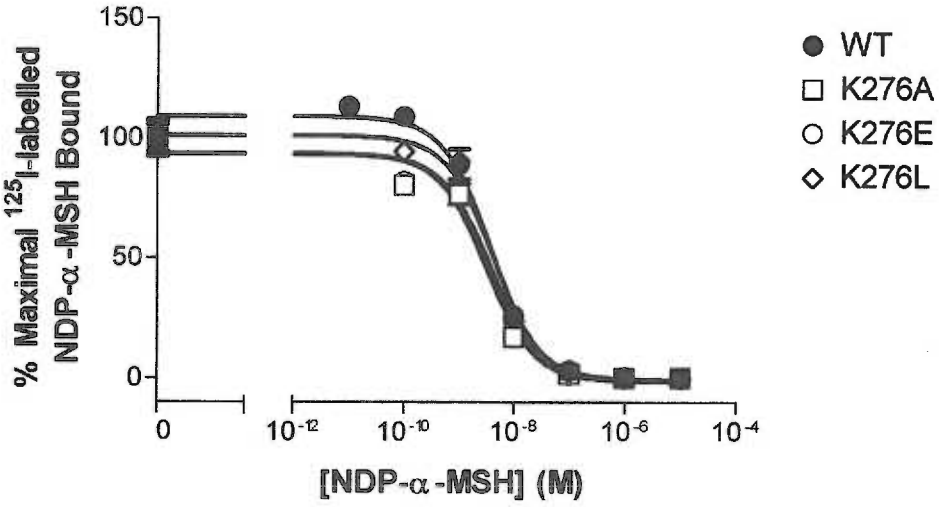

Figure 5.5D

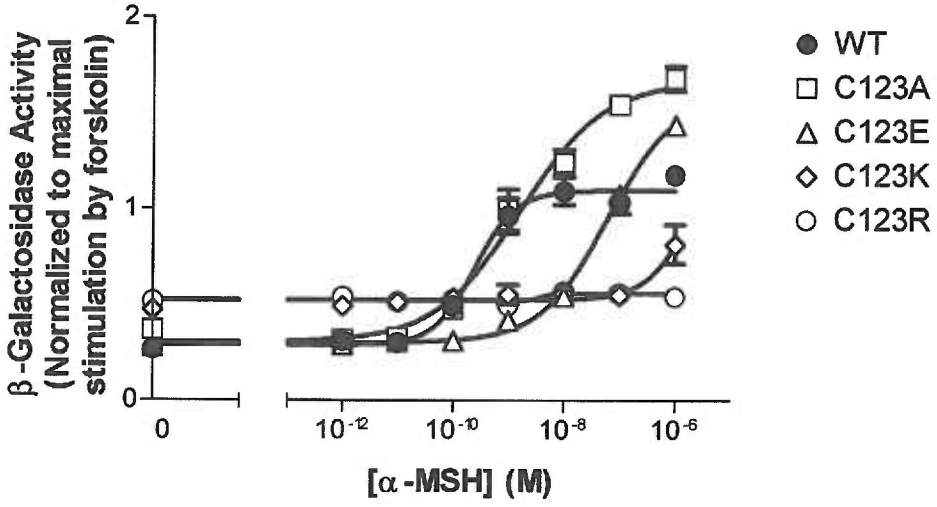

Figure 5.6A

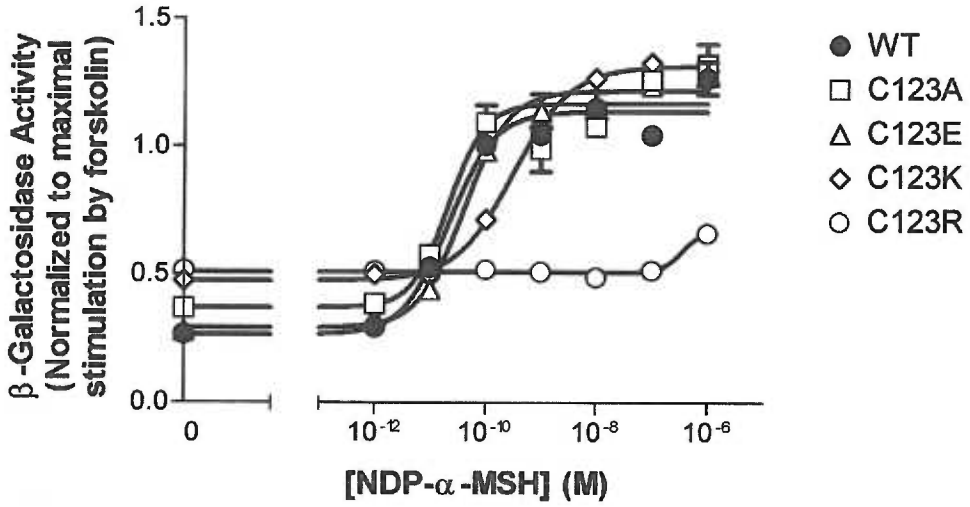

Figure 5.6B

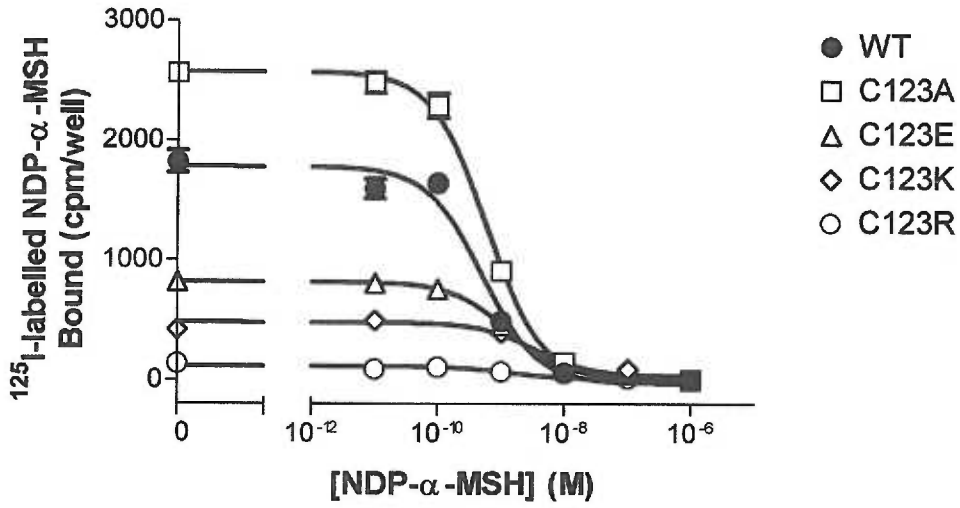

Figure 5.6C

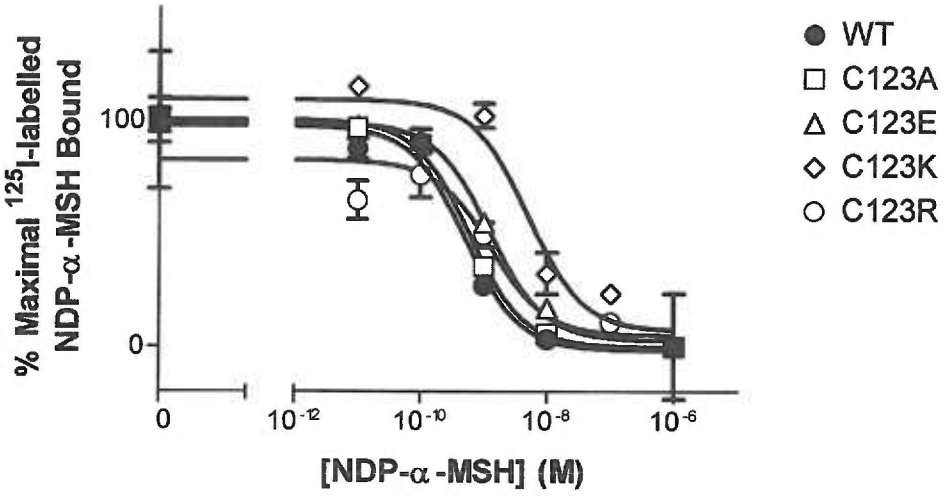

Figure 5.6D

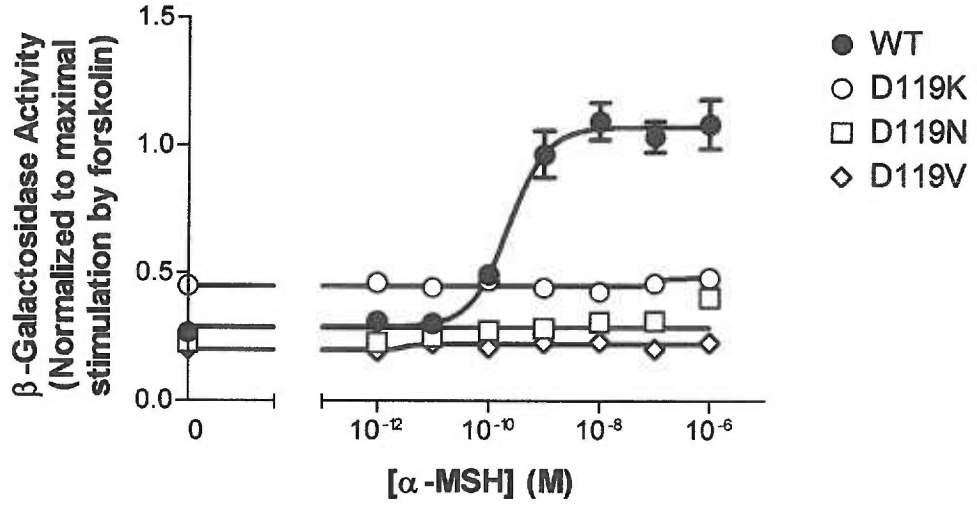

Figure 5.7A

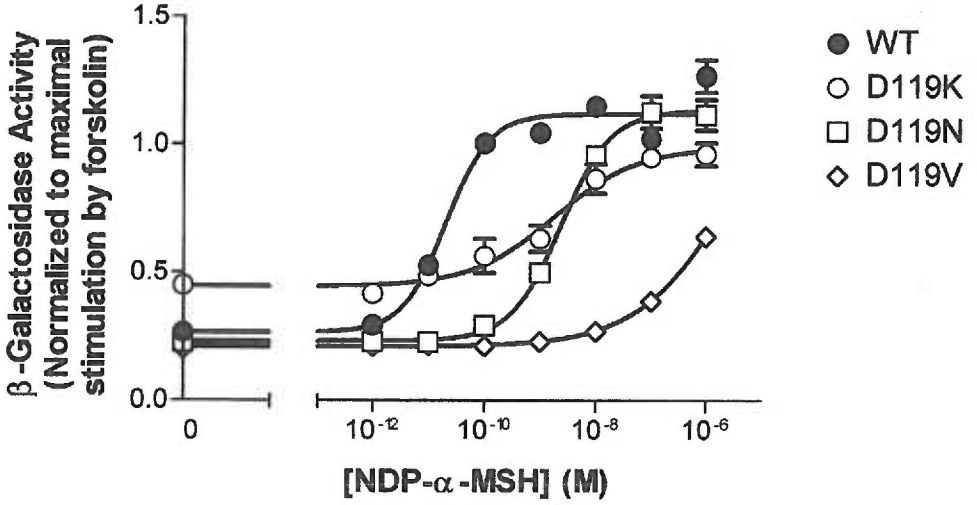

Figure 5.7B

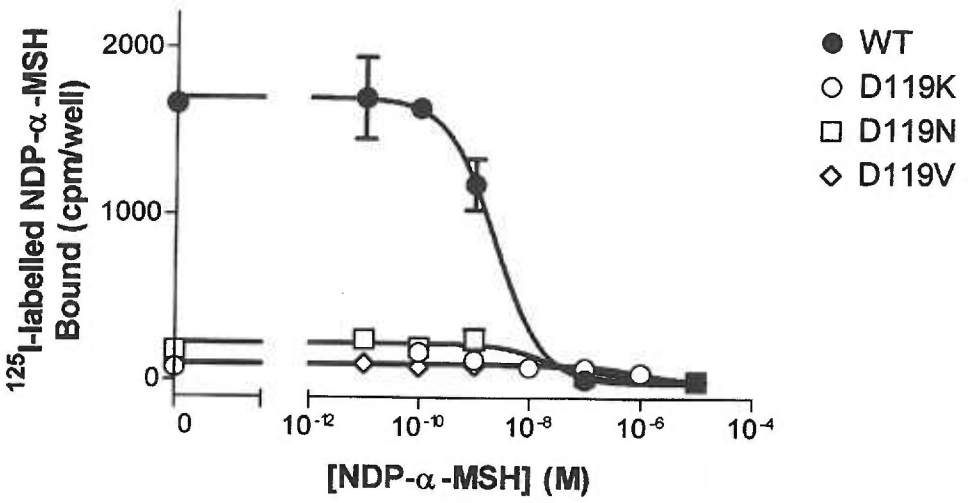

Figure 5.7C

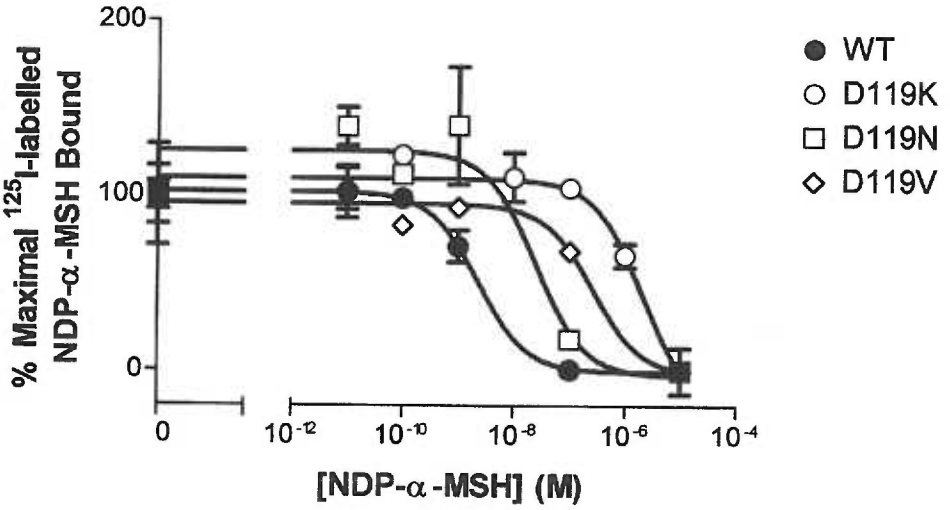

Figure 5.7D

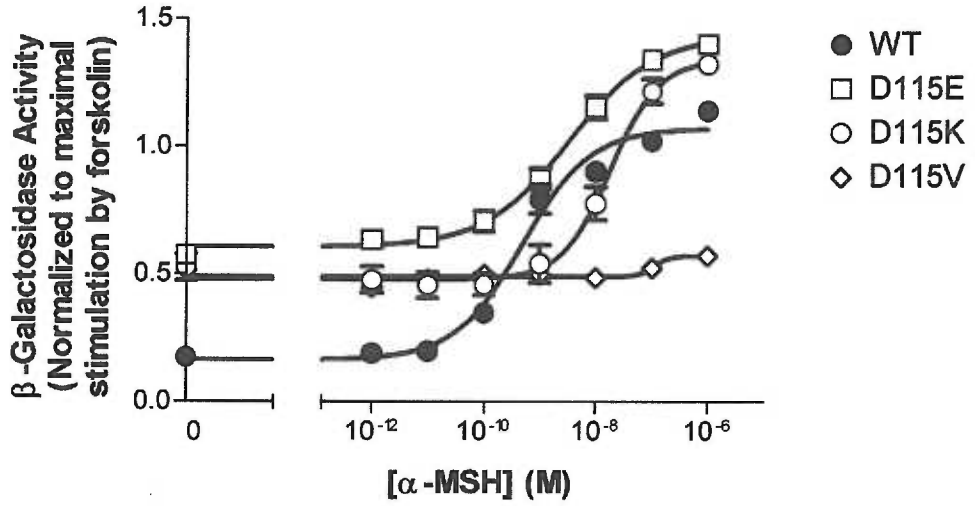

Figure 5.8A

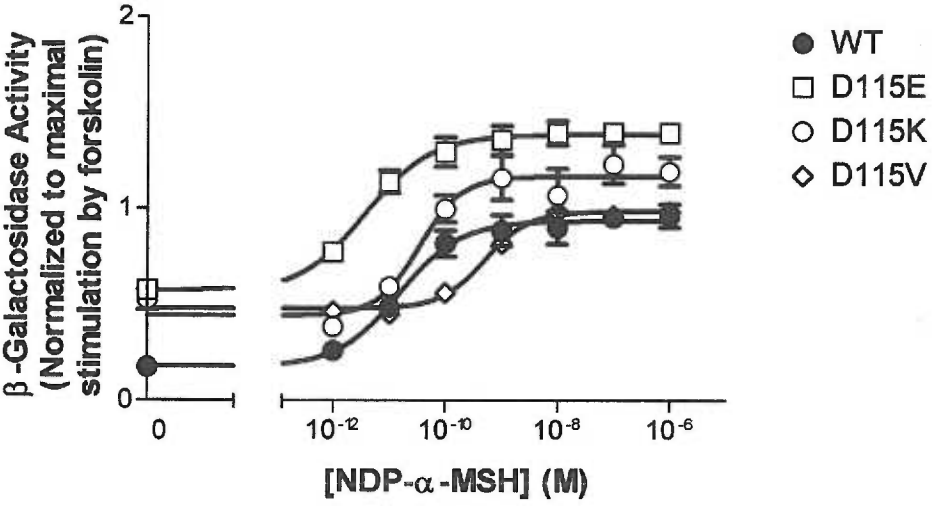

Figure 5.8B

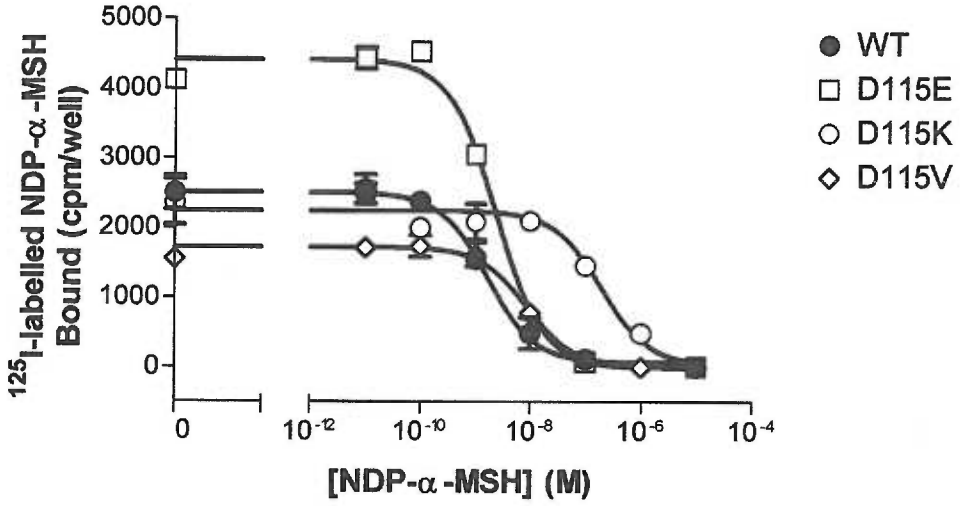

Figure 5.8C

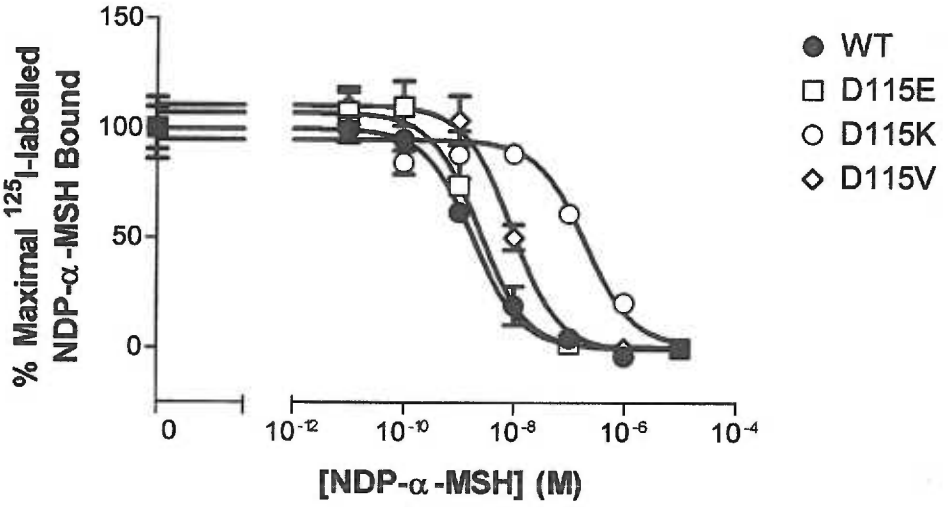

Figure 5.8D

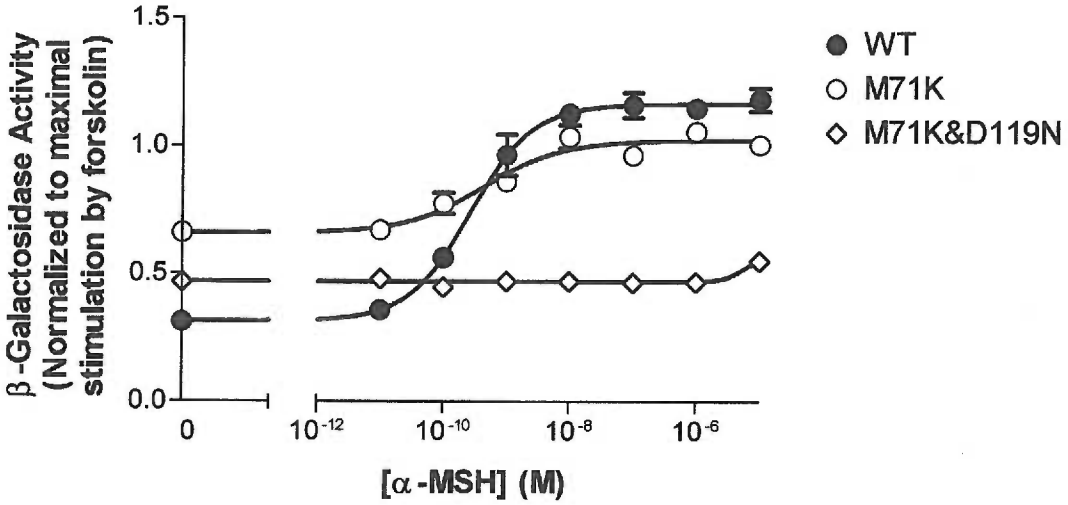

Figure 5.9A

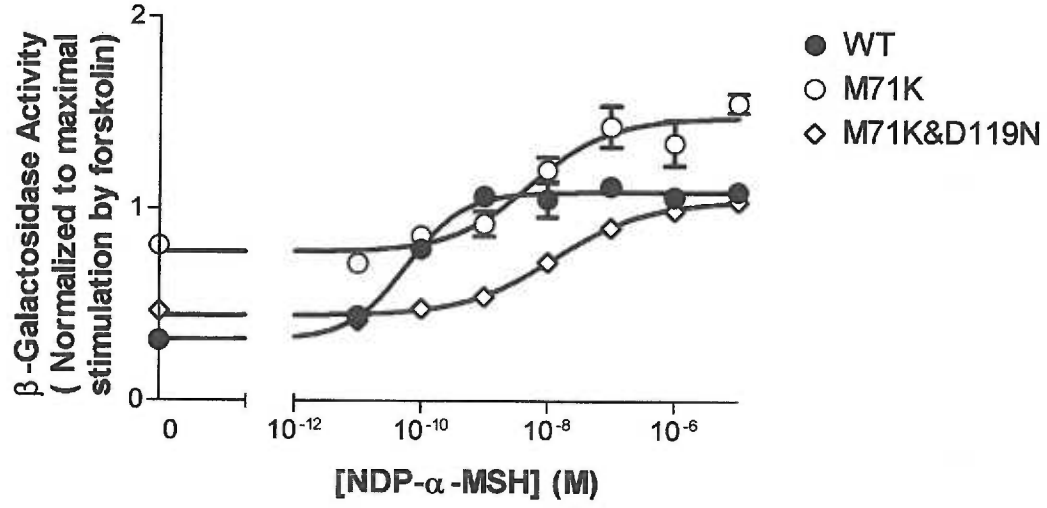

Figure 5.9B

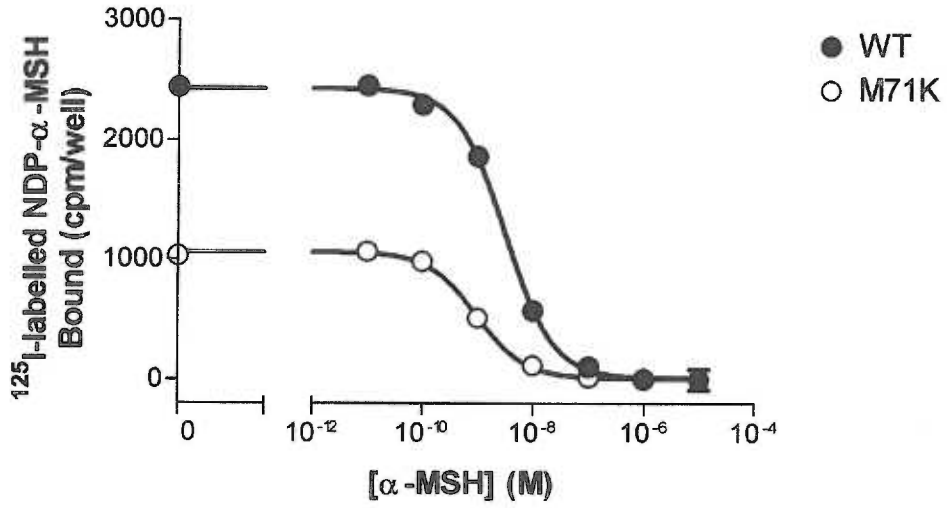

Figure 5.9C

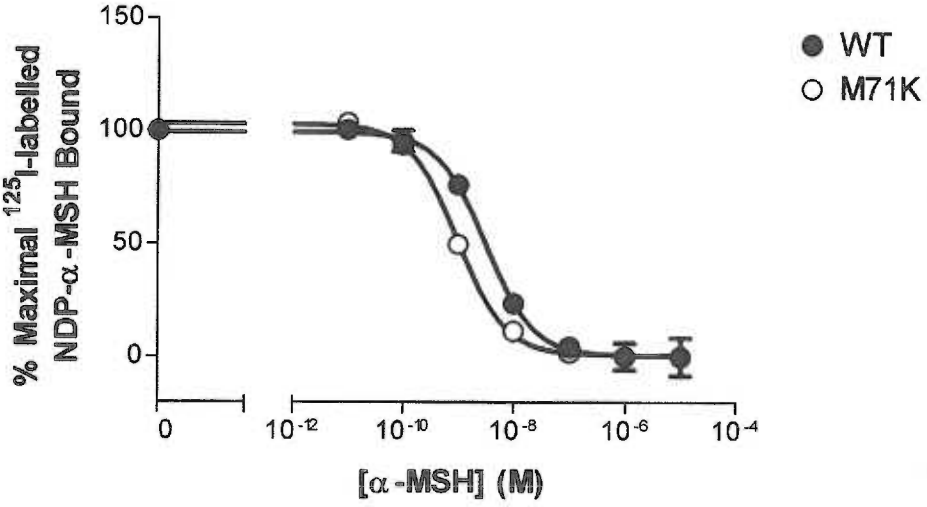

Figure 5.9D

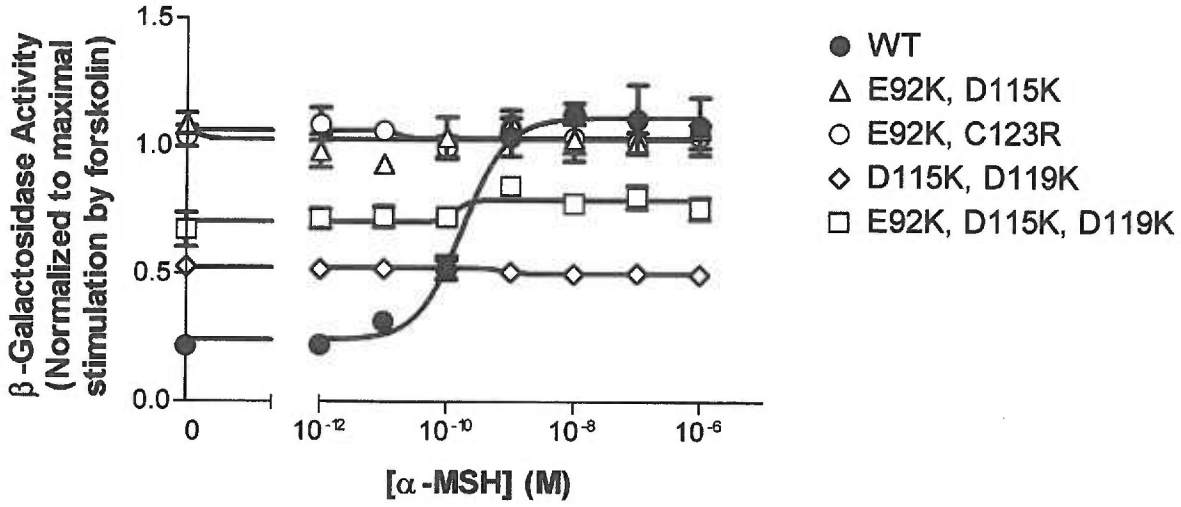

Figure 5.10A

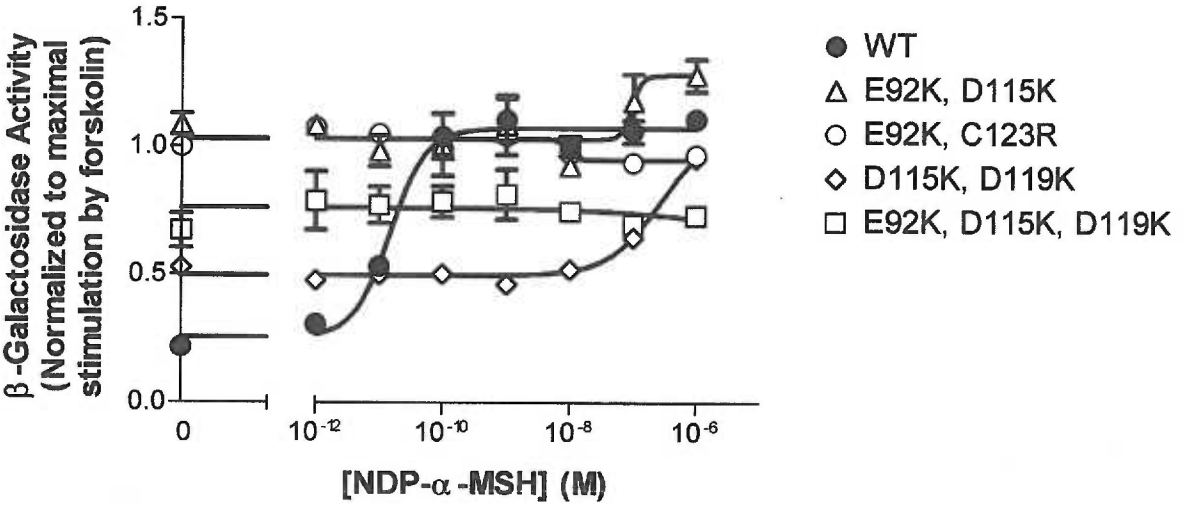

Figure 5.10B

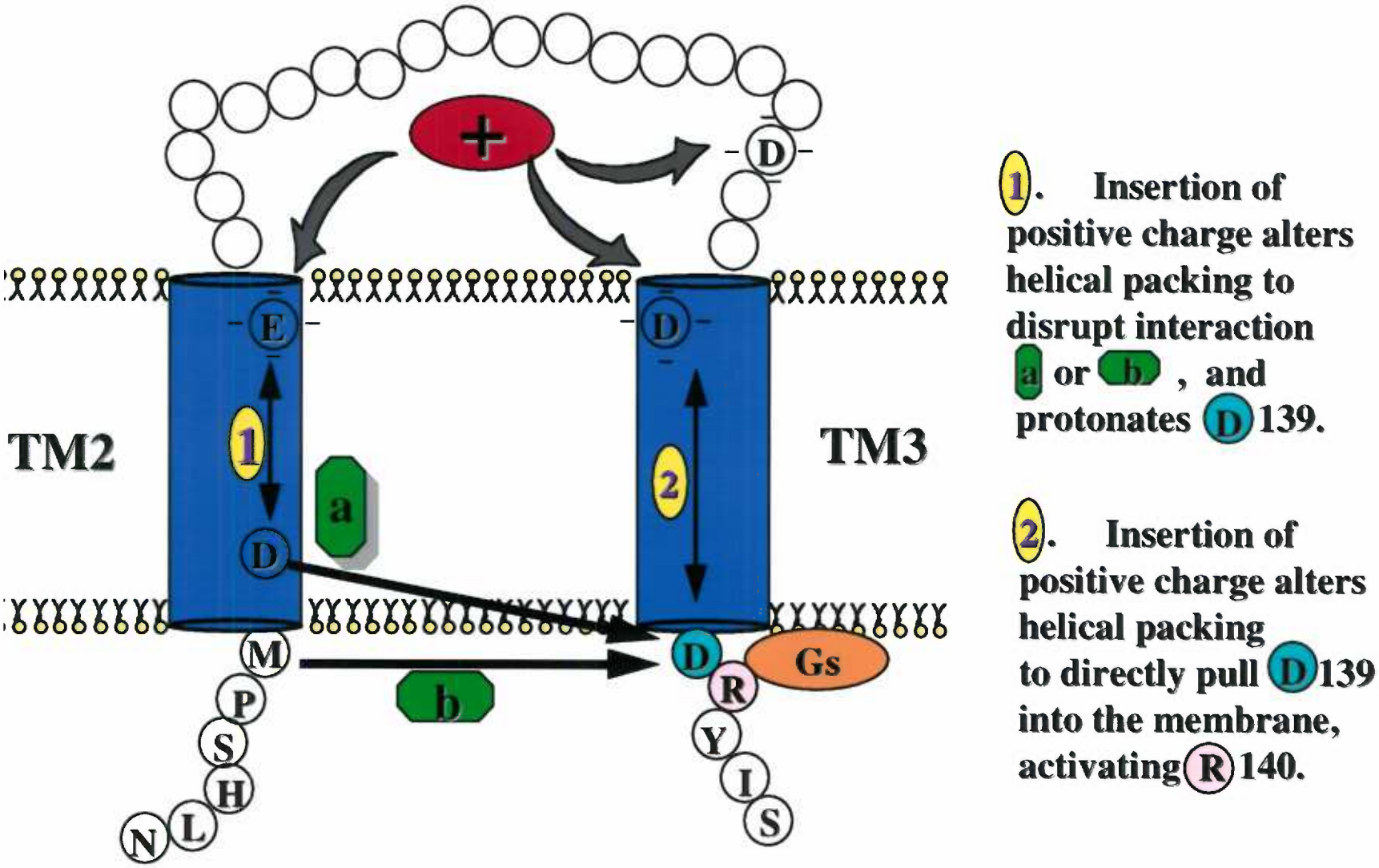

Figure 5.11 Ligand-mimetic Model for the Constitutive Activation of the Mouse Melanocortin 1 Receptor

Table 5.1. EC_{50}s for α-MSH and NDP-α-MSH Stimulation and IC_{50} of the mMC1-R Wild Type and E92 Mutants in Stably Transfected HEK 293 Cells

mMC1-R	EC_{50} (nM)[a]		IC_{50} (nM)[a]
	α-MSH	NDP-α-MSH	
WT	0.201 ± 0.109[e]	0.0162 ± 0.0055[e]	0.79 ± 0.48[c,d]
E92A	28200 ± 32500	0.554 ± 0.279	1.07 ± 0.53[c]
E92D	14.5 ± 11.4	0.165 ± 0.128	8.05 ± 4.34[c]
E92K	NA[b]	0.715 ± 0.181	13.7 ± 17.7[c]
E92Q	NA[b]	0.134 ± 0.018	3230 ± 1930[c]
E92R	NA[b]	NA[b]	NA[b]

a, Values are determined by two or more independent experiments.
b, Values can not be determined from the experiments.
c, Cold NDP-α-MSH was used for competition binding experiments.
d, Value represents mean ± standard deviation from 5 independent experiments.
e, Value represents mean ± standard deviation from 15 independent experiments.

Table 5.2. EC_{50}s for α-MSH and NDP-α-MSH Stimulation and IC_{50} of the mMC1-R Wild Type and Proline Mutants in Stably Transfected HEK 293 Cells

mMC1-R	EC_{50} (nM)[a]		IC_{50} (nM)[a]
	α-MSH	NDP-α-MSH	
WT	0.201 ± 0.109[g]	0.0162 ± 0.0055[g]	0.79 ± 0.48[c,e]
			3.68 ± 1.69[d,f]
L98P	NA[b]	3.27 ± 0.19	301 ± 55[d]
E100P	0.908 ± 0.381	0.0217 ± 0.0065	0.57 ± 0.17[c]

a, Values are determined by two or more independent experiments.
b, Values can not be determined from the experiments.
c, Cold NDP-α-MSH was used for competition binding experiments.
d, Cold α-MSH was used for competition binding experiments.
e, Value represents mean ± standard deviation from 5 independent experiments.
f, Value represents mean ± standard deviation from 9 independent experiments.
g, Value represents mean ± standard deviation from 15 independent experiments.

Table 5.3. EC_{50}s for α-MSH and NDP-α-MSH Stimulation and IC_{50} of the mMC1-R Wild Type and Histidine Mutants in Stably Transfected HEK 293 Cells

mMC1-R	EC_{50} (nM)[a]		IC_{50} (nM)[a]
	α-MSH	NDP-α-MSH	
WT	0.201 ± 0.109[e]	0.0162 ± 0.0055[e]	3.68 ± 1.69[c,d]
H183E	0.0907 ± 0.0107	0.0191 ± 0.0155	3.55 ± 2.01[c]
H258E	5.44 ± 1.68	0.0167 ± 0.0046	351 ± 94[c]
H258I	NA[b]	0.0889 ± 0.0315	656 ± 185[c]
H258W	NA[b]	0.267 ± 0.163	1360 ± 567[c]

a, Values are determined by two or more independent experiments.
b, Values can not be determined from the experiments.
c, Cold α-MSH was used for competition binding experiments.
d, Value represents mean ± standard deviation from 9 independent experiments.
e, Value represents mean ± standard deviation from 15 independent experiments.

Table 5.4. EC_{50}s for α-MSH and NDP-α-MSH Stimulation and IC_{50} of the mMC1-R Wild Type and K276 Mutants in Stably Transfected HEK 293 Cells

mMC1-R	EC_{50} (nM)[a]		IC_{50} (nM)[a]
	α-MSH	NDP-α-MSH	
WT	0.201 ± 0.109[d]	0.0162 ± 0.0055[d]	0.79 ± 0.48[b,c]
K276A	3.30 ± 2.55	0.058 ± 0.0467	2.82 ± 1.24[b]
K276E	0.320 ± 0.148	0.055 ± 0.0282	3.20 ± 0.85[b]
K276L	1.25 ± 0.07	0.0575 ± 0.0064	2.80 ± 2.41[b]

a, Values are determined by two or more independent experiments.
b, Cold NDP-α-MSH was used for competition binding experiments.
c, Value represents mean ± standard deviation from 5 independent experiments.
d, Value represents mean ± standard deviation from 15 independent experiments.

Table 5.5. EC_{50}s for α-MSH and NDP-α-MSH Stimulation and IC_{50} of the mMC1-R Wild Type and C123 Mutants in Stably Transfected HEK 293 Cells

mMC1-R	EC_{50} (nM)[a]		IC_{50} (nM)[a]
	α-MSH	NDP-α-MSH	
WT	0.201 ± 0.109[e]	0.0162 ± 0.0055[e]	0.79 ± 0.48[c,d]
C123A	0.235 ± 0.145	0.0143 ± 0.0075	3.38 ± 2.07[c]
C123E	38.9 ± 25.6	0.0400 ± 0.0201	1.50 ± 0.42[c]
C123K	NA[b]	0.193 ± 0.111	7.94 ± 3.27[c]
C123R	NA[b]	NA[b]	1.14 ± 0.24[c]

a, Values are determined by two or more independent experiments.
b, Values can not be determined from the experiments.
c, Cold NDP-α-MSH was used for competition binding experiments.
d, Value represents mean ± standard deviation from 5 independent experiments.
e, Value represents mean ± standard deviation from 15 independent experiments.

Table 5.6. EC_{50}s for α-MSH and NDP-α-MSH Stimulation and IC_{50} of the mMC1-R Wild Type and D119 Mutants in Stably Transfected HEK 293 Cells

mMC1-R	EC_{50} (nM)[a]		IC_{50} (nM)[a]
	α-MSH	NDP-α-MSH	
WT	0.201 ± 0.109[g]	0.0162 ± 0.0055[g]	0.79 ± 0.48[c,e]
			3.68 ± 1.69[d,f]
D119K	NA[b]	1.77 ± 1.02	211 ± 170[d]
D119N	NA[b]	1.70 ± 0.86	16.1 ± 7.3[c]
D119V	NA[b]	152 ± 130	179 ± 121[c]

a, Values are determined by two or more independent experiments.
b, Values can not be determined from the experiments.
c, Cold NDP-α-MSH was used for competition binding experiments.
d, Cold α-MSH was used for competition binding experiments.
e, Value represents mean ± standard deviation from 5 independent experiments.
f, Value represents mean ± standard deviation from 9 independent experiments.
g, Value represents mean ± standard deviation from 15 independent experiments.

Table 5.7. EC_{50}s for α-MSH and NDP-α-MSH Stimulation and IC_{50} of the mMC1-R Wild Type and D115 Mutants in Stably Transfected HEK 293 Cells

mMC1-R	EC_{50} (nM)[a]		IC_{50} (nM)[a]
	α-MSH	NDP-α-MSH	
WT	0.201 ± 0.109[g]	0.0162 ± 0.0055[g]	0.79 ± 0.48[c,e]
			3.68 ± 1.69[d,f]
D115E	5.74 ± 2.14	0.00945 ± 0.00834	3.14 ± 3.56[c]
D115K	23.0 ± 6.9	0.0246 ± 0.0137	187 ± 15[d]
D115V	NA[b]	4.20 ± 1.60	2.76 ± 2.29[c]

a, Values are determined by two or more independent experiments.
b, Values can not be determined from the experiments.
c, Cold NDP-α-MSH was used for competition binding experiments.
d, Cold α-MSH was used for competition binding experiments.
e, Value represents mean ± standard deviation from 5 independent experiments.
f, Value represents mean ± standard deviation from 9 independent experiments.
g, Value represents mean ± standard deviation from 15 independent experiments.

Table 5.8. EC_{50}s for α-MSH and NDP-α-MSH Stimulation and IC_{50} of the mMC1-R Wild Type and M71K Mutants in Stably Transfected HEK 293 Cells

mMC1-R	EC_{50} (nM)[a]		IC_{50} (nM)[a]
	α-MSH	NDP-α-MSH	
WT	0.201 ± 0.109[e]	0.0162 ± 0.0055[e]	3.68 ± 1.69[c,d]
M71K	1.41 ± 0.96	5.26 ± 0.40	1.01 ± 0.05[c]
M71K, D119N	NA[b]	1.30 ± 0.52	NA[b]

a, Values are determined by two or more independent experiments.
b, Values can not be determined from the experiments.
c, Cold α-MSH was used for competition binding experiments.
d, Value represents mean ± standard deviation from 9 independent experiments.
e, Value represents mean ± standard deviation from 15 independent experiments.

Chapter 5 Appendix

In addition to the mutants characterized in chapter 5, several other mutants involving phe-43, phe-278 and arg-107 were also pharmacological characterized.

F43 and F278 have different roles in the activation of the mMC1-R

The pharmacophore -His-Phe-Arg-Trp- of the α-MSH has both an arginine, with positive charge, and residues with aromatic structure, phenylalanine and tryptophan. Since cation-π interactions and π-π interactions are considered as important forces formed between ligand and receptor , the two phenyalanine residues, F43 and F278, located respectively in the presumed exterior part of the transmembrane I and transmembrane VII, were chosen to be tested for the receptor activation and ligand binding.

F43 was mutagenized to two amino acids, F43A and F43V. Both changes resulted in increased EC_{50}s for α-MSH stimulation and IC_{50}s for ligand binding (**Figure 5A.1, Table 5A.1**). The EC_{50}s for NDP-α-MSH stimulation remained the same as the wild type receptor. The difference between the F43A and F43V is that the F43V can constitutively activate the receptor and the F43A can not. F43V can also be further activated by both α-MSH and NDP-α-MSH.

The other phenylalanine residue, F278, was mutagenized to three other amino acids, alanine, valine and tyrosine. All three mutant receptors showed elevated basal level of cAMP-responsive β-galactosidase activity (**Figure 5A.2a-b**). Meanwhile, they also showed 4 fold higher total binding compared to the wild type receptor with the same IC_{50}s (**Figure 5A.2c-d, Table 5A.1**). The EC_{50}s for NDP-α-MSH stimulation is the same as the wild type receptor (**Table 5A.1**). The EC_{50}s for α-MSH stimulation are divided into two

groups: the amino acid change with aromatic structure, F278Y, showed the same EC_{50} as the wild type, while the amino acid changes without aromatic structure, F278A and F278V, showed about 20 fold increased EC_{50}s than the wild type receptor.

Disruption of arg-107 does not constitutively activate the MC1-R

As shown in chapter 1 and figure 5.1, arginine 107 in the mouse MC1-R is the homolog of arg-106 in the panther MC1-R. Arg106leu is the spontaneous mutation associated with the presumed dominant *extension* allele found in the black morph of the panther, *Panthera pardus* (chapter 1). Arginine is a positive charged residue located in the first intracellular loop. Based on the genetics and the property of arginine, it is possible that the arg-106 might be the counterion for the asp-115 of the MC1-R. Two mutations were made at arg107 of the mouse MC1-R, arg107leu and arg107asp. Surprisingly, neither mutant showed constitutive activation (**Figure 5A.3a-b**). Arg107asp has similar EC_{50} and IC_{50} values to the wild type receptor (**Figure 5A.3** and **Table 5A.2**), and the minimal elevation of the basal level of the arg107asp is probably due to the increased receptor number on the cell surface, evidenced by the higher total specific binding than with the wild type receptor. In contrast, the arg107leu mutant showed much lower total specific binding than the wild type receptor (**Figure 5A.3c**), and the basal level of the arg107leu activation was also decreased. However, the binding affinity of arg107leu was slightly increased relative to the wild type receptor (**Table 5A.2**). Due to the lack of additional genetic material, it is difficult to decide whether the arg106leu is only a polymorphism or is responsible for the dark color pigmentation in panther. So,

some other players, either other mutations of the MC1R or some other gene products may play a role in producing dark color pigmentation in the panther.

Figure legends

Figure 5A.1 Pharmacology of the F43 mutants of the mMC1-R. **a-b**, Activation of the F43 mutant receptors. Wild type and F43 mutant MC1 receptors were assayed by analyzing their ability to activate expression of a cAMP-induced β-galactosidase fusion gene. Cells stably expressing each receptor and transciently expressing the fusion construct were stimulated for 6 h with medium alone, 10 μM forskolin, or increasing concentrations of α-MSH (**a**), or NDP-α-MSH (**b**), then β-galactosidase concentrations were determined. Data points represent means of triplicate determinations divided by maximal levels of β-galactosidase activity achieved by 10 μM forskolin stimulation to normalize for transfection efficiency, and error bars indicate standard deviations. **c,d**, Competition binding studies of the mouse F43 mutants of the MC1-R along with the wild type. Different concentrations of cold NDP-α-MSH are used to compete with the ^{125}I-NDP-α-MSH. Nonspecific binding is determined as the counts bound in the presence of 10^{-5} M cold NDP-α-MSH. Data are displayed as total specific counts bound (**c**) or as a percentage of maximal specific counts bound (**d**). Data points represent means of duplicate determinations and bars indicate standard deviations.

Figure 5A.2 Pharmacology of the F278 mutants of the mMC1-R.
a-b, Activation of the F278 mutant receptors. Wild type and F278 mutant MC1 receptors were assayed by analyzing their ability to activate expression of a cAMP-induced β-galactosidase fusion gene. Cells stably expressing each

receptor and transciently expressing the fusion construct were stimulated for 6 h with medium alone, 10 μM forskolin, or increasing concentrations of α-MSH. (**a**), or NDP-α-MSH (**b**), then β-galactosidase concentrations were determined. Data points represent means of triplicate determinations divided by maximal levels of β-galactosidase activity achieved by 10 μM forskolin stimulation to normalize for transfection efficiency, and error bars indicate standard deviations.
c, d, Competition binding studies of the mouse F278 mutants of the MC1-R along with the wild type. Different concentrations of cold NDP-α-MSH are used to compete with the ^{125} I-NDP-α-MSH. Nonspecific binding is determined as the counts bound in the presence of 10^{-5} M cold NDP-α-MSH. Data are displayed as total specific counts bound (**c**) or as a percentage of maximal specific counts bound (**d**). Data points represent means of duplicate determinations and bars indicate standard deviations.

Figure 5A.3 Pharmacology of the R107 mutants of the mMC1-R.
a-b, Activation of the R107 mutant receptors. Wild type and R107 mutant MC1 receptors were assayed by analyzing their ability to activate expression of a cAMP-induced β-galactosidase fusion gene. Cells stably expressing each receptor and transciently expressing the fusion construct were stimulated for 6 h with medium alone, 10 μM forskolin, or increasing concentrations of α-MSH. (**a**), or NDP-α-MSH (**b**), then β-galactosidase concentrations were determined. Data points represent means of triplicate determinations divided by maximal levels of β-galactosidase activity achieved by 10 μM forskolin stimulation to normalize for transfection efficiency, and error bars indicate standard deviations.

c, d, Competition binding studies of the mouse R107 mutants of the MC1-R along with the wild type. Different concentrations of cold NDP-α-MSH are used to compete with the ^{125}I-NDP-α-MSH. Nonspecific binding is determined as the counts bound in the presence of 10^{-5} M cold NDP-α-MSH. Data are displayed as total specific counts bound (**c**) or as a percentage of maximal specific counts bound (**d**). Data points represent means of duplicate determinations and bars indicate standard deviations.

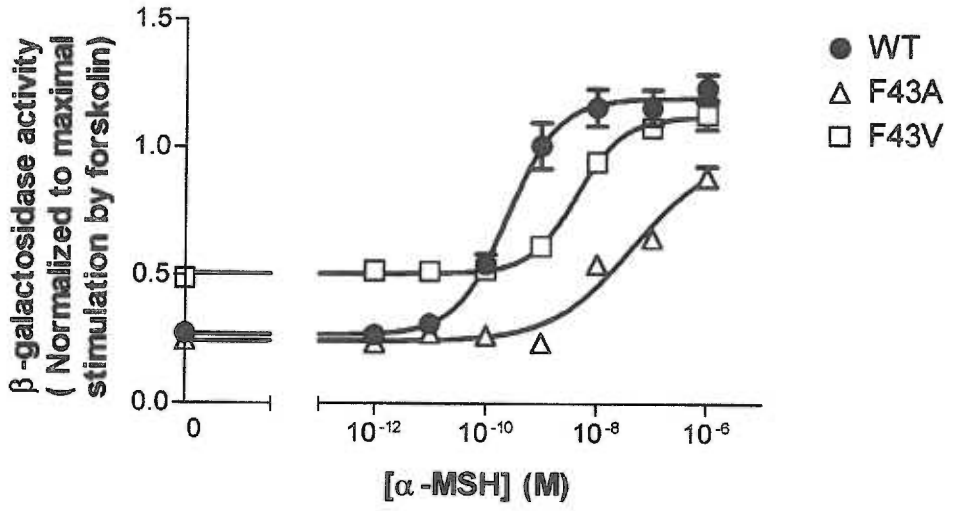

Figure 5A.1a

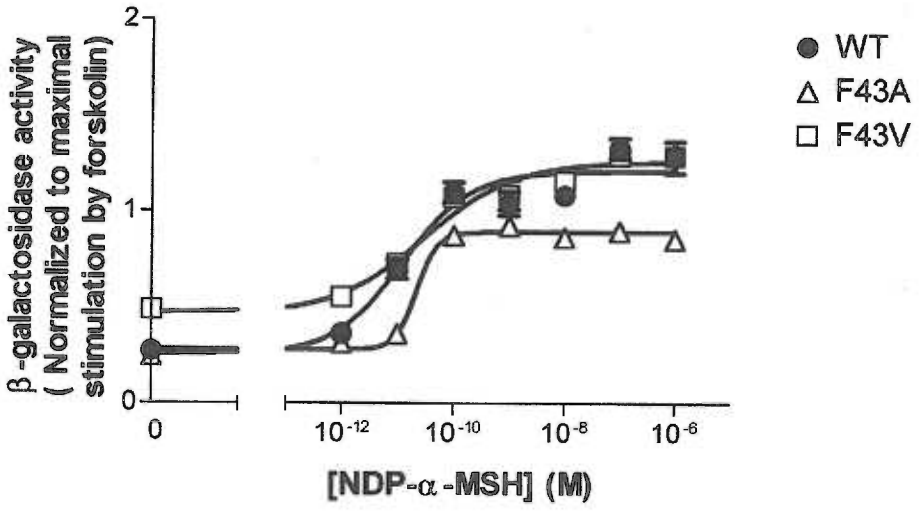

Figure 5A.1b

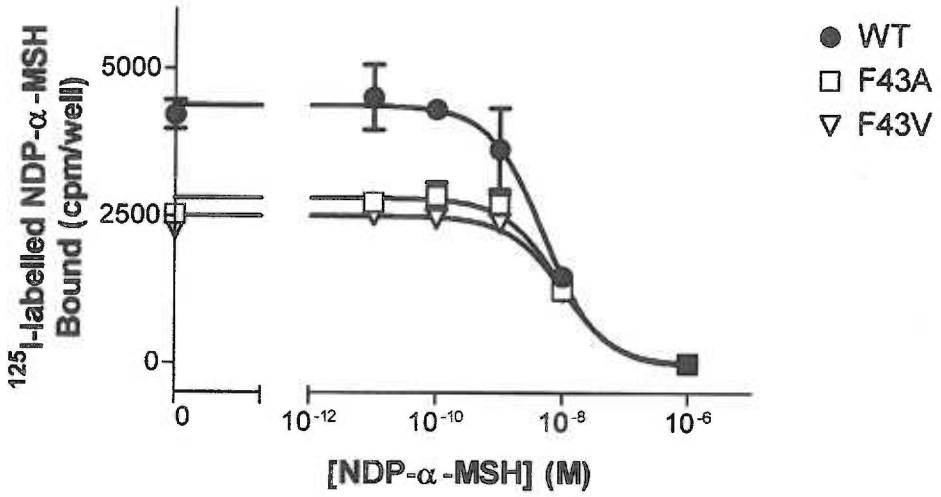

Figure 5A.1c

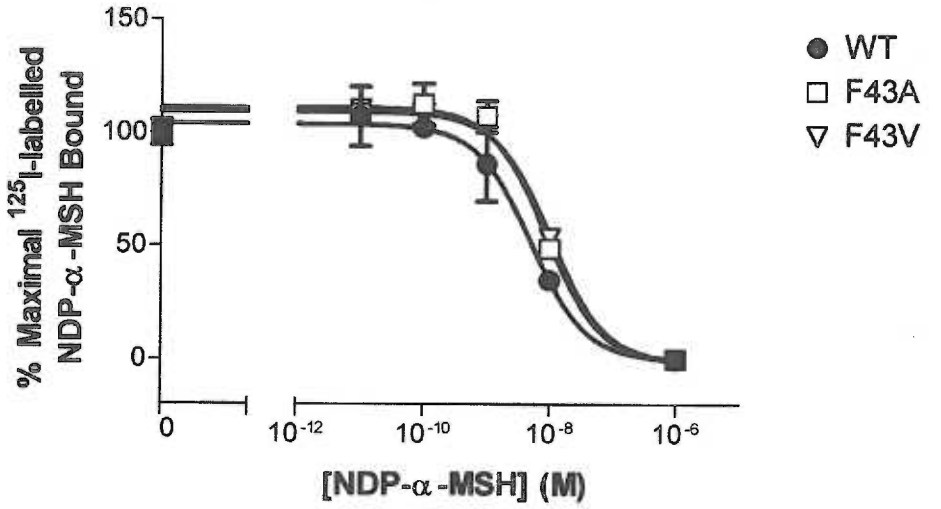

Figure 5A.1d

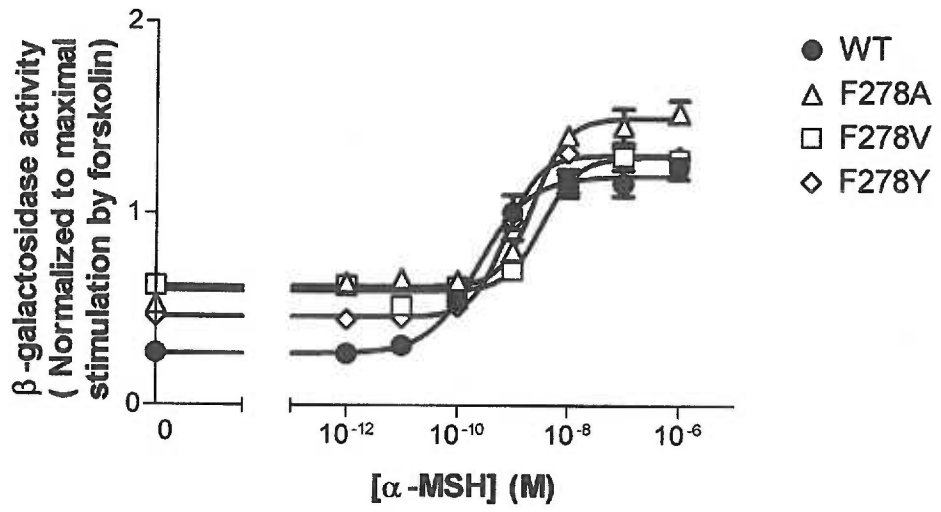

Figure 5A.2a

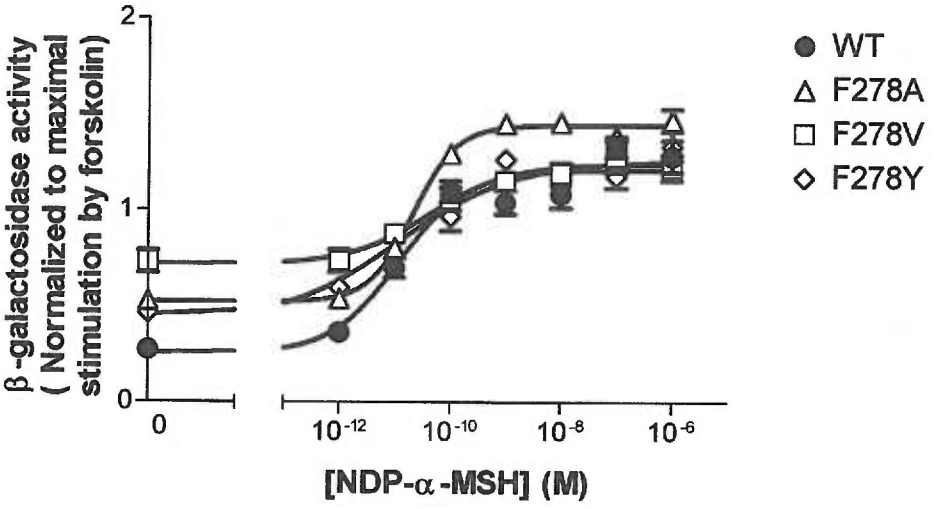

Figure 5A.2b

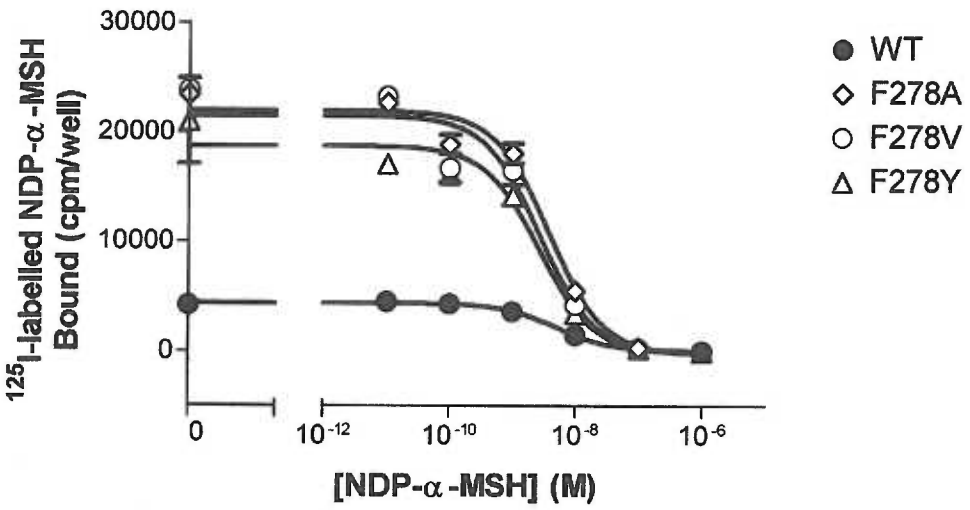

Figure 5A.2c

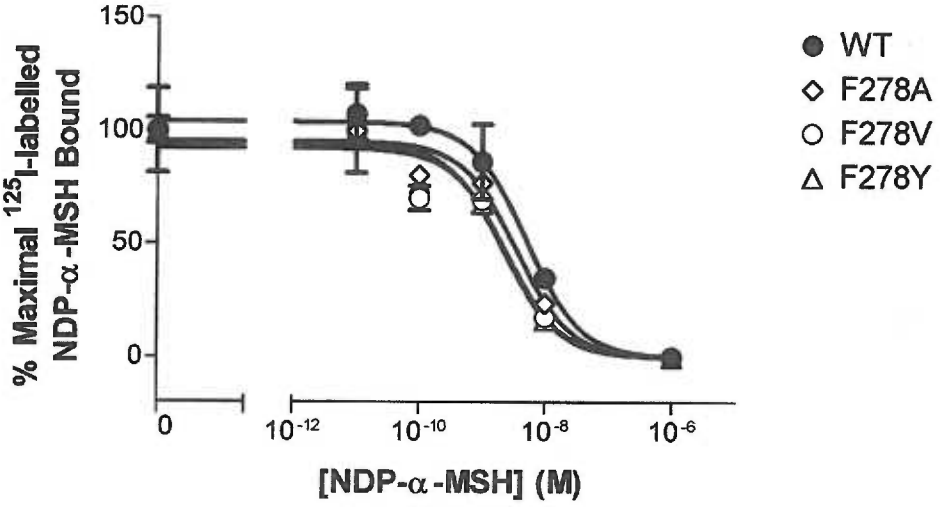

Figure 5A.2d

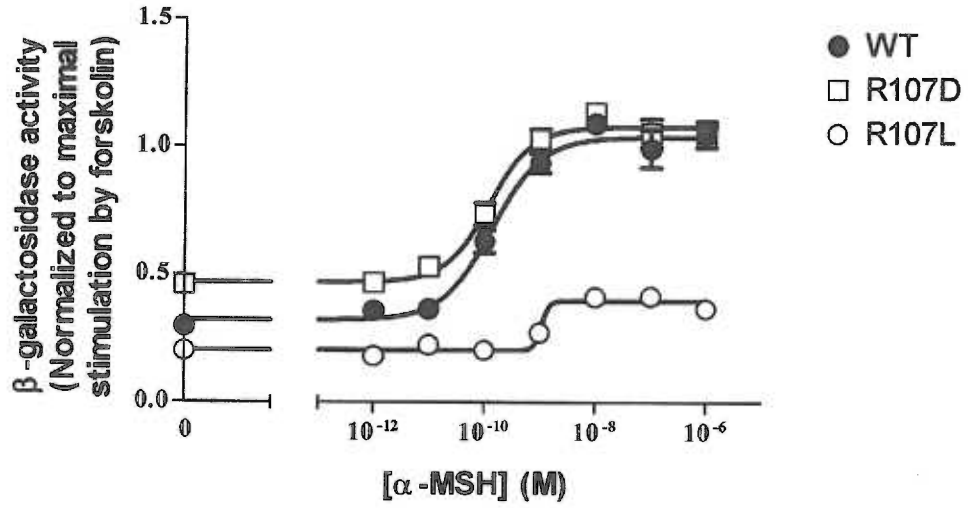

Figure 5A.3a

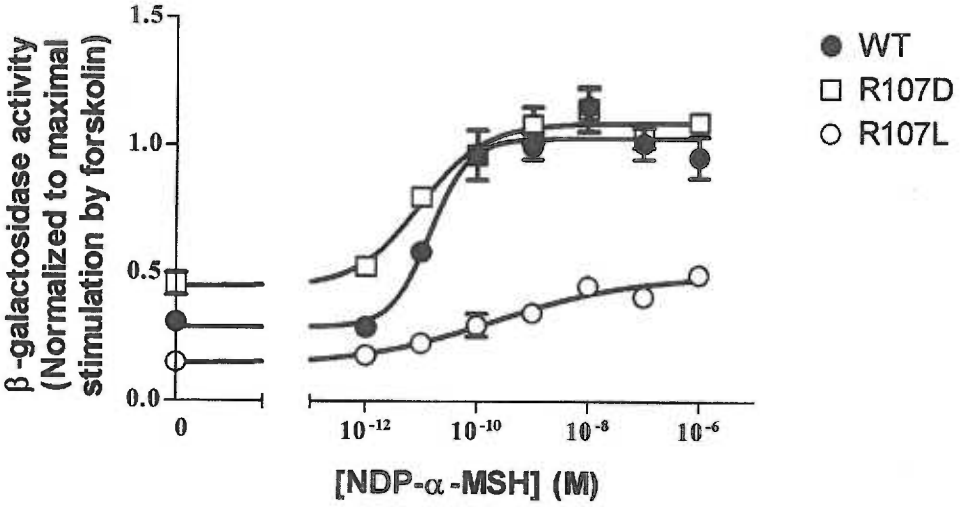

Figure 5A.3b

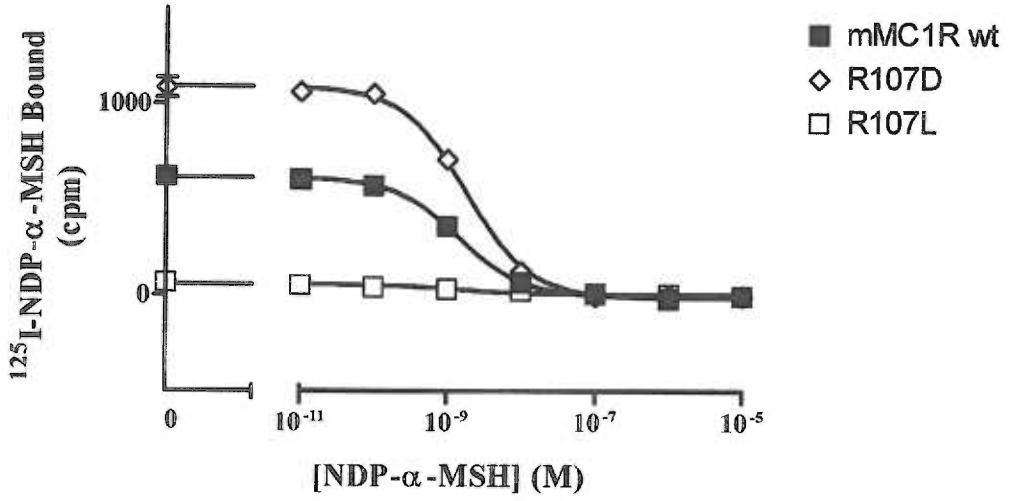

Figure 5A.3c

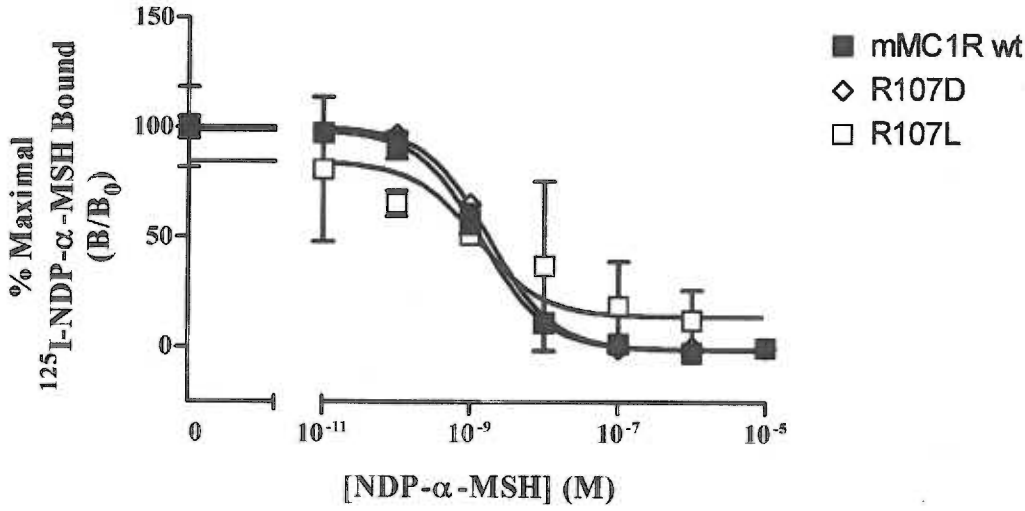

Figure 5A.3d

Table 5A.1 EC_{50}s for α-MSH and NDP-α-MSH Stimulation and IC_{50} of the mMC1-R Wild Type and Phenylalanine Mutants in Stably Transfected HEK 293 Cells

mMC1-R	EC_{50} (nM)[a]		IC_{50} (nM)[a]
	α-MSH	NDP-α-MSH	
WT	0.201 ± 0.109[d]	0.0162 ± 0.0055[d]	0.79 ± 0.48[b,c]
F43A	20.5 ± 15.4	0.0510 ± 0.0313	1.13 ± 0.33[b]
F43V	4.45 ± 0.17	0.0333 ± 0.0049	1.70 ± 0.94[b]
F278A	4.09 ± 1.97	0.0213 ± 0.0071	2.94 ± 1.25[b]
F278V	4.52 ± 1.53	0.0250 ± 0.0178	3.09 ± 1.82[b]
F278Y	3.86 ± 3.31	0.0243 ± 0.0223	3.35 ± 1.67[b]

a, Values are determined by two or more indenpendent experiments.
b, Cold NDP-α-MSH was used for competition binding experiments.
c, Value represents mean ± standard deviation from 5 indenpendent experiments.
d, Value represents mean ± standard deviation from 15 indenpendent experiments.

Table 5A.2 EC_{50}s for α-MSH and NDP-α-MSH Stimulation and IC_{50} of the mMC1-R Wild Type and R107 Mutants in Stably Transfected HEK 293 Cells

mMC1-R	EC_{50} (nM)[a]		IC_{50} (nM)[a]
	α-MSH	NDP-α-MSH	
WT	0.201 ± 0.109[d]	0.0162 ± 0.0055[d]	0.79 ± 0.48[b,c]
R107L	1.09 ± 0.61	0.211 ± 0.082	1.01 ± 0.36[b]
R107D	0.12 ± 0.01	0.0130 ± 0.0053	3.08 ± 1.79[b]

a, Values are determined by two or more indenpendent experiments.
b, Cold NDP-α-MSH was used for competition binding experiments.
c, Value represents mean ± standard deviation from 5 indenpendent experiments.
d, Value represents mean ± standard deviation from 15 indenpendent experiments.

Chapter 6

Summary and Conclusions

Receptor domain of the melanocortin receptor required for agouti function

The fact that agouti can selectively antagonize the melanocortin-1 and melanocortin-4 receptors suggested that the melanocortin-1 and melanocortin-4 receptors have a similar motif for agouti binding. Since agouti does not antagonize the function of either the melanocortin-3 or the melanocortin-5 receptors, the selectivity provides a possible way to identify the receptor domain(s) in the melanocortin-1 or the melanocortin-4 receptors required for agouti binding.

Chimeras were made using the melanocortin-3 and melanocortin-4 receptors as templates. The receptor was divided into three parts: the N-terminal fragment, including the first three transmembrane domains along with the N-terminal, and the first intracellular and extracellular loops of the receptor; the middle fragment, including the fourth transmembrane domain along with the second intracellular and extracellular loops of the receptor; and the C-terminal fragment, including the last three transmembrane domains transmembrane domain V, VI, and VII, along with the C-terminal and the third intracellular and extracellular loops of the receptor. Chimeras based on these receptor domains were tested for agouti binding, and the C-terminal domain was shown to be required for high affinity binding by agouti (Adan, R.A., Kesterson, R.A., and Cone, R.D., unpublished data). This data provides further evidence for a specific molecular interaction between agouti and the melanocortin receptors.

Additional studies of agouti function

After we first pharmacologically characterized the murine agouti peptide (Lu et al., 1994), more studies were carried out on different aspects of murine agouti peptide function, by both *in vitro* experiments using recombinant agouti protein (Blanchard et al., 1995; Hunt and Thody, 1995; Willard et al., 1995; Zemel et al., 1995; Jones et al., 1996), and *in vivo* experiments using transgenic animal studies (Klebig et al., 1995; Millar et al., 1995; Perry et al., 1995; Kim et al., 1996; Kucera et al., 1996; Perry et al., 1996). Since the human homolog of the agouti gene was also cloned in 1994 (Kwon et al., 1994; Wilson et al., 1995), the human agouti signaling peptide was made as a recombinant protein and its pharmacological properties on five human melanocortin receptors were tested (Yang et al., 1997). Furthermore, Hearing's group reported a study on the modulation of melanogenic protein expression, including tyrosinase, TRP1, and TRP2, during the switch from eu- to phaeo-melanogenesis (Kobayashi et al., 1995).

First, the effect of murine agouti peptide on endogenous mMC1-R was tested on the B16F10 murine melanoma cell line (Blanchard et al., 1995). The murine agouti peptide inhibited cAMP production stimulated by different melanocortin peptides with a similar Ki value of about 0.6 - 1.0 nM, and also inhibited the binding of ^{125}I-NDP-α-MSH to this cell line with a Kd value of 1.9 $\pm$ 0.6 nM, comparable to the results we reported earlier (chapter 2). The increased concentration of agouti peptide also reduced the crosslinking of ^{125}I-NDP-α-MSH to melanocortin receptors of intact B16F10 cells proportionally, which demonstrated again from another angle that agouti peptide blocks the ligand

binding to the receptor (Blanchard et al., 1995). Combined with our current study (chapter 2), these results indicated that the agouti peptide had similar effects in the heterogeneous cell expression system to endogenous MC1 receptors in antagonizing the function of the MC1-R.

Our results showed that murine agouti peptide functioned as a competitive antagonist of the MC1-R and the MC4-R (chapter 2). Hunt's result that agouti functions independently of α-MSH to inhibit basal melanogenesis in B16F1 murine melanoma cell (Hunt and Thody, 1995) indicated that competitive antagonism is not the only mechanism of murine agouti function, and that agouti peptide might function as an inverse agonist under some conditions (Lefkowitz et al., 1993; Samama et al., 1994), to reduce the basal activity of the mMC1-R in the B16F1 melanoma cell line. Our recent data in the fox suggests that the agouti may act as an inverse agonist in this species as well (Chapter 4). Recently, experiments related to the inhibitory action of agouti on the growth of B16F1 melanoma cells (Siegrist et al., 1996) further supported this hypothesis by demonstrating that the function of agouti peptide required the presence of the MC1-R, since agouti peptide showed no effect on the B16G4F cells, a melanoma cell line lacking functional MC1-R (Siegrist et al., 1996). Thus, reduced basal cAMP resulting from negative antagonism of the MC1-R by agouti peptide in B16F1 cells resulted in growth inhibition.

The expression and enzymatic functions of several melanogenic proteins, such as tyrosinase, TRP1, and TRP2, were examined in hair bulbs of newborn mice with normal agouti alleles (*A/A*), with one dominant agouti allele (A^y/a), and with recessive agouti alleles (*a/a*), respectively (Kobayashi et al., 1995). Neither expression of TRP1 or TRP-2 nor their enzymatic activities can be detected in the

hair bulbs of the newborn mice with one dominant agouti allele (A^y/a), and the tyrosinase activity was reduced compared to that found in the mice with either normal agouti alleles (*A/A*) or with recessive agouti alleles (*a/a*). Agouti may decrease the expression of TRP1 and TRP2 through a pathway other than antagonizing the MC1-R. Our results demonstrating that agouti peptide is a highly potent antagonist of the MC1-R (Lu et al., 1994), and the dominant *sombre* allele of the *extension* locus is epistatic to the dominant *agouti* alleles (Bateman, 1961; Wolff et al., 1978) provides genetic evidence to support our hypothesis that agouti acts through blocking α-MSH-stimulated or basal MC1-R activity. Yet, the other hypothesis that agouti peptide might act on its own receptor in addition to the MC1-R to inhibit the induction of adenylyl cyclase (Conklin and Bourne, 1993; Yen et al., 1994) has not yet been completely disproved. In this case, agouti peptide might act through its own receptor and activate the pathway which results in the reduced expression of TRP1 and TRP2 (Kobayashi et al., 1995).

Other reports claim that agouti plays a role in the regulation of intracellular calcium (Zemel et al., 1995; Jones et al., 1996; Kim et al., 1996). They showed increased intracellular [Ca^{2+}] in skeletal muscle (Zemel et al., 1995), and increased expression of both fatty acid synthase (FAS) and stearoyl-CoA desaturase (SCD) (Jones et al., 1996), two key enzymes in de novo fatty acid synthesis and desaturation, respectively, in adipose tissue from the obese viable yellow (A^{vy}/a) mice. Similar results were shown in cultured and freshly isolated skeletal muscle myocytes from wild-type mice (Zemel et al., 1995), and the 3T3-L1 adipocyte cell line (Jones et al., 1996), respectively. Calcium channel blockade nifedipine was used in both systems and partially reversed the agouti obesity phenotype (Kim et

al., 1996), and reduced the expressions of FAS and SCD in both systems (Jones et al., 1996; Kim et al., 1996). Since agouti peptide shared homology with the agatoxin/conotoxin family of proteins (Manne et al., 1995), a hypothesis that the pleiotropic effects of agouti are mediated, at least partially, through a $[Ca^{2+}]_i$-dependent mechanism was raised (Zemel et al., 1995; Jones et al., 1996; Kim et al., 1996).

However, there are some concerns about this hypothesis. First, the agatoxin/conotoxin family of proteins are calcium channel blockers (Olivera et al., 1994), which have the opposite effect as the proposed function of agouti peptide. Second, the recombinant agouti peptide is only 60-90% pure, due the lack of a suitable control for the effect of baculovirus protein, it is difficult to attribute the effects to agouti peptide directly. In this regard, it is important to note that the very delayed and modest increases (2 fold) in intracellular $[Ca^{2+}]$ could have easily resulted from the effects of contaminating growth factors from the baculovirus supernatants. Third, calcium is thought to play a role in mediating insulin action (Draznin, 1993), which is involved in the pleiotropic effects of dominant *agouti* allele. One of the melanocortin receptors, MC3-R, was also shown to couple to PKC pathway (Konda et al., 1994). The change of calcium might be the downstream effect of agouti peptide function on either MC3 or MC4 melanocortin receptors or on an unidentified melanocortin receptor. The effect of calcium channel blockade nifedipine can not link the agouti peptide directly to a calcium channel, since blockage of any effector downstream of agouti function would show the same results as blockage by agouti itself.

Previously, melanocyte transplantation experiments suggested that agouti functions as a paracrine factor, since the *agouti* phenotype could not be

produced by melanocyte transplantation, but rather only by hair follicle transplantation (Silvers and Russel, 1955; Silvers, 1958). Reported in 1995 and 1996, different laboratories used transgenic mice techniques to test whether agouti functions as a paracrine factor or through the circulation as an endocrine factor. When the expression of agouti cDNA was directed to all tissues examined with a β-actin promoter, the transgenic mice developed obesity, hyperinsulinemia, hyperglycemia and yellow fur, that is, the complete agouti obesity syndrome (Klebig et al., 1995). This result suggested that ectopic expression of agouti is the reason for the agouti obesity syndrome seen in lethal yellow (A^y) mice instead of the defects of other genes close to the agouti locus (Klebig et al., 1995). Furthermore, when the expression of agouti cDNA was targeted specifically to epithelial-associated keratinocytes in the skin (cells in the hair follicle) through the Keratin 14 promoter (Vassar et al., 1989), the transgenic mice showed yellow hair pigmentation in regions of transgene expression (Millar et al., 1995; Kucera et al., 1996), and a correlation between the expression level and degree of yellow pigmentation was established (Kucera et al., 1996). The transgenic mice with skin directed agouti expression showed no difference in weight and blood glucose levels compared to control animals (Kucera et al., 1996), which suggested that the agouti peptide acts as a paracrine factor, only has local effects, and must be expressed somewhere outside the skin to cause obesity. In order to test whether the agouti effect on hair pigmentation is through the MC1-R, those transgenic mice were backcrossed to *sombre* mice (Kucera et al., 1996), which are black due to a constitutively active MC1-R. All the resulting mice have the same hair color as the *sombre* mice, showing that the yellow hair resulted from the antagonism of agouti on the wild type MC1-R (Kucera et al., 1996).

Very recently, the effect of agouti-signaling protein (ASP), the human homolog of mouse agouti, on both receptor activation and ligand binding to the 5 human melanocortin receptors was tested (Yang et al., 1997). Similar to its counterpart in mouse, ASP is a potent inhibitor of both the hMC1-R and the hMC4-R. However, it also showed antagonist activity at both the hMC3-R and the hMC5-R at higher concentration. Since appropriate controls were not performed, there is some possibility that these activities were non-specific or the result of a contaminating baculovirus protein. In addition, the ASP showed potent inhibitory effects on the hMC2-R. However, ASP not only shifted the EC_{50} to the right, but also reduced the maximal stimulation level (Yang et al., 1997). This pharmacological property indicated that ASP is not a competitive antagonist of the hMC2-R, but more prone to noncompetitive antagonism. However, since the EC_{50} values at different concentrations of ASP are different, ASP did not act as a classic noncompetitive antagonist either. Gantz's group defined it as a nonsurmountable antagonist (Yang et al., 1997).

The structure/function relationship studies of agouti protein

Identification of the functional domain(s) in the agouti peptide would help to better understand agouti's action. In 1995, Willard *et al.* demonstrated that the C-terminal cysteine rich domain of murine agouti peptide alone retained full antagonist activity, using a biochemical approach (Willard et al., 1995). The full-length murine agouti peptide was digested with endoproteinase Lys-C to yield a C-terminal fragment val83-cys131, which was isolated by HPLC. The C-terminal fragment val83-cys131 contains all 10 cysteines connected to each other by forming 5 disulfide bonds and resembled the cysteine-rich domain of the full-

length murine agouti peptide. The ability of the C-terminal fragment to antagonize the mouse MC1-R was tested in both the adenylyl cyclase assay and the competition binding assay. This C-terminal fragment antagonized the activation of the MC1-R with a *K*i of 0.79 nM, and inhibited the binding of ^{125}I-NDP-α-MSH to the MC1-R with a *K*d of 3.0 $\pm$ 0.2 nM. Both values were similar to those of the full-length agouti peptide.

In order to further determine the required element for agouti function, fourteen agouti mutations were made and characterized for their effects on coat color and obesity using transgenic techniques (Perry et al., 1995; Perry et al., 1996). Three types of mutations were generated: 1), mutations in the putative signal peptide sequence, including the point mutation cys16arg found in the a^{16H} allele of agouti (Hustad et al., 1995; Perry et al., 1995), a recessive *agouti* allele, and a deletion from arg-5 to phe-14 (Perry et al., 1996); 2), mutations in the lysine rich basic domain, including a deletion from arg-64 to lys-77, and an asn39asp change in the only N-linked glycosylation site of murine agouti peptide (Bultman et al., 1992; Miller et al., 1993; Willard et al., 1995); and 3), mutations of each individual cysteine residue to serine residues in the C-terminal cysteine rich domain (Perry et al., 1996). Each mutant *agouti* cDNA was cloned into the pHβApr-2 plasmid containing the human β-ACTIN promoter and an SV40 polyadenylation signal, and the fragments containing each individual agouti mutant form fused to the β-ACTIN promoter were microinjected into C57BL/6J X DBA/2J)F_2 fertilized eggs to make transgenic mice (Perry et al., 1995; Perry et al., 1996). All mutants have equivalent agouti mRNA levels as in the control animals as quantitated by RNAse protection assay. Thus, effects on the coat color change and obesity could be attributed to the function of agouti peptide.

The transgenic animals with wild type agouti cDNA showed completely yellow coats and agouti obesity syndrome due to the ectopic expression of functional agouti peptide. All mutants tested showed partial loss of agouti activity or complete loss of agouti activity except the deletion from arg-64 to lys-77 in the lysine rich basic domain, which showed no apparent effect on agouti activity, indicating that at least part of the basic rich domain is not required for agouti function. The asn39asp mutant showed partial loss of agouti activity, indicating that the N-linked glycosylation probably accelerates the folding of agouti but is not absolutely necessary for producing an active protein. The mutations in the signal sequence resulted in complete loss of agouti activity suggesting that the signal peptide is necessary for agouti function probably by facilitating the secretion of agouti peptide.

Eight of the ten cysteine mutants in the cysteine rich domain resulted in the complete loss of agouti activity. The other two cysteine mutants, cys110ser and cys131ser, showed partial loss of agouti activity. The cysteines in ω-conotoxins and ω-agatoxins, which are arranged in a similar spacing pattern to that seen in agouti, have been suggested to play a critical role in stabilizing the tertiary structure of the protein through the formation of disulfide bonds (Olivera et al., 1994) (**Figure 6.1**). Interestingly, the eight cysteines critical for agouti function are those that closely align with the cysteines found in ω-agatoxins where the disulfide bond configuration is known (Olivera et al., 1994). In comparison, the function of these cysteines in agouti are probably similar to that seen in the toxins. Since the phenotypes of the cys110ser and cys131ser are nearly identical, and all cysteines in the cysteine rich domain were suggested to

be involved in disulfide bonding (Willard et al., 1995), these two cysteines probably also form a disulfide bond.

Selective antagonists are beneficial in the exploration of receptor function

After the discovery of an antagonist with high potency and selectivity for the melanocortin receptor family, these analogues were used for the exploration of specific receptor function. For example, analogue Ac-Nle^4-c[Asp^5,D-Phe^7,Lys^{10}]α-MSH-(4-10)-NH_2 (MTII) and analogue Ac-Nle^4-c[Asp^5,D-Nal(2)^7,Lys^{10}]α-MSH-(4-10)-NH_2 (SHU9119) have opposite effects on the neural melanocortin receptors, the melanocortin-3 and the melanocortin-4 receptors. SHU9119 is a potent antagonist of both MC3 and MC4 receptors, but SHU9119 is ten times more potent for the melanocortin-4 receptor ($pA_2 = 9.3$) than for the melanocortin-3 receptor ($pA_2 = 8.3$) (Hruby et al., 1995). MTII is a potent agonist for melanocortin-3 ($EC_{50} = 0.27 \pm 0.23$ nM) and melanocortin-4 receptors ($EC_{50} = 0.057 \pm 0.024$ nM) (Fan et al., 1997). Both analogues were used to determine the role of melanocortinergic neurons in feeding behavior, utilizing intracerebroventricular administration of the compounds. The experiment shows that MTII inhibits feeding, SHU9119 stimulates feeding, and SHU9119 can completely block the effect of MTII (Fan et al., 1997). These results provide strong experimental evidence in support of our previous hypothesis of the role of the MC4 receptor in the agouti obesity syndrome. Recently, the melanocortin-4 receptor has been knocked out, and the MC4-R knockout mouse showed a phenotype nearly identical to the agouti obesity syndrome with maturity-onset obesity, hyperphagia, hyperinsulinemia and hyperglycemia (Huszar et al., 1997).

The knockout experiments provide further support for our hypothesis that MC4-R plays a role in nutrient intake and energy balance.

As shown above, a selective agonist or antagonist can be very useful in helping us to understand the function of a particular receptor. Carefully analysis of the structure of these compounds will lead to identification of the key component for their function. This information can be used to develop new compounds by modification of the old ones with better specificity at different melanocortin receptors. Meanwhile, the effects of the current compounds on the different mutant receptors can also provide information for structure and function studies.

Constitutive activation studies provide information for understanding ligand binding to and activation of the MC1-R

Different studies related to the constitutive activation of G-protein coupled receptor have been conducted for more than 6 years. This phenomenon has been found in different kinds of G-protein coupled receptors, and the major receptors involved in these studies include adrenergic receptors, thyrotropin receptor (TSHR), luteinizing hormone receptor (LHR), rhodopsin, and melanocortin-1 receptor, the topic of this dissertation.

The first report of a constitutively active receptor involved chimeras of the α_1-and β_2-adrenergic receptors (Cotecchia et al., 1990), and the residues at the C-terminal end of the third intracellular loop, particular ala-293, were shown to be important in the activation of the adrenergic receptors. Subsequently, any amino acid substitutions at ala-293 was found to constitutively activate the α_1-adrenergic receptor (Kjelsberg et al., 1992). All of these mutations have higher

affinities for agonist binding than the wild type receptor, yet, the degree of increased binding affinity did not correlated to the degree of constitutive activation of the mutant receptor. Similarly, the activating mutations of the G protein-coupled α-factor pheromone receptor in the yeast *Saccharomyces cerevisiae*, with mutation pro258leu, or double mutation pro258leu and ser259leu, correlate as in the adrenergic receptor (Konopka et al., 1996). Although both mutations have higher binding affinity and higher level of constitutive activity than the wild type receptor, the pro258leu has higher affinity than the double mutation, but has lower level of constitutive activities than the double mutation (Konopka et al., 1996). The hydroxyl group of serine has been hypothesized to involved in intramolecular interaction(s), which constrain the receptor in an inactive state. Continuing with this hypothesis the mutations are proposed to release the constraint and activate the receptor.

Combined with other studies of members of the same adrenergic receptor family, such as β-adrenergic (Samama et al., 1993) and α2-adrenergic receptors (Ren et al., 1993), a new model related to the activation of the G-protein coupled receptor was suggested, the allosteric ternary complex model (Lefkowitz et al., 1993), or extended ternary complex model (Samama et al., 1993). This model indicates that there are two conformation states of the receptor, the inactive state, R, and the active state, R*, which exist in an equilibrium. Mutations that constitutively activate alter the conformation of the receptor, moving the equilibrium towards the active state, R*, similar to changes that occur when agonist binds to the receptor. According to this model, increased ratio of R* to R decreases the dissociation constant of the ligand, which explains why these

constitutive active receptors have higher affinities for the agonist (Kjelsberg et al., 1992; Ren et al., 1993; Samama et al., 1993).

However, the study of the melanocortin-1 receptor mutations shows different results. For the activating mutations tested in this receptor, binding affinities were inversely correlated with activation. The affinities for agonist are greatly reduced for mutations involving position glu-92, leu-98, asp-115, and asp-119 (1-2 magnitude higher than the wild type). Affinities remain the same as the wild type in mutations involving position met-71 and cys-123. These results in the melanocortin-1 receptor suggest a different mechanism than the adrenergic receptor discussed above. These mutations, with lower affinities for agonist, are located in different positions than the mutations of the adrenergic receptor. They are located in the exterior portions of the second and third transmembrane domains, and are probably involved in both ligand binding and activation of the receptor. Therefore, mutations in these positions will disrupt the ligand binding pocket, by mimicking ligand binding in order to constitutively activate the receptor. The adrenergic receptor mutations described above are located in the intracellular loop of the receptor, and involved in the coupling to G proteins; the binding pocket is intact and thus agonist binding is not impaired by the mutation. In contrast, the agonist binds much easier to the activating mutant receptor, since the energy required for the conformation change is greatly reduced due to the higher percentage of activating conformation R* of the mutant receptor.

In 1993, Parma *et al.* first identified that mutant TSH receptors from hyperfunctioning thyroid adenoma tissues confer constitutive activation of adenylyl cyclase when tested by transfection in COS cells (Parma et al., 1993). Two residues in the carboxyl-terminal portion of the third cytoplasmic loop of the

TSHR, asp-619 and ala-623, were mutated to glycine and isoleucine, respectively. These two mutations have increased the basal levels of cAMP to about 2-3 fold that resulting from transfection of the wild type receptor. However, unlike the homologous residue ala-293 of the α_{1B}-adrenergic receptor, at which all amino acid substitutions can cause constitutive activation (Kjelsberg et al., 1992), two other mutations of the TSHR, ala623glu and ala623lys made by *in vitro* mutagenesis, had the same basal activity as the wild type receptor (Kosugi et al., 1992). These results demonstrated that these residues probably function somewhat differently in each of the two different receptors.

As of this writing, 19 somatic and germline mutations of 13 different residues of the TSHR in tissues from hyperfunctioning thyroid adenoma (Parma et al., 1993; Paschke et al., 1994; Parma et al., 1995; Porcellini et al., 1995; Russo et al., 1995; Russo et al., 1996), from toxic thyroid hyperplasia (Tonacchera et al., 1996), from congenital hyperthyroidism (Kopp et al., 1995), and from differentiated thyroid carcinomas (Russo et al., 1995) have been identified to cause constitutive activation of the TSHR (Van Sande et al., 1995; Vassart et al., 1995; Tonacchera et al., 1996). These mutations are scattered in different regions of the TSHR. Three categories of regions are involved: 1) The carboxyl-terminal portion of the third intracellular loop (Asp-619 and Ala-623); 2) The transmembrane domains (Met-453 in the second transmembrane domain; Ser-505 and Val-509 in the third transmembrane domain; Phe- 631, Thr-632, Asp-633, and Asn-650 in the sixth transmembrane domain; and Asn-670 and Cys-672 in the seventh transmembrane domain); and 3) the extracellular loops (Ile-486 in the first extracellular loop and Ile-568 in the second extracellular loop, respectively) (**Table 6.1**).

Previous studies demonstrated that the third intracellular loop is believed to play a key role in the interaction of TSHR and other G-protein coupled receptors with their cognate G-proteins (Chazenbalk et al., 1990; Cotecchia et al., 1990; Kjelsberg et al., 1992; Kosugi et al., 1993; Yamada et al., 1994; Carlson et al., 1996). Obviously, the mutations in this important region are likely to affect this interaction.

Table 6.1 Positions of all 19 Constitutively Active Mutations of the TSHR in presumed regions of the receptor

Location	Mutations
The third intracellular loop	Asp619Gly,
	Ala623Ile/Val/Ser
Transmembrane domain II	Met453Thr
Transmembrane domain III	Ser505Arg,
	Val509Ala
Transmembrane domain VI	Phe631Leu/Cys,
	Thr632Ile,
	Asp633Glu/Tyr/His,
	Asn650Tyr
Transmembrane domain VII	Asn670Ser,
	Cys672Tyr
The first extracellular loop	Ile486Phe/Met
The second extracellular loop	Ile568Thr

However, the mutations in the transmembrane domains and in the extracellular loops are probably acting through different mechanisms than the mutations in the intracellular loop. Two hypotheses related to the constitutive activation of mutant receptors with mutations in the extracellular loops of the receptor have been suggested (Parma et al., 1995). One hypothesis is that the amino acid substitution may distort the connecting loop between transmembrane domains, thus changing the receptor to an active form with normal receptor activation by TSH; this hypothesis is probably suitable for explaining extracellular loop mutations in other receptors as well. The other hypothesis is probably unique to the extracellular loop mutations of the TSHR since it is related to the function of the characteristic long amino-terminal extracellular portion of 398 amino acids in the TSHR, which is considered to play an important role in the binding to its ligand TSH (Nagayama et al., 1990; Atassi et al., 1991; Nagayama et al., 1991; Morris et al., 1993; Bryant et al., 1994). In this model, the long extracellular portion of the TSHR is considered as the domain responsible for a negative constraint. Ligand binding to this domain would release the negative constraint, and mutations of the isoleucine residues in the second and third extracellular loops of the receptor would also interfere with the inhibitory interactions between the extracellular amino-terminal domain and the extracellular loops of the receptor (Parma et al., 1995).

The wide distribution of constitutive active TSH receptor mutations raised a question about whether a receptor is liable to be constitutively active. Tonacchera et al. made a helical wheel representation of the transmembrane segments of the TSHR according to the model of Baldwin (Baldwin, 1993), and showed all these mutations are randomly distributed (Tonacchera et al., 1996).

These results indicate that: 1) The energy requirement of conformation change from inactive to active state of the TSH-R is low (Kosugi et al., 1993; Tonacchera et al., 1996); 2) Different mechanisms might exist for different mutations; and 3) Mutations in different regions might also cause similar conformational changes since experiments showed that there are interactions among different transmembrane domains of other G-protein coupled receptors (Huang et al., 1994; Zhou et al., 1994; Liu et al., 1995; Sealfon et al., 1995; Sheikh et al., 1996).

The visual pigment rhodopsin, is another member of the G-protein coupled receptor (GPCR) superfamily. Rhodopsin contains an 11-cis-retinal chromophore covalently attached to the apoprotein, opsin, through a protonated Schiff base linkage to the ε-amino group of lys-296 in the middle portion of the seventh transmembrane domain (Findlay and Pappin, 1986). All mutations tested at lys-296 (lys296ala, lys296gly, lys296glu) and mutation of the Schiff base counterion, glu-113 (glu113gln) in the interior portion of the third transmembrane domain, result in constitutive activation of opsin in the absence of added chromophore (Robinson et al., 1992). One of the mutations, lys296gly was found in patients with retinitis pigmentosa (Keen et al., 1991). Another mutation of opsin, also found in patients with retinitis pigmentosa, lys296met, was constitutively active as well (Sullivan et al., 1993).

A salt bridge model was proposed in which the wild type opsin is normally constrained in an inactive state by an electrostatic attraction, or salt bridge, between lys296 and glu113. Mutations at either residue will disrupt the salt bridge, release the internal constraint, and activate the opsin. Later, 7 more amino acid substitutions at lys-296 also showed constitutive activity (Cohen et al., 1993), which supplied more evidence for the salt bridge model. However, the salt

bridge model is probably only part of the picture for activation of opsin, since the lys296 mutants show maximal activity at a different pH than the glu-113 mutant (Cohen et al., 1992). Since the charged residues play important roles in the activation of opsin, several other charged residues of opsin were also tested. Only one other residue, glu-134, showed the constitutive activity similar to the lys-296 mutants (Cohen et al., 1993).

The glu-134 was mutagenized to two different amino acids, gln and asp, to test the requirements for constitutive activation via this residue. The glu134gln mutation increased the activity of opsin, while the glu134asp inhibited the activity of opsin. Furthermore, the glu134gln, lys296his double mutation had more activity than the activating mutant lys296his, while glu134asp, lys296his had less activity than the activating mutant lys296his (Cohen et al., 1993). These results suggested that a negatively charged residue in position glu134 is important to stabilize the receptor in an inactive state, also functioning as a counterion in the salt bridge model (Robinson et al., 1992).

Two more missense mutations in the rhodopsin gene, gly90asp and ala292glu, found in patients with congenital stationary night blindness, were also constitutive active when expressed in COS cells (Dryja et al., 1993; Rao et al., 1994). Gly-90 is in the second transmembrane domain of rhodopsin, and close to both glu-113 and lys-296 in the three dimensional model (Rao et al., 1994). Ala-292 is in the same transmembrane domain as lys-296, and is approximately one helical turn away from lys-296. Introduction of a negatively charged residue at either position will probably affect the electrostatic interaction between the lys-296 and glu-113, competing the protonated nitrogen of the lys-296 with glu-113, and could indirectly disrupt the salt bridge (Dryja et al., 1993; Rao et al., 1994).

Since the glu113gln can not protonate the Schiff base to retain the salt bridge, the mutant glu113gln was constitutively active (Cohen et al., 1992; Robinson et al., 1992). In order to test whether introduction of a negative charged residue at gly-90, an adjacent position to glu-113, can reprotonate the Schiff base, the double mutant, gly90asp plus glu113gln, was constructed, and the double mutant showed similar absorption maximum as the wild type (Rao et al., 1994). This double mutant result demonstrated that not only the lys-296 and glu-113 can form a salt bridge to stabilize the opsin in an inactive state, but also an alternative salt bridge between lys-296 and asp-90 can be functional when the original one was broken.

The mutations of lys-296 have different profiles from those of the mutations of glu-113, gly-90 and ala-292. The mutations of lys-296, except lys296arg, can not bind the chromophore, and are constitutively active in the absence of added 11-cis-retinal chromophore or light (Keen et al., 1991; Cohen et al., 1992; Robinson et al., 1992). The mutations of the other three positions with an intact lys-296, can bind the 11-cis-retinal chromophore, and are constitutively active in the absence of added 11-cis-retinal chromophore (Cohen et al., 1992; Robinson et al., 1992; Dryja et al., 1993; Rao et al., 1994). However, when the 11-cis-retinal chromophore was added to these mutant in the dark, the activating mutants were suppressed (Cohen et al., 1992; Robinson et al., 1992; Dryja et al., 1993; Rao et al., 1994). Even though the salt bridge is directly disrupted by glu-113 mutations, or indirectly disrupted by gly90asp and ala292glu, the form of 11-cis-retinal chromophore is still sufficient to lock the receptor in an inactive state (Robinson et al., 1992). This is probably the reason that retinitis pigmentosa

results in photoreceptor degeneration but congenital stationary night blindness doesn't (Dryja et al., 1993; Rao et al., 1994).

This mechanism of indirect disruption of the salt bridge by ala292glu may explain the effects of residue asp-119 and cys-123 in the melanocortin-1 receptor. The mutagenesis data of asp-115 shows constitutive activation when this negatively charge amino acid has been removed, which indicates a potential role in a constraining interaction as is seen for lys-296 in rhodopsin. Since asp-115 is approximately one and two helical turns away from asp-119 and cys-123, respectively, and only positive charge residue changes at either of these positions can cause constitutive activation of the receptor, the simple explanation is that the interaction of the asp-115 with either of the basic residue changes mimics the interaction of arg-8 in the ligand. However, asp-119 and cys-123 may be in the membrane, with asp-115 in the extracellular milieu, and this could limit their interaction. Furthermore, no obvious counterion for asp-115 exists.

Extensive *in vitro* mutagenesis studies have been conducted on the melanocortin-1 receptor in the present study. A total of 41 mutations of the mouse melanocortin-1 receptor have been pharmacologically characterized using competition binding and functional activation methods. Scatchard analysis has also been done on the wild type receptor and some important mutants, such as the somber-3J mutant (E92K). In contrast to the constitutively active mutant of the adrenergic receptors, the E92K mutant has similar receptor number as the wild type receptor at the cell surface, but has lower affinity than the wild type receptor. α-MSH analogue NDP-α-MSH has ten times higher affinity for the wild type MC1-R (K_D(wt) = 0.62 $\pm$ 0.30 nM) than the E92K mutant receptor (K_D(E92K) = 6.41 $\pm$ 2.52 nM). As mentioned above, this result indicates that

mutants of the melanocortin-1 receptor are constitutively activated via a different mechanism than the adrenergic receptors.

Polar residues have been identified to play crucial roles in high affinity receptor binding and activation of the GPCRs. A polar allosteric pocket has been suggested by in vitro mutagenesis studies and computer modeling (Trumpp-Kallmeyer et al., 1992; Oliveira et al., 1994; Fanelli et al., 1995), in which polar residues from different transmembrane domains form a pocket for the ligand to dock in and subsequently change the receptor to an active conformation.

An aspartic acid residue, located in the third transmembrane domain, is conserved in many GPCRs that bind monoamines. Computer modeling of ligand docking for five cationic neurotransmitter receptors (serotonergic 5-HT_2, dopaminergic D_2, muscarinic m_2, α_2 and β_2 adrenergic receptors) showed that this aspartic residue belongs to the binding pocket and interacts with cationic neurotransmitters (Trumpp-Kallmeyer et al., 1992). Another independent computer model of the β_2-adrenergic receptor highlighted two aspartic acid residues, one in the second transmembrane domain (asp-79) and the other is the same one in the third transmembrane domain as above (asp-113). Asp-113 is shown as the principle anchor for the ligand in either clockwise or counterclockwise models for the β_2-adrenergic receptor helix bundles, whereas asp-79 is shown only in the clockwise model, which is turned away from the presumed binding pocket in the counterclockwise model (Kontoyianni et al., 1996). Furthermore, another report related to the asp-397 in the boundary of the second transmembrane domain and the first extracellular loop of the LH/CG-R indicated that the asp-397 formed an ion pair with lys-91 of the ligand, α-subunit of hCG (Ji et al., 1993). They postulated that ligand binding may alter the

conformation of the unoccupied receptor by reorienting the second transmembrane domain and the aspartic acid residue was important in signaling but was not essential for binding (Ji and Ji, 1993). The hypothesis they proposed is similar to our model for the present study for the roles of several acidic residues involved, glu-92, asp-115, and asp-119, located in the exterior portion of the second and the third transmembrane domain of the MC1-R. The computer modeling of the melanocortin-1 receptor shows all these three residues cluster together. As mentioned in chapter 1, the pharmacophore of the ligand α-MSH also contains a basic residue arg-8. This residue is proposed to contact the site of the negative residue cluster when the ligand is docked in the receptor in the computer model. However, the interaction is clearly more complicated than only a direct interaction between the arg-8 and the negative residue cluster in the receptor.

It will be interesting to examine some analogues of α-MSH with modification at the arg-8 position on these acidic residue mutations. For example, it will be interesting to test the effect of acidic amino acid substitution at the arg-8 position of α-MSH on the glu92lys, asp115lys, asp119lys, and double or triple substitution mutants. However, since ligand binding probably also needs other interactions, the substitution of one amino acid might affect the conformation of the ligand and produce complicated results.

The pharmacological profile of the met71lys mutation of the melanocortin-1 receptor is different from other constitutively active MC1-R mutations. As shown in chapter 5, this mutation constitutively activates the receptor, but retains wild type affinity for the ligand. Also, this mutation is located in the carboxyl-terminal portion of the first intracellular loop, unlike the other activating

mutations located closed to the extracellular side of the membrane. This mutation is likely to constitutively activate the receptor through a different mechanism than the others, and behaves much more like constitutively activating mutations of the adrenergic receptors in which high affinity agonist binding is retained or even enhanced.

In human platelet-activating factor receptor, two adjacent amino acids in the carboxyl-terminal portion of the third intracellular loop, ala-230 and leu-231, have been mutagenized to glutamic acid and glutamine in ala-230, and arginine in leu-231, respectively (Parent et al., 1996). Besides the activation of all these mutants, high and low affinity binding to the agonist were also tested in the absence and presence of GTPγs to determine the mutation's effects on the interaction between the receptor and the G protein. The leu231arg mutant has been shown to have a higher level of basal activity, has higher affinity for the agonist and 60% of leu231arg mutant is in a high affinity state compared to 40% with the wild type receptor. However, the ala230glu mutant showed no increased level of basal activity and seems not to couple well to the G-protein. The ala230gln mutation also showed no increased level of basal activity, has lower affinity for the agonist, and has the same percentage of mutant receptor in high affinity state as the wild type receptor (Parent et al., 1996). Since the difference appears to be the charge status of those residues, they speculate that the leu231arg added one more positively charged residue in an already basic microenvironment (KRRARL) that could favor the attachment of the G-protein (Parent et al., 1996). The met71lys mutant of the melanocortin-1 receptor has the same charge change as the leu231arg, and is also proximal to the DRY sequence of the second intracellular loop, which is known to be important in the coupling

to G-proteins, so there might be some similarities between these two mutations in the mechanism of constitutive activation of GPCRs. It would be interesting to see the effect of GTPγs on the pharmacological profile of the met71lys mutant.

In conclusion, the studies presented in this dissertation demonstrated the following:

1) Agouti peptide is a high affinity competitive antagonist with specificity for two of the five melanocortin receptors. It antagonizes the stimulation of mouse melanocortin-1 receptor, which provides the molecular basis for a variety of mammalian coat color pigmentation patterns. Besides the effect of agouti peptide in coat color pigmentation, antagonism of the melanocortin-4 receptor by agouti peptide suggested that disruption of hypothalamic MC4-R signaling by ectopically expressed agouti might be the molecular basis of the obesity syndrome in the lethal yellow mouse (A^y).

2) Bulky aromatic amino acid substitution in the 7-position of the cyclic MSH analogue Ac-Nle^4-c[Asp^5,D-Phe^7,Lys^{10}]α-MSH-(4-10)-NH_2 produces a potent and selective antagonist of the melanocortin-3 and melanocortin-4 receptors. Analogue 3 (SHU8914), Ac-Nle^4-c[Asp^5,D-Phe(pI)^7,Lys^{10}]α-MSH-(4-10)-NH_2, is a partial agonist and potent antagonist for both human melanocortin-3 and human melanocortin-4 receptors. The more selective analogue 4 (SHU9119), Ac-Nle^4-c[Asp^5,D-Nal(2)^7,Lys^{10}]α-MSH-(4-10)-NH_2, is a potent antagonist for the human melanocortin-3 receptor with minimal agonist activity. However, SHU9119 is a complete antagonist for the human melanocortin-4 receptor with no agonist activity. Both analogue 3 and analogue 4, along with other analogues tested, are full agonists of the mouse and human melanocortin-1 and mouse melanocortin-5 receptors.

3) In contrast to mice, in which dominant *extension* alleles are epistatic to *agouti*, a non-epistatic interaction of *agouti* and *extension* in the fox, *Vulpes vulpes* is suggested. Instead of acting as a competitive antagonist, such as in the mouse, the fox agouti peptide might function as an inverse agonist to inhibit the basal activity of the wild type fox MC1-R, thus explaining the non-epistatic interaction.

4) *In vitro* mutagenesis studies of the mouse melanocortin-1 receptor indicated that constitutive activation of the melanocortin-1 receptor is responsible for dark coat pigmentation in a variety of mammalian species, such as in the mouse, fox, sheep, and cattle. More detailed analysis of amino acid substitutions with different chemical properties demonstrated that introduction of a basic residue at glu-92, asp-119, and cys-123 is required for the constitutive activation of the receptor, while simple removal of the negative charge of asp-115 can also constitutively activate the receptor. In addition, both met71lys in the first intracellular loop, and leu98pro, one turn of the helix up from the glu-92 position, can constitutively activate the receptor as well. However, mutations at the conserved basic residues, his-183, his-258, and lys-276, can not make the melanocortin-1 receptor constitutively active. Furthermore, removal of the acidic residue in asp-119 position decreased affinity for ligand 10-100 fold, which indicates that this residue might participate in high affinity ligand binding. Computer-modeling suggested that the three acidic residues, glu-92, asp-115 and asp-119, may form a highly negatively charged pocket in the receptor, and a basic residue, arg-8 in the pharmacophore of the ligand, docks into this pocket. Based

on the in vitro mutagenesis studies and the computer modeling, a "ligand-mimetic" hypothesis is proposed for the mechanism of constitutive activation of the melanocortin-1 receptor by mutations at glu-92, asp-119 and cys-123. Insertion of basic residues at these positions are mimicking the docking of the arg-8 of the ligand pharmacophore to constitutively activate the receptor. The asp-115 interacts with an unidentified residue(s) of the receptor, and is involved in the constraint of the receptor in an inactive state.

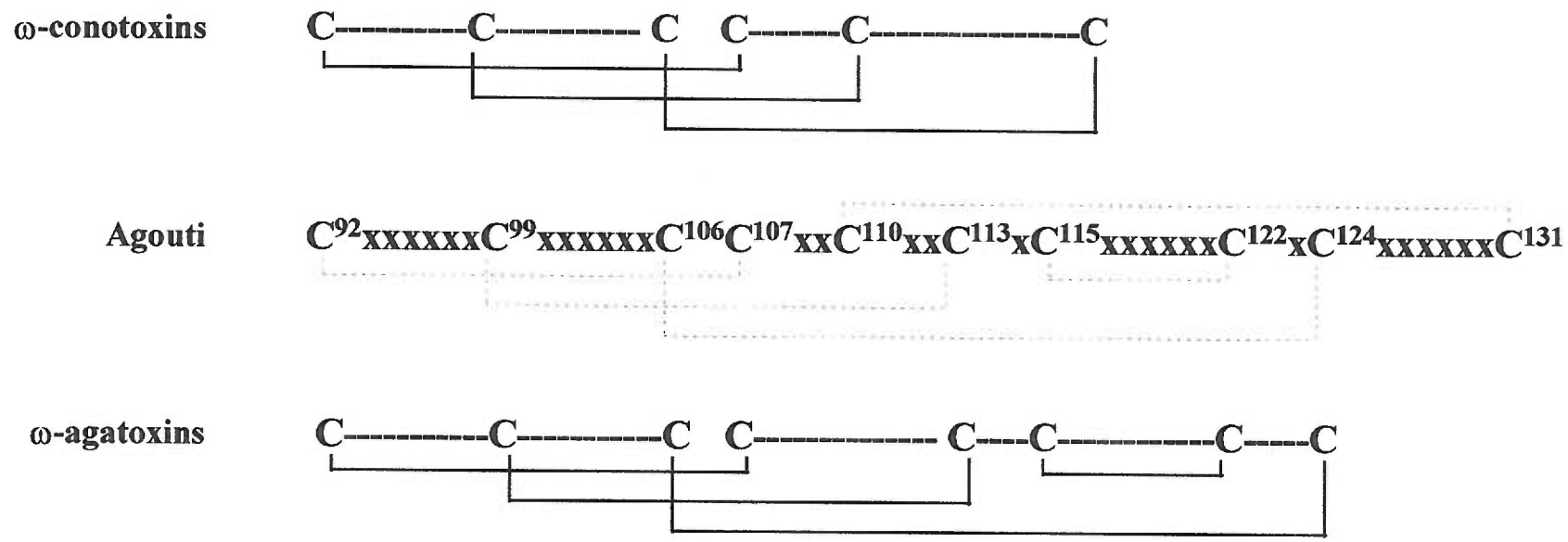

Figure 6.1 Alignment of the C-terminal cysteine residues of the murine agouti peptide with those found in ω-conotoxins and ω-agatoxins. ω-conotoxins represent all homologous calcium channel-targeted peptides isolated from the venom of cone snails of the *Conus* genus (Olivera et al., 1994). ω-agatoxins represent selective peptide antagonists of voltage-activated calcium channels isolated from venom of spiders of *Agelenopsis aperta* (Olivera et al., 1994). The pattern of ω-agatoxins cysteins spacing shown here is of peptides ω-AgaIVA and ω-AgaIVB. In agouti, "x" represents non-cys residues, and the numbers showed the position of these cysteines. The dashes in toxins help to align cysteines with those in agouti, and no actural amino acids were represented. The disulfide bonds of Cys in ω-conotoxins and ω-agatoxins are shown with connecting lines. The predicted disulfide bonds in agouti are shown with dotted lines.

REFERENCES

Abdel-Malek, Z., Swope, V. B., Suzuki, I., Akcali, C., Harriger, M. D., Boyce, S. T., Urabe, K., and Hearing, V. J. (1995). Mitogenic and melanogenic stimulation of normal human melanocytes by melanotropic peptides. Proceedings of the National Academy of Sciences of the United States of America *92*, 1789-93.

Adalsteinsson, S., Bjarnadottir, S., Vage, D. I., and Jonmundsson, J. V. (1995). Brown coat color in Icelandic cattle produced by the loci Extension and Agouti. Journal of Heredity *86*, 395-8.

Adalsteinsson, S., Hersteinsson, P., and Gunnarsson, E. (1987). Fox colors in relation to colors in mice and sheep. Journal of Heredity *78*, 235-7.

Adan, R. A., Oosterom, J., Ludvigsdottir, G., Brakkee, J. H., Burbach, J. P., and Gispen, W. H. (1994). Identification of antagonists for melanocortin MC3, MC4 and MC5 receptors. European Journal of Pharmacology *269*, 331-7.

Akamizu, T., Inoue, D., Kosugi, S., Ban, T., Kohn, L. D., Imura, H., and Mori, T. (1993). Chimeric studies of the extracellular domain of the rat thyrotropin (TSH) receptor: amino acids (268-304) in the TSH receptor are involved in ligand high affinity binding, but not in TSH receptor-specific signal transduction. Endocrine Journal *40*, 363-72.

Allen, L. F., Lefkowitz, R. J., Caron, M. G., and Cotecchia, S. (1991). G-protein-coupled receptor genes as protooncogenes: constitutively activating mutation of the alpha 1B-adrenergic receptor enhances mitogenesis and tumorigenicity. Proceedings of the National Academy of Sciences of the United States of America *88*, 11354-8.

Al-Obeidi, F., Castrucci, A. M., Hadley, M. E., and Hruby, V. J. (1989). Potent and prolonged acting cyclic lactam analogues of alpha-melanotropin: design based on molecular dynamics. Journal of Medicinal Chemistry *32*, 2555-61.

Al-Obeidi, F., Hadley, M. E., Pettitt, B. M., and Hruby, V. J. (1989). Design of a New Class of Superpotent Cyclic alpha-Melanotropins Based on Quenched Dynamic Simulations. J. Am. Chem. Soc. *111*, 3413-3416.

Al-Obeidi, F., Hruby, V. J., Darman, J., Sawyer, T. K., Castrucci, A. M., and Hadley, M. E. (1989). Discovery and Experimental Analysis of alpha-MSH Antagonists. In Peptides 1988, G. a. B. Jung, E., ed. (Berlin, Germany: W. de Gruyer), pp. 598-600.

al-Obeidi, F., Hruby, V. J., Hadley, M. E., Sawyer, T. K., and Castrucci, A. M. (1990). Design, synthesis, and biological activities of a potent and selective alpha-melanotropin antagonist. International Journal of Peptide & Protein Research *35*, 228-34.

Arvanitakis, L., Geras-Raaka, E., Varma, A., Gershengorn, M. C., and Cesarman, E. (1997). Human herpesvirus KSHV encodes a constitutively active G-protein-coupled receptor linked to cell proliferation [see comments]. Nature *385*, 347-50.

Ashbrook, F. G. (1937). The Breeding of Fur Animals. In Yearbook of Agriculture, pp. 1379-1395.

Atassi, M. Z., Manshouri, T., and Sakata, S. (1991). Localization and synthesis of the hormone-binding regions of the human thyrotropin receptor. Proceedings of the National Academy of Sciences of the United States of America *88*, 3613-7.

Baldwin, J. (1993). The probable arrangement of helices in the G protein-coupled receptors. EMBO J. *12*, 1693-1703.

Barret, P., MacDonald, A., Helliwell, R., Davidson, G., and Morgan, P. (1994). Cloning and expression of a new member of the melanocyte-stimulating hormone receptor family. J. Mol. Endocrinol. *12*, 203-213.

Barsh, G. S. (1996). The genetics of pigmentation: from fancy genes to complex traits. [Review]. Trends in Genetics *12*, 299-305.

Bateman, N. (1961). J. Hered. *52*, 186-189.

Bateman, N. (1961). Sombre, a viable dominant mutant in the house mouse. J. Hered. *52*, 186-189.

Beckwith, B. E., and Sandman, C. A. (1982). Central nervous system and peripheral effects of ACTH, MSH, and related neuropeptides. Peptides *3*, 411-20.

Beermann, F., Ruppert, S., Hummler, E., Bosch, F. X., Muller, G., Ruther, U., and Schutz, G. (1990). Rescue of the albino phenotype by introduction of a functional tyrosinase gene into mice. EMBO Journal *9*, 2819-26.

Bertagna, X. (1994). Proopiomelanocortin-derived peptides. [Review]. Endocrinology & Metabolism Clinics of North America *23*, 467-85.

Bertolini, A., Guarini, S., Rompianesi, E., and Ferrari, W. (1986). Alpha-MSH and other ACTH fragments improve cardiovascular function and survival in experimental hemorrhagic shock. European Journal of Pharmacology *130*, 19-26.

Bhardwaj, R. S., and Luger, T. A. (1994). Proopiomelanocortin production by epidermal cells: evidence for an immune neuroendocrine network in the epidermis. [Review]. Archives of Dermatological Research *287*, 85-90.

Bijlsma, W. A., Schotman, P., Jennekens, F. G., Gispen, W. H., and De Wied, D. (1983). The enhanced recovery of sensorimotor function in rats is related to the melanotropic moiety of ACTH/MSH neuropeptides. European Journal of Pharmacology *92*, 231-6.

Blanchard, S. G., Harris, C. O., Ittoop, O. R., Nichols, J. S., Parks, D. J., Truesdale, A. T., and Wilkison, W. O. (1995). Agouti antagonism of melanocortin binding and action in the B16F10 murine melanoma cell line. Biochemistry *34*, 10406-11.

Bownds, D. (1967). Site of attachment of retinal in rhodopsin. Nature *216*, 1178-81.

Bryant, W. P., Bergert, E. R., and Morris, J. C. (1994). Delineation of amino acid residues within hTSHr 256-275 that participate in hormone binding. Journal of Biological Chemistry *269*, 30935-8.

Buckley, D. I., and Ramachandran, J. (1981). Characterization of corticotropin receptors on adrenocortical cells. Proceedings of the National Academy of Sciences of the United States of America *78*, 7431-5.

Bultman, S. J., Michaud, E. J., and Woychik, R. P. (1992). Molecular characterization of the mouse agouti locus. Cell *71*, 1195-204.

Burchill, S. A., Thody, A. J., and Ito, S. (1986). Melanocyte-stimulating hormone, tyrosinase activity and the regulation of eumelanogenesis and phaeomelanogenesis in the hair follicular melanocytes of the mouse. J. Endocrinol. *109*, 15-21.

Burchill, S. A., Virden, R., and Thody, A. J. (1989). Regulation of Tyrosinase Synthesis and its Processing in the Hair Follicular Melanocytes of the Mouse During Eumelanogenesis and Phaeomelanogenesis. J. Invest. Dermatol. *93*, 236-240.

Burley, S. K., and Petsko, G. A. (1986). Amino-aromatic interactions in proteins. FEBS Letters *203*, 139-43.

Carlson, S. A., Chatterjee, T. K., and Fisher, R. A. (1996). The third intracellular domain of the platelet-activating factor receptor is a critical determinant in receptor coupling to phosphoinositide phospholipase C-activating G proteins. Studies using intracellular domain minigenes and receptor chimeras. Journal of Biological Chemistry *271*, 23146-53.

Castrucci, A. M., Hadley, M. E., and Hruby, V. J. (1984). Melanotropin bioassays: in vitro and in vivo comparisons. General & Comparative Endocrinology *55*, 104-11.

Castrucci, A. M., Hadley, M. E., Lebl, M., Zechel, C., and Hruby, V. J. (1989). Melanocyte stimulating hormone and melanin concentration hormone may be structurally and evolutionarily related. Regulatory Peptides *24*, 27-35.

Catania, A., and Lipton, J. M. (1994). The neuropeptide alpha-melanocyte-stimulating hormone: a key component of neuroimmunomodulation. Neuroimmunomodulation *1*, 93-9.

Ceriani, G., Diaz, J., Murphree, S., Catania, A., and Lipton, J. M. (1994). The neuropeptide alpha-melanocyte-stimulating hormone inhibits experimental arthritis in rats. Neuroimmunomodulation *1*, 28-32.

Chakraborty, A. K., Platt, J. T., Kim, K. K., Kwon, B. S., Bennett, D. C., and Pawelek, J. M. (1996). Polymerization of 5,6-dihydroxyindole-2-carboxylic acid to melanin by the pmel 17/silver locus protein. European Journal of Biochemistry *236*, 180-8.

Chazenbalk, G. D., Nagayama, Y., Russo, D., Wadsworth, H. L., and Rapoport, B. (1990). Functional analysis of the cytoplasmic domains of the human thyrotropin receptor by site-directed mutagenesis. Journal of Biological Chemistry *265*, 20970-5.

Chen, C., and Okayama, H. (1987). High-efficiency transformation of mammalian cells by plasmid DNA. Molecular & Cellular Biology *7*, 2745-52.

Chen, W., Shields, T. S., Stork, P. J., and Cone, R. D. (1995). A colorimetric assay for measuring activation of Gs- and Gq-coupled signaling pathways. Analytical Biochemistry *226*, 349-54.

Chhajlani, V., Muceniece, R., and Wikberg, J. E. S. (1993). Molecular cloning of a novel human melanocortin receptor. Biochem. Biophys. Res. Comm. *195*, 866-873.

Chhajlani, V., and Wikberg, J. E. S. (1992). Molecular cloning and expression of the human melanocyte stimulating hormone receptor cDNA. FEBS Lett. *309*, 417-420.

Chiao, H., Foster, S., Thomas, R., Lipton, J., and Star, R. A. (1996). Alpha-melanocyte-stimulating hormone reduces endotoxin-induced liver inflammation. Journal of Clinical Investigation *97*, 2038-44.

Chowdhary, B. P., Gustavsson, I., Wikberg, J. E., and Chhajlani, V. (1995). Localization of the human melanocortin-5 receptor gene (MC5R) to chromosome band 18p11.2 by fluorescence in situ hybridization. Cytogenetics & Cell Genetics *68*, 79-81.

Cody, W. L., Hadley, M. E., and Hruby, V. J. (1988). Mechanisms of Action and Biomedical Applications. In The Melanotropic Peptides, Vol. III, M. E. Hadley, ed. (Boca Raton, FL: CRC Press), pp. 75-92.

Cohen, G. B., Oprian, D. D., and Robinson, P. R. (1992). Mechanism of activation and inactivation of opsin: role of Glu113 and Lys296. Biochemistry *31*, 12592-601.

Cohen, G. B., Yang, T., Robinson, P. R., and Oprian, D. D. (1993). Constitutive activation of opsin: influence of charge at position 134 and size at position 296. Biochemistry *32*, 6111-5.

Cone, R. D., Lu, D., Koppula, S., Vage, D. I., Klungland, H., Boston, B., Chen, W., Orth, D. N., Pouton, C., and Kesterson, R. A. (1996). The melanocortin receptors: agonists, antagonists, and the hormonal control of pigmentation. [Review]. Recent Progress in Hormone Research *51*, 287-317.

Cone, R. D., and Mountjoy, K. G. (1993). Molecular Genetics of the ACTH and MSH Receptors. Trends Endocrinol. Metab. *4*, 242-247.

Cone, R. D., Mountjoy, K. G., Robbins, L. S., Nadeau, J. H., Johnson, K. R., Roselli-Rehfuss, L., and Mortrud, M. T. (1993). Cloning and functional characterization of a family of receptors for the melanotropic peptides. [Review]. Annals of the New York Academy of Sciences *680*, 342-63.

Conklin, B. R., and Bourne, H. R. (1993). Mouse coat colour reconsidered [letter; comment]. Nature *364*, 110.

Cotecchia, S., Exum, S., Caron, M. G., and Lefkowitz, R. J. (1990). Regions of the alpha 1-adrenergic receptor involved in coupling to phosphatidylinositol hydrolysis and enhanced sensitivity of biological function. Proceedings of the National Academy of Sciences of the United States of America *87*, 2896-900.

de Wied, D. (1990). Neurotrophic effects of ACTH/MSH neuropeptides. [Review]. Acta Neurobiologiae Experimentalis *50*, 353-66.

de Wied, D. (1977). Pituitary adrenal system hormones and behaviour. Acta Endocrinologica. Supplementum *214*, 9-18.

del Marmol, V., and Beermann, F. (1996). Tyrosinase and related proteins in mammalian pigmentation. [Review]. FEBS Letters *381*, 165-8.

del Marmol, V., Ito, S., Jackson, I., Vachtenheim, J., Berr, P., Ghanem, G., Morandini, R., Wakamatsu, K., and Huez, G. (1993). TRP-1 expression correlates with eumelanogenesis in human pigment cells in culture. FEBS Letters *327*, 307-10.

DeLean, A., Stadel, J. M., and Lefkowitz, R. J. (1980). A ternary complex model explains the agonist-specific binding properties of the adenylate cyclase-coupled β-adrenergic receptor. J. Biol. Chem. *255*, 7108-7117.

Desarnaud, F., Labbe, O., Eggerickx, D., Vassart, G., and Parmentier, M. (1994). Molecular cloning, functional expression and pharmacological characterization of a mouse melanocortin receptor gene. Biochemical Journal *299*, 367-73.

Dickerson, G. E., and Gowen, J. W. (1947). Hereditary obesity and efficient food utilization in mice. Science *105*, 496-498.

Dixon, R. A., Sigal, I. S., Candelore, M. R., Register, R. B., Scattergood, W., Rands, E., and Strader, C. D. (1987). Structural features required for ligand binding to the beta-adrenergic receptor. EMBO Journal *6*, 3269-75.

Donovan, B. T. (1978). The behavioural actions of the hypothalamic peptides: a review. [Review]. Psychological Medicine *8*, 305-16.

Dougherty, D. A. (1996). Cation-pi interactions in chemistry and biology: a new view of benzene, Phe, Tyr, and Trp. [Review] [66 refs]. Science *271*, 163-8.

Dratz, E. A., and Hargrave, P. A. (1083). The structure of rhodopsin and the rod outer segment disk membrane. Trends biochem. Sci. *8*, 128-131.

Draznin, B. (1993). Cytosolic calcium and insulin resistance. [Review] [40 refs]. American Journal of Kidney Diseases *21*, 32-8.

Dryja, T. P., Berson, E. L., Rao, V. R., and Oprian, D. D. (1993). Heterozygous missense mutation in the rhodopsin gene as a cause of congenital stationary night blindness. Nature Genetics *4*, 280-3.

Duhl, D. M., Stevens, M. E., Vrieling, H., Saxon, P. J., Miller, M. W., Epstein, C. J., and Barsh, G. S. (1994). Pleiotropic effects of the mouse lethal yellow (Ay) mutation explained by deletion of a maternally expressed gene and the simultaneous production of agouti fusion RNAs. Development *120*, 1695-708.

Eberle, A. N. (1988). The Melanotropins: Chemistry, Physiology and Mechanisms of Action (Basel, Switzerland: Karger).

Eberle, A. N., de Graan, P. N. E., Baumann, J. B., Girard, J., van Hees, G., and van de Veerdonk, F. C. G. (1984). Structural requirements of a-MSH for the stimulation of MSH receptors on different pigment cells. Yale J. Biol. Med. *57*, 353-354.

Edwards, P. M., Van der Zee, C. E., Verhaagen, J., Schotman, P., Jennekens, F. G., and Gispen, W. H. (1984). Evidence that the neurotrophic actions of alpha-MSH may derive from its ability to mimick the actions of a peptide formed in degenerating nerve stumps. Journal of the Neurological Sciences *64*, 333-40.

Fan, W., Boston, B. A., Kesterson, R. A., Hruby, V. J., and Cone, R. D. (1997). Role of melanocortinergic neurons in feeding and the *agouti* obesity syndrome. Nature *385*, 165-168.

Fanelli, F., Menziani, M. C., and De Benedetti, P. G. (1995). Computer simulations of signal transduction mechanism in alpha 1B-adrenergic and m3-muscarinic receptors. Protein Engineering *8*, 557-64.

Fathi, Z., Iben, L. G., and Parker, E. M. (1995). Cloning, expression, and tissue distribution of a fifth melanocortin receptor subtype. Neurochem. Res. *20*, 107-113.

Felgner, J. H., Kumar, R., Sridhar, C. N., Wheeler, C. J., Tsai, Y. J., Border, R., Ramsey, P., Martin, M., and Felgner, P. L. (1994). Enhanced gene delivery and mechanism studies with a novel series of cationic lipid formulations. Journal of Biological Chemistry *269*, 2550-61.

Findlay, J. B., and Pappin, D. J. (1986). The opsin family of proteins. [Review] [299 refs]. Biochemical Journal *238*, 625-42.

Findlay, J. B. C., and Pappin, D. J. C. (1986). The opsin family of proteins. Biochem J *238*, 625-642.

Frandberg, P. A., Muceniece, R., Prusis, P., Wikberg, J., and Chhajlani, V. (1994). Evidence for alternate points of attachment for alpha-MSH and its stereoisomer [Nle4, D-Phe7]-alpha-MSH at the melanocortin-1 receptor. Biochemical & Biophysical Research Communications *202*, 1266-71.

Frazier, A. L., Robbins, L. S., Stork, P. J., Sprengel, R., Segaloff, D. L., and Cone, R. D. (1990). Isolation of TSH and LH/CG receptor cDNAs from human thyroid: regulation by tissue specific splicing. Molecular Endocrinology *4*, 1264-76.

Gantz, I., Konda, Y., Tashiro, T., Shimoto, Y., Miwa, H., Munzert, G., Watson, S. J., DelValle, J., and Yamada, T. (1993a). Molecular cloning of a novel melanocortin receptor. Journal of Biological Chemistry *268*, 8246-50.

Gantz, I., Miwa, H., Konda, Y., Shimoto, Y., Tashiro, T., Watson, S. J., DelValle, J., and Yamada, T. (1993b). Molecular cloning, expression, and gene localization of a fourth melanocortin receptor. Journal of Biological Chemistry *268*, 15174-9.

Gantz, I., Shimoto, Y., Konda, Y., Miwa, H., Dickinson, C. J., and Yamada, T. (1994a). Molecular cloning, expression, and characterization of a fifth melanocortin receptor. Biochemical & Biophysical Research Communications *200*, 1214-20.

Gantz, I., Yamada, T., Tashiro, T., Konda, Y., Shimoto, Y., Miwa, H., and Trent, J. M. (1994b). Mapping of the gene encoding the melanocortin-1 (alpha-melanocyte stimulating hormone) receptor (MC1R) to human chromosome 16q24.3 by Fluorescence in situ hybridization. Genomics *19*, 394-5.

Geschwind, I. I. (1966). Change in hair color in mice induced by injection of a-MSH. *79*, 1165-1167.

Geschwind, I. I., Huseby, R. A., and Nishioka, R. (1972). The effect of melanocyte-stimulating hormone on coat color in the mouse. Rec. Prog. Horm. Res. *28*, 91-130.

Gether, U., Lin, S., and Kobilka, B. K. (1995). Fluorescent labeling of purified beta 2 adrenergic receptor. Evidence for ligand-specific conformational changes. Journal of Biological Chemistry *270*, 28268-75.

Griffon, N., Mignon, V., Facchinetti, P., Diaz, J., Schwartz, J.-C., and Sokoloff, P. (1994). Molecular cloning and characterization of the rat fifth melanocortin receptor. Biochem. Biophys. Res. Comm. *200*, 1007-1014.

Hadley, M. E. (1988). The Melanotropic Peptides (Boca Raton, FL: CRC Press).

Hadley, M. E., Heward, C. B., Hruby, V. J., Sawyer, T. K., and Yang, Y. C. (1981). Biological actions of melanocyte-stimulating hormone. Ciba Foundation Symposium *81*, 244-62.

Halaban, R., Pomerantz, S. H., Marshall, S., and Lerner, A. B. (1984). Tyrosinase activity and abundance in cloudman melanoma cells. Arch. Biochem. Biophys. *230*, 383-387.

Haskell-Luevano, C., Sawyer, T. K., and Hruby, V. J. (1995). Molecular model of the G-protein coupled melanocortin receptor, hMC1R, and possible interactions with α-MSH peptides. In Peptides: Chemistry, structure and biology, Proceedings of the Fourteenth American Peptide Symposium, P. T. P. Kaumaya and R. S. Hodges, eds. (England: Mayflower Scientific Ltd.), pp. 378-379.

Haskell-Luevano, C., Sawyer, T. K., Trumpp-Kallmeyer, S., Bikker, J., Humblet, C., Gantz, I., and Hruby, V. J. (1996). Three-dimensional molecular models of the hMC1R melanocortin receptor: Complexes with melanotropin peptide agonists. Drug design and discovery *14*, 197-211.

Hearing, V. J. (1987). Mammalian monophenol monooxygenase (tyrosinase): purification, properties and reactions catalyzed. In Methods in Enzymology-Metabolism of Aromatic Amion Acids and Amines, S. Kaufman, ed. (New York: Academic), pp. 154-165.

Hearing, V. J., and Jimenez, M. (1987). Mammalian tyrosinase: The critical regulatory control point in melanocyte pigmentation. Int. J. Biochem. *19*, 1141-1147.

Hearing, V. J., and Tsukamoto, K. (1991). Enzymatic control of pigmentation in mammals. FASEB *5*, 2902-9209.

Hiltz, M. E., Catania, A., and Lipton, J. M. (1992). Alpha-MSH peptides inhibit acute inflammation induced in mice by rIL-1 beta, rIL-6, rTNF-alpha and endogenous pyrogen but not that caused by LTB4, PAF and rIL-8. Cytokine *4*, 320-8.

Hoganson, G. E., Ledwitz-Rigby, F., Davidson, R. L., and Fuller, B. B. (1989). Regulation of tyrosinase mRNA levels in mouse melanoma cell clones by melanocyte-stimulating hormone and cyclic AMP. Som. Cell. Mol. Gen. *15*, 255-263.

Hruby, V. J. (1992). Strategies in the Development of Peptide Antagonists. In Progress in Brain Research, J. Joosse, Buijs, R. M., and Tilders, F. J. H., ed. (Amsterdam, The Netherlands: Elsevier Sci. Publ.), pp. Chapter 18, 215-224.

Hruby, V. J., Al-Obeidi, F., and Smith, D. D. (1990). Synthesis of Cyclic Peptides by Solid Phase Methods. In Innovations and Perspectives in Solid Phase Synthesis, R. Epton, ed. (Brimingham, U.K.: SPCC (U.K.) Ltd.), pp. 197-203.

Hruby, V. J., Lu, D., Sharma, S. D., Castrucci, A. L., Kesterson, R. A., al-Obeidi, F. A., Hadley, M. E., and Cone, R. D. (1995). Cyclic lactam alpha-melanotropin analogues of Ac-Nle4-cyclo[Asp5, D-Phe7,Lys10] alpha-melanocyte-stimulating hormone-(4-10)-NH2 with bulky aromatic amino acids at position 7 show high antagonist potency and selectivity at specific melanocortin receptors. Journal of Medicinal Chemistry *38*, 3454-61.

Hruby, V. J., and Sharma, S. D. (1991). Designing peptide and protein ligands for biological receptors. Current Opinion in Biotechnology *2*, 599-605.

Hruby, V. J., Sharma, S. D., Toth, K., Jaw, J. Y., Al-Obeidi, F., Sawyer, T. K., Castrucci, A. M. L., and Hadley, M. E. (1993). Synthesis and Conformation of Superpotent and Prolonged Acting Melanotropins. Ann. N. Y. Acad. Sci. *3*, 140-146.

Hruby, V. J., Wilkes, B. C., Cody, W. L., Sawyer, T. K., and Hadley, M. E. (1984). Melanotropins: Structural, Conformational, and Biological Considerations in the Development of Superpotent and Superprolonged Analogues. Pept. Protein Rev. *3*, 1-64.

Hruby, V. J., Wilkes, B. C., Hadley, M. E., Al-Obeidi, F., Sawyer, T. K., Staples, D. J., de Vaux, A. E., Dym, O., Castrucci, A. M., Hintz, M. F., and et al. (1987). alpha-Melanotropin: the minimal active sequence in the frog skin bioassay. Journal of Medicinal Chemistry *30*, 2126-30.

Huang, R. R., Yu, H., Strader, C. D., and Fong, T. M. (1994). Interaction of substance P with the second and seventh transmembrane domains of the neurokinin-1 receptor. Biochemistry *33*, 3007-13.

Hunt, G., Kyne, S., Wakamatsu, K., Ito, S., and Thody, A. J. (1995). Nle4DPhe7 alpha-melanocyte-stimulating hormone increases the eumelanin:phaeomelanin ratio in cultured human melanocytes. Journal of Investigative Dermatology *104*, 83-5.

Hunt, G., and Thody, A. J. (1995). Agouti protein can act independently of melanocyte-stimulating hormone to inhibit melanogenesis. Journal of Endocrinology *147*, R1-4.

Hunt, G., Todd, C., Cresswell, J. E., and Thody, A. J. (1994). Alpha-melanocyte stimulating hormone and its analogue Nle4DPhe7 alpha-MSH affect morphology, tyrosinase activity and melanogenesis in cultured human melanocytes. Journal of Cell Science *107*, 205-11.

Hunt, G., Todd, C., Kyne, S., and Thody, A. J. (1994). ACTH stimulates melanogenesis in cultured human melanocytes. Journal of Endocrinology *140*, R1-3.

Huntington, T., and Hadley, M. E. (1974). Evidence against mass action direct feedback control of melanophore-stimulating hormone (MSH) release. Endocrinology *95*, 472-9.

Hustad, C. M., Perry, W. L., Siracusa, L. D., Rasberry, C., Cobb, L., Cattanach, B. M., Kovatch, R., Copeland, N. G., and Jenkins, N. A. (1995). Molecular genetic characterization of six recessive viable alleles of the mouse agouti locus. Genetics *140*, 255-65.

Huszar, D., Lynch, C. A., Fairchild-Huntress, V., Dunmore, J. H., Fang, Q., Berkemeier, L. R., Gu, W., Kesterson, R. A., Boston, B. A., Cone, R. D., Smith, F. J., Campfield, L. A., Burn, P., and Lee, F. (1997). Targeted disruption of the melanocortin-4 receptor results in obesity in mice. Cell *88*, 131-141.

Jackson, I. J. (1988). A cDNA encoding tyrosinase-related protein maps to the mouse brown locus. Proc. Natl. Acad. Sci. USA *85*, 4392-4396.

Jackson, I. J. (1994). Molecular and developmental genetics of mouse coat color. Annu. Rev. Genet. *28*, 189-217.

Jackson, I. J. (1993). Molecular genetics. Colour-coded switches [news] [see comments]. Nature *362*, 587-8.

Jackson, I. J., Chambers, D. M., Tsukamoto, K., Copeland, N. G., Jenkins, N. A., and Hearing, V. (1992). A second tyrosinase-related protein, TRP-2, maps to and is mutated at the mouse slaty locus. EMBO J. *11*, 527-535.

Jayawickreme, C. K., Quillan, J. M., Graminski, G. F., and Lerner, M. R. (1994). Discovery and structure-function analysis of alpha-melanocyte-stimulating hormone antagonists. Journal of Biological Chemistry *269*, 29846-54.

Jhamandas, K. H. (1984). Opioid-neurotransmitter interactions: significance in analgesia, tolerance and dependence. Progress in Neuro-Psychopharmacology & Biological Psychiatry *8*, 565-70.

Ji, I., and Ji, T. H. (1993). Receptor activation is distinct from hormone binding in intact lutropin-choriogonadotropin receptors and Asp397 is important for receptor activation. Journal of Biological Chemistry *268*, 20851-4.

Ji, I., Zeng, H., and Ji, T. H. (1993). Receptor activation of and signal generation by the lutropin/choriogonadotropin receptor. Cooperation of Asp397 of the receptor and alpha Lys91 of the hormone. Journal of Biological Chemistry *268*, 22971-4.

Johnson, P. D., Dawson, B. V., Dorr, R. T., Hadley, M. E., Levine, N., and Hruby, V. J. (1994). Coat color darkening in a dog in response to a potent melanotropic peptide. American Journal of Veterinary Research *55*, 1593-6.

Johnson, R. A., and Salomon, Y. (1991). Assay of adenylyl cyclase catalytic activity. Methods in Enzymology *195*, 3-21.

Jones, B. H., Kim, J. H., Zemel, M. B., Woychik, R. P., Michaud, E. J., Wilkison, W. O., and Moustaid, N. (1996). Upregulation of adipocyte metabolism by agouti protein: possible paracrine actions in yellow mouse obesity. American Journal of Physiology *270*, E192-6.

Kaiser, E., Colescott, R. L., Bossinger, C. D., and Cook, P. I. (1970). Color test for detection of free terminal amino groups in the solid-phase synthesis of peptides. Analytical Biochemistry *34*, 595-8.

Karnik, S. S., Sakmar, T. P., Chen, H. B., and Khorana, H. G. (1988). Cysteine residues 110 and 187 are essential for the formation of correct structure in bovine rhodopsin. Proceedings of the National Academy of Sciences of the United States of America *85*, 8459-63.

Kawate, N., Kletter, G. B., Wilson, B. E., Netzloff, M. L., and Menon, K. M. (1995). Identification of constitutively activating mutation of the luteinising hormone receptor in a family with male limited gonadotrophin independent precocious puberty (testotoxicosis). Journal of Medical Genetics *32*, 553-4.

Keen, T. J., Inglehearn, C. F., Lester, D. H., Bashir, R., Jay, M., Bird, A. C., Jay, B., and Bhattacharya, S. S. (1991). Autosomal dominant retinitis pigmentosa: four new mutations in rhodopsin, one of them in the retinal attachment site. Genomics *11*, 199-205.

Kim, J. H., Mynatt, R. L., Moore, J. W., Woychik, R. P., Moustaid, N., and Zemel, M. B. (1996). The effects of calcium channel blockade on agouti-induced obesity. FASEB Journal *10*, 1646-52.

Kjelsberg, M. A., Cotecchia, S., Ostrowski, J., Caron, M. G., and Lefkowitz, R. J. (1992). Constitutive activation of the alpha 1B-adrenergic receptor by all amino acid substitutions at a single site. Evidence for a region which constrains receptor activation. Journal of Biological Chemistry *267*, 1430-3.

Klebig, M. L., Wilkinson, J. E., Geisler, J. G., and Woychik, R. P. (1995). Ectopic expression of the agouti gene in transgenic mice causes obesity, features of type II diabetes, and yellow fur [see comments]. Proceedings of the National Academy of Sciences of the United States of America *92*, 4728-32.

Klungland, H., Vage, D. I., Gomez-Raya, L., Adalsteinsson, S., and Lien, S. (1995). The role of melanocyte-stimulating hormone (MSH) receptor in bovine coat color determination. Mammalian Genome *6*, 636-9.

Kobayashi, T., Urabe, K., Orlow, S. J., Higashi, K., Imokawa, G., Kwon, B. S., Potterf, B., and Hearing, V. J. (1994). The Pmel 17/silver locus protein. Characterization and investigation of its melanogenic function. Journal of Biological Chemistry *269*, 29198-205.

Kobayashi, T., Vieira, W. D., Potterf, B., Sakai, C., Imokawa, G., and Hearing, V. J. (1995). Modulation of melanogenic protein expression during the switch from eu- to pheomelanogenesis. Journal of Cell Science *108*, 2301-9.

Konda, Y., Gantz, I., DelValle, J., Shimoto, Y., Miwa, H., and Yamada, T. (1994). Interaction of dual intracellular signaling pathways activated by the melanocortin-3 receptor. Journal of Biological Chemistry *269*, 13162-6.

Konopka, J. B., Margarit, S. M., and Dube, P. (1996). Mutation of Pro-258 in transmembrane domain 6 constitutively activates the G protein-coupled alpha-factor receptor. Proceedings of the National Academy of Sciences of the United States of America *93*, 6764-9.

Kontoyianni, M., DeWeese, C., Penzotti, J. E., and Lybrand, T. P. (1996). Three-dimensional models for agonist and antagonist complexes with β_2 adrenergic receptor. J. Med. Chem. *39*, 4406-4420.

Kopp, P., van Sande, J., Parma, J., Duprez, L., Gerber, H., Joss, E., Jameson, J. L., Dumont, J. E., and Vassart, G. (1995). Brief report: congenital hyperthyroidism caused by a mutation in the thyrotropin-receptor gene [see comments]. New England Journal of Medicine *332*, 150-4.

Koppula, S. V., Robbins, L. S., Lu, D., Baack, E., White, C. R., Swanson, J. N. A., and Cone, R. D. (1997). Identification of common polymorphisms in the coding sequence of the human MSH receptor with possible biological effects. Human mutation *9*, 30-36.

Korner, A., and Pawelek, J. (1982). Mammalian tyrosinase catalyzes three reactions in the biosynthesis of melanin. Science *217*, 1163-5.

Kosugi, S., Kohn, L. D., Akamizu, T., and Mori, T. (1994). The middle portion in the second cytoplasmic loop of the thyrotropin receptor plays a crucial role in adenylate cyclase activation. Molecular Endocrinology *8*, 498-509.

Kosugi, S., and Mori, T. (1994). The third exoplasmic loop of the thyrotropin receptor is partially involved in signal transduction. FEBS Letters *349*, 89-92.

Kosugi, S., Okajima, F., Ban, T., Hidaka, A., Shenker, A., and Kohn, L. D. (1992). Mutation of alanine 623 in the third cytoplasmic loop of the rat thyrotropin (TSH) receptor results in a loss in the phosphoinositide but not cAMP signal induced by TSH and receptor autoantibodies. Journal of Biological Chemistry *267*, 24153-6.

Kosugi, S., Okajima, F., Ban, T., Hidaka, A., Shenker, A., and Kohn, L. D. (1993). Substitutions of different regions of the third cytoplasmic loop of the thyrotropin (TSH) receptor have selective effects on constitutive, TSH-, and TSH receptor autoantibody-stimulated phosphoinositide and 3',5'-cyclic adenosine monophosphate signal generation. Molecular Endocrinology *7*, 1009-20.

Kosugi, S., Van Dop, C., Geffner, M. E., Rabl, W., Carel, J. C., Chaussain, J. L., Mori, T., Merendino, J. J., Jr., and Shenker, A. (1995). Characterization of heterogeneous mutations causing constitutive activation of the luteinizing hormone receptor in familial male precocious puberty. Human Molecular Genetics *4*, 183-8.

Kraaij, R., Post, M., Kremer, H., Milgrom, E., Epping, W., Brunner, H. G., Grootegoed, J. A., and Themmen, A. P. (1995). A missense mutation in the second transmembrane segment of the luteinizing hormone receptor causes familial male-limited precocious puberty. Journal of Clinical Endocrinology & Metabolism *80*, 3168-72.

Kucera, G. T., Bortner, D. M., and Rosenberg, M. P. (1996). Overexpression of an Agouti cDNA in the skin of transgenic mice recapitulates dominant coat color phenotypes of spontaneous mutants. Developmental Biology *173*, 162-73.

Kwon, B. S. (1993). Pigmentation genes: the tyrosinase gene family and the pmel 17 gene family. Journal of Investigative Dermatology *100*, 134S-140S.

Kwon, B. S., Chintamaneni, C. D., Kozak, C. A., Copeland, N. G., Gilbert, D. J., Jenkins, N. A., Barton, D. E., Francke, U., Kobayashi, Y., and Kim, K. K. (1991). A melanocyte-specific gene, Pmel 17, maps near the silver coat color locus on mouse chromosome 10, and is a syntenic region on human chromosome 12. Proc.Natl. Acad. Sci. USA *88*, 9228-9232.

Kwon, B. S., Wakulchik, M., Haq, A. Q., Halaban, R., and Kestler, D. (1988). Sequence analysis of mouse tyrosinase cDNA and the effect of melanotropin on its gene expression. Biochem. Biophys. Res. Commun. *153*, 1301-1309.

Kwon, H. Y., Bultman, S. J., Loffler, C., Chen, W. J., Furdon, P. J., Powell, J. G., Usala, A. L., Wilkison, W., Hansmann, I., and Woychik, R. P. (1994). Molecular structure and chromosomal mapping of the human homolog of the agouti gene. Proceedings of the National Academy of Sciences of the United States of America *91*, 9760-4.

Labbe, O., Desarnaud, F., Eggerickx, D., Vassart, G., and Parmentier, M. (1994). Molecular cloning of a mouse melanocortin 5 receptor gene widely expressed in peripheral tissues. Biochem. *33*, 4543-4549.

Lamoreux, M. L., and Mayer, T. C. (1975). Site of gene action in the development of hair pigment in recessive yellow (e/e) mice. Developmental Biology *46*, 160-6.

Latronico, A. C., Anasti, J., Arnhold, I. J., Mendonca, B. B., Domenice, S., Albano, M. C., Zachman, K., Wajchenberg, B. L., and Tsigos, C. (1995). A novel mutation of the luteinizing hormone receptor gene causing male gonadotropin-independent precocious puberty. Journal of Clinical Endocrinology & Metabolism *80*, 2490-4.

Laue, L., Chan, W.-Y., Hsueh, A. J. W., Kudo, M., Hsu, S. Y., Wu, S.-M., Blomberg, L., and Cutler, J., G.B. (1995). Genetic heterogeneity of constitutively activating mutations of the human lutenizing hormone receptor in familial male-limited precocious puberty. Proc. Natl. Acad. Sci. USA *92*, 1906-1910.

Lee, Z. H., Hou, L., Moellmann, G., Kuklinska, E., Antol, K., Fraser, M., Halaban, R., and Kwon, B. S. (1996). Characterization and subcellular localization of human Pmel 17/silver, a 110-kDa (pre)melanosomal membrane protein associated with 5,6,-dihydroxyindole-2-carboxylic acid (DHICA) converting activity. Journal of Investigative Dermatology *106*, 605-10.

Lefkowitz, R. J., Cotecchia, S., Samama, P., and Costa, T. (1993). Constitutive activity of receptors coupled to guanine nucleotide regulatory proteins. [Review]. Trends in Pharmacological Sciences *14*, 303-7.

Lerner, A. B., and McGuire, J. S. (1961). Effect of alpha- and beta-melanocyte stimulating hormones on the skin color of man. Nature *189*, 176-177.

Li, T., Franson, W. K., Gordon, J. W., Berson, E. L., and Dryja, T. P. (1995). Constitutive activation of phototransduction by K296E opsin is not a cause of photoreceptor degeneration. Proceedings of the National Academy of Sciences of the United States of America *92*, 3551-5.

Little, C. C. (1957). The Inheritance of Coat Colors in Dogs (New York: Macmillan).

Liu, J., Schoneberg, T., van Rhee, M., and Wess, J. (1995). Mutational analysis of the relative orientation of transmembrane helices I and VII in G protein-coupled receptors. Journal of Biological Chemistry *270*, 19532-9.

Low, M. J., Simerly, R. D., and Cone, R. D. (1994). Receptors for the Melanocortin Peptides in the Central Nervous Sustem. Curr. Opin. Endocrinol. Diabet. *1*, 79-88.

Lu, D., Willard, D., Patel, I. R., Kadwell, S., Overton, L., Kost, T., Luther, M., Chen, W., Woychik, R. P., Wilkison, W. O., and et al. (1994). Agouti protein is an antagonist of the melanocyte-stimulating-hormone receptor. Nature *371*, 799-802.

Lucas, A., Shuster, S., Thody, A. J., Eberle, A. N., and Girard, J. (1987). A comparison of structure-activity relationships within alpha-MSH on melanophores of Anolis carolinensis and Rana pipiens. Regulatory Peptides *18*, 43-50.

Lynch, P. J. (1994). Dermatology for the house officer (3rd ed.), T. S. Satterfield, ed. (Baltimore, Maryland: Williams & Wilkins).

Lyson, K., Ceriani, G., Takashima, A., Catania, A., and Lipton, J. M. (1994). Binding of anti-inflammatory alpha-melanocyte-stimulating-hormone peptides and proinflammatory cytokines to receptors on melanoma cells. Neuroimmunomodulation *1*, 121-6.

Magenis, R. E., Smith, L., Nadeau, J. H., Johnson, K. R., Mountjoy, K. G., and Cone, R. D. (1994). Mapping of the ACTH, MSH, and neural (MC3 and MC4) melanocortin receptors in the mouse and human. Mammalian Genome *5*, 503-8.

Malas, S., Peters, J., and Abbott, C. (1994). The genes for endothelin 3, vitamin D 24-hydroxylase, and melanocortin 3 receptor map to distal mouse chromosome 2, in the region of conserved synteny with human chromosome 20. Mammalian Genome *5*, 577-9.

Manne, J., Argeson, A. C., and Siracusa, L. D. (1995). Mechanisms for the pleiotropic effects of the agouti gene [comment]. Proceedings of the National Academy of Sciences of the United States of America *92*, 4721-4.

Marklund, L., Moller, M. J., Sandberg, K., and Andersson, L. (1996). A missense mutation in the gene for melanocyte-stimulating hormone receptor (MC1R) is associated with the chestnut coat color in horses. Mammalian Genome *7*, 895-9.

Michaud, E. J., Bultman, S. J., Klebig, M. L., van Vugt, M. J., Stubbs, L. J., Russell, L. B., and Woychik, R. P. (1994). A molecular model for the genetic and phenotypic characteristics of the mouse lethal yellow (Ay) mutation. Proceedings of the National Academy of Sciences of the United States of America *91*, 2562-6.

Michaud, E. J., Bultman, S. J., Stubbs, L. J., and Woychik, R. P. (1993). The embryonic lethality of homozygous lethal yellow mice (Ay/Ay) is associated with the disruption of a novel RNA-binding protein. Genes & Development *7*, 1203-13.

Millar, S. E., Miller, M. W., Stevens, M. E., and Barsh, G. S. (1995). Expression and transgenic studies of the mouse agouti gene provide insight into the mechanisms by which mammalian coat color patterns are generated. Development *121*, 3223-32.

Miller, M. W., Duhl, D. M., Vrieling, H., Cordes, S. P., Ollmann, M. M., Winkes, B. M., and Barsh, G. S. (1993). Cloning of the mouse agouti gene predicts a secreted protein ubiquitously expressed in mice carrying the lethal yellow mutation. Genes & Development *7*, 454-67.

Morris, J. C., Bergert, E. R., and McCormick, D. J. (1993). Structure-function studies of the human thyrotropin receptor. Inhibition of binding of labeled thyrotropin (TSH) by synthetic human TSH receptor peptides. Journal of Biological Chemistry *268*, 10900-5.

Mountjoy, K. G. (1994). The human melanocyte stimulating hormone receptor has evolved to become "super-sensitive" to melanocortin peptides. Molecular & Cellular Endocrinology *102*, R7-11.

Mountjoy, K. G., Mortrud, M. T., Low, M. J., Simerly, R. B., and Cone, R. D. (1994). Localization of the melanocortin-4 receptor (MC4-R) in neuroendocrine and autonomic control circuits in the brain. Molecular Endocrinology *8*, 1298-308.

Mountjoy, K. G., Robbins, L. S., Mortrud, M. T., and Cone, R. D. (1992). The cloning of a family of genes that encode the melanocortin receptors. Science *257*, 1248-51.

Nagayama, Y., and Rapoport, B. (1992). The thyrotropin receptor 25 years after its discovery: new insight after its molecular cloning. Molecular Endocrinology *6*, 145-56.

Nagayama, Y., Russo, D., Chazenbalk, G. D., Wadsworth, H. L., and Rapoport, B. (1990). Extracellular domain chimeras of the TSH and LH/CG receptors reveal the mid-region (amino acids 171-260) to play a vital role in high affinity TSH binding. Biochemical & Biophysical Research Communications *173*, 1150-6.

Nagayama, Y., Russo, D., Wadsworth, H. L., Chazenbalk, G. D., and Rapoport, B. (1991). Eleven amino acids (Lys-201 to Lys-211) and 9 amino acids (Gly-222 to Leu-230) in the human thyrotropin receptor are involved in ligand binding. Journal of Biological Chemistry *266*, 14926-30.

Nathans, J. (1990). Determinants of visual pigment absorbance: identification of the retinylidene Schiff's base counterion in bovine rhodopsin. Biochemistry *29*, 9746-52.

Nikiforovich, G. V., Sharma, S. D., Hadley, M. E., and Hruby, V. J. (1992). Chemistry and Biology, Proceedings of the Twelfth American Peptide Symposium. In Peptides, J. A. a. R. Smith, J. E., ed. (Leiden, The Netherlands: ESCOM), pp. 389-392.

Nyakas, C., Veldhuis, H. D., and De Wied, D. (1985). Beneficial effect of chronic treatment with Org 2766 and alpha-MSH on impaired reversal learning of rats with bilateral lesions of the parafascicular area. Brain Research Bulletin *15*, 257-65.

O. Donohue, T. L., and Dorsa, D. M. (1982). The opiomelanotropinergic neuronal and endocrine systems. [Review]. Peptides *3*, 353-95.

Oliveira, L., Paiva, A. C., Sander, C., and Vriend, G. (1994). A common step for signal transduction in G protein-coupled receptors. [Review]. Trends in Pharmacological Sciences *15*, 170-2.

Olivera, B. M., Miljanich, G. P., Ramachandran, J., and Adams, M. E. (1994). Calcium channel diversity and neurotransmitter release: the omega-conotoxins and omega-agatoxins. [Review]. Annual Review of Biochemistry *63*, 823-67.

Ovchinnikov, Y. A., Abdulaev, N. G., Feigina, M. Y., Artamonov, I. D., Zolotarev, A. S., Kostina, M. B., Bogachuk, A. S., Miroshnikov, A. I., Marinov, V. I., and Kudelin, A. B. (1982). The complete amino acid sequence of visual rhodopsin. Bioorg. Khim. *8*, 1011-1014.

Parent, J. L., Le Gouill, C., de Brum-Fernandes, A. J., Rola-Pleszczynski, M., and Stankova, J. (1996). Mutations of two adjacent amino acids generate inactive and constitutively active forms of the human platelet-activating factor receptor. Journal of Biological Chemistry *271*, 7949-55.

Parma, J., Duprez, L., Van Sande, J., Cochaux, P., Gervy, C., Mockel, J., Dumont, J., and Vassart, G. (1993). Somatic mutations in the thyrotropin receptor gene cause hyperfunctioning thyroid adenomas [see comments]. Nature *365*, 649-51.

Parma, J., Van Sande, J., Swillens, S., Tonacchera, M., Dumont, J., and Vassart, G. (1995). Somatic mutations causing constitutive activity of the thyrotropin receptor are the major cause of hyperfunctioning thyroid adenomas: identification of additional mutations activating both the cyclic adenosine 3',5'-monophosphate and inositol phosphate-Ca2+ cascades. Molecular Endocrinology *9*, 725-33.

Paschke, R., Tonacchera, M., Van Sande, J., Parma, J., and Vassart, G. (1994). Identification and functional characterization of two new somatic mutations causing constitutive activation of the thyrotropin receptor in hyperfunctioning autonomous adenomas of the thyroid. Journal of Clinical Endocrinology & Metabolism *79*, 1785-9.

Pawelek, J. (1976). Factors regulating growth and pigmentation of melanoma cells. J. Invest. Dermatol. *66*, 201-209.

Perry, W. L., Hustad, C. M., Swing, D. A., Jenkins, N. A., and Copeland, N. G. (1995). A transgenic mouse assay for agouti protein activity. Genetics *140*, 267-74.

Perry, W. L., Nakamura, T., Swing, D. A., Secrest, L., Eagleson, B., Hustad, C. M., Copeland, N. G., and Jenkins, N. A. (1996). Coupled site-directed mutagenesis/transgenesis identifies important functional domains of the mouse agouti protein. Genetics *144*, 255-264.

Pollak, M. R., Brown, E. M., Estep, H. L., McLaine, P. N., Kifor, O., Park, J., Hebert, S. C., Seidman, C. E., and Seidman, J. G. (1994). Autosomal dominant hypocalcaemia caused by a Ca(2+)-sensing receptor gene mutation. Nature Genetics *8*, 303-7.

Porcellini, A., Ciullo, I., Pannain, S., Fenzi, G., and Avvedimento, E. (1995). Somatic mutations in the VI transmembrane segment of the thyrotropin receptor constitutively activate cAMP signalling in thyroid hyperfunctioning adenomas. Oncogene *11*, 1089-93.

Probst, W. C., Snyder, L. A., Schuster, D. I., Brosius, J., and Sealfon, S. C. (1992). Sequence alignment of the G-protein coupled receptor superfamily. [Review] [167 refs]. DNA & Cell Biology *11*, 1-20.

Rainey, W. E., Viard, I., and Saez, J. M. (1989). Transforming growth factor beta treatment decreases ACTH receptors on ovine adrenocortical cells. Journal of Biological Chemistry *264*, 21474-7.

Rao, V. R., Cohen, G. B., and Oprian, D. D. (1994). Rhodopsin mutation G90D and a molecular mechanism for congenital night blindness. Nature *367*, 639-42.

Rao, V. R., and Oprian, D. D. (1996). Activating mutations of rhodopsin and other G protein-coupled receptors. [Review] [120 refs]. Annual Review of Biophysics & Biomolecular Structure *25*, 287-314.

Ren, Q., Kurose, H., Lefkowitz, R. J., and Cotecchia, S. (1993). Constitutively active mutants of the alpha 2-adrenergic receptor [published erratum appears in J Biol Chem 1994 Jan 14;269(2):1566]. Journal of Biological Chemistry *268*, 16483-7.

Rim, J., and Oprian, D. D. (1995). Constitutive activation of opsin: interaction of mutants with rhodopsin kinase and arrestin. Biochemistry *34*, 11938-45.

Robbins, L. S., Nadeau, J. H., Johnson, K. R., Kelly, M. A., Roselli-Rehfuss, L., Baack, E., Mountjoy, K. G., and Cone, R. D. (1993). Pigmentation phenotypes of variant extension locus alleles result from point mutations that alter MSH receptor function. Cell *72*, 827-34.

Robinson, P. R., Cohen, G. B., Zhukovsky, E. A., and Oprian, D. D. (1992). Constitutively active mutants of rhodopsin. Neuron *9*, 719-25.

Roselli-Rehfuss, L., Mountjoy, K. G., Robbins, L. S., Mortrud, M. T., Low, M. J., Tatro, J. B., Entwistle, M. L., Simerly, R. B., and Cone, R. D. (1993). Identification of a receptor for gamma melanotropin and other proopiomelanocortin peptides in the hypothalamus and limbic system. Proceedings of the National Academy of Sciences of the United States of America *90*, 8856-60.

Russo, D., Arturi, F., Schlumberger, M., Caillou, B., Monier, R., Filetti, S., and Suarez, H. G. (1995). Activating mutations of the TSH receptor in differentiated thyroid carcinomas. Oncogene *11*, 1907-11.

Russo, D., Arturi, F., Suarez, H. G., Schlumberger, M., Du Villard, J. A., Crocetti, U., and Filetti, S. (1996). Thyrotropin receptor gene alterations in thyroid hyperfunctioning adenomas. Journal of Clinical Endocrinology & Metabolism *81*, 1548-51.

Russo, D., Arturi, F., Wicker, R., Chazenbalk, G. D., Schlumberger, M., DuVillard, J. A., Caillou, B., Monier, R., Rapoport, B., Filetti, S., and et al. (1995). Genetic alterations in thyroid hyperfunctioning adenomas. Journal of Clinical Endocrinology & Metabolism *80*, 1347-51.

Russo, D., Chazenbalk, G. D., Nagayama, Y., Wadsworth, H. L., and Rapoport, B. (1991). Site-directed mutagenesis of the human thyrotropin receptor: role of asparagine-linked oligosaccharides in the expression of a functional receptor. Molecular Endocrinology *5*, 29-33.

Sakmar, T. P., Franke, R. R., and Khorana, H. G. (1989). Glutamic acid-113 serves as the retinylidene Schiff base counterion in bovine rhodopsin. Proceedings of the National Academy of Sciences of the United States of America *86*, 8309-13.

Salomon, Y. (1991). Cellular responsiveness to hormones and neurotransmitters: conversion of [3H]adenine to [3H]cAMP in cell monolayers, cell suspensions, and tissue slices. Methods in Enzymology *195*, 22-8.

Samama, P., Cotecchia, S., Costa, T., and Lefkowitz, R. J. (1993). A mutation-induced activated state of the beta 2-adrenergic receptor. Extending the ternary complex model. Journal of Biological Chemistry *268*, 4625-36.

Samama, P., Pei, G., Costa, T., Cotecchia, S., and Lefkowitz, R. J. (1994). Negative antagonists promote an inactive conformation of the beta 2-adrenergic receptor. Molecular Pharmacology *45*, 390-4.

Sandman, C. A., Beckwith, B. E., and Kastin, A. J. (1980). Are learning and attention related to the sequence of amino acids in ACTH/MSH peptides? Peptides *1*, 277-80.

Sawyer, T. K., Hadley, M. E., Hruby, V. J., Castrucci, A. M., Staples, D. J., Farah, J., and TL, O. D. (1988). Alpha-melanocyte-stimulating hormone structure-activity studies: comparative analysis of melanotropic and CNS bioactivities. Synapse *2*, 289-92.

Sawyer, T. K., Sanfilippo, P. J., Hruby, V. J., Engel, M. H., Heward, C. B., Burnett, J. B., and Hadley, M. E. (1980). 4-Norleucine, 7-D-phenylalanine-alpha-melanocyte-stimulating hormone: a highly potent alpha-melanotropin with ultralong biological activity. Proceedings of the National Academy of Sciences of the United States of America *77*, 5754-8.

Sawyer, T. K., Staples, D. J., Castrucci, A. M., Hadley, M. E., al-Obeidi, F. A., Cody, W. L., and Hruby, V. J. (1990). Alpha-melanocyte stimulating hormone message and inhibitory sequences: comparative structure-activity studies on melanocytes. Peptides *11*, 351-7.

Sawyer, T. K., Staples, D. J., de Lauro Castrucci, A. M., and Hadley, M. E. (1989). Discovery and structure-activity relationships of novel alpha-melanocyte-stimulating hormone inhibitors. Peptide Research *2*, 140-6.

Scheer, A., Fanelli, F., Costa, T., De Benedetti, P. G., and Cotecchia, S. (1996). Constitutively active mutants of the alpha 1B-adrenergic receptor: role of highly conserved polar amino acids in receptor activation. EMBO Journal *15*, 3566-78.

Schild, H. A. (1947). A New Scale for the Measurement of Drug Antagonism. Br. J. Pharmacol. *2*, 189-206.

Schipani, E., Kruse, K., and Juppner, H. (1995). A constitutively active mutant PTH-PTHrP receptor in Jansen-type metaphyseal chondrodysplasia. Science *268*, 98-100.

Sealfon, S. C., Chi, L., Ebersole, B. J., Rodic, V., Zhang, D., Ballesteros, J. A., and Weinstein, H. (1995). Related contribution of specific helix 2 and 7 residues to conformational activation of the serotonin 5-HT2A receptor. Journal of Biological Chemistry *270*, 16683-8.

Searle, A. G. (1968). Comparative Genetics of Coat Colors in Mammals (London: Logos Press Limited).

Sharma, S. D., Nikiforovich, G. V., Jiang, J., Castrucci, A. M., Hadley, M. E., and Hruby, V. J. (1993). . In Peptides 1992, C. H. a. E. Schneider, A. N., ed. (Leiden, The Netherlands: ESCOM Sci. Publ.), pp. 95-96.

Sharma, S. D., Toth, G., and Hruby, V. J. (1991). A Simple General Method for (Radio)-Indination of a Phenylalanine Residue in Peptides: Preparation of [D-Pen^2, ^{125}IPhe^4,D-Pen^5]enkephalin, a Peptide With Extraordinary Selectivity for Delta Opioid Receptors. J. Org. Chem. *56*, 4981-4983.

Sheikh, S. P., Zvyaga, T. A., Lichtarge, O., Sakmar, T. P., and Bourne, H. R. (1996). Rhodopsin activation blocked by metal-ion-binding sites linking transmembrane helices C and F. Nature *383*, 347-50.

Shenker, A., Laue, L., Kosugi, S., Merendino, J. J., Jr., Minegishi, T., and Cutler, G. B., Jr. (1993). A constitutively activating mutation of the luteinizing hormone receptor in familial male precocious puberty [see comments]. Nature *365*, 652-4.

Shizume, K., Lerner, A. B., and Fitzpatrick, T. B. (1954). In Vitro Bioassay for the Melanocyte Stimulating Hormone. Endocrinology *54*, 533-560.

Siegrist, W., Oestreicher, M., Stutz, S., Girard, J., and Eberle, A. N. (1988). Radioreceptor assay for alpha-MSH using mouse B16 melanoma cells. Journal of Receptor Research *8*, 323-43.

Siegrist, W., Willard, D. H., Wilkison, W. O., and Eberle, A. N. (1996). Agouti protein inhibits growth of B16 melanoma cells in vitro by acting through melanocortin receptors. Biochemical & Biophysical Research Communications *218*, 171-5.

Silvers, W. K. (1979). The Coat Colors of Mice: A Model for Mammalian Gene Action and Interaction (New York: Springer).

Silvers, W. K. (1958). An experimental approach to action of genes at the agouti locus in the mouse. III. Transplants of newborn A^w-, A-, and a^t- skin to A^y-, A^w-, A-, and *aa* hosts. J. Exp. Zool. *137*, 189-196.

Silvers, W. K., and Russel, E. S. (1955). An experimental approach to action of genes at the agouti locus in the mouse. J. Exp. Zool. *130*, 199-220.

Siracusa, L. D. (1994). The agouti gene: turned on to yellow [published erratum appears in Trends Genet 1995 Mar;11(3):116]. Trends in Genetics *10*, 423-8.

Solca, F., Siegirist, W., Drozdz, R., Girard, J., and Eberle, A. N. (1989). The receptor for alpha-melanotropin of mouse and human melanoma cells. J. Biol. Chem *264*, 14277-14280.

Star, R. A., Rajora, N., Huang, J., Stock, R. C., Catania, A., and Lipton, J. M. (1995). Evidence of autocrine modulation of macrophage nitric oxide synthase by alpha-melanocyte-stimulating hormone. Proceedings of the National Academy of Sciences of the United States of America *92*, 8016-20.

Strand, F. L., Zuccarelli, L. A., Williams, K. A., Lee, S. J., Lee, T. S., Antonawich, F. J., and Alves, S. E. (1993). Melanotropins as growth factors. [Review]. Annals of the New York Academy of Sciences *680*, 29-50.

Sugawa, H., Ueda, Y., Akamizu, T., Kosugi, S., Okuda, J., Ohta, C., Kiho, Y., and Mori, T. (1995). Statistical analysis of functional region(s) of the TSH receptor. Journal of Endocrinological Investigation *18*, 710-7.

Sugg, E. E., Castrucci, A. M., Hadley, M. E., van Binst, G., and Hruby, V. J. (1988). Cyclic lactam analogues of Ac-[Nle4]alpha-MSH4-11-NH2. Biochemistry *27*, 8181-8.

Sullivan, J. M., Scott, K. M., Falls, H. F., Richards, J. H., and Sieving, P. A. (1993). A novel rhodopsin mutation at the retinal binding site (Lys296-Met) in ADRP. Invest. Ophthalmol. Vis. Sci. *34*, 1149.

Summers, M. D., and Smith, G. E. (1987). A manual of methods for baculovirus vectors and cloned insect cell culture procedures.: Texas Agriculture Experiment Station, College Station).

Swaab, D. F., Boer, G. J., and Visser, M. (1978). The fetal brain and intrauterine growth. Postgraduate Medical Journal *1*, 63-73.

Swaab, D. F., and Martin, J. T. (1981). Functions of alpha-melanotropin and other opiomelanocortin peptides in labour, intrauterine growth and brain development. Ciba Foundation Symposium *81*, 196-217.

Swaab, D. F., and Visser, M. (1977). A function for alpha-MSH in fetal development and the presence of an alpha-MSH-like compound in nervous tissue. Frontiers of Hormone Research *4*, 170-8.

Swaab, D. F., Visser, M., and Tilders, F. J. (1976). Stimulation of intra-uterine growth in rat by alpha-melanocyte-stimulating hormone. Journal of Endocrinology *70*, 445-55.

Szabo, G., Gerald, A. B., Pathak, M. A., and T.B., F. (1972). The ultrastructure of racial color differences in man, in Riley. In Pigmentation: Its Genesis and Biologic Control. (New York: Appleton-Century-Crofts).

Takeuchi, S., Suzuki, H., Yabuuchi, M., and Takahashi, S. (1996). A possible involvement of melanocortin 1-receptor in regulating feather color pigmentation in the chicken. Biochimica et Biophysica Acta *1308*, 164-8.

Takeuchi, T., Kobunai, T., and Yamamoto, H. (1989). Genetic control of signal transduction in mouse melanocytes. Soc. Invest. Dermatol. *92*, 239-S-242S.

Tamate, H. B., and Takeuchi, T. (1984). Action of the e locus of mice in the response of phaeomelanic hair follicles to alpha-melanocyte stimulating hormone in vitro. Science *224*, 1241-1242.

Thody, A. J., Cooper, M. F., Bowden, P. E., Meddis, D., and Shuster, S. (1976). Effect of alpha-melanocyte-stimulating hormone and testosterone on cutaneous and modified sebaceous glands in the rat. Journal of Endocrinology *71*, 279-88.

Thody, A. J., and Shuster, S. (1975). Control of sebaceous gland function in the rat by alpha-melanocyte-stimulating hormone. Journal of Endocrinology *64*, 503-10.

TL, O. D., Handelmann, G. E., Chaconas, T., Miller, R. L., and Jacobowitz, D. M. (1981). Evidence that N-acetylation regulates the behavioral activity of alpha-MSH in the rat and human central nervous system. Peptides *2*, 333-44.

TL, O. D., and Jacobowitz, D. M. (1980). Studies of alpha-MSH-containing nerves in the brain. Progress in Biochemical Pharmacology *16*, 69-83.

Tobin, D., Quinn, A. G., Ito, S., and Thody, A. J. (1994). The presence of tyrosinase and related proteins in human epidermis and their relationship to melanin type. Pigment Cell Research *7*, 204-9.

Tominaga, Y., and Takagi, H. (1996). Molecular genetics of hyperparathyroid disease. [Review] [55 refs]. Current Opinion in Nephrology & Hypertension *5*, 336-41.

Tonacchera, M., Van Sande, J., Cetani, F., Swillens, S., Schvartz, C., Winiszewski, P., Portmann, L., Dumont, J. E., Vassart, G., and Parma, J. (1996). Functional characteristics of three new germline mutations of the thyrotropin receptor gene causing autosomal dominant toxic thyroid hyperplasia. Journal of Clinical Endocrinology & Metabolism *81*, 547-54.

Tonacchera, M., Van Sande, J., Parma, J., Duprez, L., Cetani, F., Costagliola, S., Dumont, J. E., and Vassart, G. (1996). TSH receptor and disease. Clinical Endocrinology *44*, 621-33.

Trumpp-Kallmeyer, S., Hoflack, J., Bruinvels, A., and Hibert, M. (1992). Modeling of G-protein-coupled receptors: application to dopamine, adrenaline, serotonin, acetylcholine, and mammalian opsin receptors. Journal of Medicinal Chemistry *35*, 3448-62.

Tsukamoto, K., Jackson, I. J., Urabe, K., Montague, P. M., and Hearing, V. J. (1992). A second tyrosinase-related protein, TRP-2, is a melanogenic enzyme termed DOPAchrome tautomerase. EMBO J. *11*, 519-526.

Vage, D. I., Lu, D., Klungland, H., Lien, S., Adalsteinsson, S., and Cone, R. D. (1997). A non-epistatic interaction of *agouti* and *extension* in the fox, *Vulpes vulpes*. Nat. Genet. *15*, 311-315.

Valverde, P., Healy, E., Jackson, I., Rees, J. L., and Thody, A. J. (1995). Variants of the melanocyte-stimulating hormone receptor gene are associated with red hair and fair skin in humans [see comments]. Nature Genetics *11*, 328-30.

Vamvakopoulos, N. C., Rojas, K., Overhauser, J., Durkin, A. S., Nierman, W. C., and Chrousos, G. P. (1993). Mapping the human melanocortin 2 receptor (adrenocorticotropic hormone receptor; ACTHR) gene (MC2R) to the small arm of chromosome 18 (18p11.21-pter). Genomics *18*, 454-5.

Van Sande, J., Parma, J., Tonacchera, M., Swillens, S., Dumont, J., and Vassart, G. (1995). Somatic and germline mutations of the TSH receptor gene in thyroid diseases. Journal of Clinical Endocrinology & Metabolism *80*, 2577-85.

van Wimersma Greidanus, T. B., de Rotte, G. A., Thody, A. J., and Eberle, A. N. (1981). Melanocyte-stimulating hormone and adaptive behaviour. Ciba Foundation Symposium *81*, 277-94.

Vanetti, M., Schonrock, C., Meyerhof, W., and Hollt, V. (1994). Molecular cloning of a bovine MSH receptor which is highly expressed in the testis. FEBS Letters *348*, 268-72.

Vassar, R., Rosenberg, M., Ross, S., Tyner, A., and Fuchs, E. (1989). Tissue-specific and differentiation-specific expression of a human K14 keratin gene in transgenic mice. Proceedings of the National Academy of Sciences of the United States of America *86*, 1563-7.

Vassart, G., Desarnaud, F., Duprez, L., Eggerickx, D., Labbe, O., Libert, F., Mollereau, C., Parma, J., Paschke, R., Tonacchera, M., and et al. (1995). The G protein-coupled receptor family and one of its members, the TSH receptor. Annals of the New York Academy of Sciences *766*, 23-30.

Vassart, G., Van Sande, J., Parma, J., Tonacchera, M., Duprez, L., Swillens, S., and Dumont, J. (1996). Activating mutations of the TSH receptor gene cause thyroid diseases. Annales d Endocrinologie *57*, 50-4.

Vaudry, H., and Eberle, A. N. (1993). The Melanotropic Peptides. In Annals of the New York Academy of Sciences, pp. 1-687.

Vrieling, H., Duhl, D. M., Millar, S. E., Miller, K. A., and Barsh, G. S. (1994). Differences in dorsal and ventral pigmentation result from regional expression of the mouse agouti gene. Proceedings of the National Academy of Sciences of the United States of America *91*, 5667-71.

Wesley, C. R., and Gilmore, J. P. (1985). Effects of oxytocin, vasotocin and alpha-MSH on renal function in the nonhuman primate. Hormone Research *21*, 55-9.

Willard, D. H., Bodnar, W., Harris, C., Kiefer, L., Nichols, J. S., Blanchard, S., Hoffman, C., Moyer, M., Burkhart, W., Weiel, J., and et al. (1995). Agouti structure and function: characterization of a potent alpha-melanocyte stimulating hormone receptor antagonist. Biochemistry *34*, 12341-6.

Wilson, B. D., Ollmann, M. M., Kang, L., Stoffel, M., Bell, G. I., and Barsh, G. S. (1995). Structure and function of ASP, the human homolog of the mouse agouti gene. Human Molecular Genetics *4*, 223-30.

Wolff, G. L., Galbraith, D. B., Domon, O. E., and Row, J. M. (1978). Phaeomelanin synthesis and obesity in mice. Interaction of the viable yellow (Avy) and sombre (eso) mutations. Journal of Heredity *69*, 295-8.

Wong, G., and Pawelek, J. (1975). Melanocyte stimulating hormone promotes activation of preexisting tyrosinase molecules in Cloudman S91 melanoma cells. Nature *255*, 644-646.

Xu, X., M., T., Lundin, L., and Chhajlani, V. (1996). Val92met variant of the melanocyte stimulating hormone receptor gene. Nature genetics *14*, 384.

Yamada, M., Yamada, M., Watson, M. A., and Richelson, E. (1994). Deletion mutation in the putative third intracellular loop of the rat neurotensin receptor abolishes polyphosphoinositide hydrolysis but not cyclic AMP formation in CHO-K1 cells. Molecular Pharmacology *46*, 470-6.

Yang, Y., Ollmann, M. M., Wilson, B. D., Dickinson, C., Yamada, T., Barsh, G. S., and Gantz, I. (1997). Effects of Recombinant Agouti-Signaling Protein on Melanocortin Action. Molecular Endocrinology *11*, 274-280.

Yano, K., Saji, M., Hidaka, A., Moriya, N., Okuno, A., Kohn, L. D., and Cutler, J., G.B. (1995). A new constitutively activating point mutation in the luteinizing hormone/choriogonadotropin receptor gene in cases of male-limited precocious puberty. J. Clin. Endocrinol. Metabol. *80*, 1162-1168.

Yen, T. T., Gill, A. M., Frigeri, L. G., Barsh, G. S., and Wolff, G. L. (1994). Obesity, diabetes, and neoplasia in yellow A(vy)/- mice: ectopic expression of the agouti gene. FASEB Journal *8*, 479-88.

Zemel, M. B., Kim, J. H., Woychik, R. P., Michaud, E. J., Kadwell, S. H., Patel, I. R., and Wilkison, W. O. (1995). Agouti regulation of intracellular calcium: role in the insulin resistance of viable yellow mice [see comments]. Proceedings of the National Academy of Sciences of the United States of America *92*, 4733-7.

Zhao, H., Eling, D. J., Medrano, E. E., and Boissy, R. E. (1996). Retroviral infection with human tyrosinase-related protein-1 (TRP-1) cDNA upregulates tyrosinase activity and melanin synthesis in a TRP-1-deficient melanoma cell line. Journal of Investigative Dermatology *106*, 744-52.

Zhou, W., Flanagan, C., Ballesteros, J. A., Konvicka, K., Davidson, J. S., Weinstein, H., Millar, R. P., and Sealfon, S. C. (1994). A reciprocal mutation supports helix 2 and helix 7 proximity in the gonadotropin-releasing hormone receptor. Molecular Pharmacology *45*, 165-70.

Zhukovsky, E. A., and Oprian, D. D. (1989). Effect of carboxylic acid side chains on the absorption maximum of visual pigments. Science *246*, 928-30.

Zhukovsky, E. A., Robinson, P. R., and Oprian, D. D. (1991). Transducin activation by rhodopsin without a covalent bond to the 11-cis-retinal chromophore. Science *251*, 558-60.